Leibniz-Institut für Nutztierbiologie & Teagasc Food Research Center

---

The impact on meat quality of strategies to improve feed conversion efficiency in pigs and the functional networks underpinning the relationship

Dissertation

zur Erlangung des Grades

Doktorin der Ernährungs- und Lebensmittelwissenschaften
(Dr. troph.)

der Landwirtschaftlichen Fakultät

der Rheinischen Friedrich–Wilhelms–Universität Bonn

von

Justyna Horodyska

aus

Radlin, Poland

Bonn 2018

Referent: Prof. Dr. Klaus Wimmers

Korreferent: Prof. Dr. Matthias Wüst

Tag der mündlichen Prüfung: 18 06 2018

Diese Dissertation ist auf dem Hochschulschriftenserver der ULB Bonn http://hss.ulb.uni-bonn.de/diss_online elektronisch publiziert.

Abstract

Feed efficiency (FE) is defined as a measure of efficiency in converting metabolizable energy acquired from macronutrients into muscle and/or adipose tissue. The overall aims of this thesis were to identify genomic regions associated with FE in a commercial line of Maxgro boars, to evaluate the molecular and phenotypic relationship between FE and meat quality in Maxgro x (German Landrace x Large White) pigs and to investigate the molecular mechanisms contributing to differences in FE, in liver, fat and skeletal muscle tissue. Firstly, 952 boars having measures of FE traits were genotyped and used for a genome-wide association study (GWAS). Most of the quantitative trait loci (QTL) identified by this method were described for the first time, although some of them were located not far from previously associated genomic regions. Putative candidate genes located in the QTL regions derived for FE traits had functions related to lipogenesis, glucose homeostasis, olfactory reception and immunological status. Secondly, three metabolically important tissues, including muscle, adipose and liver were analysed. Significant differences in meat traits such as sensory profile, texture and cook loss suggest a minor impairment of meat quality from high-FE pigs. This group also exhibited leaner carcasses, greater muscle content and an improved fatty acid profile compared to low-FE pigs. Ontology analysis predicted a more efficient immune defence in the muscle of high-FE pigs, which may indicate that these animals are also more efficient in conserving resources for growth. Shifts in carbohydrate conversion into glucose in FE-divergent muscle may underpin the altered *post-mortem* muscle pH profiles between FE groups. Moreover, differences in amino acid metabolism may influence growth in FE-divergent muscle, whereas decreased degradation of fibroblasts could impact on collagen turnover and alter tenderness of meat. Metabolism of lipids was also predicted to be affected by FE suggesting an altered fat metabolism in FE-divergent muscle. Transcriptomic profiling of adipose tissue of FE-divergent pigs suggested the establishment of a dense extracellular matrix and inhibition of capillary formation might be underlying mechanisms to achieve suppressed adipogenesis and increased utilisation of fatty acids by other tissues. Lipid metabolism was also affected by FE whereby over-expression of cholesterol-related genes suggests more efficient cholesterol disposal from high-FE adipose tissue. Furthermore, gene expression patterns in the liver of high-FE pigs suggested improved hepatic absorption of carbohydrates and cholesterol, and enhanced reverse cholesterol transport. The liver of high-FE pigs may be characterised by higher protein turnover and increased epithelial cell differentiation, whilst enhanced quantity of invariant natural killer T-cells and viability of

natural killer cells could induce a faster and more effective hepatic response to inflammatory stimuli. Overall, this study showed that FE is a highly complex trait affected by a number of genomic regions. Transcriptomic profiling of muscle, adipose and liver tissue from FE-divergent pigs provided mechanistic insights on the biological events prevailing differences in FE, which impacts meat quality. The findings of this thesis will assist the meat animal industry in identifying strategies to improve FE without compromising meat quality.

Kurzbeschreibung

Die Futterverwertung (FE) beschreibt die Effektivität von Nutztieren, die metabolisierbare Energie aus Makronährstoffen in Muskel- und/oder Fettgewebe umzuwandeln. Die übergeordneten Ziele dieser Arbeit waren a) genomische Regionen zu bestimmen, die mit der Ausprägung von FE-Merkmalen in einer kommerziellen Linie von Maxgro Ebern in Zusammenhang stehen, b) molekulare und phänotypische Beziehung zwischen FE und Fleischqualität in einer Maxgro x (German Landrace x Large White) Population aufzuzeigen, und c) zugrundeliegende molekulare Mechanismen in drei relevanten Geweben zu identifizieren. Im ersten Teil der Studie wurden 952 FE-getestete Eber genotypisiert und im Rahmen einer genomweiten Assoziationsstudie (GWAS) analysiert. Die meisten der mit dieser Methode identifizierten *Quantitative Trait Loci* (QTL) wurden erstmals beschrieben, obwohl einige von ihnen in der Nähe von zuvor assoziierten genomischen Regionen lagen. Die für die FE-Merkmale abgeleiteten Kandidatengene in den QTL-Regionen haben Funktionen in Bezug auf Lipogenese, Glukosehomöostase, olfaktorische Rezeption und den immunologischen Status. Der zweite Teil dieser Dissertation betrachtet Muskel-, Fett- und Lebergewebe. Signifikante Unterschiede in den Fleischmerkmalen, wie zum Beispiel von sensorischen Profilen, Fleischtextur und Kochverlust, deuten auf eine geringfügige Beeinträchtigung der Fleischqualität bei Schweinen mit hoher FE hin. Andererseits wies diese Gruppe magerere Schlachtkörper, einen höheren Muskelanteil und ein verbessertes Fettsäureprofil im Vergleich zu Schweinen mit niedriger FE auf. Die Analyse der Genontologie prognostizierte eine erhöhte Effizienz der Abwehr im Muskel von Schweinen mit hoher FE, was darauf hindeuten könnte, dass diese Tiere auch effizienter in ihrer Ressourcennutzung für Wachstum sind. Verschiebungen in der muskulären Umwandlung von Kohlenhydraten zu Glukose zwischen FE-divergenten Tieren wurden auch auf Ebene der post-mortalen pH-Profile zwischen den Gruppen abgebildet. Darüber hinaus könnten Unterschiede im Lipid- und Aminosäurestoffwechsel das Muskelwachstum beeinflussen, während ein verminderter Fibroblastenabbau den Kollagenumsatz und die Zartheit des Fleisches beeinflussen kann. Transkriptionelle Unterschiede im Fettgewebe FE-divergenter Schweine implizieren dass, die Bildung einer dichten extrazellulären Matrix und die Hemmung der Kapillarbildung grundlegende Mechanismen sein könnten, um die Adipogenese zu unterdrücken, und eine erhöhte Verfügbarkeit von Fettsäuren für andere Gewebe zu erreichen. Dementsprechend zeigte sich auch der Lipidstoffwechsel durch FE beeinflusst, wobei die Überexpression von cholesterinverwandten Genen auf einen

effizienteren Cholesterinexport aus dem Fettgewebe von Tieren mit hoher FE hindeutete. Die Analyse der hepatischen Genontologie deutete auf eine verbesserte Aufnahme von Kohlenhydraten und Cholesterin sowie einen verbesserten Rücktransport von Cholesterin in Schweinen mit hoher FE hin. Basierend auf transkriptionellen Expressionsprofilen, charakterisiert sich die Leber von Schweinen mit hoher FE durch einen höheren Proteinumsatz und eine erhöhte Differenzierung der Epithelzellen. Dabei liefert die Auslenkung von Genen, welche die Funktion natürlicher Killerzellen beeinflussen, Hinweise darauf, dass eine schnellere und effektivere hepatische Reaktion auf Entzündungsreize in Tieren mit höherer FE induzieren werden könnte. Insgesamt zeigte diese Studie, dass FE ein hochkomplexes Merkmal ist, das von einer Reihe genomischer Regionen beeinflusst wird. Transkriptionelle Profile aus Muskel-, Fett- und Lebergewebe von FE-divergenten Schweinen lieferten Erkenntnisse über biologische Mechanismen, welche für die Unterschiede in der FE fundamental sind. Die Ergebnisse dieser Arbeit werden die Tierhaltung und Züchtung dabei unterstützen, Strategien zur Verbesserung der FE zu identifizieren, ohne die Fleischqualität zu beeinträchtigen.

Table of Contents

CHAPTER 1

Introduction

1. 1 Feed efficiency

1.1.1 Feed efficiency definition and indexes

Feed efficiency (FE) is an economically and ecologically significant trait in pig production and determines the ability of an animal to efficiently convert feed into muscle and adipose tissue (Wilkinson 2011). Feed conversion ratio (FCR) is an indicator of feed efficiency and defines a ratio of feed intake to weight gain. Feed efficiency can also be expressed as residual feed intake (RFI), which refers to a difference between actual feed intake and its expected nutritional requirements due to maintenance and growth (Saintilan et al. 2013). Both FCR and RFI indexes are included in the breeding program to achieve efficient pork production. Nevertheless RFI takes into consideration that a large proportion of feed efficiency is not explained by body growth and composition, and unlike FCR, is independent of phenotypic production traits and denotes an inherent variation in the maintenance energy requirements (Young and Dekkers 2012; Willems et al. 2013).

Figure 1.1 Feed efficiency in pigs depicted as a ratio of the amount of feed to the amount of meat produced including energy conversion efficiency between the feed and meat. Adapted from http://farmfolly.com/2011/03/complete-costs-of-raising-pigs/.

1.1.2 Physiological factors affecting feed efficiency

Carbohydrates, fats and proteins are the main macronutrients present in feed providing energy in the form of calories (the amount of heat required to raise 1 gram of water by 1 degree Celsius). Burned energy is used for maintenance and growth processes and is also released as heat. Approximately a third of dietary energy is designated towards maintenance processes, thus reducing unnecessary stress, maintaining appropriate environment

temperature and ensuring good health of pigs would vastly contribute towards shifting the dietary energy towards more efficient growth (Patience et al. 2015). A study has shown that low-RFI (high-FE) pigs exhibit reduced maintenance requirements and heat production when compared to high-RFI (low-FE) line (Barea et al. 2010). Differences in feed digestibility have also been reported in pigs divergent for RFI (Harris et al. 2012).

Carbohydrates such as starch are the main source of energy in feedstuff (Nafikov and Beitz 2007; Bach-Knudsen et al. 2012). On the other hand, fibre, which is a type of carbohydrate, contributes to the energy production in a much smaller scale, if any, and may impede absorption of other nutrients (Zhang et al. 2013). When ingested, carbohydrates (excluding fibre) are broken down to glucose and either used up in energetically costly processes or stored in the form of glycogen in the liver and muscle for later usage (Granlund et al. 2010). Glucose can also be converted to fatty acids via de novo lipogenesis and transported to adipose tissue for storage as triacylglycerol (Hua et al. 2016). Fats are the highest energy source in feedstuff yielding more than double amount of energy when compared to carbohydrates and proteins (Park et al. 2012). Similarly to carbohydrates, fuel from fats can be expended to drive energy requiring processes. Alternatively, excess of fats can be exported to adipose tissue and deposited as triacylglycerol, or converted to glucose in the process known as gluconeogenesis (Kaleta et al. 2011; Kerr et al. 2015). The main destination of dietary proteins is to provide amino acids needed for synthesis of new proteins. However, if an organism experiences excess of amino acids, the subsequently ingested dietary proteins would be used to produce energy but not very efficiently as it is an energetically expensive process (Van Milgen and Noblet 2002). This diverse ways of macronutrients partitioning and energy utilization have a great impact on the efficiency of feed, which provides fuel for various maintenance processes and tissue growth.

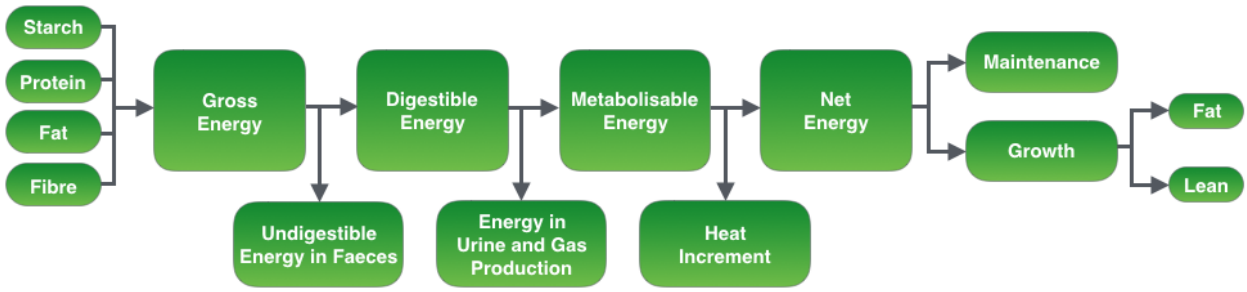

Figure 1.2 Energy partitioning and utilization derived from macronutrients ingestion. Adapted from Euken (2012).

Variation in feed intake and physical activity has been demonstrated to contribute to divergence in feed efficiency. Low-RFI pigs were shown to eat faster, less and not as frequently compared to high-RFI counterparts (Young et al. 2011). Moreover, low-RFI pigs exhibited lower physical activity (Meunier-Salaun et al. 2014). Body composition has also an influence in feed efficiency due to the fact that accretion of adipose tissue is more energy consuming than lean muscle growth (Gaines et al. 2012). Consistent with that, more efficient utilisation of energy by low-RFI pigs were shown to result in decreased deposition of fat in this line of pigs (Lefaucheur et al. 2011; Smith et al. 2011; Faure et al. 2013).

1.1.3 Quantitative trait loci for feed efficiency

Some phenotypic traits, e.g. feed efficiency, are termed as polygenic/quantitative traits, meaning that they are impacted by several genes/loci. Quantitative trait loci (QTLs) mapping serves as a powerful tool for detecting genomic regions associated with a particular trait. A number of QTLs for feed efficiency in pigs have been detected using various techniques (Figure 1.3).

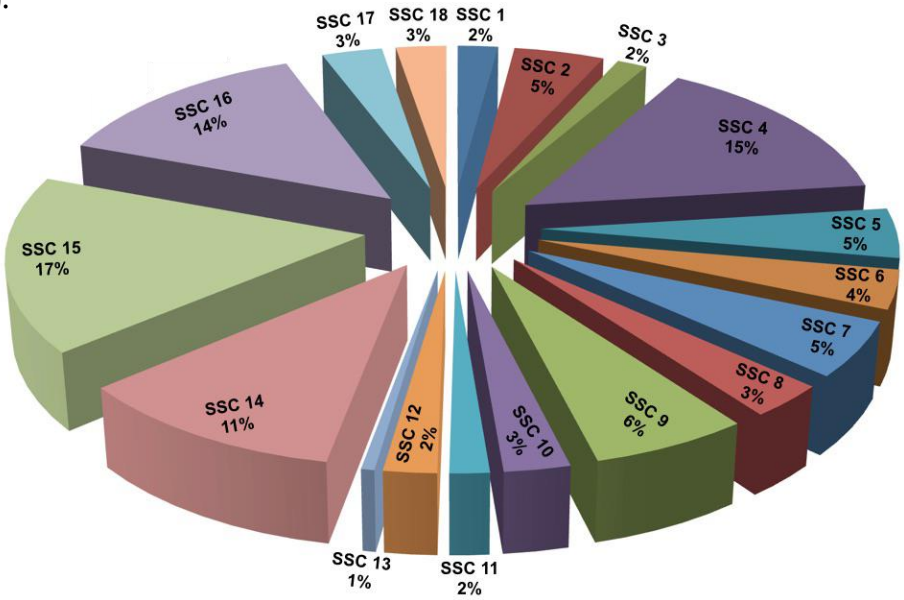

Figure 1.3 Pie chart representing a total number of 191 quantitative trait loci (QTLs) across porcine genome for feed efficiency and a percentage of these QTLs mapped to a particular chromosome (SSC). Each segment denotes a chromosome. Data gathered from Pig QTLdb (http://animalgenome.org/cgi-bin/QTLdb).

A genome-wide association study (GWAS) approach has been used in some studies to identify QTLs for feed efficiency in pigs. Specifically, a number of significant QTLs for FCR on porcine chromosomes (SSC) 4, 7, 8 and 14 were detected by GWAS in Duroc pigs

(Sahana et al. 2013), however other GWAS study in the same breed identified only one QTL for FCR on SSC 4 (Jiao et al. 2014). Several QTLs influencing RFI on SSC 3, 8, 9, 10, 15 and 17 (Do et al. 2014b), as well as 7 and 14 (Onteru et al. 2013) were reported in Yorkshire pigs also using GWAS. Additionally, QTLs on SSC 1, 8, 9, 13 and 18 were inferred from a GWAS in RFI divergent Duroc boars (Do et al. 2014a).

1.2 Meat quality

1.2.1 Key meat quality traits

Meat quality is an economically important and complex trait that includes a number of objectively and subjectively evaluated parameters including technological and sensory attributes, as well as nutritional value (Erkens et al. 2010). Tenderness is one of the most important characteristics of meat influencing consumers' acceptance (Huffman et al. 1996; Mubashera et al. 2013). *Post-mortem* degradation of cytoskeletal protein by calpain system is a key factor contributing to meat tenderness (Polidori et al. 2001). Meat tenderness is also affected by concentration of a total collagen, types of collagen and collagen matrix cross-linkages. This influence of connective tissue on meat tenderness is known as 'background toughness' (Purslow 2014). Moreover sarcomeres, which begin to shorten during rigor, also play a role in reducing tenderness of meat (Maher et al. 2005).

Intramuscular fat (IMF), known as marbling, greatly contributes to the flavour of meat. Flavour is a mixture of taste and aroma (Spence 2015). During heating, fatty acids undergo oxidation, which leads to decomposition and development of aroma volatiles (Resconi et al. 2013). Increased marbling was significantly correlated with reduced drip loss and cook loss, as well as improved sensory tenderness and juiciness (Cannata et al. 2010). IMF contains higher proportion of phospholipids comparing to subcutaneous adipose tissue and this is due to the fact that muscle tissue is richer in the amount of cell membranes (Wood et al. 2008).

Water holding capacity (WHC) is the ability of meat to hold its water after cutting, heating, grinding or pressing (Zayas 1997). It is one of the most important meat quality traits contributing to the yield of the product (Cheng and Sun 2008). Various factors such as stress of animal before slaughter, methods of stunning, post-slaughter chilling and aging of meat contribute to WHC (Cheng and Sun 2008). WHC can be determined by measuring drip loss

of fresh meat, which is a high protein fluid lost from meat upon gravity (Torres-Filho et al. 2017).

Myoglobin is a major pigment found in meat that contributes to the red colour of meat. Meat that is not exposed to oxygen (deoxymyoglobin) is characterised by purplish-red or purplish-pink colour, however upon exposure to oxygen (oxymyoglobin) meat changes colour to bright red. This colour change is known as bloom. Both deoxymyoglobin and oxymyoglobin can form metmyoglobin which is associated with oxidation of iron molecules resulting in brownish-red colour (Mubashera et al. 2013). The rate of colour change can be influenced by temperature, pH and *post-mortem* aging (Gasperlin et al. 2001; Andrés-Bello et al. 2013).

1.2.2 Factors influencing conversion of muscle to meat and the quality of meat

Muscle pH evolution influences the rate and extent of converting muscle into meat. In the first 24 hours after slaughter level of glycogen in muscle is low due to anaerobic glycolysis resulting in accumulation of lactic acid, which in turn causes the pH of muscle to drop from 7.4 to 5.5 (Scheffler et al. 2013). Acute or short term stress before killing is the major cause of Pale Soft Exudative **(**PSE**)** meat. Rapid pH decline **(**< 6 at 45 minutes *post-mortem*) due to lactic acid accumulation in the muscle is observed while the temperature of meat is still high. Low pH and high temperature lead to a decreased water-holding capacity of meat as a consequence of muscle protein denaturation (Adzitey and Nurul 2011). On the other hand, chronic or long term stress results in Dark Firm Dry (DFD) meat, which is characterised by higher ultimate pH **(**≥ 6**)** in the muscle. The cause of very restricted pH decline is limited glycogen content at death which does not allow significant production of lactic acid (Adzitey and Nurul 2011). Due to the higher pH, little denaturation of protein is observed therefore the water-holding capacity of the meat is relatively high (Penny 1969; Adzitey and Nurul 2011).

Conversion of muscle to meat begins immediately *post-mortem* through degradation of myofibril and cytoskeletal proteins known as proteolysis. There are four main proteolytic systems including calpains, caspases, cathepsins and proteasomes (Kemp et al. 2010). Calpains belong to intracellular cysteine proteases family requiring Ca2+ for activation and are expressed in skeletal muscle as three isoforms: μ-calpain (calpain 1), m-calpain (calpain 2) and calpain 3. Calpain 1 and its inhibitor, calpastatin, play the most important role in *post-mortem* proteolysis and meat tenderisation (Koohmaraie and Geesink 2006). Caspases are cysteine aspartate-specific proteases and can be divided into initiator caspases (caspase 8, 9,

10 and 12) and effector caspases (caspase 3, 6 and 7) (Kemp and Parr 2012). Calpain inhibition via up-regulation of calpastatin has been shown to increase caspase 3 activity and apoptosis (Kemp et al. 2010). Furthermore, calpastatin is proteolysed by caspase 1, 3 and 7 (Wang et al. 1998). Thus activated caspases present in muscle *post-mortem* can contribute to meat quality through indirect up-regulation of calpains. Moreover, proteasomes together with cathepsins, which are located in the lysosomes and released in the cytosol upon apoptosis, also influence muscle proteolysis (Nowak 2011).

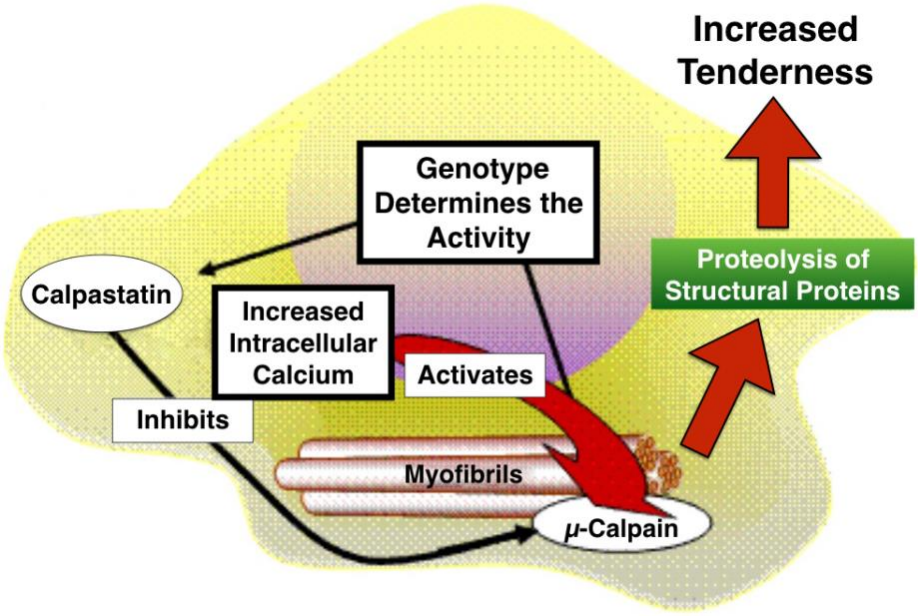

Figure 1.4 The impact of calpastatin and calcium on meat tenderness through inhibition/activation of μ-calpain (calpain 1). Adapted from http://beltiebeef.com.

Moreover, *post-mortem* carcass temperatures also affect the rate and extent of converting muscle into meat, with temperatures below 10°C in early *post-mortem* muscle being associated with 'cold shortening', also referred to as 'sarcomere shortening' (James and James 2010). This phenomenon can be reduced by permitting the temperature of muscle to drop below 10°C until the pH of muscle had fallen below 6.2 (Bendall 1973). Meat tenderness can be enhanced by applying electrical stimulation to pre-rigor carcass causing muscle contraction, which leads to rapid depletion of muscle glycogen before chilling (Adeyemi and Sazili 2014), or through pre-rigor alteration in carcass position causing some muscle to stretch and other muscle to relax (Herring et al. 1965).

1.2.3 Genetic markers for pork meat quality traits

Similarly to feed efficiency, meat quality is a complex trait influenced by animal's genetic makeup. A number of molecular markers have been identified with the aim to improve meat quality traits through genetic selection. Single nucleotide polymorphisms (SNP) in halothane (*HAL*) and ryanodine receptor 1 (*RYR1*) genes involved in Ca2+ release (Pabelick et al. 2001; Lanner et al. 2010), were associated with lower ultimate pH, lighter meat colour and greater drip loss (Guardia et al. 2004; Škrlep et al. 2010; Silveira et al. 2011). A variation in the promoter region of the insulin-like growth factor 2 (*IGF2*) regulating cell proliferation, differentiation and apoptosis was associated with intramuscular fat content (Aslan et al. 2012). Peroxisome proliferator-activated receptor gamma coactivator 1-alpha (*PPARGC1A*) is another candidate gene for meat quality traits. It plays a part in energy and fat metabolism, adipogenesis and muscle fibre type formation (Erkens et al. 2010). Polymorphisms in this gene have been associated with fat related traits (Kunej et al. 2005) and tenderness (Erkens et al. 2010). A number of SNPs in calpain 1 (*CAPN1*), which is involved in proteolysis of myofibril proteins, demonstrated associations with pork tenderness (Yang et al. 2007). Moreover, variations in calpastatin (*CAST*), known for inhibiting calpain 1 activity, has also been associated with meat tenderness (Lindholm-Perry et al. 2009). Protein kinase AMP-Activated non-catalytic subunit gamma 3 (PRKAG3; also known as rendement napole, RN) participates in muscle energy metabolism and a polymorphism within this gene has been associated with intramuscular fat deposition and drip loss (Škrlep et al. 2010; Ryan et al. 2012; Salas and Mingala 2017).

1.3 Impact of feed efficiency on meat traits and functional networks underpinning the relationship between meat quality and feed efficiency

Processes related to muscle growth, e.g. skeletal muscle differentiation and proliferation were identified to be significantly enriched amongst up-regulated genes in low-RFI muscle (Jing et al. 2015). Surprisingly, Gondret et al. (2017) reported a suppression of skeletal muscle development in low-RFI line. Higher abundance of genes involved in protein synthesis (Vincent et al. 2015; Gondret et al. 2017) and degradation, more specifically 'ribonucleoprotein complex biogenesis' and 'ubiquitin-dependent catabolic process' in low-RFI pigs (Gondret et al. 2017) were also identified. These biochemical processes occurring in RFI divergent muscle could explain phenotypically observed enhanced muscle

content (Lefaucheur et al. 2011), Moreover, processes related to lipid metabolism such as lipid localisation and transport, cellular lipid catabolic processes, and fatty acids metabolism and beta-oxidation were significantly enriched with differentially expressed genes in relation to RFI (Le Naou et al. 2012; Jing et al. 2015; Vincent et al. 2015; Gondret et al. 2017). Accordingly, reduced back-fat thickness (Lefaucheur et al. 2011; Faure et al. 2013) while increased leanness (Lefaucheur et al. 2011; Smith et al. 2011; Faure et al. 2013) and decreased intramuscular fat content (Lefaucheur et al. 2011; Smith et al. 2011), as well as reduced sensory scores for marbling (Faure et al. 2013) were reported.

No significant association between RFI and tenderness, evaluated by sensory panel, was found in a study carried out by Faure et al. (2013). In contrast, another sensory analysis has shown a positive correlation between RFI and tenderness, whilst negative correlation between RFI and chewiness (Smith et al. 2011). The same author postulated that tenderness of meat produced by low-RFI pigs could be negatively affected by greater calpastatin activity resulting in decreased *post-mortem* protein degradation (Smith et al. 2011). Consistent with this, calpain 2 was found over-expressed in muscle from low-RFI pigs (Vincent et al. 2015).

Observed reduced mitochondrial energy metabolism (Le Naou et al. 2012; Jing et al. 2015; Vincent et al. 2015; Fu et al. 2017) and greater glycolytic potential (Lefaucheur et al. 2011; Faure et al. 2013) in low-RFI could have resulted in decreased ultimate pH, greater drip loss (Lefaucheur et al. 2011; Faure et al. 2013) and increased values for lightness (Lefaucheur et al. 2011) in muscle from low-RFI pigs. Moreover, these changes in energy metabolism and glycolytic potential could be attributable to observed differences in fibre type and a switch away from oxidative metabolism in low-RFI muscle (Lefaucheur et al. 2011). However, no evidence for the switch from oxidative to glycolytic fibres was detected by other study (Smith et al. 2011).

1.4 Research aims

This study is part of the pan-European ECO-FCE project, of which overall findings will assist the meat animal industry in predicting the effect of management and feeding strategies on feed efficiency and meat quality, and identifying strategies to improve efficiency without compromising meat quality. There is some evidence that divergence in feed efficiency affect meat quality (Lefaucheur et al. 2011; Smith et al. 2011; Faure et al. 2013), nevertheless the

relationship between feed efficiency and meat quality is not fully elucidated and the biological processes associated with feed efficiency which impact meat quality are not well understood. The current study was conducted at both Teagasc Food Research Centre (Dublin, Ireland) and Leibniz Institute for Farm Animal Biology (FBN; Dummerstorf, Germany) and the aims were to:

Aim 1: Identify candidate genes for feed efficiency in pigs using the genome-wide association (GWAS) study, and elucidate pathways and biological functions enriched with positional genes closest to significantly associated quantitative trait loci.

Aim 2: Examine technological, sensory and nutritional quality of *Longissimus thoracis et lumborum* (LTL) muscle from pigs differing in feed efficiency, investigate the molecular mechanisms induced in that muscle contributing to differences in feed efficiency and the functional networks underpinning the relationship between meat quality and feed efficiency.

Aim 3: Illuminate the biological processes in major metabolic and growth-related tissues, i.e. adipose and liver, that underpin the differences in feed efficiency.

Additionally, through obtaining the Teagasc Overseas Training Award, the study programme was expanded from European to global scale through conducting research for a three-month period at U.S. Meat Animal Research Center (U.S. MARC; Nebraska, USA). The primary purpose of this visit was to validate candidate genes for feed efficiency, identified through the GWAS, in U.S. pig population.

CHAPTER 2

Materials and Methods

2.1 Experimental design

In the Aim 1 of this project blood samples from n = 952 Maxgro boars (Hermitage Genetics, Ireland), which is predominately Pietrain based terminal line, were used. Estimated breeding values (EBV) for feed conversion ratio (FCR) and its related trait, days to 110 kg (D110), were recorded by Hermitage Genetics following the method of Varley et al. (2011). In the Aim 2, *Longissimus thoracis et lumborum* (LTL) muscle from two batches of animals was utilised for phenotypic and transcriptomic evaluation. The first batch included n = 20 Maxgro (Hermitage Genetics) x (German Landrace x Large White) gilts from low-RFI (high-FE) and high-RFI (low-FE) groups, selected from a total of n = 80 RFI-divergent pigs. Phenotypic and transcriptomic analysis were carried out on all 20 animals. The second batch included n = 40 Maxgro (Hermitage Genetics) x (German Landrace x Large White) pigs from low-RFI (high-FE) and high-RFI (low-FE) groups, selected from a total of n = 138 RFI-divergent pigs. In this batch, n = 40 were used for phenotypic evaluation, whilst n = 16 (selected of the 40) were utilised for molecular examination. RFI tests and animal selection based on RFI values are described in details in the manuscripts (see Annex A2 and A3). In the Aim 3, blood parameters and liver weight of n = 40 Maxgro (Hermitage Genetics) x (German Landrace x Large White) pigs from the second batch of animals (Aim 2) were measured. For molecular experiments, adipose and liver tissue samples of n = 16 pigs, selected of the 40, were utilised.

The experimental design, which is depicted in Figure 2.1, consisted of the following parts: a genome wide association study for feed efficiency in Maxgro boars using PorcineSNP60 BeadChip; transcriptome analysis of the LTL muscle from the first batch of Maxgro x (German Landrace x Large White) pigs from low-RFI (high-FE) and high-RFI (low-FE) groups using Porcine Snowball Array; RNA sequencing of the LTL muscle, adipose and liver tissue from the second batch of Maxgro x (German Landrace x Large White) pigs from low-RFI (high-FE) and high-RFI (low-FE) groups using Illumina HiSeq2500; analysis of carcass and meat quality traits, as well as biochemical and haematological blood parameters of Maxgro x (German Landrace x Large White) pigs from low-RFI (high-FE) and high-RFI (low-FE); and elucidation of biological processes affecting feed efficiency and functional networks underpinning the relationship between meat quality and feed efficiency.

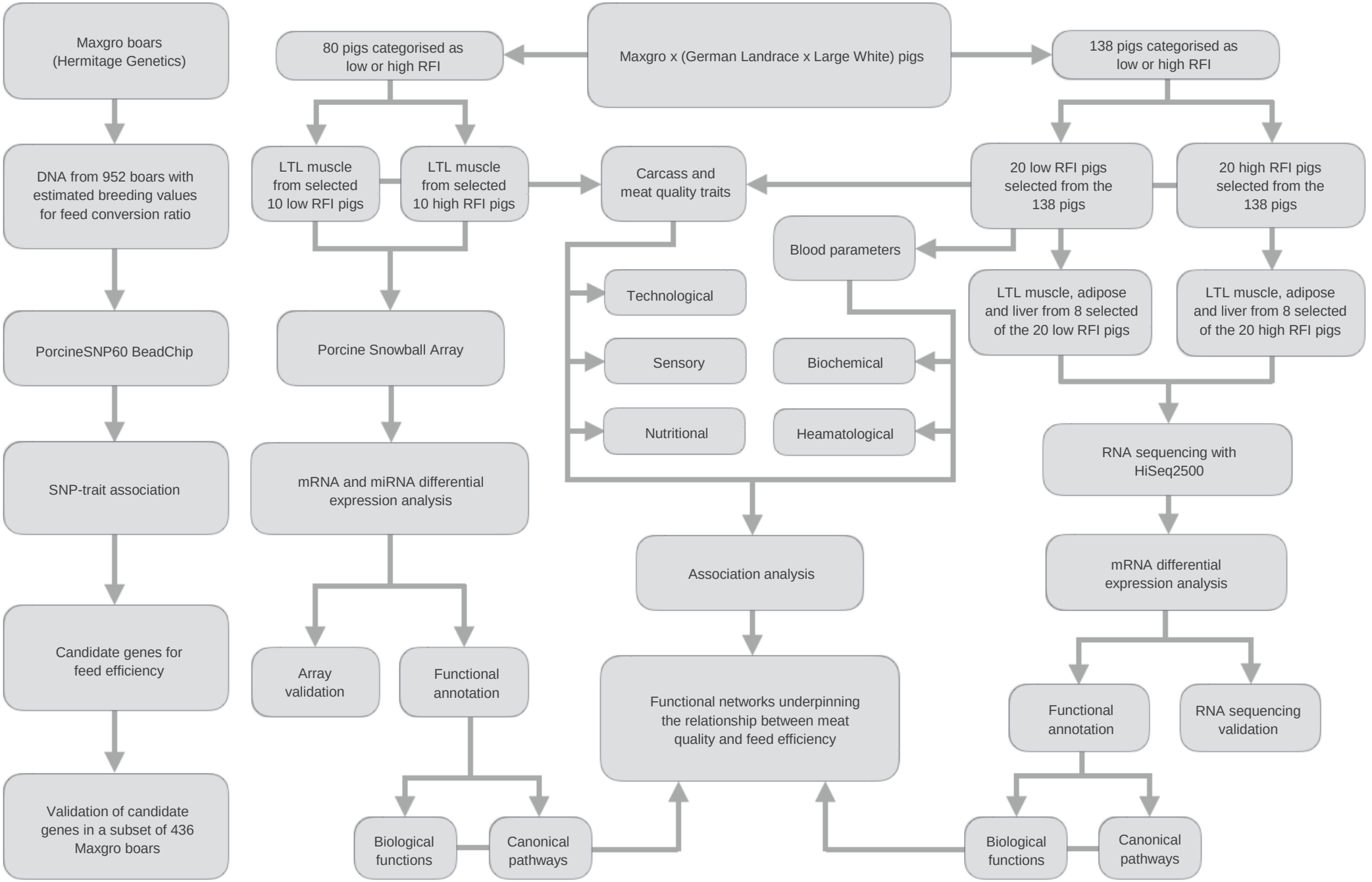

Figure 2.1 Pipeline depiction of the experimental design. LTL: *Longissimus thoracis et lumborum*; RFI: residual feed intake.

2.2 Sample collection

Animal care, slaughter and tissue collection of the animals used in this study were performed in compliance with national regulations related to animal research and commercial slaughtering and were approved by the local committees for the care and use of animals of Teagasc and Leibniz Institute for Farm Animal Biology. In this project, samples for both molecular and phenotypic analysis were collected. Molecular sampling was conducted as follows - Aim 1: blood from *Vena jugularis* was collected from each boar and preserved by Hermitage Genetics; Aim 2: for the first batch of animals, samples of the LTL muscle were collected, cut up finely and preserved in RNALater® (Ambion Inc., Austin, USA) within 10 minutes *post-mortem* and then stored overnight at 4°C followed by storage at -80°C; for the second batch of animals, samples of the LTL muscle were collected and snap frozen in liquid nitrogen within 10 minutes *post-mortem* and stored at -80°C. Aim 3: samples of the subcutaneous adipose tissues (above the LTL muscle) and the right liver lobe (*Lobus spigelii*) were collected and snap frozen in liquid nitrogen within 10 minutes *post-mortem* followed by storage at -80°C. The sample collection for phenotypic analysis was conducted as follows - Aim 2: carcass traits were measured on day 0 *post-mortem*, whilst for meat quality analysis the LTL muscle was excised 24 hours *post-mortem*. Aim 3: liver weights were recorded and blood samples were collected during slaughter. For biochemical analysis, upon allowing the blood to clot at room temperature, the samples were centrifuged and the serum was collected and stored at -80°C until analysed. For haematological analysis, blood was treated with EDTA to prevent clotting and analysed within 4 hours of sample collection. This chapter briefly summarises the main methods used for the molecular and phenotypic analysis. A detailed methodology is described in the publications (see Annex A1 - A5).

2.3 Approaches for Aim 1

2.3.1 SNP array genotyping, quality control and statistical analysis

Genotyping with PorcineSNP60 BeadChip (Illumina Inc., San Diego, CA, USA) was performed in compliance with the SNP Infinium HD assay protocol (http://illumina.com). Subsequently, data was analysed using GenomeStudio (Version 2011.1, Illumina Inc.). Individuals with call rate ≤ 97% and SNPs with call frequency ≤ 95% and minor allele frequency (MAF) ≤ 0.03 were excluded. After quality control, remaining SNPs were tested for an association with EBVs FCR and days to 110 kg (D110). SNP-trait association analysis

was implemented with a mixed linear model using JMP Genomics 6 software (version 6, SAS INST., Inc., Cary, NC, 2002–2010). In order to correct for population structure, the relationship matrix tool implemented in JMP Genomics 6 was used to compute identity-by-state (IBS) relations between individuals based on genotype data (Yu et al. 2006). After compression of K matrices, these relations were included as a random effect in the model. Threshold p-values for suggestive and Bonferroni-adjusted genome-wide significance were set to -log10[p-value] = 4.7 and -log10[p-value] = 6, respectively.

2.3.2 Functional enrichment among mapped genes and validation of candidate genes

A list of genes closest to the significant SNPs (-log10[p-value] ≥ 6) was created allowing a maximum distance of 1Mb between the marker and genes, using the Ensembl database (http://ensembl.org, release 78) and was uploaded into Ingenuity Pathways Analysis (IPA; Ingenuity® Systems, http://ingenuity.com) Benjamini-Hochberg corrected *P*-values (< 0.01) were used to map the genes to the most significant molecular, cellular and physiological systems development functions. Genotyping of selected SNPs, located in positional candidate genes that are not represented on the PorcineSNP60 BeadChip, was performed in a subset of Maxgro boars using TaqMan® SNP Genotyping Assays (Applied Biosystems, Foster City, CA, USA). Allele frequencies were computed and deviations from Hardy–Weinberg equilibrium (HWE) ($P < 0.05$) were tested using Haploview software (Barrett et al. 2005). Mixed linear model using JMP Genomics 6 software (version 6, SAS INST., Inc., Cary, NC, 2002–2010) was used to evaluate associations between the SNPs with allele frequency as predicted and greater than 5% and EBVs for FCR and D110 in the Maxgro boars. Compressed IBS relations were included as a random effect in the model.

2.4 Approaches for Aim 2

2.4.1 Microarray hybridisation and differential expression analysis

Double stranded cDNA was synthesised using total RNA. Antisense cRNA was then purified and sense-strand cDNA was synthesised by the reverse transcription of cRNA, using a GeneChip® WT Amplification Kit (Affymetrix, Santa Clara, CA, USA). Biotin-labeled cDNA was then fragmented with GeneChip® WT Terminal Labeling Kit (Affymetrix) and injected onto porcine snowball arrays (Affymetrix) containing 47,845 probe sets with a mean coverage of 22 probes per transcript (Freeman et al. 2012). The arrays were incubated for 16

hours at 45°C in Affymetrix GeneChip Hybridization Oven 640. After hybridisation, the arrays were washed and stained with streptavidin-phycoerythrin antibody solution (Affymetrix) on an Affymetrix GeneChip® Fluidic Station 450 station. The arrays were then scanned with Affymetrix GeneChip Scanner 3000 and microarray images were quantified using GCOS 1.1.1 (Affymetrix). Bioinformatic analysis, including pre-processing and normalisation, was implemented using R (version 3.1.1, http://R-project.org/). Robust multi-array average normalisation (Log2) was performed and probe sets with a low standard deviation (std $\leq$ 0.23) were discarded. A further filtering step involved filtering by both control probe sets and means (means $\leq$ 2.5 were rejected). PROC MIXED including RFI groups and sow as fixed effects and birth weight as a covariate was implemented in JMP Genomics 6 software of SAS (version 6, SAS INST.) to determine relative changes in transcript abundances (fold change).

2.4.2 RNA sequencing and differential expression analysis

RNA library preparation was carried out using the TruSeq® Stranded mRNA protocol. Following RNA sequencing with Illumina HiSeq2500, paired-end reads were mapped to the reference Sscrofa10.2 (Ensembl release 84) using TopHat (2.1.0) (Kim et al. 2013). Read counts were assigned to the gene features using the HTSeq 0.6.1 program (Anders et al. 2015). Differential gene expression analysis in relation to FE was performed using the Wald test implemented in DESeq2 package (3.4.0, http://R-project.org), including RFI groups and sow as fixed effects.

2.4.3 Functional annotation of microarray and RNA sequencing data

For microarray data, gene symbols for differentially expressed (DE) genes at a $P < 0.05$ and related fold changes were subjected to ontology analysis (IPA; Ingenuity® Systems, http://ingenuity.com) and Benjamini-Hochberg (B-H) corrected *P*-values (< 0.05) were used to detect the most significant canonical pathways and biological functions. For RNA-seq data, a list of DE genes at a $P < 0.01$ and corresponding fold changes were submitted to IPA, whereby B-H corrected *P*-values (< 0.01) were used to extract significantly enriched bio-functions and canonical pathways. Functional annotations with a z-score greater than 2 and lower than -2 were considered significantly activated and inhibited in low-RFI (high-FE) pigs, respectively. Information contained in the Ingenuity® Knowledge Base was used to create potential important networks of DE genes. Additionally for microarray data, a list of

DE microRNAs (miRNAs; represented on the *snowball* array) along with DE transcripts and related fold changes ($P \leq 0.05$) were submitted to Ingenuity miRNA Target Filter (http://www.ingenuity.com/) to predict target transcripts regulated by these miRNAs. Furthermore, potential networks of the DE transcripts that were predicted to be regulated by the DE miRNAs were generated.

2.4.4 Phenotypic measurements

Based on the difference in light reflectance of tissues, carcass was measured for fat thickness and muscle depth using Hennessy Grading Probe (Hennessy Grading Systems Ltd., Auckland, New Zealand). pH of LTL muscle was measured at several time points *post-mortem* (45min, 3h and 24h for the first batch of animals, whilst 45min, 2h, 3h, 4h, 5h and 24h for the second batch of animals), using a portable Hanna pH meter (Hanna Instruments, Woonsocket, RI, USA). Meat colour was measured with MiniScan XE Plus (Hunter Associates Laboratory Inc., Virginia, USA) using CIE L* (lightness), a* (redness) and b* (yellowness) colour scale. Drip loss was determined using the bag method of Honikel (1998), whereby pork chops measuring 2.5 cm in thickness and trimmed to a weight of 80.0 g ± 1.0 g were suspended by string inside an inflated and sealed plastic bag for 48h at 4°C, patted dry and reweighed and the percentage change recorded. For cook loss (CL) evaluation, muscle chops were placed in plastic bags and immersed in a water bath (Grant Instruments Ltd., England) at 77°C until they reached a core temperature of 75°C. Meat tenderness was measured using the Warner Bratzler shear force (WBSF) method, whereby six cores of 1.25 cm diameter, obtained from the previously cooked samples, were cut in parallel to the longitudinal orientation of fibres and sheared perpendicularly to the muscle fibres long axis (Instron model 5543). Data was analysed using Blue Hill software (Instron Ltd., Buckinghamshire, UK). Protein content was measured with a Leco Nitrogen/Protein Analyser (FP-528, Leco Corp., MI, USA) using the Dumas method in accordance with AOAC method 992.15, 1990. Intramuscular fat (IMF) content was measured with NMR Smart Trac and Smart 5 Rapid Fat Analyser (CEM Corporation, USA) using AOAC method 985.14. Fatty acid (FA) profile of IMF was analysed using Gas Chromatography - Flame Ionization Detector (GC - FID) in accordance with SAL Cam Nut003 method (Pearson's Chemical Analysis of Foods, 9th Edition, Longman Group UK Limited, 1991, 0-582-40910-1). For sensory assessment, chops aged at 4°C for 7 days were grilled (Velox grill, Silesia Velox UK Ltd., Oxfordshire, England) until the core temperature reached 70°C and cut into 2.5 cm x

2 cm cubes. Randomised samples were evaluated by trained panellists rating the pork chops sensory attributes on a scale of 1 (very poorly detectable attribute) to 100 (extremely detectable attribute). To evaluate associations between FE and meat quality traits, PROC MIXED procedure in the SAS system was used. The model for the first batch of animals included RFI groups as a fixed effect, sow as a random effect and pre-slaughter live weight as a covariate, as well as the absolute values of RFI as a weight statement to account for differences in RFI values within the RFI groups. The model for the second batch of animals incorporated RFI groups, gender and slaughter day as fixed effects, sow as a random effect, live weight as a covariate and the absolute values of RFI as a weight statement.

2.5 Approaches for Aim 3

2.5.1 RNA sequencing and differential expression analysis

Total RNA was used as input for the library preparation according to the TruSeq Stranded mRNA protocol (Illumina, San Diego, CA, USA). Subsequently, sequencing was performed on an Illumina HiSeq2500 generating paired-end reads. Reads were mapped to the reference (Ensembl release 84) using TopHat (2.1.0) (Kim et al. 2013) and read counts were assigned to the gene features employing HTSeq 0.6.1 (Anders et al. 2015). The assessment of the differentially expressed genes included RFI groups and sow as fixed effects for adipose tissue, whilst RFI groups and slaughter date as fixed effects for liver tissue, and was performed using the Wald test implemented in DESeq2 (3.4.0, www.R-project.org).

2.5.2 Gene ontology analysis

To integrate gene expression data, the list of DE genes ($P < 0.01$) and corresponding fold changes were passed to Ingenuity Pathway Analysis (IPA; Ingenuity® Systems, http://ingenuity.com), whereby Fisher's exact test *P*-values (< 0.01) were used to extract significantly enriched bio-functions and canonical pathways. Potential important interaction networks enriched with DE genes were generated using the Ingenuity® Knowledge Base. Additionally for adipose tissue, IPA Upstream Regulator analysis was utilised to identify potential transcription factors, growth factors etc., that can elucidate the differences in gene expression. Functional annotations and upstream regulators with a z-score greater than 2 and lower than -2 were considered significantly activated and inhibited in low-RFI (high-FE) pigs, respectively.

2.5.3 Phenotypic measurements

Biochemical serum parameters, such as creatinine, creatine kinase, total protein, blood urea nitrogen, triglycerides, glucose and cholesterol, were analysed with ABS Pentra 400 clinical chemistry analyser (Horiba, ABX, North Hampton, UK). For haematological analysis, white blood cells, lymphocytes, monocytes, granulocytes, red blood cells, red blood cell distribution width, haemoglobin, haematocrit, mean corpuscular volume, mean corpuscular haemoglobin, platelets and mean platelet volume were measured with a Beckman Coulter Ac T Diff analyser (Beckman Coulter Ltd., High Wycombe, UK). The PROC MIXED procedure in the SAS system was used to evaluate associations between FE and liver weight as well as biochemical and haematological parameters. The model included RFI group as a fixed effect, slaughter day as a random effect, and the absolute values of RFI as a weight statement. Additionally for liver weight, final live body weight was incorporated in the model as a covariate.

CHAPTER 3

Results and Discussion

There is some evidence that selection for improved feed efficiency (FE) is associated with leaner carcasses and may alter meat quality (Lefaucheur et al. 2011; Smith et al. 2011; Faure et al. 2013). Nevertheless the relationship between FE and meat quality is not fully elucidated, therefore this thesis aimed to identify genomic regions associated with FE in a commercial pig population, evaluate the consequences of FE on meat quality and investigate the molecular mechanisms contributing to differences in FE as well as understand the functional networks relating FE to meat quality. In order to gain deeper insights of biological processes governing differences in FE and meat quality, three metabolically important tissues, including muscle, adipose and liver were analysed.

3.1 Aim 1

Genome-wide association analysis and functional annotation of positional candidate genes for feed conversion efficiency and growth rate in pigs

In this study, a genome-wide association study (GWAS) was performed to elucidate the genetic architecture of feed conversion efficiency and growth rate in pigs. After quality control, 940 individuals and 48,440 SNPs, mapped to the Sscrofa 10.2 pig genome assembly, remained for the further analysis. In total 132 and 71 SNPs reached the threshold of suggestive significance (-log10[p-value] $\geq$ 4.7) for an association with EBVs FCR and D110, respectively. 25 SNPs mapping to 10 porcine autosomes and 12 SNPs mapping to 7 porcine autosomes crossed the Bonferroni-adjusted genome-wide significance threshold (-log10[p-value] $\geq$ 6) for an association with EBVs FCR and D110, respectively. Most of the identified quantitative trait loci (QTLs) are novel, although some of them were located not far from previously reported QTLs. Specifically, a QTL located at 78.3 to 80.5 Mb on SSC 6 coincided with a QTL for FCR in a European Wild Boar x Meishan cross mapped in the region of 127.3 cM (64.9 to 89 Mb, PigQTLdb) (Yue et al. 2003). Additionally this QTL overlapped with a QTL for body weight detected at 78.3 to 78.7 Mb in Iberian x Landrace and Iberian x Meishan crosses (Muñoz et al. 2009). This QTL has thus been independently discovered in different populations, which supports attributing it to biologically relevant common genetic variation (Becker et al. 2013). QTL located at 86.7 to 89.1 Mb on SSC 4 found in this study was in a close proximity to QTL for FCR in a European Wild Boar x Pietrain cross (Cepica et al. 2003) at 75 cM (89.5 to 98.2 Mb, PigQTLdb). Another QTL on SSC 4 was detected at 20 cM (7.2 to 12.6 Mb, PigQTLdb) in a three-generation full-sib population, created by crossing Pietrain sires with Large White x Landrace x Leicoma dam

line (Duthie et al. 2008), which is very distant from the QTL identified in this study. These QTLs were detected by linkage analysis and therefore were mapped with very low resolution and cover large intervals. A GWAS in a Danish Duroc population identified QTL for FCR located on SSC 4 at 63.8 to 64 Mb (Sahana et al. 2013). Another GWAS revealed QTL for FCR on SSC 4 at 4 to 5 Mb in a Duroc terminal sire population (Jiao et al. 2014). The very small number of overlapping QTL regions is in accordance with Gregersen et al. (Gregersen et al. 2012) who reported limited overlap of QTL for a particular trait between breeds. This might suggest that different QTLs regulate feed efficiency traits in the Maxgro boars compared to other breeds (de Oliveira et al. 2014).

A total of 86 and 16 genes mapped within 1Mb upstream and downstream of significant markers for EBV FCR and D110, respectively, were uploaded into Ingenuity Pathways Analysis. Functional annotation revealed 'organismal development' and 'organ morphology', 'lymphoid tissue and 'haematological system development' and 'immune cell trafficking' to be significantly enriched among the genes located in QTL regions for EBV FCR. Furthermore, statistically associated biological functions with the positional candidate genes for EBV D110 were 'energy and lipid metabolism', 'endocrine system development', and 'small molecule biochemistry'. Four SNPs located near the QTLs for EBV FCR (rs80900450, rs319738340, rs340456509 and a novel SNP) in protein kinase, DNA-activated, catalytic polypeptide *(PRKDC*), selectin L (*SELL*), nuclear receptor subfamily 2 group E member 1 (*NR2E1*) and opioid receptor delta 1 (*OPRD1*) respectively and two SNPs mapped close to the QTL for EBV D110 (rs332368013 and rs81508945) in methyl-CpG binding domain protein 5 (*MBD5*) and aldo-keto reductase family 1 member C3 (*AKR1C3*) respectively were confirmed to be polymorphic in target populations by sequencing. Subsequently, these SNPs were genotyped in 436 Maxgro boars. *OPRD1* was not tested for association with EBVs due to its minor allele frequency being less than 5 percent. SNP in *MBD5* significantly departured from HWE ($P < 0.05$) and for this reason was also excluded from further analysis. SNP rs80900450 and rs319738340 in *PRKDC* and *SELL* respectively, were confirmed to be significantly associated with EBV for FCR. PRKDC is involved in the signalling pathway responsible for the formation of fat from carbohydrates in the liver and its deficiency has been shown to impair lipogenesis (Wong et al. 2009). SELL plays a role in lymphocyte trafficking to lymph nodes and Peyer's patches, as well as targeting lymphocytes and neutrophils to an inflammation source (Raffler et al. 2005). Moreover, rs340456509 SNP in the *NR1E2* was significantly associated with breeding values for FCR and D110. A previous

study showed a reduced volume of olfactory bulb in NR2E1 knockout mice (Raffler et al. 2005). Olfactory bulb plays an important part in regulating feed intake as it is targeted by signals responsible for the regulation of energy balance (Aime et al. 2014).

In this part of the study, a number of chromosomal regions significantly associated with feed conversion efficiency and growth rate were demonstrated in the examined terminal pig sire line. Also, by validation of putative candidate genes from GWAS mapping near the significant SNPs, a number of genes significantly associated with feed conversion efficiency were confirmed. Feed efficiency is a highly complex trait affected by a number of factors and this study suggests that the genetic predisposition to greater efficiency traits is associated with lipogenesis, olfactory reception, and also immunological status.

3.2 Aim 2

Analysis of meat quality traits and gene expression profiling of pigs divergent in residual feed intake

Here, gene expression profiling of muscle from FE-divergent pigs using microarray technology was performed to elucidate mechanistic insights on the biological events governing differences in FE that have consequences for eating quality. First, various meat and carcass quality parameters were measured. High-FE pigs were associated with leaner carcasses ($P < 0.05$), greater muscle content ($P < 0.05$) with lower intramuscular fat (IMF; $P < 0.05$). The pH at 45min *post-mortem* had a tendency toward increased values in the high-FE group ($P = 0.055$), however pH at 3h and 24h *post-mortem* did not differ between the two groups. Moreover meat from high-FE pigs tended to have increased cook loss at day 1 *post-mortem* ($P = 0.053$) but there was no difference detected at day 7 *post-mortem*. Muscle from high-FE pigs was significantly associated with increased Warner Bratzler shear force values (WBSF; less tender) at day 1 *post-mortem* ($P < 0.01$) and had a tendency towards increased WBSF scores at day 7 *post-mortem* ($P = 0.057$). Significant difference in tenderness between the FE groups was also detected by sensory panellists who scored the high-FE meat (day 7 *post-mortem*) as less tender ($P < 0.05$). Pork sensory assessment also revealed that meat produced from high-FE pigs had higher scores for stringy and chewy texture ($P < 0.05$). Additionally, meat from high-FE pigs was found less crumbly in texture ($P < 0.05$), less sweet ($P < 0.001$) and more sour ($P < 0.05$). From a nutritional point of view, meat from high-FE group contained significantly lower amounts of saturated fatty acids

(SFA) such as myristic, palmitic and stearic ($P < 0.05$) and monounsaturated fatty acids (MUFA) including palmitoleic, oleic ($P < 0.05$) and eicosenoic ($P < 0.1$). The IMF from high-FE group had significantly higher amounts of polyunsaturated fatty acid (PUFA) such as linoleic ($P < 0.001$) and alpha-linolenic ($P < 0.05$), and lower level of palmitic acid ($P < 0.01$) belonging to a SFA family.

Gene expression profiling revealed a total of 30,992 probe-sets to remain after filtering and 1,035 probes differentially expressed ($P \leq 0.05$, $q < 0.75$) between high- and low-FE groups (645 probes were up-regulated and 390 were down-regulated in high-FE pigs). Of the 1,035 probes, 875 were annotated and assigned to 800 genes (481 genes were up-regulated and 319 genes were down-regulated in high- compared to low-FE pigs) and 33 miRNAs (27 miRNAs were up-regulated and 6 miRNAs were down-regulated in high- compared to low-FE pigs). Gene ontology analysis exposed twenty six molecular and cellular functions significantly associated with genes DE in relation to FE ($P < 0.05$). Twenty five over-represented gene networks were generated for differentially expressed genes in relation to FE. The most significant network was represented by functions related to 'molecular transport', 'nucleic acid metabolism' and 'small molecule biochemistry', and contained 32 DE tumor suppressor p53 (TP53)-associated molecules. In agreement with increased muscle depth and decreased IMF content in high-FE pigs, a number of biological processes related to growth. Specifically, 'cell survival' and 'cell differentiation' were significantly activated in high-FE pigs. Other significantly enriched functions related to growth were 'protein synthesis and degradation', suggesting greater muscle protein turnover in high-FE pigs. Our data supports the possibility that high-FE pigs reuse existing proteins and thus conserve energy, which otherwise would be utilised for protein synthesis, directing it towards more efficient muscle growth. Moreover, the interactions depicted in the *TP53* rooted network supports the role of *TP53* as a central hub in mediating the modulation of muscle cell growth and differentiation (Tamir and Bengal 1998; Porrello et al. 2000). The connection of these DE genes to *TP53*, which was over-expressed in high-FE pigs, suggests their importance in lean growth. Furthermore, a number of DE genes were significantly overrepresented in 'adhesion of connective tissue' function with a tendency towards activation in the high-FE pigs. During the process of muscle growth, connective tissue undergoes dynamic remodelling which involves its proteolytic degradation, and the establishment of expanded networks through synthesis of new connective tissue components (Purslow 2014). Accordingly, high-FE pigs which showed signs of increased muscle mass also over-expressed matrix metallopeptidase 2

(*MMP2*) belonging to a family of enzymes associated with connective tissue degradation and remodelling (Woessner 1991; Rodier et al. 1999). Although this pattern might be expected to be associated with more tender meat, increased toughness of high-FE muscle was observed in this study. Collagen type I alpha 1 chain (*COL1A1*), one of the predominant collagen types in the skeletal muscle (McCormick 1994), was up-regulated in high-FE pigs. Over-expression of *COL1A1* was previously associated with increased drip loss (Ponsuksili et al. 2008; McBryan et al. 2010). In the present study, while drip loss did not differ significantly between FE groups, a tendency towards increased cook loss at day 1 *post-mortem* was observed in meat from high-FE pigs. Upon heating, collagen fibrils shrink which consequently leads to fluid loss (Weston et al. 2002). This finding may relate to the stringy/fibrous and chewy texture of meat produced by high-FE pigs. Moreover, 29 DE miRNAs were mapped and predicted to regulate 379 DE genes. Molecular connectivity of DE genes regulated by 11 miRNAs revealed networks related to connective tissue development and function. In accordance with the relation of FE to IMF content, a number of DE genes were significantly enriched in 'adipogenesis pathway' and lipid metabolism functions. Peroxisome proliferator activated receptor gamma (*PPARG*), which is a master regulator of adipogenesis in a variety of tissues (Norris et al. 2003), was over-expressed in muscle of high-FE pigs. A previous study reported that muscle-specific deletion of *PPARG* is associated with enhanced adiposity in mice (Norris et al. 2003), which could explain the muscle of high-FE pigs exhibiting reduced IMF content while enhanced *PPARG* expression. Previous studies reported reduced mitochondrial energy metabolism in the *Longissimus* muscle of high- versus low-FE pigs (Le Naou et al. 2012; Jing et al. 2015; Fu et al. 2017). In this study, functional annotation revealed 'oxidation of fatty acids' significantly over-represented amongst DE genes with the direction towards inhibition in high-FE pigs, which suggests that the high-FE pigs might exhibit reduced mitochondrial energy metabolism. Similarly, enrichment of DE genes in lipid catabolic processes was previously reported in FE divergent pigs (Jing et al. 2015). Moreover, succinate dehydrogenase complex iron sulphur subunit B (*SDHB*), involved in complex II of the mitochondrial electron transport chain (Liu et al. 2015), and transcription factor A mitochondrial (*TFAM*), a key modulator of mitochondrial DNA replication and transcription (Zou et al. 2016), were down-regulated in high-FE pigs.

This part of the project identified a number of differentially expressed genes significantly over-represented with functions in muscle growth and development, lipid metabolism and

connective tissue metabolism. Up-regulation of genes involved in the synthesis and degradation of protein suggest a greater muscle protein turnover in low-RFI pigs, while the divergence in adhesion of connective tissue may contribute to differences in tenderness. Moreover, a tendency towards suppression of fatty acid oxidation and down-regulation of *SDHB* and *TFAM* could possibly contribute to reduced mitochondrial activity in low-RFI muscle.

RNA-seq of muscle from pigs divergent in feed efficiency and product quality identifies differences in immune response, growth, and macronutrient and connective tissue metabolism

This study utilised next-generation sequencing (NGS) technology to profile the transcriptomes of FE-divergent pigs to provide clues with regards to biological mechanisms driving FE and associated with the relationship between FE and observed alteration in product quality traits. First, various meat and carcass quality parameters were examined. IMF content significantly differed between the FE groups ($P < 0.05$), with the high-FE carcasses having leaner muscle (1.49% IMF) comparing to low-FE carcasses (1.89% IMF). Muscle depth and percent lean meat did not differ significantly between the FE groups however pH at 45min *post-mortem* showed a tendency toward decreased values in the high-FE pigs ($P < 0.1$) while pH measured at 2h, 3h, 4h, 5h and 24h *post-mortem* was significantly lower in the high-FE group ($P < 0.05$). Drip loss did not vary between the FE groups. Muscle from high-FE pigs had increased cook loss at day 1 *post-mortem* ($P < 0.01$) but there was no difference detected at day 7 *post-mortem*. Although meat produced by high-FE pigs was significantly associated with increased WBSF values (less tender) at day 1 *post-mortem* ($P < 0.05$) and had a tendency towards increased WBSF values at day 7 *post-mortem* ($P < 0.1$), this difference in tenderness between the FE groups was not detected by sensory panellists. However, pork sensory assessment revealed that meat produced from high-FE pigs had higher scores for salty taste ($P < 0.05$) and a tendency towards increased barny flavour ($P < 0.1$). SFA did not differ significantly in LTL muscle of FE-divergent pigs, however, a tendency towards decreased proportions for each of palmitic and stearic acids in high-FE muscle was observed ($P < 0.1$). Muscle from high-FE group contained significantly lower amounts of the MUFA, palmitoleic acid ($P < 0.05$) and had a tendency towards decreased proportions of eicosenoic and oleic acids ($P < 0.1$). While PUFA content of muscle did not differ, when comparing the IMF *per se*, high-FE muscle had significantly greater concentrations of linoleic and alpha-linolenic acids ($P < 0.05$).

RNA sequencing resulted in an average of 104.4 million high quality paired-end reads per sample mapped to the reference with a mean of 80.9% mapping efficiency. A total of 14,497 genes were expressed in the muscle and of these 272 annotated genes were differentially expressed between high- and low-FE samples with a $P < 0.01$ corresponding to false discovery rate (q) ≤ 0.47. Of these annotated genes, 176 were up- and 96 were down-regulated in high- versus low-FE pigs. Enrichment analysis of the DE genes was utilised to investigate biological processes and pathways altered in response to differences in FE. Thirty nine biological functions and forty six canonical pathways were significantly ($P < 0.01$) enriched with DE genes. Analysis of molecule connectivity revealed nineteen networks enriched with DE genes. A number of biological processes related to immune response as being relevant to FE in porcine muscle and suggested more efficient conserving of resources by high-FE pigs through availing to a greater extent of adaptive rather than innate immunity, which may reduce feed requirements. pH evolution in the pre-rigor period was highly divergent in relation to FE status and this is consistent with previous studies demonstrating greater glycolytic potential in high-FE pigs (Lefaucheur et al. 2011; Faure et al. 2013). Genes involved in glycolysis and energy metabolism were previously reported to be up-regulated in chickens exhibiting lower ultimate pH (Beauclercq et al. 2017). Here, pH evolution was significantly different in the FE-divergent muscle, and trehalase (*TREH*) that codes for an enzyme catalysing the conversion of trehalose to glucose (Sode et al. 2001) was the most up-regulated gene in high-FE pigs. This might indicate that this group of pigs could potentially exhibit more efficient energy conversion in growth, but with potential consequences for *post-mortem* energy metabolism and product quality. Indeed, ontology analysis highlighted 'catabolism of oligosaccharides' as being highly relevant to the gene expression changes in divergent FE muscle. These findings suggest that shifts in carbohydrate conversion into glucose in FE-divergent muscle may underpin the altered evolution of pH profile in meat from the divergent groups. Syndecan-4 (*SDC4*), which was the most down-regulated gene in high-FE muscle, encodes plasma membrane proteoglycans and has been previously shown to have an impact on muscle cell proliferation and differentiation (Velleman et al. 2007). Knock down of *SDC4* has been associated with increased myogenic regulatory transcription factor (Shin et al. 2012) and myogenin expressions, as well as increased muscle differentiation (Ronning et al. 2015), which signify its importance to muscle growth. Integrating functional annotations of DE genes revealed a number of biological processes related to growth. Moreover, annotations related to amino acid and protein metabolism were significantly enriched amongst DE genes. Pathway analysis highlighted several functions related to connective tissue for example, 'apoptosis of fibroblast cell lines',

which was significantly inhibited in high-FE pigs. Fibroblasts are the key players in the synthesis of extracellular matrix components such as collagen (Russell et al. 1981; Scherzer et al. 2015). Amongst down-regulated transcripts in muscle of high-FE pigs were nuclear factor of activated T-cells 1 (*NFATC1*), nuclear factor of activated T-cells 2 (*NFATC2*) and transcription factor P64 (*MYC*) that have previously been shown to induce apoptosis in fibroblasts (Evan et al. 1992; Neal and Clipstone 2003; Robbs et al. 2008). Besides connective tissue, tenderness of meat is vastly influenced by greater calpastatin activity through decreased *post-mortem* protein degradation (Smith et al. 2011). In the present study, calpastatin (*CAST*) was down-regulated in high-FE pigs suggesting an enhancing effect on tenderness, which is in contrast to our observation that tenderness was impaired in high-FE pigs. Nevertheless, the altered tenderness of FE-divergent meat could be partially impacted by shifts in collagen turnover resulted from decreased degradation of fibroblasts. Biological functions important in metabolism of lipids were also affected by FE, specifically, 'concentration of lipids, cholesterol and triacylglycerol' and 'fatty acid metabolism'. In addition, the second most significant network (network 2) contained several features related to 'lipid metabolism', 'molecular transport' and 'protein synthesis'. In this network, triacylglycerol lipase (*LIPC)* encoding an enzyme catalysing hydrolysis of phospholipids and triacylglycerols (Chatterjee and Sparks 2011) was over-expressed in high-FE muscle suggesting enhanced lipid degradation in this group of pigs.

In this part of the study, a number of biological events related to immune response, growth, carbohydrate and lipid metabolism, and connective tissue were elucidated indicating that these might be important mechanisms governing differences in FE. Enhanced activity of adaptive immunity in high-FE pigs suggests more efficient conserving of resources. Shifts in carbohydrate conversion into glucose in FE-divergent muscle may underpin the divergent evolution of pH profile in meat from the FE-groups and altered amino acid metabolism may influence growth in FE-divergent muscle. Furthermore, decreased degradation of fibroblasts in FE-divergent muscle could impact on collagen turnover and alter tenderness of meat, whilst enhanced lipid degradation in high-FE pigs may potentially underlie a more efficient fat metabolism in these animals.

3.3 Aim 3

RNA-seq of adipose from pigs divergent in feed efficiency reveals alteration in adipose growth, lipid metabolism, extracellular matrix and immune response

Our prior study (Horodyska et al. in review) demonstrated that high-FE pigs exhibit reduced muscle adiposity, however muscle and subcutaneous fat tissue depth remained unaffected by FE. In this study the transcriptome of subcutaneous adipose tissue was examined, using NGS technology, to identify biological processes contributing to differences in FE and explore the functional networks driving the relationship between muscle adiposity and FE. Upon sequencing and data processing of the RNA libraries from subcutaneous adipose tissue of FE-divergent pigs, high quality reads were mapped with 87.5% efficiency to the reference yielding an average of 105.5 million paired-end reads per sample. Assigning of read counts to gene features revealed a total of 15,477 genes to be expressed in adipose tissue. Based on a significance threshold of $P < 0.01$ (corresponding to a false discovery rate of $q \leq 0.64$), 209 (111 up- and 98 down-regulated) annotated genes were found to be affected by FE. Gene ontology analysis revealed forty biological functions and nine canonical signalling pathways were significantly ($P < 0.01$) associated with DE genes in relation to FE. Sixteen networks were inferred by integration of genes affected by FE, whereby the most significant network (network 1) comprised twenty four DE genes involved in cell death and survival, and embryonic development. Of these annotations, several categories related to adipose tissue growth, whereby 'quantity of connective tissue' was significantly inhibited and 'stimulation of connective tissue' tended towards suppression in high-FE pigs. Furthermore, 'movement of endothelial cells' and 'quantity of blood vessels' categories were repressed in high-FE pigs. Growth of adipose tissue is angiogenesis dependent and inhibition of vascular growth has been previously shown to prevent adipose tissue expansion (Rupnick et al. 2002). Here, an important regulator of angiogenesis in adipose tissue (Ledoux et al. 2008), vascular endothelial growth factor A (*VEGFA*), was down-regulated in high-FE pigs. Prediction of potential upstream regulators identified CCAAT/enhancer binding protein alpha (CEBPA), nuclear factor, erythroid 2 like 2 (NFE2L2) and epidermal growth factor (EGF) to control expression of 11, 5 and 10 DE genes, respectively, in the direction consistent with the activation state of the particular regulator. CEBPA, together with peroxisome proliferators activated receptor gamma (PPARG), is a master regulator of adipogenesis (Prokesch et al. 2009). *NFE2L2* encodes a transcription factor which is activated during oxidative stress and

induces transcription of protective genes (von Otter et al. 2014), while EGF has previously been linked to proliferation and differentiation of adipose-derived stem cells (Hebert et al. 2009) and obesity (Kurachi et al. 1993). In the present study this growth factor, along with CEBPA and NFE2L2, was predicted to be inhibited in adipose tissue of high-FE pigs. mRNAs coding for these transcription regulators were not significantly differentially expressed between the FE-divergent groups *per se*, albeit abundance of transcripts encoding these factors is not expected to affect their activity (Filtz et al. 2014). Analysis of molecule connectivity revealed a network 2 enriched with functions related to 'connective tissue development and function'. The most up-regulated gene in high-FE pigs, collagen type XI alpha 2 chain (*COL11A2*) coding for extracellular minor fibrillar collagen (Fang et al. 2010) was represented in this network. Collagen is a predominant structural element of interstitial extracellular matrix (Frantz et al. 2010), which provides mechanical support to the cellular constituents (Neve et al. 2014). Extracellular matrix has also been proven to play a part in regulation of angiogenesis (Neve et al. 2014). Formation of a dense extracellular matrix may suppress adipogenesis through inhibiting capillary formation (Bouloumie et al. 2002). 'Synthesis of fatty acids and lipids' were significantly enriched with DE genes tending towards inhibition in high-FE pigs. Differential expression of genes involved in cholesterol metabolism in the adipose tissue of high-FE animals suggest increased mobilisation of fat depots for hepatic metabolism and utilisation of fat resources (Reyer et al. 2017). 'High mobility group box 1 (HMGB1) signalling' and 'p38 mitogen-activated protein kinase (p38MAPK) signalling' were pathways significantly affected by FE. p38MAPK and HMGB1 are involved in the immune response through synthesis of pro-inflammatory cytokines (Yang et al. 2005; Cuenda and Rousseau 2007; Lee et al. 2014). A previous study postulated that production of HMGB1 in adipose tissue is triggered by inflammatory signals associated with obesity (Gunasekaran et al. 2013). Accordingly 'complement system', which is a major constituent of the innate immunity (Rus et al. 2005), was inferred from ontology analysis. Furthermore 'proliferation of immune cells', 'chemotaxis of phagocytes' and 'phagocytosis' were significantly inhibited in high-FE adipose tissue, and 'prostaglandin synthesis' had a tendency towards suppression in high-FE pigs. Cytokines and prostaglandins are inflammatory molecules that are synthesized and secreted by macrophages upon tissue exposure to inflammatory stimuli (Arango-Duque and Descoteaux 2014). Studies carried out on obese mice and humans reported a strong positive correlation between adipocyte size and accumulation of pro-inflammatory macrophages in adipose tissue (Cinti et al. 2005; Ortega

Martinez de Victoria et al. 2009). In addition, cytokines communicate with skeletal muscle, liver and brain and regulate appetite and lipid and glucose metabolism (Guerre-Millo 2002).

This part of the project identified a number of candidate biological functions and pathways affiliated with adipose tissue growth, extracellular matrix formation, lipid metabolism and immune response. Establishment of a dense extracellular matrix and inhibition of capillary formation may be one underlying mechanism to achieve suppressed adipogenesis. Moreover, mechanisms ensuring an efficient utilisation of lipids in high-FE pigs might be orchestrated by upstream regulators including CEBPA, NFE2L2 and EGF. Consequently, high-FE adipose tissue could exhibit more efficient cholesterol disposal, whilst inhibition of inflammatory and immune response in high-FE pigs may be an indicator of an optimally functioning adipose tissue.

RNA-seq of liver from pigs divergent in feed efficiency highlights shifts in macronutrient metabolism, hepatic growth and immune response

In this study the hepatic transcriptome of pigs divergent in FE was investigated to illuminate the physiology of FE, which corroborate with the recorded biochemical and haematological parameters. RNA sequencing resulted in mapping of 89.2% of sequences to the reference with an average of 105.6 million high quality paired-end reads per sample being assigned to 14,910 genes expressed in liver. A total of 922 genes were differentially expressed with a $P < 0.01$ corresponding to false discovery rate (q) ≤ 0.16, and of these 818 (464 up- and 354 down-regulated) were annotated. Forty-two biological functions were significantly enriched ($P < 0.01$) amongst the DE genes in relation to FE, as inferred from functional enrichment analysis. Twenty five networks were obtained upon integration of all DE genes. The most significant network (network 1) contained functions related to gastrointestinal and hepatic system disease and liver cirrhosis. Carbohydrate and lipid metabolism, and small molecule biochemistry were represented in network 12. Enrichment of DE genes in this network suggests increased reverse cholesterol transport in high-FE livers. Indeed, serum analysis pointed towards enhanced cholesterol level in high-FE pigs. A previous study has also shown reverse cholesterol transport to be over-expressed in the livers of high-FE pigs (Gondret et al. 2017). 'Fibroblast growth factor (FGF) signalling', which is involved in bile acid metabolism (Ornitz and Itoh 2015), was predicted to be activated in high-FE livers. In this pathway, fibroblast growth factor receptor substrate 2 (*FRS2*) was up-regulated in high-FE pigs. FRS2α

deficiency led to increased bile acid synthesis in mouse liver (Wang et al. 2014) therefore it seems probable that high-FE pigs experience decreased bile acid production. Besides its well established functions, bile acids are also involved in lowering glucose levels (Staels and Fonseca 2009) and hindering gluconeogenesis (Chai et al. 2015). Differential expression of cholesterol-related genes in the livers divergent for FE points towards increased absorption of dietary cholesterol and reverse cholesterol transport in high-FE pigs, thus the inferred reduction in bile acid synthesis may be a measure to prevent drops in serum glucose level rather than explained by high density lipoprotein (HDL) cholesterol shortage. This presumption is in accordance with observed greater glucose in serum of high-FE pigs. Enhancement of serum in total protein level observed in high-FE pigs reflects a suggested activation of 'protein catabolism and secretion' in the high-FE livers inferred from the functional enrichment analysis. Over-expression of genes involved in protein synthesis and degradation has elsewhere been reported in livers of high-FE pigs (Gondret et al. 2017). In the prior report it was suggested that high-FE muscle exhibits increased protein turnover and potentially reuses existing proteins, while directing the conserved energy towards more efficient growth (Horodyska et al. 2018). This phenomenon could also be occurring in the livers of high-FE pigs. 'Hepatocyte growth factor (HGF) signalling', 'epidermal growth factor (EGF) signalling' and 'FGF signalling' were significantly activated pathways in high-FE pigs. Previous studies revealed a role of growth factors, e.g. HGF, EGF and FGF, in stimulating proliferation and differentiation of hepatic oval cells (Hu et al. 1993; Jones et al. 2009; Sanchez and Fabregat 2010) and also in liver regeneration (Jiang et al. 1993; Steiling et al. 2003; Zimmers et al. 2017). Accordingly, 'differentiation of epithelial cells' was activated whilst 'senescence of cells', characterised by cell cycle arrest leading to loss of its ability to divide (Hoare et al. 2010), was suppressed in high-FE pigs. In the present study liver weights did not significantly differ between the FE groups, although a prior report demonstrated significantly increased liver weights of high-FE pigs (Reyer et al. 2017). Cyclin T2 (*CCNT2*), coding for a protein regulating cell differentiation through activation of cyclin-dependent kinase 9 (CDK9) (Simone et al. 2002; Garriga et al. 2003), was the most down-regulated gene in high-FE pigs. CDK9 also functions in the inflammatory response (Han et al. 2014). Here, *CDK9* was down-regulated in high-FE pigs at a $P < 0.05$. It is possible that suppression of *CCNT2* could influence CDK9 function in differentiation of monocytes (De Falco et al. 2005) rather than hepatic epithelial cells. Gene ontology analysis also suggested that livers of more efficient pigs may be characterised by more prompt and effective hepatic response to inflammatory stimuli. Specifically, 'role of nuclear factor of activated T cells (NFAT) in

regulation of the immune response' was significantly activated in high-FE pigs. NFAT proteins play a role in the first line of defence through regulating innate leukocytes response to inflammatory stimuli (Zanoni and Granucci 2012). Furthermore, 'quantity of invariant natural killer T-cells' and 'cell viability of natural killer cells' were also significantly activated in high-FE pigs. Consistent with this, haematological analysis demonstrated higher percentage of lymphocytes in the high-FE group. Several studies have reported a diverse hepatic inflammatory response in high- versus low-FE pigs (Gondret et al. 2017) and cattle (Alexandre et al. 2015; Paradis et al. 2015), supporting this connection. Moreover, it has been postulated that high-FE animals exhibit more efficient immune response to fight off inflammation, which in turn translates to more energy for growth and muscle deposition (Paradis et al. 2015; Horodyska et al. in review).

In this part of the study a number of biological mechanisms governing differences in FE were identified. In particular, improved hepatic absorption of carbohydrates and cholesterol as well as enhanced reverse cholesterol transport were inferred in high-FE pigs. The suggested decrease in bile acid synthesis in high-FE pigs may contribute to the increased concentrations of serum glucose observed. Moreover, enhanced quantity of invariant natural killer T-cells and viability of natural killer cells could induce a faster and more effective hepatic response to inflammatory stimuli.

CHAPTER 4

Synthesis and Implications

Synthesis and Implications

In this project, a number of high-throughput platforms including SNP chip, microarray and next-generation sequencing were availed of with the aim to identify genomic regions associated with feed efficiency and detect genes of which expression is affected by divergence in feed efficiency. Validation of these platforms was performed through quantitative real-time PCR, which confirmed reliability of all three technologies. Although a high level of correlation between microarray and RNA-seq platforms have been reported (Nazarov et al. 2017), RNA-seq technology presents some advantages over microarrays, for example, it does not require transcript-specific probes and therefore RNA-seq does not encounter issues associated with cross hybridisation and non-specific hybridisation (Zhao et al. 2014). Nevertheless, shorter and less abundant transcripts have a higher possibility to be detected using microarray approach (Nazarov et al. 2017). Therefore in these cases and particularly in quantifying microRNA, microarray might outperform RNA sequencing (Git et al. 2010; Nazarov et al. 2017). On the other note, a number of genes / mRNA isoforms are not incorporated on microarrays (Bumgarner 2013).

In summary this study identified a number of chromosomal regions significantly associated with feed efficiency. Ontology analysis of FE-divergent muscle predicted differences in fat metabolism and immune defence. Shifts in carbohydrate conversion into glucose in FE-divergent muscle may underpin observed changes in *post-mortem* muscle pH between FE groups, whilst differences in amino acid metabolism may influence growth in FE-divergent muscle. Moreover, decreased degradation of fibroblasts may alter tenderness of meat. Furthermore, establishment of a dense extracellular matrix and inhibition of capillary formation in high-FE adipose tissue may be underlying mechanisms to achieve suppressed adipogenesis and increased utilisation of fatty acids by other tissues. Over-expression of cholesterol-related genes suggests more efficient cholesterol disposal from high-FE adipose tissue. The liver of high-FE pigs may exhibit improved carbohydrate absorption, enhanced reverse cholesterol transport and higher protein turnover, as well as increased epithelial cell differentiation and a more effective inflammatory response.

In the first muscle transcriptome analysis using a microarray platform, small differences in gene expression between FE groups were observed. These limited differences could be explained by a relatively low number of pigs from which a subset of pigs was selected for the

study. For this very reason, transcripts with a $P \leq 0.05$ were considered significantly differentially expressed. Samples from the second batch of animals analysed through next-generation sequencing (NGS) were selected from a much larger group of FE-divergent pigs, which resulted in greater differences in gene expression at a more stringent *P*-value (< 0.01). In this section for the purpose to elucidate the overlapping differentially expressed (DE) genes and biological themes in FE-divergent muscle between microarray and NGS technology, a $P < 0.05$ was used for both datasets. Subsequently, the comparison analysis revealed 54 DE genes and a number of biological processes (Table 4.1) shared between the two platforms.

Furthermore, common DE genes ($P < 0.01$) (Figure 4.1) and biological processes between muscle, adipose and liver of pigs divergent in FE (Table 4.2) were identified. *PON3* was the only common DE gene between the three tissues. *PON3* codes for an enzyme that associates with high density lipoproteins (Getz and Reardon 2004). Increased adipose deposition observed in PON3 knockout mice (Shih et al. 2015) is consistent with a potential role of PON3 in promoting lean growth and this is in keeping with decreased intramuscular fat content in the high-FE pigs shown in this thesis. Eight DE genes were identified to be shared between muscle and adipose tissue. Trehalase (*TREH*), coding for an enzyme catalysing the conversion of trehalose to glucose (Sode et al. 2001) was among these genes. Moreover, twenty eight DE gene overlapped between liver and adipose tissue. Amongst these genes was selectin L (*SELL*). SELL is involved in leukocyte adhesion to blood vessels during inflammatory and immunological response (Nelson et al. 1992). Interestingly, a single nucleotide polymorphism in the *SELL* gene was identified as a positional and functional candidate gene for FE through the genome-wide association study. Fourteen DE genes were common between muscle and liver, including pyruvate dehydrogenase kinase 4 (*PDK4*), which is an important regulator of lactate and energy production (Liu et al. 2017). A number of common biological processes between the three tissues were elucidated; for example protein and lipid metabolism, cellular growth and proliferation, tissue and cardiovascular system development, immune cell trafficking, lymphoid tissue structure, and organ morphology. Many of these processes were also inferred from the functional annotation of positional candidate genes in the GWAS study, with *SELL* being significantly enriched in a number of these themes.

Table 4.1 Common biological processes, significantly enriched with differentially expressed genes in muscle from pigs divergent in feed efficiency, identified through next-generation sequencing and microarray technology.

Molecular and cellular function	Physiological system development and function
Cellular movement and development**	Haematological system development and function**
Carbohydrate metabolism**	Immune cell trafficking***
Cellular growth and proliferation**	Lymphoid tissue structure and development**
Cell-to-cell signalling and interaction**	Tissue morphology**
Cell death and survival**	Organismal development**
Protein synthesis**	Humoral immune response**
Free radical scavenging***	Haematopoiesis***
Lipid metabolism**	Tissue development**
Small molecule biochemistry**	Organ development**
Cellular compromise**	Skeletal and muscular system development and function**
Molecular transport**	Organ morphology**
Post-translational modification**	Connective tissue development and function**
Cell morphology**	Cardiovascular system development and function**
Cellular assembly and organization**	Cell-mediated immune response***
Cell cycle**	
Gene expression**	

**$P < 0.01$, ***$P < 0.001$; data was analysed in IPA, Ingenuity® Systems, http://ingenuity.com.

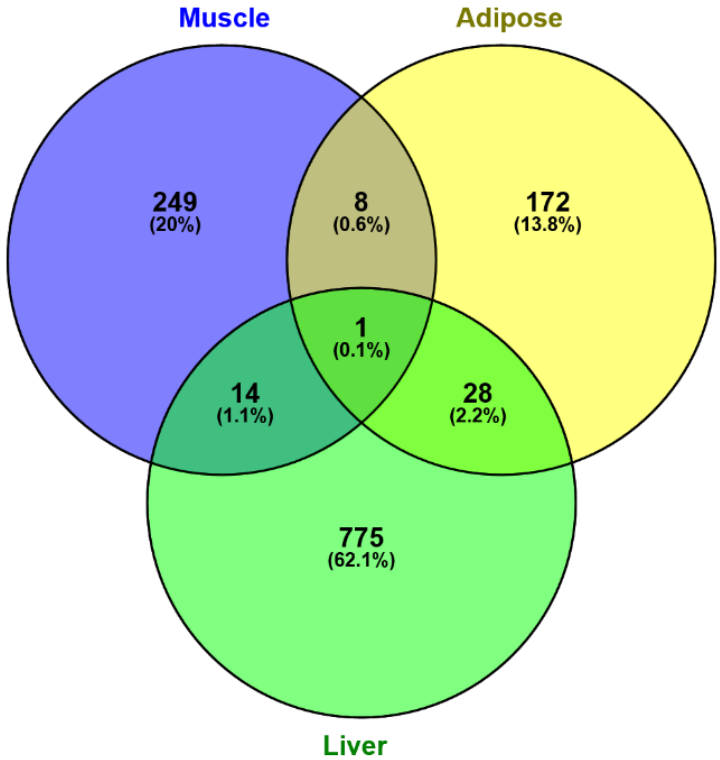

Figure 4.1 Venn diagram illustrating numbers of overlapping differentially expressed genes ($P < 0.01$), identified through next-generation sequencing, between three tissues from pigs divergent in feed efficiency. Diagram was constructed using VENNY tool, (http://bioinfogp.cnb.csic.es/tools/venny/).

Table 4.2 Biological processes significantly enriched with differentially expressed genes, identified through next-generation sequencing, overlapped between muscle, adipose and liver tissues from pigs divergent in feed efficiency.

Molecular and cellular function	Physiological system development and function
Gene expression***	Cardiovascular system development and function**
Cellular movement and development**	Tissue development**
Cellular growth and proliferation**	Haematological system development and function**
Cell cycle**	Lymphoid tissue structure and development**
Cell death and survival**	Organ development**
Molecular transport**	Organ morphology**
Small molecule biochemistry**	Nervous system development and function**
Cell morphology**	Haematopoiesis**
Cell-to-cell signalling and interaction**	Immune cell trafficking**
Protein synthesis***	
Cellular assembly and organization**	
Lipid metabolism**	

**$P < 0.01$, ***$P < 0.001$; data was analysed in IPA, Ingenuity® Systems, http://ingenuity.com.

Previous studies utilised animals selected in divergent lines for multiple generations (Lefaucheur et al. 2011; Smith et al. 2011; Faure et al. 2013; Vincent et al. 2015; Gondret et al. 2017). The experimental model used in this project involved animals selected within the same family. As a result of using animals from the same family, the genetic variability, and transcriptomic response is unlikely to be driven by genetic divergence and drift. However, functional annotation of DE genes revealed commonalities in processes among over-expressed genes with previous studies. In muscle, overlapping processes related to growth, such as protein synthesis and degradation (Vincent et al. 2015; Zhao et al. 2016; Gondret et al. 2017) and skeletal muscle differentiation and proliferation (Jing et al. 2015). Surprisingly, Gondret et al. (2017) also reported suppression of skeletal muscle development in high-FE pigs. Differential expression of genes involved in muscle lipid metabolism (Jing et al. 2015; Gondret et al. 2017) was a further commonality between the studies. Functional annotation of DE genes in FE-divergent muscle, such as that of Jing et al. (2015) and Vincent et al. (2015) revealed under-expression of genes involved in mitochondrial energy metabolism, which relates to greater proportion of glycolytic fibres. Lefaucheur et al. (2010) observed differences in fibre type and a switch away from oxidative metabolism in high-FE muscle. However here, and in the paper of Smith et al. (2011), which also selected for divergence in FE over a number of generations, some evidence for the switch from oxidative to glycolytic metabolism, such as inferred over-representation of DE genes in lipid oxidation and oligosaccharide catabolism processes, but no evidence for difference in fibre type between

FE conditions were detected. For this reason, it is likely that a variety of mechanisms can contribute to differing FE status depending on the experimental model. To gain deeper insights into biological processes that underpin observed differences in FE, other metabolic organs such as adipose and liver were analysed. Lipid and fatty acid metabolism, cellular homeostasis and immune response were the common processes altered in adipose tissue identified here and in previous studies (Lkhagvadorj et al. 2010; Gondret et al. 2017). Moreover, common biological processes observed to be differentially regulated in livers from FE-divergent pigs included cell proliferation, protein synthesis and catabolism, lipid and carbohydrate metabolism, reverse cholesterol transport, and immune response (Zhao et al. 2016; Gondret et al. 2017; Reyer et al. 2017). It can be inferred that these processes are the main mechanisms contributing to differences in feed efficiency.

Factors other than mRNA abundance, for instance levels of microRNAs regulating translation of mRNAs and thus influencing functions of resulting proteins (Rajewsky 2006), could be relevant to feed efficiency. Taking this matter into consideration, expression levels of microRNAs were measured in this study using microarray platform. Nevertheless this platform contained a limited number of microRNAs. Therefore, evaluating abundance of microRNAs with a specialised microRNA array would further elucidate the events regulating protein levels and functionality. Moreover, identification of proteins affected by feed efficiency through proteomic analysis would be of great benefit. This holistic approach would offer a wider understanding of biological processes illuminating the differences in feed efficiency.

CHAPTER 5

Summary

Summary

In the framework of this thesis a number of chromosomal regions significantly associated with feed efficiency (FE), were identified in a commercial pig line (Maxgro, Hermitage Genetics). Most of the significantly associated regions were described for the first time, although some of them were located not far from previously reported quantitative trait loci. Validation of candidate genes mapping near the significant SNPs, confirmed a number of genes significantly associated with FE suggesting that the genetic predisposition to increased FE is driven by lipogenesis, glucose homeostasis, olfactory reception and also immunological status.

The next aim of this thesis was to evaluate the consequences of FE on pork quality and to investigate the molecular mechanisms contributing to differences in FE as well as to understand the functional networks relating FE to meat quality. Analysis of meat from FE-divergent pigs revealed characteristics generally within the normal range for the production of acceptable quality pork. However, small but significant differences in traits such as sensory profile, texture, and technological aspects such as cook loss suggest there is a minor impairment of meat quality in high-FE pigs. High-FE pigs were also associated with leaner carcasses, greater muscle content and enhanced nutritional value in terms of fatty acid composition. Genome-wide transcriptomics of FE-divergent muscle revealed molecular bio-functions of adaptive immunity and phagocytosis to be enriched, indicating for a resource conservation strategy which enables high-FE pigs to allocate resources for other growth-related biological processes. Shifts in carbohydrate conversion into glucose in FE-divergent muscle may underpin the altered evolution of pH profile in meat from the divergent groups. These transcriptomic findings indicate that altered amino acid metabolism may influence growth in FE-divergent muscle. Moreover, decreased degradation of fibroblasts, the key players in the synthesis of the extracellular matrix, could impact on collagen turnover and alter tenderness of meat. Biological functions important in metabolism of lipids were also affected by FE.

In order to gain deeper insights on the biological processes governing differences in FE and meat quality, besides muscle, other metabolically important tissues, including adipose and liver were analysed. Adipose tissue is a master regulator of systemic lipid storage as well as an active endocrine organ influencing energy homeostasis. Hence this thesis also focused on identifying relevant biological processes in adipose that underpin observed differences in FE.

Adipose growth, extracellular matrix formation, lipid metabolism and inflammatory and immune response were significantly enriched biological processes among the DE genes. Conclusively, the establishment of a dense extracellular matrix and inhibition of capillary formation might suppress adipogenesis and increase the utilisation of fatty acids. Accordingly, lipid metabolism was also affected by FE whereby over-expression of cholesterol-related genes suggests more efficient cholesterol disposal from high-FE adipose tissue. The mechanisms ensuring an efficient utilisation of lipids in high-FE pigs might be orchestrated by upstream regulators including CEBPA, NFE2L2 and EGF. Moreover, inhibition of inflammatory and immune responses in high-FE pigs may be an indicator of an optimally functioning adipose tissue.

Liver influences nutrient partitioning and it is hypothesised to modulate FE, therefore important biological processes that underpin the differences in liver phenotype were analysed between FE groups. Ontology analysis illuminated carbohydrate, lipid and protein metabolism significantly enriched with the differentially expressed genes, confirming the hepatic influence on divergent energy utilization in high- versus low-FE pigs. In particular, high-FE pigs exhibited gene expression patterns suggesting improved hepatic absorption of carbohydrates and cholesterol as well as enhanced reverse cholesterol transport. Furthermore, the inferred decrease in bile acid synthesis in high-FE pigs may contribute to the increased concentration of serum glucose observed. This increased glucose can be delivered to cells and utilised for increased growth. Gene ontology analysis also suggests that the liver of high-FE pigs may be characterised by higher protein turnover and increased epithelial cell differentiation, whilst bio-functions dedicated to natural killer T-cells argue for a faster and more effective hepatic response to inflammatory stimuli.

Overall, the study showed that FE is a highly complex trait affected by a number of genomic regions. Transcriptomic profiling of muscle, adipose and liver tissue from FE-divergent pigs provided mechanistic insights on the biological events prevailing differences in FE, which impacts meat quality. The findings of this thesis will assist the meat industry in optimising the strategies to improving FE without compromising meat quality. These results are also relevant to the biomedical field including metabolic studies.

Zusammenfassung

Im Rahmen dieser Arbeit wurden eine Reihe von chromosomalen Regionen, die signifikant mit der Futterverwertung (FE), assoziiert sind, in einer kommerziellen Schweinelinie (Maxgro, Hermitage Genetics) identifiziert. Die meisten der signifikant assoziierten Regionen wurden zum ersten Mal beschrieben, obwohl einige von ihnen nicht weit von bereits bekannten assoziierten genomischen Regionen entfernt lagen. Die Validierung von positionellen Kandidatengenen bestätigte eine Reihe von FE-assoziierten Genen. Die funktionelle Annotation dieser Gene deutet auf eine genetische Prädisposition zur erhöhten FE hin, die durch biologische Prozesse wie der Lipogenese, Glukosehomöostase, olfaktorische Rezeption und auch den immunologischen Status getrieben wird.

Das nächste Ziel dieser Arbeit war es, die Auswirkungen von FE auf die Schweinefleischqualität zu bewerten und den molekularen Zusammenhang zwischen FE und Fleischqualität zu beleuchten. Die Analyse des Fleisches von FE-divergenten Schweinen ergab Eigenschaften, die im Allgemeinen im normalen Bereich für die Produktion von Schweinefleisch akzeptabler Qualität liegen. Kleine, aber signifikante Unterschiede wie z.B. im sensorischen Profil, der Textur und von technologischen Aspekten wie dem Kochverlust deuten jedoch darauf hin, dass die Fleischqualität bei Schweinen mit hoher FE geringfügig beeinträchtigt ist. Gute Futterverwerter zeigten zudem magerere Schlachtkörper, einem höheren Muskelanteil und eine vorteilhafte Fettsäurezusammensetzung. Die genomweiten Transkriptomanalysen von FE-divergenten Muskeln deuten darauf hin, dass molekulare Biofunktionen der adaptiven Immunität und Phagozytose ausgelenkt sind. Dies impliziert eine Strategie zur Ressourcenschonung, die es Schweinen mit hoher FE ermöglicht, Ressourcen für andere wichtige biologische Prozesse zu nutzen. Verschiebungen bei der Umwandlung von Kohlenhydraten in Glukose im Muskel FE-divergenter Tiere könnten die veränderte Entwicklung des pH-Profils im Fleisch begründen. Die Analysen zeigen weiter, dass ein veränderter Aminosäurenstoffwechsel das Wachstum des Muskels in Tieren mit guter Futterverwertung beeinflussen kann. Darüber hinaus könnte sich ein verminderter Abbau von Fibroblasten, den Hauptakteuren bei der Synthese der extrazellulären Matrix, auf den Kollagenumsatz auswirken und die Zartheit des Fleisches verändern. Biologische Funktionen, die für den Fettstoffwechsel wichtig sind, scheinen ebenfalls mit FE im Zusammenhang zu stehen. Um tiefere Einblicke in die biologischen Prozesse zu gewinnen,

welche die Unterschiede im FE und der Fleischqualität bestimmen, wurden neben dem Muskel auch andere metabolisch wichtige Gewebe wie Fett und Leber analysiert.

Fettgewebe ist ein Hauptregulator der systemischen Lipidspeicherung sowie ein aktives endokrines Organ, das die Energiehomöostase beeinflusst. Daher konzentrierte sich diese Arbeit auch auf die Identifizierung relevanter biologischer Prozesse im Fettgewebe, die die beobachteten Unterschiede in der FE untermauern. Adipogenese, extrazelluläre Matrixbildung, Lipidstoffwechsel sowie Entzündungs- und Immunantwort wurden als signifikant angereicherte biologische Prozesse identifiziert. Die Etablierung einer dichten extrazellulären Matrix und die Hemmung der Kapillarbildung könnten die Adipogenese unterdrücken und die systemische Verfügbarkeit von Fettsäuren erhöhen. Dementsprechend zeigte sich auch der Lipidstoffwechsel durch divergente FE beeinflusst, wobei die Überexpression von cholesterinverwandten Genen auf einen effizienteren Cholesterinexport aus dem Fettgewebe bei Tieren mit hoher FE hindeutet. Die Mechanismen, die eine effiziente Nutzung von Lipiden bei Schweinen mit hoher FE gewährleisten, könnten von vorgeschalteten Regulatoren wie CEBPA, NFE2L2 und EGF koordiniert werden. Darüber hinaus kann die Hemmung von Entzündungs- und Immunreaktionen bei guten Futterverwertern ein Indikator für ein optimal funktionierendes Fettgewebe sein.

Die Leber ist wesentlich an der Nährstoffbereitstellung beteilig. Daher wurden im Rahmen der Dissertation auch die biologischen Prozesse, welche die Unterschiede im Leberphänotyp untermauern, zwischen den FE Gruppen analysiert. Genontologie-Analysen identifizierten den Kohlenhydrat-, Lipid- und Proteinstoffwechsel als signifikant ausgelenkt, was den hepatischen Einfluss auf die divergierende Energieausnutzung bei Schweinen mit hoher und niedriger FE bestätigte. Insbesondere zeigten Schweine mit hoher FE Genexpressionsmuster, die auf eine verbesserte hepatische Absorption von Kohlenhydraten und Cholesterin sowie auf einen verbesserten Rücktransport von Cholesterin hindeuten. Die daraus abgeleitete Abnahme der Gallensäure-Synthese bei Schweinen mit hoher FE ist in Übereinstimmung mit einer erhöhten Konzentration an Serumglukose. Diese erhöhte Glukose kann an die Zellen abgegeben und für ein verstärktes Wachstum genutzt werden. Die Analyse der Genontologie deutet auch darauf hin, dass sich die Leber von Schweinen mit hoher FE durch einen höheren Proteinumsatz und eine erhöhte Differenzierung der Epithelzellen auszeichnet. Die Auslenkung von Genen, welche die Funktion natürlicher Killerzellen beeinflussen, liefert Hinweise darauf, dass eine schnellere und effektivere hepatische Reaktion auf Entzündungsreize induzieren werden könnte.

Insgesamt zeigte die Studie, dass FE ein hochkomplexes Merkmal ist, das von einer Reihe genomischer Regionen beeinflusst wird. Expressionsprofile von Muskel-, Fett- und Lebergewebe FE-divergenter Schweine lieferten mechanistische Erkenntnisse über die biologischen Zusammenhänge zwischen FE und Fleischqualität bzw. Schlachtkörpermerkmalen. Die Ergebnisse dieser Arbeit werden die Tierhaltung und Züchtung dabei unterstützen, Strategien zur Verbesserung der FE zu identifizieren, ohne die Fleischqualität zu beeinträchtigen. Diese Ergebnisse sind auch für den biomedizinischen Bereich einschließlich Stoffwechselstudien relevant.

CHAPTER 6

References

References

Adeyemi KD, Sazili AQ (2014) Efficacy of Carcass Electrical Stimulation in Meat Quality Enhancement: A Review. Asian-Australas J Anim Sci 27:447-456

Adzitey F, Nurul H (2011) Pale soft exudative (PSE) and dark firm dry (DFD) meats: causes and measures to reduce these incidences - a mini review. Int Food Res J 18(1):11-20

Aime P, Palouzier-Paulignan B, Salem R, Al Koborssy D, Garcia S, Duchamp C, Romestaing C, Julliard AK (2014) Modulation of olfactory sensitivity and glucose-sensing by the feeding state in obese Zucker rats. Front Behav Neurosci 8:326

Alexandre PA, Kogelman LJA, Santana MHA, Passarelli D, Pulz LH, Fantinato-Neto P, Silva PL, Leme PR, Strefezzi RF, Coutinho LL, Ferraz JBS, Eler JP, Kadarmideen HN, Fukumasu H (2015) Liver transcriptomic networks reveal main biological processes associated with feed efficiency in beef cattle. BMC Genomics 16:1073

Anders S, Pyl PT, Huber W (2015) HTSeq--a Python framework to work with high-throughput sequencing data. Bioinformatics 31:166-169

Andrés-Bello A, Barreto-Palacios V, García-Segovia P, Mir-Bel J, Martínez-Monzó J (2013) Effect of pH on Color and Texture of Food Products. Food Eng Rev 5:158-170

Arango-Duque G, Descoteaux A (2014) Macrophage cytokines: involvement in immunity and infectious diseases. Front Immunol 5:491

Aslan O, Hamill R, Davey G, McBryan J, Mullen A, Gispert M, Sweeney T (2012) Variation in the IGF2 gene promoter region is associated with intramuscular fat content in porcine skeletal muscle. Mol Biol Rep 39

Bach-Knudsen KE, Hedemann MS, Lærke HN (2012) The role of carbohydrates in intestinal health of pigs. Anim Feed Sci Technol 173:41-53

Barea R, Dubois S, Gilbert H, Sellier P, van Milgen J, Noblet J (2010) Energy utilization in pigs selected for high and low residual feed intake. J Anim Sci 88:2062-2072

Barrett JC, Fry B, Maller J, Daly MJ (2005) Haploview: analysis and visualization of LD and haplotype maps. Bioinformatics 21:263-265

Beauclercq S, Hennequet-Antier C, Praud C, Godet E, Collin A, Tesseraud S, Metayer-Coustard S, Bourin M, Moroldo M, Martins F, Lagarrigue S, Bihan-Duval EL, Berri C (2017) Muscle transcriptome analysis reveals molecular pathways and biomarkers involved in extreme ultimate pH and meat defect occurrence in chicken. Sci Rep 7:6447

Becker D, Wimmers K, Luther H, Hofer A, Leeb T (2013) A genome-wide association study to detect QTL for commercially important traits in Swiss Large White boars. PLoS One 8:e55951

Bendall JR (1973) The biochemistry of rigor mortis and cold-contracture. In: Proc. European Meet. Meat Res. Workers Paris, France, pp 1-27

Bouloumie A, Lolmede K, Sengenes C, Galitzky J, Lafontan M (2002) Angiogenesis in adipose tissue. Ann Endocrinol (Paris) 63:91-95

Bumgarner R (2013) DNA microarrays: Types, Applications and their future. CPMB, Frederick M. Ausubel et al. 0 22:Unit-22.21.

Cannata S, Engle TE, Moeller SJ, Zerby HN, Radunz AE, Green MD, Bass PD, Belk KE (2010) Effect of visual marbling on sensory properties and quality traits of pork loin. Meat Sci 85:428-434

Cepica S, Stratil A, Kopecny M, Blazkova P, Schröffel J, Davoli R, Fontanesi L, Reiner G, Bartenschlager H, Moser G, Geldermann H (2003) Linkage and QTL mapping for Sus scrofa chromosome 4. J Anim Breed Genet 120:28-37

Chai J, Zou L, Li X, Han D, Wang S, Hu S, Guan J (2015) Mechanism of bile acid-regulated glucose and lipid metabolism in duodenal-jejunal bypass. Int J Clin Exp Pathol 8:15778-15785

Chatterjee C, Sparks DL (2011) Hepatic Lipase, High Density Lipoproteins, and Hypertriglyceridemia. Am J Pathol 178:1429-1433

Cheng Q, Sun DW (2008) Factors affecting the water holding capacity of red meat products: a review of recent research advances. Crit Rev Food Sci Nutr 48:137-159

Cinti S, Mitchell G, Barbatelli G, Murano I, Ceresi E, Faloia E, Wang S, Fortier M, Greenberg AS, Obin MS (2005) Adipocyte death defines macrophage localization and function in adipose tissue of obese mice and humans. J Lipid Res 46:2347-2355

Cuenda A, Rousseau S (2007) p38 MAP-kinases pathway regulation, function and role in human diseases. Biochim Biophys Acta 1773:1358-1375

De Falco G, Bellan C, D'Amuri A, Angeloni G, Leucci E, Giordano A, Leoncini L (2005) Cdk9 regulates neural differentiation and its expression correlates with the differentiation grade of neuroblastoma and PNET tumors. Cancer Biol Ther 4:277-281

de Oliveira PS, Cesar AS, do Nascimento ML, Chaves AS, Tizioto PC, Tullio RR, Lanna DP, Rosa AN, Sonstegard TS, Mourao GB, Reecy JM, Garrick DJ, Mudadu MA, Coutinho LL, Regitano LC (2014) Identification of genomic regions associated with feed efficiency in Nelore cattle. BMC Genetics 15:100

Do DN, Ostersen T, Strathe AB, Mark T, Jensen J, Kadarmideen HN (2014a) Genome-wide association and systems genetic analyses of residual feed intake, daily feed consumption, backfat and weight gain in pigs. BMC Genetics 15:27

Do DN, Strathe AB, Ostersen T, Pant SD, Kadarmideen HN (2014b) Genome-wide association and pathway analysis of feed efficiency in pigs reveal candidate genes and pathways for residual feed intake. Front Genet 5:307

Duthie C, Simm G, Doeschl-Wilson A, Kalm E, Knap PW, Roehe R (2008) Quantitative trait loci for chemical body composition traits in pigs and their positional associations with body tissues, growth and feed intake. Anim Genet 39:130-140

Erkens T, De Smet S, Van den Maagdenberg K, Stinckens A, Buys N, Van Zeveren A, Peelman LJ (2010) Association analysis of PPARGC1A mutations with meat quality parameters in a commercial hybrid pig population. Czech J Anim Sci 55:200-208

Euken RM (2012) Swine Feed Efficiency: Effect of Dietary Energy on Feed Efficiency Iowa Pork Industry Center Fact Sheets 8

Evan GI, Wyllie AH, Gilbert CS, Littlewood TD, Land H, Brooks M, Waters CM, Penn LZ, Hancock DC (1992) Induction of apoptosis in fibroblasts by c-myc protein. Cell 69:119-128

Fang M, Adams JS, McMahan BL, Brown RJ, Oxford JT (2010) The expression patterns of minor fibrillar collagens during development in zebrafish. Gene Expr Patterns 10:315-322

Faure J, Lefaucheur L, Bonhomme N, Ecolan P, Meteau K, Coustard SM, Kouba M, Gilbert H, Lebret B (2013) Consequences of divergent selection for residual feed intake in pigs on muscle energy metabolism and meat quality. Meat Sci 93:37-45

Filtz TM, Vogel WK, Leid M (2014) Regulation of transcription factor activity by interconnected post-translational modifications. Trends Pharmacol Sci 35:76-85

Frantz C, Stewart KM, Weaver VM (2010) The extracellular matrix at a glance. J Cell Sci 123:4195-4200

Freeman TC, Ivens A, Baillie JK, Beraldi D, Barnett MW, Dorward D, Downing A, Fairbairn L, Kapetanovic R, Raza S, Tomoiu A, Alberio R, Wu C, Su AI, Summers KM,

Tuggle CK, Archibald AL, Hume DA (2012) A gene expression atlas of the domestic pig. BMC Biol 10:90

Fu L, Xu Y, Hou Y, Qi X, Zhou L, Liu, Luan Y, Jing L, Miao Y, Zhao S, Liu H, Li X (2017) Proteomic analysis indicates that mitochondrial energy metabolism in skeletal muscle tissue is negatively correlated with feed efficiency in pigs. Sci Rep 7:45291

Gaines AM, Peterson BA, Mendoza OF (2012) Herd management factors that influence whole herd feed efficiency. In: Patience JF (ed) Feed efficiency in swine. Wageningen Academic Press, Wageningen, pp 15–39

Garriga J, Bhattacharya S, Calbo J, Marshall RM, Truongcao M, Haines DS, Grana X (2003) CDK9 is constitutively expressed throughout the cell cycle, and its steady-state expression is independent of SKP2. Mol Cell Biol 23:5165-5173

Gasperlin L, Zlender B, Abram V (2001) Colour of beef heated to different temperatures as related to meat ageing. Meat Sci 59:23-30

Getz GS, Reardon CA (2004) Paraoxonase, a cardioprotective enzyme: continuing issues. Curr Opin Lipidol 15:261-267

Git A, Dvinge H, Salmon-Divon M, Osborne M, Kutter C, Hadfield J, Bertone P, Caldas C (2010) Systematic comparison of microarray profiling, real-time PCR, and next-generation sequencing technologies for measuring differential microRNA expression. RNA 16:991-1006

Gondret F, Vincent A, Houée-Bigot M, Siegel A, Lagarrigue S, Causeur D, Gilbert H, Louveau I (2017) A transcriptome multi-tissue analysis identifies biological pathways and genes associated with variations in feed efficiency of growing pigs. BMC Genomics 18:244

Granlund A, Kotova O, Benziane B, Galuska D, Jensen-Waern M, Chibalin AV, Essén-Gustavsson B (2010) Effects of exercise on muscle glycogen synthesis signalling and enzyme activities in pigs carrying the PRKAG3 mutation. Exp Physiol 95:541-549

Gregersen VR, Conley LN, Sorensen KK, Guldbrandtsen B, Velander IH, Bendixen C (2012) Genome-wide association scan and phased haplotype construction for quantitative trait loci affecting boar taint in three pig breeds. BMC Genomics 13:22

Guardia MD, Estany J, Balasch S, Oliver MA, Gispert M, Diestre A (2004) Risk assessment of PSE condition due to pre-slaughter conditions and RYR1 gene in pigs. Meat Sci 67:471-478

Guerre-Millo M (2002) Adipose tissue hormones. J Endocrinol Invest 25:855-861

Gunasekaran MK, Viranaicken W, Girard AC, Festy F, Cesari M, Roche R, Hoareau L (2013) Inflammation triggers high mobility group box 1 (HMGB1) secretion in adipose tissue, a potential link to obesity. Cytokine 64:103-111

Han Y, Zhan Y, Hou G, Li L (2014) Cyclin-dependent kinase 9 may as a novel target in downregulating the atherosclerosis inflammation (Review). Biomed Rep 2:775-779

Harris AJ, Patience JF, Lonergan SM, C JMD, Gabler NK (2012) Improved nutrient digestibility and retention partially explains feed efficiency gains in pigs selected for low residual feed intake. J Anim Sci 90 Suppl 4:164-166

Hebert TL, Wu X, Yu G, Goh BC, Halvorsen YD, Wang Z, Moro C, Gimble JM (2009) Culture effects of epidermal growth factor (EGF) and basic fibroblast growth factor (bFGF) on cryopreserved human adipose-derived stromal/stem cell proliferation and adipogenesis. J Tissue Eng Regen Med 3:553-561

Herring HK, Cassens RG, Rriskey EJ (1965) Further Studies on Bovine Muscle Tenderness as Influenced by Carcass Position, Sarcomere Length, and Fiber Diameter. J Food Sci 30:1049-1054

Hoare M, Das T, Alexander G (2010) Ageing, telomeres, senescence, and liver injury. J Hepatol 53:950-961

Honikel KO (1998) Reference methods for the assessment of physical characteristics of meat. Meat Sci 49:447-457

Horodyska J, Oster M, Reyer H, Mullen AM, Lawlor PG, Wimmers K, Hamill RM (2018) Analysis of meat quality traits and gene expression profiling of pigs divergent in residual feed intake. Meat Sci 137:265–274

Horodyska J, Wimmers K, Reyer H, Trakooljul N, Mullen AM, Lawlor PG, Hamill RM (in review) RNA-seq of muscle from pigs divergent in feed efficiency and product quality identifies differences in immune response, growth, and macronutrient and connective tissue metabolism

Hu Z, Evarts RP, Fujio K, Marsden ER, Thorgeirsson SS (1993) Expression of hepatocyte growth factor and c-met genes during hepatic differentiation and liver development in the rat. Am J Pathol 142:1823-1830

Hua ZG, Xiong LJ, Yan C, Wei DH, YingPai ZX, Qing ZY, Lin QZ, Fei FR, Ling WY, Ren MZ (2016) Glucose and Insulin Stimulate Lipogenesis in Porcine Adipocytes: Dissimilar and Identical Regulation Pathway for Key Transcription Factors. Mol Cells 39:797-806

Huffman KL, Miller MF, Hoover LC, Wu CK, Brittin HC, Ramsey CB (1996) Effect of beef tenderness on consumer satisfaction with steaks consumed in the home and restaurant. J Anim Sci 74:91-97

James C, James SJ (2010) Freezing/Thawing. In: Handbook of Meat Processing. Wiley-Blackwell, pp 105-124

Jiang WG, Hallett MB, Puntis MC (1993) Hepatocyte growth factor/scatter factor, liver regeneration and cancer metastasis. Br J Surg 80:1368-1373

Jiao S, Maltecca C, Gray KA, Cassady JP (2014) Feed intake, average daily gain, feed efficiency, and real-time ultrasound traits in Duroc pigs: II. Genomewide association. J Anim Sci 92:2846-2860

Jing L, Hou Y, Wu H, Miao Y, Li X, Cao J, Brameld JM, Parr T, Zhao S (2015) Transcriptome analysis of mRNA and miRNA in skeletal muscle indicates an important network for differential Residual Feed Intake in pigs. Sci Rep 5:11953

Jones CN, Tuleuova N, Lee JY, Ramanculov E, Reddi AH, Zern MA, Revzin A (2009) Cultivating liver cells on printed arrays of hepatocyte growth factor. Biomaterials 30:3733-3741

Kaleta C, de Figueiredo LF, Werner S, Guthke R, Ristow M, Schuster S (2011) In Silico Evidence for Gluconeogenesis from Fatty Acids in Humans. PLoS Comput Biol 7:e1002116

Kemp CM, Parr T (2012) Advances in apoptotic mediated proteolysis in meat tenderisation. Meat Sci 92:252-259

Kemp CM, Sensky PL, Bardsley RG, Buttery PJ, Parr T (2010) Tenderness – An enzymatic view. Meat Sci 84:248-256

Kerr BJ, Kellner TA, Shurson GC (2015) Characteristics of lipids and their feeding value in swine diets. J Anim Sci Technol 6:30

Kim D, Pertea G, Trapnell C, Pimentel H, Kelley R, Salzberg SL (2013) TopHat2: accurate alignment of transcriptomes in the presence of insertions, deletions and gene fusions. Genome Biol 14:R36

Koohmaraie M, Geesink GH (2006) Contribution of postmortem muscle biochemistry to the delivery of consistent meat quality with particular focus on the calpain system. Meat Sci 74:34-43

Kunej T, Wu XL, Berlic TM, Michal JJ, Jiang Z, Dovc P (2005) Frequency distribution of a Cys430Ser polymorphism in peroxisome proliferator-activated receptor-gamma

coactivator-1 (PPARGC1) gene sequence in Chinese and Western pig breeds. J Anim Breed Genet 122:7-11

Kurachi H, Adachi H, Ohtsuka S, Morishige K, Amemiya K, Keno Y, Shimomura I, Tokunaga K, Miyake A, Matsuzawa Y, et al. (1993) Involvement of epidermal growth factor in inducing obesity in ovariectomized mice. Am J Physiol 265:E323-331

Lanner JT, Georgiou DK, Joshi AD, Hamilton SL (2010) Ryanodine Receptors: Structure, Expression, Molecular Details, and Function in Calcium Release. Cold Spring Harb Perspect Biol 2:a003996

Le Naou T, Le Floc'h N, Louveau I, Gilbert H, Gondret F (2012) Metabolic changes and tissue responses to selection on residual feed intake in growing pigs. J Anim Sci 90:4771-4780

Ledoux S, Queguiner I, Msika S, Calderari S, Rufat P, Gasc JM, Corvol P, Larger E (2008) Angiogenesis associated with visceral and subcutaneous adipose tissue in severe human obesity. Diabetes 57:3247-3257

Lee SA, Kwak MS, Kim S, Shin JS (2014) The role of high mobility group box 1 in innate immunity. Yonsei Med J 55:1165-1176

Lefaucheur L, Lebret B, Ecolan P, Louveau I, Damon M, Prunier A, Billon Y, Sellier P, Gilbert H (2011) Muscle characteristics and meat quality traits are affected by divergent selection on residual feed intake in pigs. J Anim Sci 89:996-1010

Lindholm-Perry AK, Rohrer GA, Holl JW, Shackelford SD, Wheeler TL, Koohmaraie M, Nonneman D (2009) Relationships among calpastatin single nucleotide polymorphisms, calpastatin expression and tenderness in pork longissimus. Anim Genet 40:713-721

Liu X, Du Y, Trakooljul N, Brand B, Muráni E, Krischek C, Wicke M, Schwerin M, Wimmers K, Ponsuksili S (2015) Muscle Transcriptional Profile Based on Muscle Fiber, Mitochondrial Respiratory Activity, and Metabolic Enzymes. Int J Biol Sci 11:1348-1362

Liu XH, Zuo RJ, Bao YR, Qu XX, Sun K, Ying H (2017) Down-regulation of PDK4 is Critical for the Switch of Carbohydrate Catabolism during Syncytialization of Human Placental Trophoblasts. Sci Rep 7

Lkhagvadorj S, Qu L, Cai W, Couture OP, Barb CR, Hausman GJ, Nettleton D, Anderson LL, Dekkers JC, Tuggle CK (2010) Gene expression profiling of the short-term adaptive response to acute caloric restriction in liver and adipose tissues of pigs differing in feed efficiency. Am J Physiol Regul Integr Comp Physiol 298:R494-507

Maher SC, Mullen AM, Moloney AP, Reville W, Buckley DJ, Kerry JP, Troy DJ (2005) Ultrastructural Variation in Beef M. longissimus dorsi as an Explanation of the Variation in Beef Tenderness. J Food Sci 70:E579-E584

McBryan J, Hamill RM, Davey G, Lawlor P, Mullen AM (2010) Identification of suitable reference genes for gene expression analysis of pork meat quality and analysis of candidate genes associated with the trait drip loss. Meat Sci 86:436-439

McCormick RJ (1994) The flexibility of the collagen compartment of muscle. Meat Sci 36:79-91

Meunier-Salaun MC, Guerin C, Billon Y, Sellier P, Noblet J, Gilbert H (2014) Divergent selection for residual feed intake in group-housed growing pigs: characteristics of physical and behavioural activity according to line and sex. Animal 8:1898-1906

Mubashera A, Khan MI, Imran P, Tariq MR, Muhammad S (2013) Quality assessment of meat in relation to colour and muscle fiber types. Pak J Food Sci 23:80-86

Muñoz G, Ovilo C, Silió L, Tomás A, Noguera JL, Rodríguez MC (2009) Single- and joint-population analyses of two experimental pig crosses to confirm quantitative trait loci

on Sus scrofa chromosome 6 and leptin receptor effects on fatness and growth traits1. J Anim Sci 87:459-468

Nafikov RA, Beitz DC (2007) Carbohydrate and lipid metabolism in farm animals. J Nutr 137:702-705

Nazarov PV, Muller A, Kaoma T, Nicot N, Maximo C, Birembaut P, Tran NL, Dittmar G, Vallar L (2017) RNA sequencing and transcriptome arrays analyses show opposing results for alternative splicing in patient derived samples. BMC Genomics 18:443

Neal JW, Clipstone NA (2003) A constitutively active NFATc1 mutant induces a transformed phenotype in 3T3-L1 fibroblasts. J Biol Chem 278:17246-17254

Nelson RM, Aruffo A, Dolich S, Cecconi O, Mannori G, Bevilacqua MP (1992) Quantitative determination of selectin-carbohydrate interactions. Cold Spring Harb Symp Quant Biol 57:271-279

Neve A, Cantatore FP, Maruotti N, Corrado A, Ribatti D (2014) Extracellular Matrix Modulates Angiogenesis in Physiological and Pathological Conditions. BioMed Res Int 2014:10

Norris AW, Chen L, Fisher SJ, Szanto I, Ristow M, Jozsi AC, Hirshman MF, Rosen ED, Goodyear LJ, Gonzalez FJ, Spiegelman BM, Kahn CR (2003) Muscle-specific PPARgamma-deficient mice develop increased adiposity and insulin resistance but respond to thiazolidinediones. J Clin Invest 112:608-618

Nowak D (2011) Enzymes in Tenderization of Meat - The System of Calpains and Other Systems - a Review. In: Pol J Food Nutr Sci, p 231

Onteru SK, Gorbach DM, Young JM, Garrick DJ, Dekkers JC, Rothschild MF (2013) Whole Genome Association Studies of Residual Feed Intake and Related Traits in the Pig. PLoS One 8:e61756

Ornitz DM, Itoh N (2015) The Fibroblast Growth Factor signaling pathway. Wiley Interdisciplinary Reviews. Dev Biol 4:215-266

Ortega Martinez de Victoria E, Xu X, Koska J, Francisco AM, Scalise M, Ferrante AW, Jr., Krakoff J (2009) Macrophage content in subcutaneous adipose tissue: associations with adiposity, age, inflammatory markers, and whole-body insulin action in healthy Pima Indians. Diabetes 58:385-393

Pabelick CM, Prakash YS, Kannan MS, Warner DO, Sieck GC (2001) Effects of halothane on sarcoplasmic reticulum calcium release channels in porcine airway smooth muscle cells. Anesthesiology 95:207-215

Paradis F, Yue S, Grant JR, Stothard P, Basarab JA, Fitzsimmons C (2015) Transcriptomic analysis by RNA sequencing reveals that hepatic interferon-induced genes may be associated with feed efficiency in beef heifers. J Anim Sci 93:3331-3341

Park JC, Kim SC, Lee SD, Jang HC, Kim NK, Lee SH, Jung HJ, Kim IC, Seong HH, Choi BH (2012) Effects of Dietary Fat Types on Growth Performance, Pork Quality, and Gene Expression in Growing-finishing Pigs. Asian-Australasian J Anim Sci 25:1759-1767

Patience JF, Rossoni-Serão MC, Gutiérrez NA (2015) A review of feed efficiency in swine: biology and application. J Anim Sci Biotechnol 6:33

Penny IF (1969) Protein denaturation and water-holding capacity in pork muscle. Int J Food Sci Technol 4:269-273

Polidori P, Trabalza-Marinucci M, Fantuz F, Polidori F (2001) Post mortem proteolysis and tenderization of beef muscle through infusion of calcium chloride. Anim Res 50:223-226

Ponsuksili S, Jonas E, Murani E, Phatsara C, Srikanchai T, Walz C, Schwerin M, Schellander K, Wimmers K (2008) Trait correlated expression combined with expression QTL

analysis reveals biological pathways and candidate genes affecting water holding capacity of muscle. BMC Genomics 9:367

Porrello A, Cerone MA, Coen S, Gurtner A, Fontemaggi G, Cimino L, Piaggio G, Sacchi A, Soddu S (2000) p53 regulates myogenesis by triggering the differentiation activity of pRb. J Cell Biol 151:1295-1304

Prokesch A, Hackl H, Hakim-Weber R, Bornstein SR, Trajanoski Z (2009) Novel insights into adipogenesis from omics data. Curr Med Chem 16:2952-2964

Purslow PP (2014) New developments on the role of intramuscular connective tissue in meat toughness. Annu Rev Food Sci Technol 5:133-153

Raffler NA, Rivera-Nieves J, Ley K (2005) L-selectin in inflammation, infection and immunity. Drug Discov Today Ther Strateg 2:213-220

Rajewsky N (2006) microRNA target predictions in animals. Nature Genetics 38:S8

Resconi VC, Escudero A, Campo MM (2013) The development of aromas in ruminant meat. Molecules 18:6748-6781

Reyer H, Oster M, Magowan E, Dannenberger D, Ponsuksili S, Wimmers K (2017) Strategies towards Improved Feed Efficiency in Pigs Comprise Molecular Shifts in Hepatic Lipid and Carbohydrate Metabolism. Int J Mol Sci 18

Robbs BK, Cruz AL, Werneck MB, Mognol GP, Viola JP (2008) Dual roles for NFAT transcription factor genes as oncogenes and tumor suppressors. Mol Cell Biol 28:7168-7181

Rodier MH, El Moudni B, Kauffmann-Lacroix C, Daniault G, Jacquemin JL (1999) A Candida albicans metallopeptidase degrades constitutive proteins of extracellular matrix. FEMS Microbiol Lett 177:205-210

Ronning SB, Carlson CR, Stang E, Kolset SO, Hollung K, Pedersen ME (2015) Syndecan-4 Regulates Muscle Differentiation and Is Internalized from the Plasma Membrane during Myogenesis. PLoS One 10:e0129288

Rupnick MA, Panigrahy D, Zhang CY, Dallabrida SM, Lowell BB, Langer R, Folkman MJ (2002) Adipose tissue mass can be regulated through the vasculature. Proc Natl Acad Sci U S A 99:10730-10735

Rus H, Cudrici C, Niculescu F (2005) The role of the complement system in innate immunity. Immunol Res 33:103-112

Russell SB, Russell JD, Trupin KM (1981) Collagen synthesis in human fibroblasts: effects of ascorbic acid and regulation by hydrocortisone. J Cell Physiol 109:121-131

Ryan MT, Hamill RM, O'Halloran AM, Davey GC, McBryan J, Mullen AM, McGee C, Gispert M, Southwood OI, Sweeney T (2012) SNP variation in the promoter of the PRKAG3gene and association with meat quality traits in pig. BMC Genetics 13:66

Sahana G, Kadlecova V, Hornshoj H, Nielsen B, Christensen OF (2013) A genome-wide association scan in pig identifies novel regions associated with feed efficiency trait. J Anim Sci 91:1041-1050

Saintilan R, Merour I, Brossard L, Tribout T, Dourmad JY, Sellier P, Bidanel J, van Milgen J, Gilbert H (2013) Genetics of residual feed intake in growing pigs: Relationships with production traits, and nitrogen and phosphorus excretion traits. J Anim Sci 91:2542-2554

Salas RC, Mingala CN (2017) Genetic Factors Affecting Pork Quality: Halothane and Rendement Napole Genes. Anim Biotechnol 28:148-155

Sanchez A, Fabregat I (2010) Growth factor- and cytokine-driven pathways governing liver stemness and differentiation. World J Gastroenterol 16:5148-5161

Scheffler TL, Scheffler JM, Kasten SC, Sosnicki AA, Gerrard DE (2013) High glycolytic potential does not predict low ultimate pH in pork. Meat Sci 95:85-91

Scherzer MT, Waigel S, Donninger H, Arumugam V, Zacharias W, Clark G, Siskind LJ, Soucy P, Beverly L (2015) Fibroblast-Derived Extracellular Matrices: An Alternative Cell Culture System That Increases Metastatic Cellular Properties. PLoS One 10:e0138065

Shih DM, Yu JM, Vergnes L, Dali-Youcef N, Champion MD, Devarajan A, Zhang P, Castellani LW, Brindley DN, Jamey C, Auwerx J, Reddy ST, Ford DA, Reue K, Lusis AJ (2015) PON3 knockout mice are susceptible to obesity, gallstone formation, and atherosclerosis. FASEB J 29:1185-1197

Shin J, McFarland DC, Velleman SG (2012) Heparan sulfate proteoglycans, syndecan-4 and glypican-1, differentially regulate myogenic regulatory transcription factors and paired box 7 expression during turkey satellite cell myogenesis: implications for muscle growth. Poult Sci 91:201-207

Silveira AC, Freitas PF, Cesar AS, Cesar AS, Antunes RC, Guimaraes EC, Batista DF, Torido LC (2011) Influence of the halothane gene (HAL) on pork quality in two commercial crossbreeds. Genet Mol Res 10:1479-1489

Simone C, Stiegler P, Bagella L, Pucci B, Bellan C, De Falco G, De Luca A, Guanti G, Puri PL, Giordano A (2002) Activation of MyoD-dependent transcription by cdk9/cyclin T2. Oncogene 21:4137-4148

Škrlep M, Kavar T, Čandek-Potokar M (2010) Comparison of PRKAG3 and RYR1 gene effect on carcass traits and meat quality in Slovenian commercial pigs. Czech J Anim Sci 55

Smith RM, Gabler NK, Young JM, Cai W, Boddicker NJ, Anderson MJ, Huff-Lonergan E, Dekkers JC, Lonergan SM (2011) Effects of selection for decreased residual feed intake on composition and quality of fresh pork. J Anim Sci 89:192-200

Sode K, Akaike E, Sugiura H, Tsugawa W (2001) Enzymatic synthesis of a novel trehalose derivative, 3,3'-diketotrehalose, and its potential application as the trehalase enzyme inhibitor. FEBS Lett 489:42-45

Spence C (2015) Just how much of what we taste derives from the sense of smell? Flavour 4:30

Staels B, Fonseca VA (2009) Bile Acids and Metabolic Regulation: Mechanisms and clinical responses to bile acid sequestration. Diabetes Care 32:S237-S245

Steiling H, Wustefeld T, Bugnon P, Brauchle M, Fassler R, Teupser D, Thiery J, Gordon JI, Trautwein C, Werner S (2003) Fibroblast growth factor receptor signalling is crucial for liver homeostasis and regeneration. Oncogene 22:4380-4388

Tamir Y, Bengal E (1998) p53 protein is activated during muscle differentiation and participates with MyoD in the transcription of muscle creatine kinase gene. Oncogene 17:347

Torres-Filho RA, Cazedey HP, Fontes PR, Ramos ALS, Ramos EM (2017) Drip Loss Assessment by Different Analytical Methods and Their Relationships with Pork Quality Classification. J Food Quality 2017:8

Van Milgen J, Noblet J (2002) Partitioning of energy intake to heat protein and fat in growing pigs. J Anim Sci:86-93

Varley PF, Sweeney T, Ryan MT, O'Doherty JV (2011) The effect of phosphorus restriction during the weaner-grower phase on compensatory growth, serum osteocalcin and bone mineralization in gilts. Livest Sci 135:282-288

Velleman SG, Coy CS, McFarland DC (2007) Effect of syndecan-1, syndecan-4, and glypican-1 on turkey muscle satellite cell proliferation, differentiation, and responsiveness to fibroblast growth factor 2. Poult Sci 86:1406-1413

Vincent A, Louveau I, Gondret F, Trefeu C, Gilbert H, Lefaucheur L (2015) Divergent selection for residual feed intake affects the transcriptomic and proteomic profiles of pig skeletal muscle. J Anim Sci 93:2745-2758

von Otter M, Bergström P, Quattrone A, De Marco EV, Annesi G, Söderkvist P, Wettinger SB, Drozdzik M, Bialecka M, Nissbrandt H, Klein C, Nilsson M, Hammarsten O, Nilsson S, Zetterberg H (2014) Genetic associations of Nrf2-encoding NFE2L2 variants with Parkinson's disease – a multicenter study. BMC Med Genet 15:131

Wang C, Yang C, Chang JY, You P, Li Y, Jin C, Luo Y, Li X, McKeehan WL, Wang F (2014) Hepatocyte FRS2alpha is essential for the endocrine fibroblast growth factor to limit the amplitude of bile acid production induced by prandial activity. Curr Mol Med 14:703-711

Wang KKW, Posmantur R, Nadimpalli R, Nath R, Mohan P, Nixon RA, Talanian RV, Keegan M, Herzog L, Allen (1998) Caspase-Mediated Fragmentation of Calpain Inhibitor Protein Calpastatin during Apoptosis. Arch Biochem Biophys 356:187-196

Weston AR, Rogers RW, Althen TG (2002) Review: The Role of Collagen in Meat Tenderness. PAS 18:107-111

Wilkinson JM (2011) Re-defining efficiency of feed use by livestock. Animal 5:1014-1022

Willems OW, Miller SP, Wood BJ (2013) Assessment of residual body weight gain and residual intake and body weight gain as feed efficiency traits in the turkey (Meleagris gallopavo). Genet Sel Evol 45:26-26

Woessner JF, Jr. (1991) Matrix metalloproteinases and their inhibitors in connective tissue remodeling. FASEB J 5:2145-2154

Wong RH, Chang I, Hudak CS, Hyun S, Kwan HY, Sul HS (2009) A role of DNA-PK for the metabolic gene regulation in response to insulin. Cell 136:1056-1072

Wood JD, Enser M, Fisher AV, Nute GR, Sheard PR, Richardson RI, Hughes SI, Whittington FM (2008) Fat deposition, fatty acid composition and meat quality: A review. Meat Sci 78:343-358

Yang H, Wang H, Czura CJ, Tracey KJ (2005) The cytokine activity of HMGB1. J Leukoc Biol 78:1-8

Yang XQ, Liu H, Guo LJ, Xu Y, Liu D (2007) The mutation site analysis on CAPN1 gene of Wild boar, Min pig and Yorkshire. Yi Chuan 29:581-586

Young JM, Cai W, Dekkers JC (2011) Effect of selection for residual feed intake on feeding behavior and daily feed intake patterns in Yorkshire swine. J Anim Sci 89:639-647

Young JM, Dekkers JCM (2012) The Genetic and Biological Basis of Residual Feed Intake as a Measure of Feed Efficiency. In: Patience JF (ed) Feed Efficiency in Swine. Wageningen Academic Press, Wageningen, pp 153–166

Yu J, Pressoir G, Briggs WH, Vroh Bi I, Yamasaki M, Doebley JF, McMullen MD, Gaut BS, Nielsen DM, Holland JB, Kresovich S, Buckler ES (2006) A unified mixed-model method for association mapping that accounts for multiple levels of relatedness. Nature Genet 38:203-208

Yue G, Stratil A, Kopecny M, Schröffelova D, Schröffel J, Hojny J, Cepica S, Davoli R, Zambonelli P, Brunsch C, Sternstein I, Moser G, Bartenschlager H, Reiner G, Geldermann H (2003) Linkage and QTL mapping for Sus scrofa chromosome 6. J Anim Breed Genet 120:45-55

Zanoni I, Granucci F (2012) Regulation and dysregulation of innate immunity by NFAT signaling downstream of pattern recognition receptors (PRRs). Eur J Immunol 42:1924-1931

Zayas JF (1997) Water Holding Capacity of Proteins. In: Functionality of Proteins in Food. Springer, Berlin, Heidelberg

Zhang W, Li D, Liu L, Zang J, Duan Q, Yang W, Zhang L (2013) The effects of dietary fiber level on nutrient digestibility in growing pigs. J Anim Sci Biotechnol 4:17

Zhao S, Fung-Leung WP, Bittner A, Ngo K, Liu X (2014) Comparison of RNA-Seq and Microarray in Transcriptome Profiling of Activated T Cells. PLoS One 9:e78644

Zhao Y, Hou Y, Liu F, Liu A, Jing L, Zhao C, Luan Y, Miao Y, Zhao S, Li X (2016) Transcriptome Analysis Reveals that Vitamin A Metabolism in the Liver Affects Feed Efficiency in Pigs. G3 116.032839

Zimmers TA, Jin X, Zhang Z, Jiang Y, Koniaris LG (2017) Epidermal growth factor receptor restoration rescues the fatty liver regeneration in mice. Am J Physiol Endocrinol Metab 313:E440-e449

Zou T, Yu B, Yu J, Mao X, Zheng P, He J, Huang Z, Liu Y, Chen D (2016) Moderately decreased maternal dietary energy intake during pregnancy reduces fetal skeletal muscle mitochondrial biogenesis in the pigs. Genes Nutr 11:19

ANNEX A

Publications

List of publications

A.1 Genome-wide association analysis and functional annotation of positional candidate genes for feed conversion efficiency in pigs

Horodyska J., Hamill R.M., Varley P.F., Reyer H., Wimmers K.

Published in: PLoS ONE (20117), 12(6), e0173482, DOI: 10.1371/journal.pone.0173482

A.2 Analysis of meat quality traits and gene expression profiling of pigs divergent in residual feed intake

Horodyska J., Oster M., Reyer H., Mullen A.M., Lawlor P.G., Wimmers K., Hamill R.M.

Published in: Meat Science (2017), 137, 265–274, DOI: 10.1016/j.meatsci.2017.11.021

A.3 RNA-seq of muscle from pigs divergent in feed efficiency and product quality identifies differences in immune response, growth, and macronutrient and connective tissue metabolism

Horodyska J., Wimmers K., Reyer H., Trakooljul N., Mullen A.M., Lawlor P.G., Hamill R.M.

In review at BMC Genomics

A.4 Transcriptome analysis of adipose from pigs divergent in feed efficiency reveals alteration in gene networks related to adipose growth, lipid metabolism, extracellular matrix and immune response

Horodyska J., Reyer H., Wimmers K., Trakooljul N., Lawlor P.G., Hamill R.M.

In review at Molecular Genetics and Genomics

A.5 RNA-seq of liver from pigs divergent in feed efficiency highlights shifts in macronutrient metabolism, hepatic growth and immune response

Horodyska J., Hamill R.M., Reyer H., Trakooljul N., Lawlor P.G., McCormack U.M, Wimmers K.

In review at Frontiers in Genetics

Genome-wide association analysis and functional annotation of positional candidate genes for feed conversion efficiency and growth rate in pigs

Justyna Horodyska[1,2], Ruth M. Hamill[1], Patrick F. Varley[3], Henry Reyer[2*], Klaus Wimmers[2]

[1]Teagasc, Food Research Centre, Ashtown, Dublin, Ireland

[2]Leibniz Institute for Farm Animal Biology (FBN), Institute for Genome Biology, Dummerstorf, Germany

[3]Hermitage Genetics, Sion Road, Kilkenny, Ireland

*Corresponding author

Published in PLoS One (2017), 12(6), e0173482

The final publication is available at http://journals.plos.org/plosone/article?id=10.1371/journal.pone.0173482 [DOI: 10.1371/journal.pone.0173482]

Abstract

Feed conversion efficiency is a measure of how well an animal converts feed into live weight and it is typically expressed as feed conversion ratio (FCR). FCR and related traits like growth rate (e.g. days to 110 kg – D110) are of high interest for animal breeders, farmers and society due to implications on animal performance, feeding costs and environmental sustainability. The objective of this study was to identify genomic regions associated with FCR and D110 in pigs. A total of 952 terminal line boars, showing an individual variation in FCR, were genotyped using 60K SNP-Chips. Markers were tested for associations with estimated breeding values (EBV) for FCR and D110. For FCR, the largest number of associated SNPs was located on chromosomes 4 (30 SNPs), 1 (25 SNPs), X (15 SNPs) and 6 (12 SNPs). The most prominent genomic regions for D110 were identified on chromosomes 15 (10 SNPs), 1 and 4 (both 9 SNPs). The most significantly associated SNPs for FCR and D110 mapped 129.8 Kb from *METTL11B* (chromosome 4) and 32Kb from *MBD5* (chromosome 15), respectively. A list of positional genes, closest to significantly associated SNPs, was used to identify enriched pathways and biological functions related to the QTL for

both traits. A number of candidate genes were significantly overrepresented in pathways of immune cell trafficking, lymphoid tissue structure, organ morphology, endocrine system function, lipid metabolism, and energy production. After resequencing the coding region of selected positional and functional candidate genes, six SNPs were genotyped in a subset of boars. SNPs in *PRKDC*, *SELL* and *NR2E1* showed significant associations with EBVs for FCR/D110. The study revealed a number of chromosomal regions and candidate genes affecting FCR/D110 and pointed to corresponding biological pathways related to lipid metabolism, olfactory reception, and also immunological status.

Background

Improving feed conversion efficiency (FCE) in pigs is a major goal in pig breeding as feed accounts for a high proportion of the total production cost [1]. Selection for improved FCE is also a key factor in reducing the environmental footprint of the pig industry [2]. FCE can be defined as a measure of an animal's efficiency in converting feed into live weight [3] and it is typically expressed as feed conversion ratio (FCR, ratio of feed intake to weight gain) [4]. As such, growth rate traits which determine the weight gain in different developmental stages are closely related to FCR thus having a direct impact on efficiency [5]. However, phenotypic and genetic correlations between FCR and its components (i.e. feed intake and body weight gain) have been reported to be higher for FCR and feed intake compared to FCR and body weight gain in different pig populations [5]. Apart from FCR, other indexes such as residual feed intake (RFI), which can be described as the difference between an individual's actual feed intake and its predicted feed requirements for maintenance and growth, have been studied [2].

A number of quantitative trait loci (QTLs) affecting feed efficiency in pigs have been detected (PigQTLdb, http://www.animalgenome.org/cgi-bin/QTLdb/SS/index). However, most of them were identified using a linkage mapping approach resulting in wide genomic QTL regions. Such linkage data is limited to within-family selection only [6]. A genome-wide association study (GWAS) approach would offer the potential for improved accuracy and refinement in the identification of QTL locations at the population level [7]. To date, only a few studies have used the GWAS approach to identify QTLs for FCE traits in pigs. Sahana et al. [6] detected a number of significant QTLs for FCR on porcine chromosomes

(SSC) 4, 7, 8 and 14 in Duroc pigs. Another study identified only one QTL for FCR on SSC 4 in Duroc boars [8]. A GWAS performed on Yorkshire boars revealed several QTLs influencing RFI on SSC 7 and 14 [9]. Do et al. [10] additionally reported QTLs on SSC 3, 8, 9, 10, 15 and 17 for RFI in Yorkshire pigs. The same author also conducted a study on Duroc boars and identified significant regions for RFI on SSC 1, 8, 9, 13 and 18 [11]. While employing the GWAS approach, the objective of this study was to identify genomic regions associated with feed efficiency in an important commercial pig sire line (Maxgro, Hermitage Genetics).

Materials and Methods

Animals and phenotypes

Animal care, slaughter and tissue collection of the animals used in this study were performed in compliance with national regulations related to animal research and commercial slaughtering and were approved by the local committees for the care and use of animals of the Teagasc Research Center Ashtown and the Leibniz Institute for Farm Animal Biology. A total of 952 Maxgro boars, which is predominately Pietrain based terminal line, were used in this study. These animals, born between year 2006 and 2012, were selected as replacement boars in the artificial insemination (AI) stud and were supplied by Hermitage Genetics (Ireland). The pigs were penned in groups of fourteen with a space allowance of 0.75 m^2 per pig and were fed a pelleted finisher diet (National Research Council, 2012) consisting of 177.8 g crude protein, 5.0 g tP, 6.0 g Ca and 13.9 MJ DE, and 8.8 g ileal digestible lysine per kilogram. They also had *ad libitum* access to water through nipple drinkers. Phenotypic data such as FCR and D110 comprising 46 and 91 percent of the total number of animals used in the study, respectively, were recorded by Hermitage Genetics following the method of Varley et al [12]. Breeding values (EBV) for FCR (range: -0.44 - 0.32, mean: -0.09, SD: 0.09) and D110 (range: -20.8 - 9.18, mean: -10.2, SD: 4.00) were estimated using Best Linear Unbiased Prediction (BLUP) system [13] from a dataset that included multiple breeds, two sexes and a number of farms and AI studs. The models for the routine estimation of direct genetic effects for both traits were multivariate and included fixed effects of contemporary group, pig breed and sex. The affiliation of a pig to a litter was fit as an uncorrelated random effect in the prediction. Moreover, the status of performance testing was also included as fixed effect.

Specifically, for performance tested pigs individual feeding records were obtained using a single-space computerised feeder (Mastleistungsprüfung MLP-RAP; Schauer Agrotronic AG, Sursee, Switzerland) [12]. The pigs (age at start of the test - mean: 102.3 days, SD: 6.4 days; age at end of the test – mean: 144.1 days, SD: 6.4 days) were weighted at the start (mean: 60.9 kg, SD: 7.6 kg) and the end (mean: 109.3 kg, SD: 9.9 kg) of the test period for a minimum of 40 days (mean: 41.8 days, SD: 4.7 days). Based on these observations FCR was calculated. In order to obtain the number of days needed to gain a final body weight of 110 kg, the pig's date of birth and slaughter weight, which is slightly above or below 110 kg, was entered into the BLUP system and calculated. For the prediction of the EBVs FCR, both start weight and end weight were fit as a covariate in order to consider weight related differences in feed efficiency. Following the test period, boars were entered into the AI stud therefore no euthanasia of boars occurred.

SNP array genotyping, quality control and statistical analysis

Approximately 50 ml of blood from *Vena jugularis* was collected from each boar by Hermitage Genetics into a tube containing EDTA. Genomic DNA was extracted from the preserved blood using QIAamp DNA Blood Mini Kit (QIAGEN Ltd., West Sussex, UK) according to manufacturer's instructions. Genotyping with PorcineSNP60 BeadChip (Illumina Inc., San Diego, CA, USA) was performed in compliance with the SNP Infinium HD assay protocol (http://www.illumina.com). Subsequently, data was analysed using GenomeStudio (Version 2011.1, Illumina Inc.). Individuals with call rate ≤ 97% and SNPs with call frequency ≤ 95% and minor allele frequency (MAF) ≤ 0.03 were excluded. The departure from Hardy-Weinberg equilibrium (HWE) was not considered as indicator for consistent genotyping errors as it has been reported to be underpowered for this purpose [14].

After quality control, remaining SNPs were tested for an association with EBVs FCR and D110. SNP-trait association analysis was implemented with a mixed linear model using JMP Genomics 6 software (version 6, SAS INST., Inc., Cary, NC, 2002–2010). In order to correct for population structure, the relationship matrix tool implemented in JMP Genomics 6 was used to compute identity-by-state (IBS) relations between individuals based on genotype data [15]. After compression of K matrices, these relations were included as a random effect in the model. Moreover, this factor accounting for relatedness was applied to counteract high false-

positive rates and the misestimating of QTL effects assigned to the usage of EBVs for GWAS [16]. Threshold p-values for suggestive and Bonferroni-adjusted genome-wide significance were set to -log10[p-value] = 4.7 (1 divided by 48440 independent tests) and -log10[p-value] = 6 (0.05 divided by 48440 independent tests), respectively.

A list of genes closest to the significant SNPs ($-\log_{10}$[p-value] ≥ 6) was created allowing a maximum distance of 1Mb between the marker and genes, using the Ensembl database (http://www.ensembl.org, release 78) and was uploaded into Ingenuity Pathways Analysis (IPA; Ingenuity® Systems, http://www.ingenuity.com) in order to investigate relevant pathways and functional categories. Benjamini-Hochberg corrected P values were used to map the genes to the most significant molecular, cellular and physiological systems development functions ($P < 0.01$). To get insights into the most relevant metabolic and signalling pathways based on the designated list of genes, canonical pathways were displayed (Fisher's exact test; $P < 0.05$), although they did not differ significantly after Benjamini-Hochberg correction. Categories addressing human disease and disorder-associated pathways were excluded from the IPA analysis.

Validation of candidate genes

Twelve genes with functions relevant to feed efficiency according to IPA were selected from the candidate gene list for validation and further analysis. A set of primers for each gene was designed based on published sequence data (Ensembl database) using Primer3 (http://primer3.ut.ee/) (Table 1). Genomic DNA of low EBV FCR pigs (n=10, mean: -0.182, SD: 0.027) and high EBV FCR pigs (n=10, mean: 0.040, SD: 0.032), with a p-value of difference < 0.0001, was pooled (n=2) and used as template for PCR. All PCR reactions were carried out in a final volume of 50 µl and consisted of 10 µl PCR buffer (5x) (Promega, WI, USA), 3 µl $MgCl_2$ (25mM) (Promega), 0.4 µl dNTP mix (10mM each), 0.4 µl of each primer (100 pmol, Eurofins MWG Operon, Germany), 0.4 µl Go Taq DNA Polymerase (100U, Promega), 30 ng of the DNA pool and filled with dH_2O. The cycling conditions were as follows: initial denaturation at 95°C for 135 sec; 35 cycles of 95°C for 45 sec, annealing for 45 sec (60°C for *OPRD1*, *WDTC1*, *SMPD2* and 56°C for the remaining primers), and 72°C for 75 sec, subsequently final extension of 72°C for 10 min. PCR products were subjected to electrophoresis on 1.5% agarose gels and visualised. PCR products were purified using the

QIAquick PCR Purification Kit (QIAGEN Ltd.) and sequenced commercially (Eurofins, MWG-Biotech). Chromatograms were analysed to identify segregating SNP.

Based on the PCR product sequencing of the twelve genes, six confirmed SNPs (located in *MBD5*, *OPRD1*, *AKR1C3*, *NR2E1*, *PRKDC* and *SELL*) were selected for genotyping in 436 Maxgo boars as a representative subset of animals. The SNP genotyping was performed using TaqMan® SNP Genotyping Assays (Applied Biosystems, Foster City, CA, USA). Each 15 µl PCR reaction consisted of 7.5 µl of TaqMan® genotyping master mix (Applied Biosystems, Foster City, CA, USA), 0.375 µl 40 x genotyping assay mix (Applied Biosystems), 6.125 µl dH_2O and 1 µl of genomic DNA (10 ng/µl). Thermal cycling was performed using ABI PRISM® 7500 Real Time PCR System (Applied Biosystems) and the cycling conditions were as follows: initial denaturation at 95°C for 10 min, followed by 40 cycles of 95°C for 15 sec denaturation and 60°C for 1 min annealing/extension. Genotype calling was carried out using proprietary 7500 System SDS software (Applied Biosystems).

Allele frequencies were computed and deviations from HWE (p-value < 0.05) were tested using Haploview software [17]. Mixed linear model using JMP Genomics 6 software (version 6, SAS INST., Inc., Cary, NC, 2002–2010) was used to evaluate associations between the four SNPs with allele frequency as predicted and greater than 5% (rs340456509, rs80900450, rs319738340 and rs81508945) and EBVs for FCR and D110 in the Maxgro boars (n = 436). Compressed IBS relations were included as a random effect in the model. In order to determine additive and dominant effects for the particular SNP, indicator variables alpha (1=homozygote for the allele with higher least square means, -1=homozygote for the allele with lower least square means and 0=heterozygote), and delta (1=heterozygote and 0=homozygote) were created. Regression models were performed, using EBV FCR and EBV D110 as the dependent variables and variable alpha and delta as the independent variables, to estimate the additive and dominant effects for each significant SNP (REG procedure of the SAS v9.3 software package). Based on the squared multiple correlation (R^2) of the regression, the effect size was expressed as the phenotypic variance attributable to the genetic variance at the designated locus.

Results

Genome-wide association study

After quality control, 940 individuals and 48,440 SNPs, mapped to the Sscrofa 10.2 pig genome assembly, remained for the further analysis. In total 132 SNPs reached the threshold of suggestive significance for an association with EBV FCR ($-\log_{10}$[p-value] ≥ 4.7) (Fig 1; S1 Table). The largest number of associated SNPs were located on SSC4 (30 SNPs) and SSC1 (25 SNPs) followed by SSCX (15 SNPs) and SSC6 (12 SNPs). A total of 25 SNPs mapping to 10 porcine autosomes crossed the Bonferroni-adjusted genome-wide significance threshold ($-\log_{10}$[p-value] ≥ 6). Of the 25 SNPs, 5 were located within a 2.37 Mb segment on SSC4 and pointed to Methyltransferase like 11B (*METTL11B*) and Coagulation Factor V (*F5*) as positional candidate genes (Table 2). A search for genes in the window surrounding the significantly associated markers revealed Selectin L (*SELL*), Selectin P (*SELP*) and Protein kinase, DNA-activated, catalytic polypeptide (*PRKDC*) as putative candidate genes for FCE. On SSC15, Neuronal guanine nucleotide exchange factor (*NGEF*) and 5-hydroxytryptamine (serotonin) receptor 2B, G protein-coupled (*HTR2B*) genes were revealed as functional candidate genes, whereas *DIS3* and *ARL4C* were identified as positional candidates. Two significant SNPs on SSC6 were located near Feline Gardner-Rasheed sarcoma viral oncogene homolog (*FGR*) and Protein tyrosine phosphatase, receptor type, U (*PTPRU*). A further search for genes with putative relevance for processes related to FCE in this region revealed Tetratricopeptide repeats 1 (*WDTC1*) and Opioid receptor, delta 1 (*OPRD1*). Furthermore, a significant SNP mapped to SSC1 was located in an uncharacterised gene and the nearest annotated gene was CD164 molecule, sialomucin (*CD164*). Nuclear receptor subfamily 2, group E, member 1 (*NR2E1*) and Sphingomyelin phosphodiesterase 2, neutral membrane (*SMPD2*) were identified as functional candidate genes in this region.

In total 71 SNPs reached the threshold of suggestive significance for an association with EBV D110 ($-\log_{10}$[p-value] ≥ 4.7) (Fig 2; S1 Table). The largest number of associated SNPs was located on SSC15 (10 SNPs), SSC1 and SSC4 (9 SNPs), SSC3 (8 SNPs), followed by SSC10 and 13 (5 SNPs). A total of 12 SNPs mapping to 7 porcine autosomes crossed the Bonferroni-adjusted genome-wide significance threshold ($-\log_{10}$[p-value] ≥ 6). Of the 12 SNPs, 5 were located within a 682 Kb segment (between 2.64 and 3.32 Mb) on SSC15. Three of these markers were located within an intron of Kinesin family member 5C (*KIF5C*) gene (Table 2).

Two remaining markers mapped near Methyl-CpG binding domain protein 5 (*MBD5*) and LY6/PLAUR domain containing 6B (*LYPD6B*). A further search for genes revealed Methylmalonic aciduria cblD type, with homocystinuria (*MMADHC*) with functional relations to D110. On SSC10, Kruppel-like factor 6 (*KLF6*) and Aldo-keto reductase family 1, member C3 (*AKR1C3*) were identified as positional candidate genes with a putative contribution to D110.

Functional enrichment among mapped genes

A total of 86 and 16 genes mapped within 1Mb upstream and downstream of significant markers for EBV FCR and D110, respectively, were uploaded into Ingenuity Pathways Analysis. Functional annotation of the positional candidate genes to biological processes and canonical pathways (top 5) is presented in Table 3 and 4. The top canonical pathways significantly overrepresented among the positional candidate genes for EBV of FCR were related to cell cycle control, estrogen receptor signaling, RXR and subfamily 1 nuclear receptors activation, granulocyte mediate inflammation, and sphingomyelin metabolism. Functional annotation revealed organismal development and organ morphology, lymphoid tissue and hematological system development, and immune cell trafficking to be significantly enriched among the genes located in QTL regions for EBV FCR. Moreover, bile acid and androgen biosynthesis, TR/RXR Activation, methylglyoxal detoxification, and retinoate biosynthesis pathways were the top pathways associated with the positional candidate genes for EBV D110. Furthermore, statistically associated biological functions with the positional candidate genes for EBV D110 were energy, lipid and drug metabolism, endocrine system development, and small molecule biochemistry.

SNP array validation

Four SNPs located near the QTLs for EBV FCR (rs80900450, rs319738340, rs340456509 and a novel SNP) in *PRKDC, SELL, NR2E1* and *OPRD1* respectively, and two SNPs mapped close to the QTL for EBV D110 (rs332368013 and rs81508945) in *MBD5* and *AKR1C3* respectively were confirmed to be polymorphic in target populations by sequencing. Subsequently, these six SNPs were genotyped in 436 Maxgro boars. Allelic frequencies and HWE are presented in Table 5. SNP in *MBD5* significantly departured from HWE (P-value < 0.05) indicating a slight deficiency of homozygotes in the studied population and SNP in

OPRD1 displayed minor allele frequency less than 5%. All SNPs, with the exception of the SNP in *MBD5* and *OPRD1* were tested for association with breeding values for FCR and D110 (Table 6). SNP rs80900450 and rs319738340 showed significant association with EBV FCR. Moreover, SNP rs340456509 was found significantly associated with both traits. The occurrence of the G allele was shown to be beneficial for both growth and feed efficiency. Significant additive effects of SNPs rs80900450, rs81508945 and rs340456509 were observed. In addition, SNP rs340456509 showed a dominant effect for EBV D110, however only one percent of the phenotypic variance was attributable to the dominant genetic variance.

Discussion

In this study, a genome-wide association analysis was performed to elucidate the genetic architecture of feed conversion efficiency and growth rate in pigs. A number of candidate genes neighbouring the identified QTL regions were selected for downstream analysis. A further validation confirmed significant associations between these genes and EBV FCR / D110. The most prominent regions for EBV FCR were identified on SSC 1, 4, 6 and 15. For EBV D110, the most promising QTLs were detected on porcine chromosome 10 and 15. None of the identified QTL regions overlap for both traits. Alignment of the genetic and physical maps on the Sscrofa 10.2 genome assembly (PigQTLdb) enabled the identified QTLs from the present study to be compared with previously described QTL regions. A QTL from this study located at 78.3 to 80.5 Mb on SSC 6 coincided with a QTL for FCR in a European Wild Boar x Meishan cross mapped in the region of 127.3 cM (64.9 to 89 Mb, PigQTLdb) [18]. Additionally this QTL overlapped with a QTL for body weight detected at 78.3 to 78.7 Mb in Iberian x Landrace and Iberian x Meishan crosses [19]. This QTL has thus been independently discovered in different populations, which supports attributing it to biologically relevant common genetic variation [20]. QTL located at 86.7 to 89.1 Mb on SSC 4 found in this study was in a close proximity to QTL for FCR in a European Wild Boar x Pietrain cross mapped by Cepica et al. [21] at 75 cM (89.5 to 98.2 Mb, PigQTLdb). Another QTL on SSC 4 was detected at 20 cM (7.2 to 12.6 Mb, PigQTLdb) in a three-generation full-sib population, created by crossing Pietrain sires with Large White x Landrace x Leicoma dam line [22], which is very distant from the QTL identified in this study. These QTLs were detected by linkage analysis and therefore were mapped with very low resolution and cover

large intervals. A genome-wide association study in a Danish Duroc population identified QTL for FCR located on SSC 4 at 63.8 to 64 Mb [6]. Another GWAS revealed QTL for FCR on SSC 4 at 4 to 5 Mb in a Duroc terminal sire population [8]. The remaining QTL regions for EBV FCR / D110 identified in this study on SSC 1, 10 and 15 did not colocalize closely to regions affecting FCR and growth rate found in the literature. Furthermore, Jiao et al. [8] mapped a QTL for daily feed intake in Duroc boars at 73.1 to 73.9 Mb, which is ~700 Kb from the QTL for EBV D110 detected in the present study. The very small number of overlapping QTL regions is in accordance with Gregersen et al. [23] who reported limited overlap of QTL for a particular trait between breeds. This might suggest that different QTLs regulate feed efficiency traits in the Maxgro boars compared to other breeds [4].[4] Moreover, the EBVs, which were used as response variable in the current study, are known to behave differently compared to raw phenotypes. EBVs have been reported to be more independent from environmental factors compared to raw phenotypes [20]. However, a recent evaluation of the direct use of EBVs for GWAS revealed issues of power, type I error and QTL effect sizes related to the incorporation of familial information in the estimation of EBV [16]. To account for these weaknesses linked to EBVs, the familial relationship (i.e. as genomic relationship matrix) was included in the statistical model as previously applied in other association analyses using EBVs [24-26]. The comparison of results obtained from different GWAS methods revealed that the used methodologies provide a further source for variation of results between different studies [27].

Pathways and biological functions of genes mapped near the significant SNPs

Functional annotation revealed a number of pathways and biological processes significantly overrepresented among the positional candidate genes for EBV FCR and D110. Nearby genes to the significant markers for EBV FCR (*SELP*, *SELL*, *FGR*, *SELE*, *F5*, *FOXO3* and *OPRD1*) were identified to be involved in immune cell trafficking. Similarly, *THEMIS2*, *SELP*, *SELL*, *SELE*, *F5* and *PRKDC* were clustered in lymphoid tissue structure and development category. It is well documented that the activity of the immune system is linked to feed intake and therefore provide a relevant aspect for feed efficiency [28]. When immune response is activated, the available energy resources are shifted away from skeletal muscle accretion and prioritised to production of antibodies in order to fight the infection. This in turn might result in reduced rates of weight gain and feed conversion [29]. In addition, functional annotation of

the positional candidate genes for EBV FCR to biological processes revealed a cluster of seventeen genes overrepresented in an organ morphology category (*CEBPD, SELL, ECEL1, NR2E1, SELE, CHRNG, WASF1, GPR3, EIF4E2, HTR2B, CHRND, SELP, KIFAP3, SEC63, SYTL1, PRKDC* and *FOXO3*). A study conducted by Njoku et al. [30] on Large White pigs revealed that visceral organ growth is stimulated by feed intake. Moreover, low RFI pigs have been associated with decreased visceral organ weight [31,32]. This is in agreement with Ferrell and Jenkins [33] postulating that a lower maintenance costs are associated with reduced visceral organ weight and decreased feed intake. A number of genes (*AKR1C3, MBD5, ACVR2A, AKR1C1/AKR1C2* and *AKR1C4*) located within 1Mb of the significant markers for EBV D110 were clustered in an endocrine system function and development category. Previous study identified smaller thyroid glands in low residual feed intake pigs [34]. Moreover, Gabarrou et al. [35] reported a decreased thyroid function in low RFI cockerels. Additionally, these genes belonging to Aldo-Keto Reductase family were significantly overrepresented in lipid metabolism and energy production. Lipid metabolism pathway as well as energy pathway were statistically associated with residual feed intake in muscle and adipose tissue of pigs [36-38].

Candidate genes for feed conversion efficiency

Positional and functional genes located within 1 Mb of the GWAS SNPs significantly associated with breeding values for FCR/D110 were selected and examined. On SSC 4, SNP rs80900450 and rs319738340 in *PRKDC* and *SELL* respectively, were significantly associated with breeding value for FCR. ***PRKDC*** is a gene encoding the catalytic subunit of the DNA-dependent protein kinase (DNA-PK), which plays a part in DNA double stranded break repair [39]. *PRKDC* is involved in the signalling pathway responsible for the formation of fat from carbohydrates in the liver [40]. Wong et al. [40] conducted a study, in which they postulated that during fasting, inactivation of Fatty Acid Synthase (*FAS*) promoter occurs. However upon feeding, the *FAS* promoter becomes activated by *PRKDC* gene. In *PRKDC* deficient scid (severe combined immunodeficient) mice, feeding-induced transcriptional activation of the *FAS* gene and lipogenesis were impaired. As a result, reduced triglyceride level and decreased adipose tissue in *PRKDC* deficient scid mice were observed [40]. L-selectin (**SELL**) plays a role in lymphocyte trafficking to lymph nodes and Peyer's patches, as well as targeting lymphocytes and neutrophils to an inflammation source [41]. The *SELL*

encoded protein is a member of selectins belonging to a family of transmembrane glycoproteins and its role is to support adhesion of blood leucocytes to the vessel wall upon inflammatory and immunological response [42]. Significant reduction of L-selectin, which could affect the neutrophil's ability to activate and travel to a source of inflammation, was observed in morbidly obese patients [43]. Yang et al. [44] proposed that L-selectin is responsible for mediating leukocyte homing to islets which would suggest it might be associated with autoimmune disease such as diabetes mellitus. Moreover, T668C SNP in *SELL* was associated with insulin-dependent diabetes mellitus [45]. Additionally, allele L206 of L-selectin gene was associated with inflammatory bowel disease [46].

NR2E1 is a member of a ligand dependent transcriptional factors group, which controls a number of biological and disease related processes. *NR2E1* is abundantly expressed in the brain where it is involved in neurogenesis [47]. Christie et al. [48] and Kumar et al. [49] reported reduced neurogenesis in adult mice with *NR1E1* deletion. Moreover, the *NR2E1* knockout mice had reduced volume of olfactory bulb [49], a first central structure involved in processing of the olfactory information [50]. Interestingly, in the present study rs340456509 SNP in the *NR1E2* was significantly associated with breeding values for FCR and D110. Olfactory bulb plays an important part in regulating food intake as it is targeted by signals responsible for the regulation of energy balance [50], therefore it is hugely relevant for feed conversion efficiency.

AKR1C3 belongs to a large aldo and keto reductase enzyme family and is expressed in a wide variety of tissues including liver and adipose tissue. The protein encoded by this gene plays a role in conversion of active androgens, oestrogens and prostaglandins to their non-active metabolites [51]. *AKR1C3* has been associated with androgen inactivation induced adiposity, where large adipocytes had higher expression level compared to small adipocytes [52,53]. This finding was supported by a study conducted on obese patients having decreased *AKR1C3* expression upon diet induced weight loss [52]. Svensson et al. [52] also postulated that there might be a link between the *AKR1C3* gene and glucose intolerance. Moreover, White et al. [51] found an association between rs2211623 SNP and liver inflammation, which in turn might be related to insulin resistance. Nevertheless, in this study the selected SNP rs81508945 SNP in the *AKR1C3* was not found significantly associated with the breeding values for FCR or D110.

MBD5 is a member of the methyl-CpG-binding domain (MBD) family of proteins. It is highly expressed in neurons [54] and is involved in mediating DNA methylation [55]. MBD5 also plays an essential role in the regulation of postnatal growth and glucose homeostasis [56]. A study conducted on *MBD5* knockout mice revealed severe growth retardation and persistent hypoglycemia, hypoinsulinemia, enhanced glucose intolerance and elevated insulin sensitivity. Moreover, mice lacking the *MBD5* gene exhibited significantly smaller body size and reduction of subcutaneous and perigonadal fat [56]. Nevertheless, in this study the selected SNP rs332368013 in the *MBD5* was out of HWE. The protein encoded by ***OPRD1***, a member of the opioid family of G-protein-coupled receptor, is broadly distributed in a number of brain areas involved in the regulation of energy homeostasis [57]. In particular, ***OPRD1*** is highly expressed in olfactory bulb and anterior olfactory nucleus [58]. *OPRD1* knockout mice fed with high energy diet were found to be resistant to weight gain and had lower fat mass. They also exhibited higher energy expenditure due to increased thermogenic activity in the brown adipose tissue [57]. Additionally, a number of SNPs within the *OPRD1* gene were significantly associated with anorexia nervosa [59,60]. Although it would be interesting to examine the role of *OPRD1* for feed efficiency and growth, the minor allele frequency of the identified novel SNP within this gene was lower than 5 percent and thus it was excluded from the further analysis.

Conclusions

In summary, the present study demonstrated a number of chromosomal regions significantly associated with feed conversion efficiency and growth rate in the examined terminal pig sire line. Most of the regions were described for the first time, although some of them were located not far from previously reported QTLs. Validation of putative candidate genes from GWAS mapping near the significant SNPs confirmed a number of genes significantly associated with feed conversion efficiency and its related trait, days to 110 kg. Feed efficiency is a highly complex trait affected by a number of factors. This study suggests that the genetic predisposition of analysed traits is driven by lipogenesis, olfactory reception, and also immunological status. In depth characterisation of these genes to determine their molecular architecture and identify the causative mutations would be of benefit. Moreover, it would be useful to validate these SNPs in other commercial pig population regarding their effects on feed conversion efficiency and growth rate.

List of abbreviations

FCE: feed conversion efficiency, **FCR:** feed conversion ratio, **RFI:** residual feed intake, **D110:** days to 110 kg, **QTL:** quantitative trait locus, **GWAS:** genome-wide association study, **SSC:** Sus scrofa chromosome, **BLUP:** best linear unbiased prediction, **EBV:** estimated breeding value, **SNP:** single nucleotide polymorphism, **MAF:** minor allele frequency.

Declarations

Ethics approval and consent to participate

Animal care, slaughter and tissue collection of the animals used in this study were performed in compliance with national regulations related to animal research and commercial slaughtering and were approved by the local committees for the care and use of animals.

Competing interests

All authors declare no competing financial interests; with exception of PV, being employed by Hermitage Genetics, is involved in pig breeding and research on genetic improvement of terminal sire lines. Due to commercial restrictions, some of the data underlying the findings described in this manuscript cannot be made fully available.

Funding

This project has received funding from the European Union‘s Seventh Framework Programme for research, technological development and demonstration as part of the ECO-FCE project under grant agreement No. 311794. Hermitage Genetics is a partner of the ECO-FCE project and did not provide own funds for conducting this research.

Author’s contributions

JH performed SNP genotyping, carried out the data analysis and drafted the manuscript; RH supervised the research and edited the manuscript; HR participated in statistical analysis, supervised the research and edited the manuscript; PV provided the animals and was involved

in estimation of breeding values; KW designed and directed the study and edited the manuscript.

References

1. Patience JF, Rossoni-Serao MC, Gutierrez NA (2015) A review of feed efficiency in swine: biology and application. Journal of Animal Science and Biotechnology 6.
2. Saintilan R, Merour I, Brossard L, Tribout T, Dourmad JY, Sellier P, et al. (2013) Genetics of residual feed intake in growing pigs: Relationships with production traits, and nitrogen and phosphorus excretion traits. Journal of Animal Science 91: 2542-2554.
3. Wilkinson JM (2011) Re-defining efficiency of feed use by livestock. Animal 5: 1014-1022.
4. de Oliveira PSN, Cesar ASM, do Nascimento ML, Chaves AS, Tizioto PC, Tullio RR, et al. (2014) Identification of genomic regions associated with feed efficiency in Nelore cattle. Bmc Genetics 15.
5. Do DN, Strathe AB, Jensen J, Mark T, Kadarmideen HN (2013) Genetic parameters for different measures of feed efficiency and related traits in boars of three pig breeds. Journal of Animal Science 91: 4069-4079.
6. Sahana G, Kadlecova V, Hornshoj H, Nielsen B, Christensen OF (2013) A genome-wide association scan in pig identifies novel regions associated with feed efficiency trait. Journal of Animal Science 91: 1041-1050.
7. Luo WZ, Cheng DX, Chen SK, Wang LG, Li Y, Ma XJ, et al. (2012) Genome-Wide Association Analysis of Meat Quality Traits in a Porcine Large White x Minzhu Intercross Population. International Journal of Biological Sciences 8: 580-595.
8. Jiao S, Maltecca C, Gray KA, Cassady JP (2014) Feed intake, average daily gain, feed efficiency, and real-time ultrasound traits in Duroc pigs: II. Genomewide association. Journal of Animal Science 92: 2846-2860.
9. Onteru SK, Gorbach DM, Young JM, Garrick DJ, Dekkers JCM, Rothschild MF (2013) Whole Genome Association Studies of Residual Feed Intake and Related Traits in the Pig. Plos One 8.
10. Do DN, Strathe AB, Ostersen T, Pant SD, Kadarmideen HN (2014) Genome-wide association and pathway analysis of feed efficiency in pigs reveal candidate genes and pathways for residual feed intake. Frontiers in Genetics 5.
11. Do DN, Ostersen T, Strathe AB, Mark T, Jensen J, Kadarmideen HN (2014) Genome-wide association and systems genetic analyses of residual feed intake, daily feed consumption, backfat and weight gain in pigs. Bmc Genetics 15.
12. Varley PF, Sweeney T, Ryan MT, O'Doherty JV (2011) The effect of phosphorus restriction during the weaner-grower phase on compensatory growth, serum osteocalcin and bone mineralization in gilts. Livestock Science 135: 282-288.
13. Henderson CR (1975) Best linear unbiased estimation and prediction under a selection model. Biometrics 31: 423-447.
14. Cox DG, Kraft P (2006) Quantification of the power of Hardy-Weinberg equilibrium testing to detect genotyping error. Human Heredity 61: 10-14.
15. Yu JM, Pressoir G, Briggs WH, Bi IV, Yamasaki M, Doebley JF, et al. (2006) A unified mixed-model method for association mapping that accounts for multiple levels of relatedness. Nature Genetics 38: 203-208.

16. Ekine CC, Rowe SJ, Bishop SC, de Koning DJ (2014) Why breeding values estimated using familial data should not be used for genome-wide association studies. G3 (Bethesda) 4: 341-347.
17. Barrett JC, Fry B, Maller J, Daly MJ (2005) Haploview: analysis and visualization of LD and haplotype maps. Bioinformatics 21: 263-265.
18. Yue G, Stratil A, Kopecny M, Schroffelova D, Schroffel J, Hojny J, et al. (2003) Linkage and QTL mapping for Sus scrofa chromosome 6. Journal of Animal Breeding and Genetics 120: 45-55.
19. Munoz G, Ovilo C, Silio L, Tomas A, Noguera JL, Rodriguez MC (2009) Single- and joint- population analyses of two experimental pig crosses to confirm quantitative trait loci on Sus scrofa chromosome 6 and leptin receptor effects on fatness and growth traits. Journal of Animal Science 87: 459-468.
20. Becker D, Wimmers K, Luther H, Hofer A, Leeb T (2013) A Genome-Wide Association Study to Detect QTL for Commercially Important Traits in Swiss Large White Boars. Plos One 8.
21. Cepica S, Stratil A, Kopecny M, Blazkova P, Schroffel J, Davoli R, et al. (2003) Linkage and QTL mapping for Sus scrofa chromosome 4. Journal of Animal Breeding and Genetics 120: 28-37.
22. Duthie C, Simm G, Doeschl-Wilson A, Kalm E, Knap PW, Roehe R (2008) Quantitative trait loci for chemical body composition traits in pigs and their positional associations with body tissues, growth and feed intake. Animal Genetics 39: 130-140.
23. Gregersen VR, Conley LN, Sorensen KK, Guldbrandtsen B, Velander IH, Bendixen C (2012) Genome-wide association scan and phased haplotype construction for quantitative trait loci affecting boar taint in three pig breeds. Bmc Genomics 13.
24. Jiang L, Liu X, Yang J, Wang HF, Jiang JC, Liu LL, et al. (2014) Targeted resequencing of GWAS loci reveals novel genetic variants for milk production traits. Bmc Genomics 15.
25. Bosse M, Megens HJ, Frantz LAF, Madsen O, Larson G, Paudel Y, et al. (2014) Genomic analysis reveals selection for Asian genes in European pigs following human-mediated introgression. Nature Communications 5.
26. Jafarikia M, Methot S, Maignel L, Fortin F, Wyss S, Sullivan B, et al. (2015) Association of adiponectin and adiponectin receptor genes with sow productivity estimated breeding values. Molecular Biology Reports 42: 1391-1401.
27. Wang HY, Misztal I, Aguilar I, Legarra A, Fernando RL, Vitezica Z, et al. (2014) Genome-wide association mapping including phenotypes from relatives without genotypes in a single-step (ssGWAS) for 6-week body weight in broiler chickens. Frontiers in Genetics 5.
28. Rakhshandeh A, Dekkers JCM, Kerr BJ, Weber TE, English J, Gabler NK (2012) Effect of immune system stimulation and divergent selection for residual feed intake on digestive capacity of the small intestine in growing pigs. Journal of Animal Science 90: 233-235.
29. Roberts NE, Almond GW (2003) Infection of growing swine with porcine reproductive and respiratory syndrome virus and Mycoplasma hyopneumoniae - Effects on growth, serum metabolites, and insulin-like growth factor-I. Canadian Veterinary Journal-Revue Veterinaire Canadienne 44: 31-37.
30. Njoku CP, Adeyemi OA, Sogunle OM, Aina ABJ (20915) Growth performance, carcass yield and organ weight of growing pigs fed different levels of feed. Slovak Journal of Animal Science: 16-22.

31. Montagne L, Loisel F, Le Naou T, Gondret F, Gilbert H, Le Gall M (2014) Difference in short-term responses to a high-fiber diet in pigs divergently selected for residual feed intake. Journal of Animal Science 92: 1512-1523.
32. Vigors S, Torres S, Kelly AK, O'Shea CJ, Doyle DN, O'Doherty J (2014) Residual feed intake in pigs is associated with organ weight, nutrient digestibility and intestinal nutrient transporter gene expression. ADSA-ASAS-CSAS Joint Annual Meeting.
33. Ferrell CL, Jenkins TG (1985) Cow type and the nutritional environment: nutritional aspects. J Anim Sci 61: 725-741.
34. Lefaucheur L, Lebret B, Ecolan P, Louveau I, Damon M, Prunier A, et al. (2011) Muscle characteristics and meat quality traits are affected by divergent selection on residual feed intake in pigs. Journal of Animal Science 89: 996-1010.
35. Gabarrou JF, Geraert PA, Williams J, Ruffier L, Rideau N (2000) Glucose-insulin relationships and thyroid status of cockerels selected for high or low residual food consumption. Br J Nutr 83: 645-651.
36. Lkhagvadorj S, Qu L, Cai WG, Couture OP, Barb CR, Hausman GJ, et al. (2010) Gene expression profiling of the short-term adaptive response to acute caloric restriction in liver and adipose tissues of pigs differing in feed efficiency. American Journal of Physiology-Regulatory Integrative and Comparative Physiology 298: R494-R507.
37. Gondret F, Vincent A, Houee-Bigot M, Siegel A, Lagarrigue S, Louveau I, et al. (2016) Molecular alterations induced by a high-fat high-fiber diet in porcine adipose tissues: variations according to the anatomical fat location. Bmc Genomics 17.
38. Vincent A, Louveau I, Gondret F, Trefeu C, Gilbert H, Lefaucheur L (2015) Divergent selection for residual feed intake affects the transcriptomic and proteomic profiles of pig skeletal muscle. Journal of Animal Science 93: 2745-2758.
39. Yu YJ, Okayasu R, Weil MM, Silver A, McCarthy M, Zabriskie R, et al. (2001) Elevated breast cancer risk in irradiated BALB/c mice associates with unique functional polymorphism of the Prkdc (DNA-dependent protein kinase catalytic subunit) gene. Cancer Research 61: 1820-1824.
40. Wong RHF, Chang I, Hudak CSS, Hyun S, Kwan HY, Sul HS (2009) A Role of DNA-PK for the Metabolic Gene Regulation in Response to Insulin. Cell 136: 1056-1072.
41. Raffler NA, Rivera-Nieves J, Ley K (2005) L-selectin in inflammation, infection and immunity. Drug Discovery Today: Therapeutic Strategies 2: 213-220.
42. Nelson RM, Aruffo A, Dolich S, Cecconi O, Mannori G, Bevilacqua MP (1992) Quantitative-determination of selectin-carbohydrate interactions. Cold Spring Harbor Symposia on Quantitative Biology 57: 271-279.
43. Cottam DR, Schaefer PA, Fahmy D, Shaftan GW, Angus LDG (2002) The effect of obesity on neutrophil Fc receptors and adhesion molecules (CD16, CD11b, CD62L). Obesity Surgery 12: 230-235.
44. Yang XD, Karin N, Tisch R, Steinman L, McDevitt HO (1993) Inhibition of insulitis and prevention of diabetes in nonobese diabetic mice by blocking l-selectin and very late antigen-4 adhesion receptors. Proceedings of the National Academy of Sciences of the United States of America 90: 10494-10498.
45. Kretowski A, Kinalska I (2000) L-selectin gene T668C mutation in type 1 diabetes patients and their first degree relatives. Immunology Letters 74: 225-228.
46. Khazen D, Jendoubi-Ayed S, Aleya WB, Sfar I, Mouelhi L, Matri S, et al. (2009) Polymorphism in ICAM-1, PECAM-1, E-selectin, and L-selectin genes in Tunisian patients with inflammatory bowel disease. European Journal of Gastroenterology & Hepatology 21: 167-175.

47. Benod C, Villagomez R, Filgueira CS, Hwang PK, Leonard PG, Poncet-Montange G, et al. (2014) The Human Orphan Nuclear Receptor Tailless (TLX, NR2E1) Is Druggable. Plos One 9.
48. Christie BR, Li MA, Redila VA, Booth H, Wong BKY, Eadie BD, et al. (2006) Deletion of the nuclear receptor Nr2e1 impairs synaptic plasticity and dendritic structure in the mouse dentate gyrus. Neuroscience 137: 1031-1037.
49. Kumar RA, McGhee KA, Leach S, Bonaguro R, Maclean A, Aguirre-Hernandez R, et al. (2008) Initial association of NR2E1 with bipolar disorder and identification of candidate mutations in bipolar disorder, schizophrenia, and aggression through resequencing. American Journal of Medical Genetics Part B-Neuropsychiatric Genetics 147B: 880-889.
50. Aime P, Palouzier-Paulignan B, Salem R, Al Koborssy D, Garcia S, Duchamp C, et al. (2014) Modulation of olfactory sensitivity and glucose-sensing by the feeding state in obese Zucker rats. Frontiers in Behavioral Neuroscience 8.
51. White DL, Liu YH, Tsavachidis S, Tabasi ST, Kuzniarek J, Jiao L, et al. (2014) Sex Hormone Pathway Gene Polymorphisms Are Associated With Risk of Advanced Hepatitis C-Related Liver Disease in Males. Gastroenterology 146: S968-S968.
52. Svensson PA, Gabrielsson BG, Jernas M, Gummesson A, Sjoholm K (2008) Regulation of human aldoketoreductase 1c3 (akr1c3) gene expression in the adipose tissue. Cellular & Molecular Biology Letters 13: 599-613.
53. Gonzalez-Muniesa P, Marrades MP, Martinez JA, Moreno-Aliaga MJ (2013) Differential Proinflammatory and Oxidative Stress Response and Vulnerability to Metabolic Syndrome in Habitual High-Fat Young Male Consumers Putatively Predisposed by Their Genetic Background. International Journal of Molecular Sciences 14: 17238-17255.
54. Kwon DY, Zhou ZL (2014) Trapping MBD5 to understand 2q23.1 microdeletion syndrome. Embo Molecular Medicine 6: 993-994.
55. Walz K, Young JI (2014) The methyl binding domain containing protein MBD5 is a transcriptional regulator responsible for 2q23.1 deletion syndrome. Rare Diseases 2(1):e967151.
56. Du YR, Liu B, Guo F, Xu GF, Ding YQ, Liu Y, et al. (2012) The Essential Role of Mbd5 in the Regulation of Somatic Growth and Glucose Homeostasis in Mice. Plos One 7.
57. Czyzyk TA, Romero-Pico A, Pintar J, McKinzie JH, Tschop MH, Statnick MA, et al. (2012) Mice lacking delta-opioid receptors resist the development of diet-induced obesity. Faseb Journal 26: 3483-3492.
58. Yilmaz Z, Hardaway JA, Bulik CM (2015) Genetics and Epigenetics of Eating Disorders. Adv Genomics Genet 5: 131-150.
59. Brown KMO, Bujac SR, Mann ET, Campbell DA, Stubbins MJ, Blundell JE (2007) Further evidence of association of OPRD1 & HTR1D Polymorphisms with susceptibility to anorexia nervosa. Biological Psychiatry 61: 367-373.
60. Bergen AW, van den Bree MB, Yeager M, Welch R, Ganjei JK, Haque K, et al. (2003) Candidate genes for anorexia nervosa in the 1p33-36 linkage region: serotonin 1D and delta opioid receptor loci exhibit significant association to anorexia nervosa. Mol Psychiatry 8: 397-406.

Table 1 Forward and reverse primers for PCR amplification of the twelve selected positional candidate genes located within 1Mb of the genome-wide significant markers for EBVs FCR and D110.

Gene	Ensembl reference	Size (bp)	Forward	Reverse
CD164	*ENSSSCG00000004414*	713	TGTGTCTGTCCAGTTTCTTCGC	TGAAGTCAGGCTGGGGATTACG
NR2E1	*ENSSSCG00000004384*	706	TCTCCCTTCCCTCTCTTCACCT	ACCTACGCTGCCCTCTGATTTC
SMPD2	*ENSSSCG00000004408*	697	CCTCCTCTCTGACCCTCTCTCT	TGGGGCTGTCTGTTTCTTCC
PRKDC	*ENSSSCG00000006274*	735	AGGAAACACGCCTCAGTTGGTA	ACGCAGGAGACAGAAGGAAAGC
SELL	*ENSSSCG00000006287*	706	TCTCAAAACAAATGTCTGTGGCTGT	GGTTATCTTCTGGGCAACTCACC
SELP	*ENSSSCG00000006288*	350	ACCTGAATCCAACCTCTCTCCA	TGCATCTGAAGTAGCAAGTCGT
OPRD1	*ENSSSCG00000027401*	718	GCTCCCATCCACATCTTCGTCA	CCCCTCAATTCCACCTTCCTCA
WDTC1	*ENSSSCG00000003570*	567	CCAGGGACCAAGACAACCGA	CACCATACCTCACAGCAACGC
AKR1C3	*ENSSSCG00000030447*	792	GCTGACACTTAGCAGTTGAGGAATA	GGTGGAGGAAAGAGGAGTTAAATACA
KLF6	*ENSSSCG00000028828*	702	GACCAACAGCCTGAACTCGGA	CCCTGAGTCTCACTTCCCCAAA
MBD5	*ENSSSCG00000015667*	773	ACTTGGAAGCCCTGATGTTTTCAC	ACCCTATCGTTGACCTTGGTGAC
MMADHC	*ENSSSCG00000028646*	696	GGATTCTCCGTTGATGATCTTGGC	CCTTATTCTTCTTTCCCGCACAAAC

Table 2 Genes located closest to the genome-wide significant SNPs.

EBV[$]	SNP	Neglog$_{10}$ (p-value)	SSC*	Position (bp)	Region	Nearest gene*	Gene position (bp)
FCR	H3GA0002102	6.32	1	84,686,166	Intronic	*ENSSSCG00000004415*	84,644,862 - 84,709,541
FCR	MARC0000845	6.26	4	86,747,415	Intergenic	*ENSSSCG00000024309*	86,796,081 - 86,804,148
FCR	ALGA0026204	6.47	4	87,021,547	Intergenic	*MCM4*	87,134,012 - 87,185,073
FCR	H3GA0013204	7.96	4	88,311,790	Intergenic	*METTL11B*	88,441,595 - 88,460,670
FCR	ALGA0026230	6.84	4	89,104,182	Intronic	*F5*	89,027,936 - 89,109,573
FCR	ALGA0026233	6.91	4	89,118,147	Intergenic	*F5*	89,027,936 - 89,109,573
FCR	ASGA0028724	6.44	6	78,297,229	Intergenic	*FGR*	78,358,088 - 78,326,491
FCR	ALGA0035847	6.43	6	80,577,487	Intergenic	*PTPRU*	80,106,273 - 80,024,322
FCR	MARC0015113	7.40	15	146,404,317	Intronic	*DIS3L2*	146,381,891 - 146,596,424
FCR	ALGA0119312	6.27	15	149,350,761	Intergenic	*ARL4C*	149,122,784 - 149,123,362
D110	ALGA0060013	6.32	10	72,375,760	Intergenic	*AKR1C3*	72,091,036 - 72,106,952
D110	H3GA0030777	6.92	10	72,766,001	Intergenic	*KLF6*	72,992,245 - 73,001,823
D110	MARC0036947	6.92	15	2,640,639	Intergenic	*LYPD6B*	2,443,675 - 2,456,793
D110	ALGA0115976	6.89	15	2,798,633	Intronic	*KIF5C*	2,730,359 - 2,901,565
D110	ALGA0113899	6.78	15	2,835,746	Intronic	*KIF5C*	2,730,359 - 2,901,565
D110	MARC0072361	7.75	15	2,843,921	Intronic	*KIF5C*	2,730,359 - 2,901,565
D110	ALGA0083417	8.15	15	3,322,649	Intergenic	*MBD5*	3,354,689 - 3,361,520

[$]Estimated breeding value; *Sscrofa 10.2 assembly.

Table 3 Top molecular themes for the positional and functional candidate genes located within 1Mb of the genome-wide significant markers for EBV of FCR and D110.

EBV	Category	B-H p-value*	Genes
FCR	Hematological System Development and Function	8.53E-05-9.68E-02	*CEBPD, SRSF4,* ***SELL****, ATPIF1, FGR, SELE, F5, THEMIS2, EPB41, HTR2B,* ***SELP****, ZBTB24, WASF2,* ***PRKDC****, FOXO3,* ***OPRD1***
FCR	Immune Cell Trafficking	8.53E-05-9E-02	***SELP****,* ***SELL****, FGR, SELE, F5, FOXO3,* ***OPRD1***
FCR	Lymphoid Tissue Structure and Development	2.89E-03-9E-02	*THEMIS2,* ***SELP****,* ***SELL****, SELE, F5,* ***PRKDC***
FCR	Organ Morphology	2.89E-03-9.68E-02	*CEBPD,* ***SELL****, ECEL1,* ***NR2E1****,* ***SELE****, CHRNG, WASF1, GPR3, EIF4E2, HTR2B, CHRND,* ***SELP****, KIFAP3, SEC63, SYTL1,* ***PRKDC****, FOXO3*
FCR	Organismal Development	2.89E-03-9.14E-02	*CEBPD,* ***SELL****, ATPIF1,* ***NR2E1****, FGR, SELE, F5, NPPC, WASF1, GPR3, THEMIS2, EIF4E2, HTR2B,* ***SELP****, KIFAP3, WASF2,* ***PRKDC****, FOXO3*
D110	Endocrine System Development and Function	4.7E-06-8.62E-02	***AKR1C3****,* ***MBD5****, ACVR2A, AKR1C1/AKR1C2, AKR1C4*
D110	Small Molecule Biochemistry	4.7E-06-6.21E-02	*PFKP,* ***AKR1C3****,* ***MBD5****, ACVR2A, AKR1C1/AKR1C2, AKR1C4*
D110	Energy Production	3.51E-05-2.45E-02	***AKR1C3****, AKR1C1/AKR1C2, AKR1C4*
D110	Lipid Metabolism	6.06E-05-5.44E-02	***AKR1C3****, AKR1C1/AKR1C2, AKR1C4*
D110	Drug Metabolism	3.68E-04-3.01E-02	***AKR1C3****, AKR1C1/AKR1C2, AKR1C4*

*Range of B-H multiple testing correction p-values of enriched biological functions within the category; candidate genes selected for downstream validation are highlighted in bold.

Table 4 Top canonical pathways for the positional and functional candidate genes located within 1Mb of the genome-wide significant markers for EBV of FCR and D110.

EBV	Ingenuity Canonical Pathways	P-value	Genes
FCR	Cell Cycle Control of Chromosomal Replication	4.66E-03	*RPA2, MCM4*
FCR	Estrogen Receptor Signaling	1.27E-02	*TAF12, MED18,* ***PRKDC***
FCR	PXR/RXR Activation	2.59E-02	*UGT1A1, FOXO3*
FCR	Granulocyte Adhesion and Diapedesis	2.62E-02	***SELP***, ***SELL***, *SELE*
FCR	Sphingomyelin Metabolism	2.96E-02	***SMPD2***
D110	Bile Acid Biosynthesis, Neutral Pathway	5.57E-08	***AKR1C3***, *AKR1C1/AKR1C2, AKR1C4*
D110	TR/RXR Activation	1.87E-05	*PFKP,* ***AKR1C3***, *AKR1C1/AKR1C2*
D110	Androgen Biosynthesis	3.32E-05	***AKR1C3***, *AKR1C4*
D110	Methylglyoxal Degradation III	4.38E-05	***AKR1C3***, *AKR1C1/AKR1C2*
D110	Retinoate Biosynthesis I	1.91E-04	***AKR1C3***, *AKR1C4*

Candidate genes selected for downstream validation are highlighted in bold.

Table 5 Observed and expected heterozygosity of the SNPs selected for validation.

Gene	SNP	Location (SSC 10.2)	Alleles	Variant	MAF	Observed heterozygosity	Expected heterozygosity	HWE[£]
MBD5	rs332368013	15:3,359,994	A/G	missense	0.300	0.471	0.420	0.014*
NR2E1	rs340456509	1:83,552,036	G/T	intron	0.211	0.359	0.334	0.155
PRKDC	rs80900450	4:87,256,301	C/T	missense	0.268	0.370	0.392	0.282
SELL	rs319738340	4:88,935,116	C/T	splice region	0.166	0.276	0.276	1
AKR1C3	rs81508945	10:72,102,793	G/C	missense	0.120	0.213	0.212	1
OPRD1	NOVEL	6:79,658,669	C/A	downstream	0.022	0.044	0.043	1

[£]p-value for test for departure from Hardy-Weinberg Equilibrium (HWE); *Significant departure from HWE ($p<0.05$)

Table 6 Association of the five SNPs, located in selected functional genes mapped within 1Mb of the genome-wide significant markers, with breeding values for FCR and D110. Lower breeding values indicate higher feed efficiency.

SNP (gene)	Trait	P-value	Least squares means of EBVs per genotype			Additive effect		Dominant effect	
rs80900450 (*PRKDC*)			C/C n=36	C/T n=161	T/T n=238	P-value	a[1] (variance[2])	P-value	d[1] (variance[2])
	EBV D110	0.085	-8.771 ±5.80	-8.416 ±5.78	-9.214 ±5.78				
	EBV FCR	**<.0001**	-0.036 ±0.15	-0.057 ±0.15	-0.084 ±0.15	**<.0001**	0.0377 (5%)	0.838	0.0026
rs319738340 (*SELL*)			C/C n=303	C/T n=120	T/T n=12				
	EBV D110	0.366	-8.899 ±5.78	-8.389 ±5.78	-9.142 ±5.86				
	EBV FCR	**0.026**	-0.073 ±0.15	-0.049 ±0.15	-0.047 ±0.15	0.852	-0.0019	0.800	0.0048
rs340456509 (*NR2E1*)			G/G n=265	T/G n=156	T/T n=14				
	EBV D110	**0.033**	-9.224 ±5.78	-8.327 ±5.78	-7.631 ±5.84	**<.0001**	-0.4849 (16%)	**0.044**	-0.2665 (1%)
	EBV FCR	**<.0001**	-0.085 ±0.15	-0.047 ±0.15	-0.021 ±0.15	**0.015**	-0.0230 (1%)	0.559	-0.0101
rs81508945 (*AKR1C3*)			C/C n=6	C/G n=93	G/G n=337				
	EBV D110	0.195	-6.632 ±5.92	-8.561 ±5.79	-8.953 ±5.78				
	EBV FCR	0.468	-0.043 ±0.15	-0.058 ±0.15	-0.069 ±0.15				

Significant associations are in bold; [1]Additive (a) and dominant (d) effect of an allelic substitution on a phenotype; [2] Phenotypic variance in percentage explained by SNP; Where delta was not significant, the alpha was reported from the first regression model.

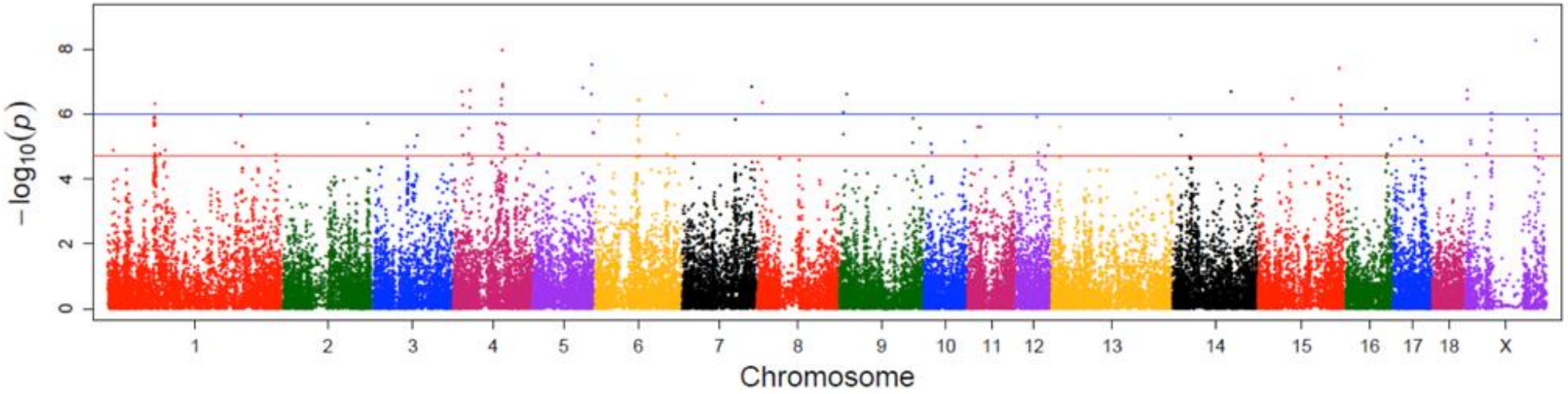

Fig 1 Manhattan plot of the genome-wide association analysis of EBV FCR. The red line indicates the suggestive significance threshold (-log10[p-value] ≥ 4.7) and the blue line corresponds to Bonferroni-adjusted genome-wide significance threshold (-log10[p-value] ≥ 6)

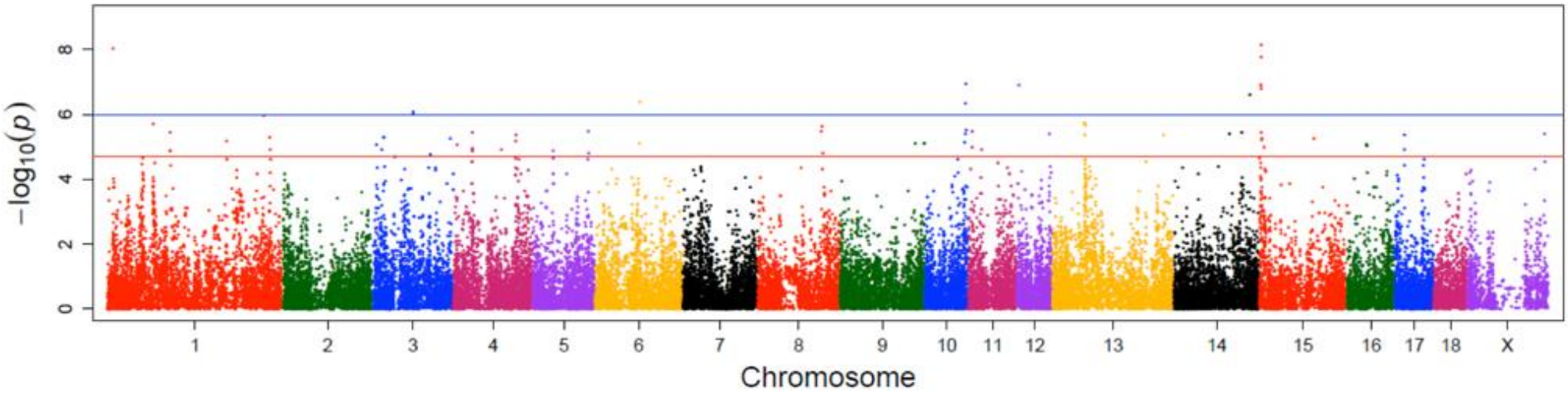

Fig 2 Manhattan plot of the genome-wide association analysis of EBV D110. The red line indicates the suggestive significance threshold (-log10[p-value] ≥ 4.7) and the blue line corresponds to Bonferroni-adjusted genome-wide significance threshold (-log10[p-value] ≥ 6).

Supporting Information

S1 Table. Chromosomal position and minor allele frequency (MAF) of markers significantly (-log10[p-value] ≥ 4.7) associated with breeding value of days to 110 kg (BV_D11) and breeding value of feed conversion ratio (BV_FCR) in a commercial pig population (n = 940). (PDF)

Analysis of meat quality traits and gene expression profiling of pigs divergent in residual feed intake

Justyna Horodyska[a,b], Michael Oster[b], Henry Reyer[b], Anne Maria Mullen[a], Peadar G. Lawlor[c], Klaus Wimmers[b,d], Ruth M. Hamill[a]*

[a] Teagasc, Food Research Centre, Ashtown, Dublin 15, Ireland

[b] Leibniz Institute for Farm Animal Biology (FBN), Institute for Genome Biology, Dummerstorf, Germany

[c] Teagasc, Pig Development Department, AGRIC, Moorepark, Fermoy, Co. Cork, Ireland

[d] Faculty of Agricultural and Environmental Sciences, University Rostock, Rostock, Germany

*Corresponding author

Published in: Meat Science (2017), 137, 265–274

The final publication is available at https://doi.org/10.1016/j.meatsci.2017.11.021 [DOI: 10.1016/j.meatsci.2017.11.021]

Abstract

Residual feed intake (RFI), the difference between actual feed intake and predicted feed requirements, is suggested to impact various aspects of meat quality. The objective of this study was to investigate the molecular mechanisms underpinning the relationship between RFI and meat quality. Technological, sensory and nutritional analysis as well as transcriptome profiling were carried out in *Longissimus thoracis et lumborum* muscle of pigs divergent in RFI (n = 20). Significant differences in sensory profile and texture suggest a minor impairment of meat quality in more efficient pigs. Low RFI animals had leaner carcasses, greater muscle content and altered fatty acid profiles compared to high RFI animals. Accordingly, differentially expressed genes were enriched in muscle growth and lipid & connective tissue metabolism. Differences in protein synthesis and degradation suggest a greater turnover of low RFI muscle, while divergence in connective tissue adhesion

may impact tenderness. Fatty acid oxidation tending towards decrease could possibly contribute to reduced mitochondrial activity in low RFI muscle.

Key words: Pork quality, Feed efficiency, FE, RFI, Transcriptomics, RNA

1 Introduction

Producing meat more feed efficiently has been a major goal in pig breeding. Improvement in pig production efficiency is being targeted through selection for enhanced feed efficiency (FE), which is an indicator of an animal's efficiency in converting feed into live weight (Wilkinson, 2011). Residual feed intake (RFI), a measure of FE, refers to a difference between an individual's actual feed intake and its expected nutritional requirements due to maintenance and growth (Saintilan, et al., 2013). A low RFI indicates a decreased energy requirement for maintenance (Hoque & Suzuki, 2009), therefore less feed is needed and production is more efficient. RFI is a moderately heritable trait with estimates ranging from 0.15 to 0.40, which makes it a suitable trait for genetic improvement (Fan, et al., 2010). A gene expression profiling of skeletal muscle from RFI divergent Large White pigs, carried out using microarrays, revealed 1,000 differentially expressed (DE) probes. Genes significantly up-regulated in low RFI pigs were mainly associated with protein synthesis, while down-regulated genes were predominantly involved in mitochondrial energy metabolism (Vincent, et al., 2015). Moreover, RNA sequencing of skeletal muscle in RFI divergent Yorkshire boars identified 99 DE genes (Jing, et al., 2015). Similarly to the study carried out on Large White pigs described above, genes associated with skeletal muscle differentiation and proliferation were up-regulated and genes involved in mitochondrial energy metabolism were down-regulated in low RFI pigs. Although a high level of correlation between microarray and RNA sequencing platforms have been reported, shorter and less abundant transcripts have a higher possibility to be detected using microarray approach (Nazarov, et al., 2017). Therefore in these cases and particularly in quantifying microRNA, microarray might outperform RNA sequencing (Git, et al., 2010; Nazarov, et al., 2017). Nevertheless, one of the downsides of using microarrays is that a number of genes / mRNA isoforms are not incorporated (Bumgarner, 2013).There is evidence that selection for reduced RFI pigs is associated with leaner carcasses (Lefaucheur, et al., 2011, Faure, et al., 2013, Smith et al., 2014) with greater muscle content (Lefaucheur, et al., 2011) and reduced

back-fat thickness (Lefaucheur, et al., 2011, Faure, et al., 2013). Moreover, decreased intramuscular fat content (Lefaucheur, et al., 2011, Smith et al., 2014) and ultimate pH as well as greater drip loss (Lefaucheur, et al., 2011, Faure, et al., 2013) and lighter meat colour (Lefaucheur, et al., 2011) have been reported in meat produced from low RFI pigs (Faure, et al., 2013). Nevertheless, the relationship between RFI and meat quality is not fully elucidated and the biological processes associated with RFI which impact meat quality are not well understood. Therefore the objectives of this study were to investigate 1) the technological, sensory and nutritional quality of pork from pigs differing in RFI, 2) the molecular mechanisms induced in muscle tissue contributing to differences in RFI using microarray platform and 3) the functional networks underpinning the potential relationship between meat quality and RFI.

2 Materials and methods

2.1 Animals and experimental design

Animal care, slaughter and tissue collection of the animals used in this study were performed in compliance with national regulations related to animal research and commercial slaughtering and were approved by the local committees for the care and use of animals of the Teagasc and the Leibniz Institute for Farm Animal Biology. This study involved 80 pigs (39 gilts and 41 boars) from the cross Maxgro (Hermitage Genetics) x (German Landrace x Large White), which represented the intact litters of 7 sows inseminated with semen from 4 boars (Hermitage Genetics, Kilkenny, Ireland) having a high estimated breeding value for feed conversion efficiency. As previously described in Metzler-Zebell, et al. (2017), pigs were weaned at 28 days of age and sibling groups were group-housed. All pigs were provided with the same sequence of diets, with the same ingredient and chemical composition (starter, link, weaner and finisher), via Feed Intake Recording Equipment (FIRE) feeders (Schauer Agrotonic, Wels, Austria). Pigs had *ad libitum* access to feed and water. Pigs were placed on test between day 42 and 91 post-weaning, whereby intake was recorded daily, and pig weight and back-fat depth was recorded weekly. Average daily feed intake (ADFI) and average daily gain (ADG) from day 42 to day 91 post-weaning were calculated for each pig. RFI was calculated at the end of the test period as the residuals from a least squares regression model of ADFI on ADG, metabolic live weight, gender and also all relevant two-way interactions, and the effects of back-fat and muscle depth using the PROC REG procedure in SAS (version

9.4; SAS Inst. Inc., Cary, NC, USA). Pigs were categorised as the highest and lowest RFI within litter and gender. Out of the 80 pigs, a total of 20 divergent sib-pairs of gilts (10 low (L) and 10 high (H) RFI from lowest and highest quartile, respectively) with an average final body weight of 101kg (SD: 7.6kg) (average birth weight: 1.2kg, SD: 0.2kg) were selected for transcriptomic and meat quality evaluation. Growth performance parameters of the pigs selected for further evaluation are depicted in Table S1. Prior to slaughter, the animals were fasted for 18 hours. The pigs were electronically stunned followed by exsanguination. A sample of the *Longissimus thoracis et lumborum* (LTL) muscle was collected from each carcass, cut up finely and preserved in RNALater® (Ambion Inc., Austin, USA) within 10 minutes post-slaughter. It was then stored overnight at 4°C followed by storage at -80°C until RNA isolation. For meat quality measurements, the LTL muscle was excised from each carcass 24 hours *post-mortem* (*pm*). Assignment of LTL muscle for transcriptome and meat quality analysis is depicted in Fig. 1.

2.2 Meat and carcass quality measurements

2.2.1 Carcass grading. Based on the difference in light reflectance of tissues, carcass was measured for fat thickness and muscle depth between 3rd and 4th rib on the day of slaughter using Hennessy Grading Probe (Hennessy Grading Systems Ltd., Auckland, New Zealand).

2.2.2 pH. pH of LTL muscle was measured at 45 minutes (pH 45m), 3 hours (pH 3h) and 24 hours (pH 24h) *pm*, using a portable Hanna pH meter (Hanna Instruments, Woonsocket, RI, USA). A previously calibrated pH probe was inserted in the LTL between the 12th and 13th rib.

2.2.3 Colour. Meat colour of the fresh chops and after 1h of blooming was recorded at day 1 pm. It was measured with MiniScan XE Plus (Hunter Associates Laboratory Inc., Virginia, USA) using CIE L* (lighteness), a* (redness) and b* (yellowness) colour scale. The measurements were taken at three locations on each chop and averaged.

2.2.4 Drip loss (DL). Drip loss was measured using the bag method of Honikel (1998), whereby pork chops measuring 2.5cm in thickness were trimmed of the adipose tissue and epimysium at day 1 pm, to a weight of 80g±1g. Each pork chop was then suspended by string inside an inflated plastic bag, ensuring that the meat did not make direct contact with the bag.

The bag was then sealed and suspended for 48 h at 4 °C. Thereafter, the samples were dried with paper towel, weighed and drip loss was expressed as percentage of the original weight of the chop.

2.2.5 Cook loss (CL). Samples frozen at -20°C on day 1 and day 7 *pm* were thawed in bags in a circulating water bath at 20°C. The muscle chops were then trimmed of external fat to a similar size, dried with a paper towel and weighed. They were placed in plastic bags and immersed in a water bath (Grant Instruments Ltd., England) at 77°C until they reached a core temperature of 75°C was measured with a temperature probe (Eirelec Ltd., Ireland). The samples were allowed to cool at room temperature. Weight of the chops was recorded followed by refrigerated storage. The cook loss was expressed as a percentage of the raw weight of the chop.

2.2.6 Warner Bratzler shear force (WBSF). After cook loss was determined, the samples were used to measure WBSF according to AMSA guidelines, 1995. Briefly, six cores of 1.25cm diameter were obtained from each sample. The cores were cut in parallel to the longitudinal orientation of fibres and were sheared perpendicularly to the muscle fibres long axis with a shear blade using 500N load cell at a crosshead spead of 50mm/min (Instron model 5543). Data was analysed using Blue Hill software (Instron Ltd., Buckinghamshire, UK).

2.2.7 Protein, moisture and intramuscular fat (IMF) and mineral content. Samples frozen at -20°C on day 1 *pm* were thawed in bags in a circulating water bath at 20°C. Muscle chops were then trimmed of external fat and homogenized using a Robot Coupe blender (R301 Ultra, Robot coupe SA, France). Protein content was measured with a Leco Nitrogen/Protein Analyser (FP-528, Leco Corp., MI, USA) using the Dumas method in accordance with AOAC method 992.15, 1990. IMF and moisture were measured with NMR Smart Trac & Smart 5 Rapid Fat and Moisture Analyser (CEM Corporation, USA) using AOAC method 985.14 and 985.26, 1990. Ash content was determined by calcination of the meat samples in a muffle furnace at 540°C (AOAC method 923.03). The analysis for each sample was carried out in duplicate and the mean recorded.

2.2.8 Fatty acid (FA) profile. Frozen samples (day 1 *pm*) were transported to a commercial laboratory for FA profile analysis. Intramuscular fat was extracted from LTL muscle and

fatty acid methyl esters were prepared and analysed using Gas Chromatography - Flame Ionization Detector (GC - FID) in accordance with SAL Cam Nut003 method (Pearson's Chemical Analysis of Foods, 9th Edition, Longman Group UK Limited, 1991, 0-582-40910-1). Results were expressed as mg fatty acid per 100g meat.

2.2.9 Sensory assessment. Panellists received a total of 60 hours training in red meat texture, flavour and after-effects (AMSA, 2015). Prior to assessment of the actual samples, the trained panellists were familiarised with pork samples from the sample set. Accuracy and repeatability of the panellists were then examined using PanelCheck software (version 2, 1991, Free Software Foundation, Inc., MA, USA). Vacuum packed chops were aged at 4°C for 7 days followed by freezing. A day before sensory assessment, the chops were thawed overnight in the fridge. The chops were then grilled (Velox grill, Silesia Velox UK Ltd., Oxfordshire, England) until the core temperature reached 70°C and cut into 2.5 cm x 2 cm cubes. The 20 samples were combined with an additional set of 40 samples from a separate trial. A total of 60 samples were assessed over 5 sessions. Each 3-hour session consisted of 12 randomised samples and was evaluated by trained panellists (n=8) rating the pork chops sensory attributes on a scale of 1 (very poorly detectable attribute) to 100 (extremely detectable attribute).

2.2.10 Statistical analysis. PROC MIXED procedure in the SAS system was used to evaluate associations between RFI and meat quality traits in the Maxgro x (Landrace x Large White) gilts (n = 20). The model included RFI groups as a fixed effect, sow as a random effect and pre-slaughter live weight as a covariate, as well as the absolute values of RFI as a weight statement to account for differences in RFI values within the RFI groups.

2.3 RNA isolation and cDNA synthesis

According to the manufacture’s protocol total RNA from preserved LTL muscle of 10 biological replicates per RFI group was extracted using Tri-Reagent (Sigma-Alrich, Taufkirchen, Germany). It was then subjected to DNase treatment and a column-based purification using the Nucleospin RNA II kit (Macherey-Nagel, Düren, Germany). RNA samples were analysed for integrity and quantity using agarose gel electrophoresis and Nanodrop ND-1000 spectrophotometer (PEQLAB, Erlangen, Germany). RNA samples were also checked for DNA contamination by PCR of the porcine glyceraldehyde-3-phosphate

dehydrogenase (GAPDH) gene (Forward primer: AAGCAGGGATGATGTTCTGG; Reverse primer: ATGCCTCCTGTACCACCAAC). For cDNA synthesis, 1 µg of total RNA was utilised in presence of random primers (Promega, Mannheim, Germany), oligo (dT) primer and Superscript® III reverse transcriptase (Invitrogen Corp., San Diego, CA, USA).

2.4. Microarray hybridisation

Double stranded cDNA was synthesised using total RNA, which served as a template in the subsequent in vitro transcription reaction. Antisense cRNA was then purified and sense-strand cDNA was synthesised by the reverse transcription of cRNA, using a GeneChip® WT Amplification Kit (Affymetrix, Santa Clara, CA, USA). Biotin-labeled cDNA was then fragmented with GeneChip® WT Terminal Labeling Kit (Affymetrix) and injected onto porcine snowball arrays (Affymetrix) containing 47,845 probe sets with a mean coverage of 22 probes per transcript (Freeman, et al., 2012). The arrays were incubated for 16 hours at 45°C in Affymetrix GeneChip Hybridization Oven 640. After hybridisation, the arrays were washed and stained with streptavidin-phycoerythrin antibody solution (Affymetrix) on an Affymetrix GeneChip Fluidic Station 450 station. The arrays were then scanned with Affymetrix GeneChip Scanner 3000. Microarray images were quantified using GCOS 1.1.1 (Affymetrix) and raw data was deposited in a MIAME-compliant database, the National Center for Biotechnology Information Gene Expression Omnibus (www.ncbi.nlm.nih.gov/geo) (accession number: GSE99653).

2.5 Analysis of microarray data and functional annotation

Bioinformatic analysis of the microarrays, including pre-processing and normalisation, was implemented using R packages (affy, arrayQualityMetrics, genefilter, affyPLM and vsn) (version 3.1.1, https://www.R-project.org/). Robust multi-array average (RMA) normalisation (Log2) was performed and probe sets with a low standard deviation (std $\leq$ 0.23) were discarded. A further filtering step involved filtering by both control probe sets and means (means $\leq$ 2.5 were rejected). PROC MIXED including RFI groups and sow as fixed effects and birth weight as a covariate was implemented in JMP Genomics 6 software of SAS (version 6, SAS INST.) to determine relative changes in transcript abundances (fold change). The corresponding false discovery rate (q-value) (Storey & Tibshirani, 2003) was calculated using the qvalue R package (version 3.1.1, https://www.R-project.org/). Relative changes in transcript abundance significant at the nominal 0.05 level were subjected to further ontology

analysis (Ingenuity Pathway Analysis; Ingenuity® Systems, http://www.ingenuity.com/). Benjamini-Hochberg corrected p-values were used to detect the most significant canonical pathways ($P < 0.05$) and to map the genes to the most significant molecular and cellular functions ($P < 0.05$) contained in the IPA library. Functional annotations with a z-score > 2 were considered significantly activated in low RFI pigs. Information contained in the Ingenuity® Knowledge Base was used to create potential important networks of DE genes. A list of DE microRNAs (miRNAs; represented on the snowball array) along with DE transcripts and related fold changes ($P \leq 0.05$) were submitted to Ingenuity miRNA Target Filter (http://www.ingenuity.com/) to predict target transcripts regulated by these miRNAs and to investigate miRNA–mRNA expression patterns. Additionally, potential networks of the DE transcripts that were predicted to be regulated by the DE miRNAs were generated.

2.6 Microarray validation

In order to validate the microarray results, six DE genes involved in lipid and energy metabolism (*ACACA*, *ACSL1*, *BCL2*, *MMP2*, *SDHB* and *TFAM*) were selected for quantitative real-time PCR (qPCR), whereby *RPL10* and *RPL32* were used as housekeeping genes. Primers for target genes were designed online with Primer3 software (http://bioinfo.ut.ee/primer3-0.4.0/) based on Sus scrofa nucleotide sequences. Specificity of primers was determined with the BLAST search tool in the NCBI database (http://www.ncbi.nlm.nih.gov/BLAST). Primer sets for selected reference and target genes are listed in Table S2. qPCR was carried out on 96-well plates using 7500 system (Applied Biosystems, Foster City, CA, USA). 2 µl of cDNA was amplified in a 21 µl reaction volume using 10 µl Power SYBR® Green Master Mix, 0.15 µl (10 µM) of each forward and reverse primer and 8.7 µl nuclease free water (QIAGEN Ltd., West Sussex, UK). All qPCR reactions were performed in triplicate for each cDNA sample. Cycling conditions for reference and DE genes of interest were as follows: 50 °C for 2 min, 95 °C for 10 min, and 40 cycles of 95 °C for 15 s and 60 °C for 1 min. In order to confirm a specificity of all individual amplification reactions, a dissociation curve analysis was included at the end of the amplification: 95 °C for 15 s, 60 °C for 1 min, 95 °C for 15 s and 60 °C for 15 s. A standard curve using 5-fold serial dilutions of a cDNA pool was generated to which relative expression values were compared. A normalization factor obtained from the expression of the reference genes was utilised for normalization of the candidate DE genes' expression values. Data was analysed using a general linear model procedure in the SAS system (version 9.3, SAS INST.) Spearman

correlations between the microarray expression values (log2) and qPCR normalised relative expression values (Ct) were carried out using R (version 3.1.1, https://www.R-project.org/).

3 Results

3.1 Meat quality

The mean RFI (g/day) of the L (low RFI - LRFI) and H group (high RFI - HRFI) was -106.6 (SD: 78.9) and 86.4 (SD: 84.7), respectively. Carcass and technological meat quality traits of LTL muscle in LRFI and HRFI pigs are shown in Table 1 and sensory attributes of LTL muscle in LRFI and HRFI pigs are presented in Fig. 2. Muscle depth and percent lean meat significantly differed between the RFI groups ($P < 0.05$), with the LRFI having greater lean meat percentage and increased muscle depth. LRFI pigs were also found to have significantly reduced IMF percentage ($P < 0.05$). The pH at 45m *pm* had a tendency towards increased values in the LRFI group ($P = 0.055$), however pH at 3h and 24h *pm* did not differ between the two groups. Moreover meat from LRFI pigs tended to have increased cook loss at day 1 *pm* ($P = 0.053$) but there was no difference detected at day 7 pm. Muscle from LRFI pigs was significantly associated with increased WBSF (less tender) at day 1 *pm* ($P < 0.01$) and had a tendency towards increased WBSF scores at day 7 *pm* ($P = 0.057$). Significant difference in tenderness between the RFI groups was also detected by sensory panellists who scored the LRFI meat (day 7 pm) as less tender ($P < 0.05$). Furthermore, meat from LRFI pigs was found to have lower b* values ($P < 0.05$) compared to meat from HRFI pigs, however the difference in yellowness scores was not significant after 1h blooming ($P > 0.1$). Lightness and redness did not differ between the two groups. Pork sensory assessment also revealed that meat produced from LRFI pigs had higher scores for stringy/fibrous/sinewy and chewy texture ($P < 0.05$). Additionally, meat from LRFI pigs was found less crumbly in texture ($P < 0.05$), less sweet ($P < 0.001$) and more sour ($P < 0.05$). Nutritional composition with regards to fatty acid (FA) content in LTL muscle (mg FA/100g meat), and percentage of FA in IMF of pigs divergent in RFI are presented in Table 2. From a nutritional point of view, meat from LRFI group contained significantly lower amounts of saturated fatty acids (SFA) such as myristic, palmitic and stearic ($P < 0.05$) and monounsaturated fatty acids (MUFA) including palmitoleic, oleic ($P < 0.05$) and eicosenoic ($P < 0.1$). Neither member of polyunsaturated fatty acid (PUFA) family differed significantly in LTL muscle of RFI divergent pigs. The IMF from LRFI group had significantly higher proportions of PUFA such as linoleic ($P <$

0.001) and alpha-linolenic ($P < 0.05$), and lower level of palmitic acid ($P < 0.01$) belonging to a SFA family. MUFA did not differ significantly in IMF between the RFI groups however.

3.2 Differential mRNA and miRNA expression profile

A total of 30,992 probe-sets remained after filtering and 1,035 probes were differentially expressed between LRFI and HRFI groups (645 probes were up-regulated and 390 were down-regulated in LRFI pigs) ($P \leq 0.05$, $q < 0.75$). Of the 1,035 probes, 875 were annotated and assigned to 800 genes (481 genes were up-regulated and 319 genes were down-regulated in LRFI compared to HRFI pigs) and 33 miRNAs (27 miRNAs were up-regulated and 6 miRNAs were down-regulated in LRFI compared to HRFI pigs). 123 annotated genes and 10 annotated miRNAs were found to be at least 1.5-fold differentially expressed. The most altered genes were *AP2M1* (2.37; LRFI > HRFI) and *NCOA2* (-3.32; LRFI < HRFI), and the most altered miRNAs were mir-675 (1.70 LRFI > HRFI) and mir-4311 (-1.90 LRFI < HRFI). Due to the relatively small differences in gene expression between the low and high RFI groups, transcripts and miRNAs with a $P \leq 0.05$ were considered significantly differentially expressed. To further refine this data, a gene ontology approach was utilised to extract molecular themes and networks.

3.3 Functional annotation, canonical pathway and network analysis

Twenty six molecular and cellular functions were significantly associated with genes DE in relation to RFI ($P < 0.05$). The six most significant biological processes altered in RFI groups were ‘gene expression’ (150 DE genes), ‘lipid metabolism’ (82 DE genes), ‘molecular transport’ (156 DE genes), ‘small molecule biochemistry’ (113 DE genes), ‘cellular growth and proliferation’ (248 DE genes), and ‘cell death and survival’ (227 DE genes). Ten canonical signalling pathways ($P < 0.05$) were significantly over-represented among DE genes in relation to RFI. The six most significant signalling pathways were ‘TR/RXR activation’ (16 DE genes), ‘PEDF signalling’ (11 DE genes), ‘HIF α signalling’ (11 DE genes), ‘myc mediated apoptosis signalling’ (8 DE genes), ‘aryl hydrocarbon receptor signalling’ (13 DE genes) and ‘adipogenesis pathway’ (12 DE genes) (Table 3). Twenty five over-represented gene networks were generated for differentially expressed genes in relation to RFI. The most significant network (Fig. 3) was represented by functions related to ‘molecular transport’, ‘nucleic acid metabolism’ and ‘small molecule biochemistry’, and contained 32 differentially expressed TP53-associated molecules.

3.4 miRNA-mRNA paired expression profiling and network analysis of target transcripts

Since miRNAs repress gene translation through base pairing with their target mRNAs, identification of their target transcripts is vital for understanding their biological function (Rajewsky, 2006; Tang, et al., 2015). In this study, potential DE target genes regulated by the 33 DE miRNAs were predicted. Of these, 29 miRNAs were mapped and predicted to regulate 379 DE genes. miRNA–mRNA expression pairing was performed to investigate expression patterns of miRNAs and potential mRNA targets. Although some studies reported miRNAs capability to activate gene expression (Orang, Safaralizadeh & Kazemzadeh-Bavili, 2014), our aim was to focus on the miRNA repression of target genes, therefore miRNA-mRNA expression patterns exhibiting the same direction were removed. 168 DE genes targeted by 28 DE miRNAs remained (Table S5), with mir3184, mir4313 and mir631 being the top three miRNAs predicted regulating 79, 44 and 44 DE target transcripts, respectively. In order to gain insights into biological functions of DE miRNAs, molecular connectivity of DE genes regulated by these miRNAs was performed. The most significant network (Fig. S1) was represented by functions related to 'cellular development, growth & proliferation' and 'respiratory system development and function' and contained 24 DE molecules. Another interesting network (Fig. 4) included 'embryonic development', 'connective tissue development & function' and 'organ morphology' and was represented by 10 DE molecules.

3.5 Microarray validation

The qPCR confirmed significant differences in the expression of *ACSL1*, *SDHB* and *TFAM* transcripts between LRFI and HRFI groups. mRNA abundances of *ACACA*, *BCL2* and *MMP2* showed a numerical change in the same direction when compared to results obtained from the microarrays. Spearman correlations between microarray expression values and qPCR Ct values were significant ($P < 0.05$) for all transcripts and ranged from 0.56 to 0.84 (Table 4).

4 Discussion

4.1 Meat quality

The first objective of this study was to examine the effect of divergence in RFI on technological, sensory and nutritional quality of pork. Our findings indicate that low RFI pigs

exhibit increased muscle size, leanness and reduced IMF content, and this is consistent with previous studies (Faure, et al., 2013; Lefaucheur, et al., 2011; Smith, et al., 2011). The similar trend in adiposity and marbling is not surprising and can be explained by a positive genetic correlation between the two traits (Lefaucheur, et al., 2011). In agreement with the fact that lipid content can influence colour measurements (Schwab, Baas, Stalder & Mabry, 2006), meat from LRFI pigs was found to be less yellow. The results regarding pH are in contrast with previous studies reporting no effect on early pH and significantly reduced ultimate pH in LRFI pigs, compared to HRFI (Faure, et al., 2013; Lefaucheur, et al., 2011). *Longissimus* (LM) is a large fast-twitch glycolytic muscle composed of approximately 74 percent type IIBW (white) fibres (Lefaucheur, et al., 2011). In a previous study, LM from pigs divergent in RFI showed no difference in proportions of muscle fibre types (Smith, et al., 2011). On the contrary, another study reported higher proportions of IIBW fibres in meat from LRFI pigs compared to HRFI group (Lefaucheur, et al., 2011). Increase in IIBW fibres and consequently greater muscle glycogen content in LRFI pigs have been associated with impaired meat quality through reduced ultimate pH, greater lightness and drip loss (Gilbert, et al., 2007; Lefaucheur, et al., 2011). In the present study, these associations were not observed, which may indicate that muscle from the LRFI pigs does not contain higher proportions of IIBW fibres. Indeed, the array contained several myosin heavy chain isoforms but no significant differences in their expression were observed here between RFI groups. Previous studies, such as that of Lefaucheur et al. (2011) and Faure et al. (2013) utilised a different experimental model for RFI, with animals being selected in divergent lines for multiple generations. The animals in the present study were selected from within families and the mechanisms underpinning the differences in RFI which we observed are likely to differ from those in previous experiments.

Shear force and sensory analysis showed that meat from LRFI pigs was tougher and more stringy compared to HRFI. No significant association with tenderness was found in a previous study carried out on low RFI pigs versus control pigs (Faure, et al., 2013). In contrast, another study (Smith, et al., 2011) did report a significant correlation between tenderness and RFI, and they postulated that tenderness of meat produced by LRFI pigs could be negatively affected by greater calpastatin activity resulting in decreased *post-mortem* protein degradation. They also suggested that the lower IMF in this group of pigs may contribute to decreased tenderness of resultant meat from LRFI pigs. While the relationship between IMF and tenderness is inconclusive (Smith, et al., 2011), many authors have

speculated on a link between IMF and tenderness, due to greater ease of tissue disruption in areas richer in fat cells. Furthermore, trained panellists scored meat from LRFI pigs as less sweet and more sour compared to meat from HRFI group. A previous study also reported that meat with elevated ultimate pH (pH = 6) was perceived as more sweet, tender and less acidic than meat with normal pH (Bryhni, et al., 2003). It is interesting that meat from HRFI pigs showed a similar trend in the sensory scores while having an ultimate pH within the normal range and although HRFI pigs had slightly higher values than meat from LRFI pigs the difference was not significant. This variation in sweet and sour taste could also be caused by a diverse proportion of particular amino acids. It has been well documented that variable concentrations of amino acids affect taste perception (Choudhuri, Delay & Delay, 2015). For example L-serine and D-serine amino acids are associated with sweet taste (Kawai, Sekine-Hayakawa, Okiyama & Ninomiya, 2012), whereas glutamic and aspartic amino acids are associated with sour taste (Birch & Kemp, 1989).

Fat content and fatty acid composition play important roles in sensory attributes and nutritional value of meat (Nieto & Ros, 2012). Meat contains considerable concentrations of cell membrane phospholipids, which are rich in PUFA (Wood, et al., 2008). Nevertheless the most predominant class of fatty acids present in meat are MUFA followed by SFA, which are the major constituents of triacylglycerol (Kasprzyk, Tyra & Babicz, 2015; Wood, et al., 2008). Reduced IMF content is frequently associated with higher proportion of PUFA and decreased levels of SFA and MUFA (Dominguez & Lorenzo, 2014; Dugan, et al., 2015; Wood, et al., 2008). Here, low RFI muscle was associated with reduced IMF content and, in keeping with previous studies, this was predominantly due to reduced SFA and MUFA content, with similar total meat PUFA content in LTL muscle of both groups. The health profile of muscle from LRFI pigs could be considered more beneficial, being 42 percent lower in SFA and with IMF 19 percent richer in PUFA.

4.2 Gene expression profile

Besides the carcass and meat quality analysis of the RFI divergent pigs, the other aim of this study was to attain insights on the biological events explaining differences in RFI and increase understanding of the biological processes linking RFI and meat quality traits such as sensory profile and technological performance. The magnitude of DE genes found in the current study is similar to a recently performed gene expression profiling of skeletal muscle

of Large White pigs selected for divergent RFI (Vincent, et al., 2015). It is important to note that the experimental model used in our study involved pairs of animals from the lowest and highest quartile chosen within the same family, i.e. divergent sib-pairs, and the work conducted by Vincent et al. (2015) utilised animals of divergently selected lines for RFI over several generations. As a result of using animals from the same family, the genetic variability, and transcriptomic response is likely due to different mendelian inheritance of parental alleles within the sib-pairs that largely contribute to the trait of interest, rather than long term selection effects and genetic drift. Hence it is of interest that very similar numbers of differentially expressed transcripts were observed in both experiments. Furthermore, downstream validation of the microarray results via qPCR of selected DE genes was successful thus confirming reliability of the expression profiles. Functional annotation revealed a number of biological processes related to growth, connective tissue and lipid metabolism suggesting that these might be important mechanisms contributing to differences in RFI.

4.2.1 Growth

Adaptor related protein complex 2 mu 1 subunit (*AP2M1*) was the most up-regulated gene (fold change = 2.37) in LRFI pigs. AP2M1 is a subunit of adaptor protein 2 (AP2) involved in clathrin-mediated endocytosis, which is the uptake of nutrients from the surface of the cell into the cell via clathrin-coated vesicles (Tian, Chang, Fan, Flajolet & Greengard, 2013). Accordingly, functional annotation revealed endocytosis significantly activated in LRFI pigs (z-score = 3.11). Nuclear receptor coactivator 2 (*NCOA2*) was the most down-regulated gene (fold change = -3.32) in LRFI pigs. NCOA2 belongs to the nuclear receptor coactivator family, which assists in the function of nuclear hormone receptors playing a vital role in cell growth, development and homeostasis via regulating expression of particular genes. In a previous study, porcine *NCOA2* transcript was positively associated with IMF content in LM muscle (Wang, et al., 2008). This is in agreement with the LRFI pigs exhibiting suppressed *NCOA2* expression and reduced IMF content. Two miRNAs, mir135a and mir3184, that were predicted to suppress *NCOA2* expression were significantly over-expressed in LRFI pigs. Thus these miRNAs could play a mechanistic role in reducing IMF content through inhibiting *NCOA2* activity in LRFI pigs.

In agreement with increased muscle depth and decreased IMF content in LRFI pigs, functional annotation revealed a number of biological processes related to growth. Specifically, 'cell survival' and 'cell differentiation' were significantly activated (z-score = 2.3 and 2.4 respectively) in LRFI pigs. Among the up-regulated genes were insulin like growth factor 2 (IGF2). Protein encoded by *IGF2* plays an essential role in skeletal muscle differentiation (Alzhanov, McInerney & Rotwein, 2010) and lean versus intramuscular fat content (Aslan, et al., 2012; Van Laere, et al., 2003). Other significantly enriched functions related to growth were 'protein synthesis and degradation', with meltrin-alpha (*ADAM12*) being over-expressed in LRFI pigs. ADAM12 is an adhesion molecule that has previously been found to play a role in skeletal muscle development and regeneration (Kurisaki, et al., 2003; Moghadaszadeh, et al., 2003; Przewozniak, et al., 2013). Up-regulation of *ADAM12* along with other genes involved in muscle protein synthesis, and also up-regulation of muscle protein degrading enzymes such as calpain 10 (*CAPN10*) and caspase 9 (*CASP9*) suggest greater muscle protein turnover in LRFI pigs. This can be supported by another study reporting up-regulation of genes involved in processes related to protein synthesis and degradation, more specifically 'ribonucleoprotein complex biogenesis' and 'ubiquitin-dependent catabolic process' in LRFI pigs (Gondret, et al., 2017). Vincent el al. (2015) also identified greater muscle protein synthesis in LRFI pigs and also a calpain, in that case calpain 2 to be over-expressed in muscle from LRFI pigs. While probes corresponding to known players in *pm* muscle proteolysis such as calpain 1 and calpastatin, (Geesink, Taylor & Koohmaraie, 2005) were not incorporated in the array, *CASP9* which is an initiator of *pm* proteolysis that has been suggested to influence meat tenderness thus the rate of proteolysis (Ouali, et al., 2006) was up-regulated in LRFI pigs. Other studies reported either no difference (Le Naou, Le Floc'h, Louveau, Gilbert & Gondret, 2012) or reduced protein degradation in LRFI pigs (Cruzen, et al., 2013; Smith, et al., 2011). Lobley (2003) postulated that muscle growth driven by enhanced synthesis and decreased degradation of protein contributes to net gain in deposition. Nevertheless, protein synthesis is much more energetically costly in comparison to protein degradation (Lobley, 2003). Our data supports the possibility that LRFI pigs reuse existing proteins and thus conserve energy, which otherwise would be utilised for protein synthesis, directing it towards more efficient muscle growth. In addition, the interactions depicted in the tumor suppressor p53 (TP53) rooted network (Figure 3) support the role of TP53 as a central hub in mediating the modulation of muscle cell growth and differentiation (Porrello, et al., 2000; Tamir & Bengal, 1998). FXYD domain containing ion transport regulator 3 (*FXYD3*) and chloride intracellular channel 2

(*CLIC2*), coding for integral membrane proteins that regulate function of ion channels (Biasiotta, D'Arcangelo, Passarelli, Nicodemi & Facchiano, 2016; Littler, et al., 2010), were differentially expressed in this network. Ion channels are vital modulators of apoptosis through permitting release of potassium and chloride ions subsequently leading to cell shrinkage (Wanitchakool, et al., 2016). TP53 regulated inhibitor of apoptosis 1 (*TRIAP1*) and ADP ribosylation factor like GTPase interacting protein 1 (*ARL6IP1*) were another over-represented genes in this network. Proteins encoded by these genes are involved in apoptosis via regulating *CASP9* activity (Adams, et al., 2015; Lui, Chen, Wang & Naumovski, 2003). The connection of these DE genes to *TP53*, which was over-expressed in LRFI pigs, suggests their importance in lean growth due to its involvement in cell proliferation. Moreover, nineteen miRNAs were predicted to be associated with 'cellular development, growth & proliferation' through regulation of their target DE genes.

4.2.2 Connective tissue

A number of DE genes were significantly overrepresented in 'adhesion of connective tissue' function with a tendency towards activation in the high FE pigs (z-score = 1.99). During the process of muscle growth, connective tissue undergoes dynamic remodelling which involves its proteolytic degradation, and the establishment of expanded networks through synthesis of new connective tissue components (Purslow, 2014). Accordingly, LRFI pigs which showed signs of increased muscle mass also over-expressed matrix metallopeptidase 2 (*MMP2*) belonging to a family of enzymes associated with connective tissue degradation and remodelling (Rodier, El Moudni, Kauffmann-Lacroix, Daniault & Jacquemin, 1999; Woessner, 1991). This pattern might be expected to be associated with more tender meat, which is often associated with elevated turnover of muscle proteins (Olsson & Pickova, 2005) but this was not observed in the present study. Collagen type I alpha 1 chain (*COL1A1*), one of the predominant collagen types in the skeletal muscle (McCormick, 1994), was up-regulated in LRFI pigs.. Over-expression of *COL1A1* was previously associated with increased drip loss (McBryan, Hamill, Davey, Lawlor & Mullen, 2010; Ponsuksili, et al., 2008). In the present study, while drip loss did not differ significantly between RFI groups, a tendency towards increased cook loss at day 1 *pm* was observed in meat from LRFI pigs. Upon heating, collagen fibrils shrink which consequently leads to fluid loss (Weston, Rogers & Althen, 2002). This finding may relate to the stringy/fibrous/sinewy and chewy texture of meat produced by LRFI pigs. Eleven miRNAs were predicted to regulate expression of genes

with functions related to ‘connective tissue development & function’. Down-regulation of mir584 and mir887 potentially resulted in the over-expression of collagen type I alpha 2 chain (*COL1A2*) and connective tissue growth factor (*CTGF*), respectively.

4.2.3 Lipid and energy metabolism

In accordance with the relation of RFI to IMF content, a number of DE genes were significantly enriched in ‘adipogenesis pathway’ and lipid metabolism functions. Peroxisome proliferator activated receptor gamma (*PPARG*) is a master regulator of adipogenesis in a variety of tissues (Norris, et al., 2003).Overexpression of *PPARG* in adipocytes of LRFI pigs would suggest enhanced adipogenesis which disagrees with the observed shifts in muscle to fat ratio. However, considering that skeletal muscle is a highly heterogeneous tissue, the observed differences in *PPARG* expression could be attributable either to muscle cells or intramuscular adipocytes. A previous study reported that muscle-specific deletion of *PPARG* is associated with enhanced adiposity in mice (Norris, et al., 2003), which could explain the muscle of LRFI pigs exhibiting reduced IMF content while enhanced *PPARG* expression. Acyl-CoA synthetase long-chain family member 1 (*ACSL1*) expression was suppressed in LRFI pigs. The enzyme encoded by this gene is involved in lipid synthesis through conversion of fatty acids to triglycerides (Parkes, et al., 2006). Over-expression of *ACSL1* was previously associated with increased triglyceride level in mouse liver (Parkes, et al., 2006). Insulin receptor (*INSR*), coding for transmembrane receptor stimulating triacylglycerol synthesis in muscle (Dimitriadis, Mitrou, Lambadiari, Maratou & Raptis, 2011) was another down-regulated gene in LRFI pigs. Repression of these two genes, *ACSL1* and *INSR*, is in agreement with reduced IMF content in meat from LRFI pigs.

Previous studies reported reduced mitochondrial energy metabolism in the *Longissimus* muscle of low vs high RFI pigs (Fu, et al., 2017; Jing, et al., 2015; Le Naou, et al., 2012). In this study, functional annotation revealed ‘oxidation of fatty acids’ significantly over-represented among DE genes with the direction towards inhibition in LRFI pigs (z-score = -1.12), which suggests that the LRFI pigs might exhibit reduced mitochondrial energy metabolism. Similarly, enrichment of DE genes in lipid catabolic processes was previously reported in RFI divergent pigs (Jing, et al., 2015). Moreover, succinate dehydrogenase complex iron sulfur subunit B (*SDHB*), involved in complex II of the mitochondrial electron transport chain (Liu, et al., 2015), and transcription factor A mitochondrial (*TFAM*), a key

modulator of mitochondrial DNA replication and transcription (Zou, et al., 2016), were down-regulated in low RFI pigs.

5 Conclusions

To conclude, improvement in feed efficiency revealed meat quality characteristics generally within the normal range for the production of acceptable quality pork. However significant differences in traits such as sensory profile, texture, and technological aspects such as cook loss suggest there is a minor impairment of meat quality in more feed efficient pigs, at least in the *M. longissimus*. High FE pigs were also associated with leaner carcasses, greater muscle content and enhanced nutritional value in terms of fatty acid composition. Gene expression profiling of muscle from RFI-divergent pigs provided mechanistic insights on the biological events governing differences in RFI that have consequences for eating quality. A number of differentially expressed genes were significantly over-represented with functions in muscle growth & development, lipid metabolism and connective tissue metabolism. Up-regulation of genes involved in the synthesis and degradation of protein suggest a greater muscle protein turnover in low RFI pigs, while the divergence in adhesion of connective tissue may contribute to differences in tenderness. Moreover, a tendency towards suppression of fatty acid oxidation and down-regulation of *SDHB* and *TFAM* could possibly contribute to reduced mitochondrial activity in low RFI muscle.

Acknowledgements

The authors wish to thank Carol Griffin for training sensory panellists and conducting sensory assessment of the samples, as well as staff and students at Teagasc in Ashtown who assisted in animal sampling. The authors also thank Hannelore Tychsen for her excellent technical help. The ECO-FCE project was funded by the European Union Seventh Framework Programme (FP7 2007/2013) under grant agreement No. 311794.

References

Adams, C., Cazzanelli, G., Rasul, S., Hitchinson, B., Hu, Y., Coombes, R. C., . . . Yague, E. (2015). Apoptosis inhibitor TRIAP1 is a novel effector of drug resistance. Oncology Reports, 34(1), 415-422.

Alzhanov, D. T., McInerney, S. F. & Rotwein, P. (2010). Long Range Interactions Regulate Igf2 Gene Transcription during Skeletal Muscle Differentiation. Journal of Biological Chemistry, 285(50), 38969-38977.

AMSA. (1995). Research guidelines for cookery, sensory evaluation and instrumental tenderness measurements Chicago: American Meat Science Association in cooperation with National Live Stock and Meat Board.

AMSA. (2015). Research guidelines for cookery, sensory evaluation and instrumental tenderness measurements of meat. Chicago: American Meat Science Association.

Aslan, O., Hamill, R. M., Davey, G., McBryan, J., Mullen, A. M., Gispert, M. & Sweeney, T. (2012). Variation in the IGF2 gene promoter region is associated with intramuscular fat content in porcine skeletal muscle. Molecular Biology Reports, 39(4), 4101-4110.

Biasiotta, A., D'Arcangelo, D., Passarelli, F., Nicodemi, E. M. & Facchiano, A. (2016). Ion channels expression and function are strongly modified in solid tumors and vascular malformations. Journal of Translational Medicine, 14(1), 285.

Birch, G. G. & Kemp, S. E. (1989). Apparent specific volumes and tastes of amino-acids. Chemical Senses, 14(2), 249-258.

Bryhni, E. A., Byrne, D. V., Rodbotten, M., Moller, S., Claudi-Magnussen, C., Karlsson, A., . . . Martens, M. (2003). Consumer and sensory investigations in relation to physical/chemical aspects of cooked pork in Scandinavia. Meat Science, 65(2), 737-748.

Bumgarner, R. (2013). DNA microarrays: Types, Applications and their future. Current Protocols in Molecular Biology / edited by Frederick M. Ausubel ... [et al.], 0 22, Unit-22.21.

Choudhuri, S. P., Delay, R. J. & Delay, E. R. (2015). L-Amino Acids Elicit Diverse Response Patterns in Taste Sensory Cells: A Role for Multiple Receptors. Plos One, 10(6), e0130088.

Cruzen, S. M., Harris, A. J., Hollinger, K., Punt, R. M., Grubbs, J. K., Selsby, J. T., . . . Huff-Lonergan, E. (2013). Evidence of decreased muscle protein turnover in gilts selected for low residual feed intake. Journal of Animal Science, 91(8), 4007-4016.

Dimitriadis, G., Mitrou, P., Lambadiari, V., Maratou, E. & Raptis, S. A. (2011). Insulin effects in muscle and adipose tissue. Diabetes Research and Clinical Practice, 93 Suppl 1, S52-59.

Dominguez, R. & Lorenzo, J. M. (2014). Effect of genotype on fatty acid composition of intramuscular and subcutaneous fat of Celta pig breed. Grasas Y Aceites, 65(3), e037.

Dugan, M. E. R., Vahmani, P., Turner, T. D., Mapiye, C., Juárez, M., Prieto, N., . . . Aalhus, J. L. (2015). Pork as a Source of Omega-3 (n-3) Fatty Acids. Journal of Clinical Medicine, 4(12), 1999-2011.

Fan, B., Lkhagvadorj, S., Cai, W., Young, J., Smith, R. M., Dekkers, J. C. M., . . . Rothschild, M. F. (2010). Identification of genetic markers associated with residual feed intake and meat quality traits in the pig. Meat Science, 84(4), 645-650.

Faure, J., Lefaucheur, L., Bonhomme, N., Ecolan, P., Meteau, K., Coustard, S. M., . . . Lebret, B. (2013). Consequences of divergent selection for residual feed intake in pigs on muscle energy metabolism and meat quality. Meat Science, 93(1), 37-45.

Freeman, T. C., Ivens, A., Baillie, J. K., Beraldi, D., Barnett, M. W., Dorward, D., . . . Hume, D. A. (2012). A gene expression atlas of the domestic pig. BMC Biology, 10, 90.

Fu, L. L., Xu, Y. Y., Hou, Y., Qi, X. L., Zhou, L., Liu, H. Y., . . . Li, X. Y. (2017). Proteomic analysis indicates that mitochondrial energy metabolism in skeletal muscle tissue is negatively correlated with feed efficiency in pigs. Scientific Reports, 7, 45291.

Geesink, G. H., Taylor, R. G. & Koohmaraie, M. (2005). Calpain 3/p94 is not involved in postmortem proteolysis. Journal of Animal Science, 83(7), 1646-1652.

Gilbert, H., Bidanel, J. P., Gruand, J., Caritez, J. C., Billon, Y., Guillouet, P., . . . Sellier, P. (2007). Genetic parameters for residual feed intake in growing pigs, with emphasis on genetic relationships with carcass and meat quality traits. Journal of Animal Science, 85(12), 3182-3188.

Git, A., Dvinge, H., Salmon-Divon, M., Osborne, M., Kutter, C., Hadfield, J., . . . Caldas, C. (2010). Systematic comparison of microarray profiling, real-time PCR, and next-generation sequencing technologies for measuring differential microRNA expression. Rna, 16(5), 991-1006.

Gondret, F., Vincent, A., Houee-Bigot, M., Siegel, A., Lagarrigue, S., Causeur, D., . . . Louveau, I. (2017). A transcriptome multi-tissue analysis identifies biological pathways and genes associated with variations in feed efficiency of growing pigs. BMC Genomics, 18(1), 244.

Honikel, K. O. (1998). Reference methods for the assessment of physical characteristics of meat. Meat Science, 49(4), 447-457.

Hoque, M. A. & Suzuki, K. (2009). Genetics of Residual Feed Intake in Cattle and Pigs: A Review. Asian-Australasian Journal of Animal Sciences, 22(5), 747-755.

Jing, L., Hou, Y., Wu, H., Miao, Y. X., Li, X. Y., Cao, J. H., . . . Zhao, S. H. (2015). Transcriptome analysis of mRNA and miRNA in skeletal muscle indicates an important network for differential Residual Feed Intake in pigs. Scientific Reports, 5, 11953.

Kasprzyk, A., Tyra, M. & Babicz, M. (2015). Fatty acid profile of pork from a local and a commercial breed. Archives Animal Breeding, 58(2), 379-385.

Kawai, M., Sekine-Hayakawa, Y., Okiyama, A. & Ninomiya, Y. (2012). Gustatory sensation of (L)- and (D)-amino acids in humans. Amino Acids, 43(6), 2349-2358.

Kurisaki, T., Masuda, A., Sudo, K., Sakagami, J., Higashiyama, S., Matsuda, Y., . . . Sehara-Fujisawa, A. (2003). Phenotypic analysis of Meltrin alpha (ADAM12)-deficient mice: Involvement of Meltrin alpha in adipogenesis and myogenesis. Molecular and Cellular Biology, 23(1), 55-61.

Le Naou, T., Le Floc'h, N., Louveau, I., Gilbert, H. & Gondret, F. (2012). Metabolic changes and tissue responses to selection on residual feed intake in growing pigs. Journal of Animal Science, 90(13), 4771-4780.

Lefaucheur, L., Lebret, B., Ecolan, P., Louveau, I., Damon, M., Prunier, A., . . . Gilbert, H. (2011). Muscle characteristics and meat quality traits are affected by divergent selection on residual feed intake in pigs. Journal of Animal Science, 89(4), 996-1010.

Littler, D. R., Harrop, S. J., Goodchild, S. C., Phang, J. M., Mynott, A. V., Jiang, L., . . . Curmi, P. M. (2010). The enigma of the CLIC proteins: Ion channels, redox proteins, enzymes, scaffolding proteins? FEBS Letters, 584(10), 2093-2101.

Liu, X., Du, Y., Trakooljul, N., Brand, B., Muryni, E., Krischek, C., . . . Ponsuksili, S. (2015). Muscle Transcriptional Profile Based on Muscle Fiber, Mitochondrial

Respiratory Activity, and Metabolic Enzymes. International Journal of Biological Sciences, 11(12), 1348-1362.

Lobley, G. E. (2003). Protein turnover—what does it mean for animal production? Canadian Journal of Animal Science, 83(3), 327-340.

Lui, H. M., Chen, J., Wang, L. L. & Naumovski, L. (2003). ARMER, apoptotic regulator in the membrane of the endoplasmic reticulum, a novel inhibitor of apoptosis. Molecular Cancer Research, 1(7), 508-518.

McBryan, J., Hamill, R. M., Davey, G., Lawlor, P. & Mullen, A. M. (2010). Identification of suitable reference genes for gene expression analysis of pork meat quality and analysis of candidate genes associated with the trait drip loss. Meat Science, 86(2), 436-439.

McCormick, R. J. (1994). The flexibility of the collagen compartment of muscle. Meat Science, 36(1-2), 79-91.

Metzler-Zebell, B. U., Lawlor, P. G., Magowan, E., McCormack, U. M., Curiao, T., Hollmann, M., . . . Zebell, Q. (2017). Finishing pigs that are divergent in feed efficiency show small differences in intestinal functionality and structure. Plos One, 12(4), e0174917 .

Moghadaszadeh, B., Albrechtsen, R., Guo, L. T., Zaik, M., Kawaguchi, N., Borup, R. H., . . . Wewer, U. M. (2003). Compensation for dystrophin-deficiency: ADAM12 overexpression in skeletal muscle results in increased α7 integrin, utrophin and associated glycoproteins. Human Molecular Genetics, 12(19), 2467-2479.

Nazarov, P. V., Muller, A., Kaoma, T., Nicot, N., Maximo, C., Birembaut, P., . . . Vallar, L. (2017). RNA sequencing and transcriptome arrays analyses show opposing results for alternative splicing in patient derived samples. BMC Genomics, 18(1), 443.

Nieto, G. & Ros, G. (2012). Modification of Fatty Acid Composition in Meat Through Diet: Effect on Lipid Peroxidation and Relationship to Nutritional Quality - A Review. Lipid Peroxidation, 239-258.

Norris, A. W., Chen, L. H., Fisher, S. J., Szanto, I., Ristow, M., Jozsi, A. C., . . . Kahn, C. R. (2003). Muscle-specific PPAR gamma-deficient mice develop increased adiposity and insulin resistance but respond to thiazolidinediones. Journal of Clinical Investigation, 112(4), 608-618.

Olsson, V. & Pickova, J. (2005). The influence of production systems on meat quality, with emphasis on pork. Ambio, 34(4-5), 338-343.

Orang, A. V., Safaralizadeh, R. & Kazemzadeh-Bavili, M. (2014). Mechanisms of miRNA-Mediated Gene Regulation from Common Downregulation to mRNA-Specific Upregulation. International Journal of Genomics, 2014, 970607.

Ouali, A., Herrera-Mendez, C. H., Coulis, G., Becila, S., Boudjellal, A., Aubry, L. & Sentandreu, M. A. (2006). Revisiting the conversion of muscle into meat and the underlying mechanisms. Meat Science, 74(1), 44-58.

Parkes, H. A., Preston, E., Wilks, D., Ballesteros, M., Carpenter, L., Wood, L., . . . Cooney, G. J. (2006). Overexpression of acyl-CoA synthetase-1 increases lipid deposition in hepatic (HepG2) cells and rodent liver in vivo. American Journal of Physiology-Endocrinology and Metabolism, 291(4), E737-E744.

Ponsuksili, S., Jonas, E., Murani, E., Phatsara, C., Srikanchai, T., Walz, C., . . . Wimmers, K. (2008). Trait correlated expression combined with expression QTL analysis reveals biological pathways and candidate genes affecting water holding capacity of muscle. BMC Genomics, 9, 367.

Porrello, A., Cerone, M. A., Coen, S., Gurtner, A., Fontemaggi, G., Cimino, L., . . . Soddu, S. (2000). p53 regulates myogenesis by triggering the differentiation activity of pRb. Journal of Cell Biology, 151(6), 1295-1304.

Przewozniak, M., Czaplicka, I., Czerwinska, A. M., Markowska-Zagrajek, A., Moraczewski, J., Streminska, W., . . . Brzoska, E. (2013). Adhesion Proteins - An Impact on Skeletal Myoblast Differentiation. Plos One, 8(5), e61760.

Purslow, P. P. (2014). New developments on the role of intramuscular connective tissue in meat toughness. Annual Review of Food Science and Technology, 5, 133-153.

Rajewsky, N. (2006). microRNA target predictions in animals. Nature Genetics, 38, S8-S13.

Rodier, M. H., El Moudni, B., Kauffmann-Lacroix, C., Daniault, G. & Jacquemin, J. L. (1999). A Candida albicans metallopeptidase degrades constitutive proteins of extracellular matrix. Fems Microbiology Letters, 177(2), 205-210.

Saintilan, R., Merour, I., Brossard, L., Tribout, T., Dourmad, J. Y., Sellier, P., . . . Gilbert, H. (2013). Genetics of residual feed intake in growing pigs: Relationships with production traits, and nitrogen and phosphorus excretion traits. Journal of Animal Science, 91(6), 2542-2554.

Schwab, C. R., Baas, T. J., Stalder, K. J. & Mabry, J. W. (2006). Effect of long-term selection for increased leanness on meat and eating quality traits in Duroc swine. Journal of Animal Science, 84(6), 1577-1583.

Smith, R. M., Gabler, N. K., Young, J. M., Cai, W., Boddicker, N. J., Anderson, M. J., . . . Lonergan, S. M. (2011). Effects of selection for decreased residual feed intake on composition and quality of fresh pork. Journal of Animal Science, 89(1), 192-200.

Storey, J. D. & Tibshirani, R. (2003). Statistical significance for genomewide studies. Proceedings of the National Academy of Sciences of the United States of America, 100(16), 9440-9445.

Tamir, Y. & Bengal, E. (1998). p53 Protein is activated during muscle differentiation and participates with MyoD in the transcription of muscle creatine kinase gene. Oncogene, 17(3), 347-356.

Tang, Z., Yang, Y., Wang, Z., Zhao, S., Mu, Y. & Li, K. (2015). Integrated analysis of miRNA and mRNA paired expression profiling of prenatal skeletal muscle development in three genotype pigs. Scientific Reports, 5, 15544.

Tian, Y., Chang, J. C., Fan, E. Y., Flajolet, M. & Greengard, P. (2013). Adaptor complex AP2/PICALM, through interaction with LC3, targets Alzheimer's APP-CTF for terminal degradation via autophagy. Proceedings of the National Academy of Sciences of the United States of America, 110(42), 17071-17076.

Van Laere, A.-S., Nguyen, M., Braunschweig, M., Nezer, C., Collette, C., Moreau, L., . . . Andersson, L. (2003). A regulatory mutation in IGF2 causes a major QTL effect on muscle growth in the pig. Nature, 425(6960), 832-836.

Vincent, A., Louveau, I., Gondret, F., Trefeu, C., Gilbert, H. & Lefaucheur, L. (2015). Divergent selection for residual feed intake affects the transcriptomic and proteomic profiles of pig skeletal muscle. Journal of Animal Science, 93(6), 2745-2758.

Wang, X., Chen, J., Liu, H., Xu, Y., Wang, X., Xue, C., . . . Jiang, Z. (2008). The pig p160 co-activator family: Full length cDNA cloning, expression and effects on intramuscular fat content in Longissimus Dorsi muscle. Domestic Animal Endocrinology, 35(2), 208-216.

Wanitchakool, P., Ousingsawat, J., Sirianant, L., MacAulay, N., Schreiber, R. & Kunzelmann, K. (2016). Cl- channels in apoptosis. European Biophysics Journal, 45(7), 599-610.

Weston, A. R., Rogers, R. W. & Althen, T. G. (2002). Review: The Role of Collagen in Meat Tenderness. The Professional Animal Scientist, 18(2), 107-111.

Wilkinson, J. M. (2011). Re-defining efficiency of feed use by livestock. Animal, 5(7), 1014-1022.

Woessner, J. F. (1991). Matrix metalloproteinases and their inhibitors in connective-tissue remodeling. Faseb Journal, 5(8), 2145-2154.

Wood, J. D., Enser, M., Fisher, A. V., Nute, G. R., Sheard, P. R., Richardson, R. I., . . . Whittington, F. M. (2008). Fat deposition, fatty acid composition and meat quality: A review. Meat Science, 78(4), 343-358.

Zou, T. D., Yu, B., Yu, J., Mao, X. B., Zheng, P., He, J., . . . Chen, D. W. (2016). Moderately decreased maternal dietary energy intake during pregnancy reduces fetal skeletal muscle mitochondrial biogenesis in the pigs. Genes and Nutrition, 11, 19.

Table 1 Carcass and technological meat quality traits of *Longissimus thoracis et lumborum* muscle from pigs divergent in RFI.

Trait	Low RFI[1]	High RFI[1]	SE	P-value
Fat depth (mm)	11.9	13.3	0.71	0.086
Muscle depth (mm)	53.4	50.9	1.10	**0.045**
Lean (%)	58.0	56.5	0.64	**0.042**
pH 45m	6.72	6.58	0.06	0.055
pH 3h	6.71	6.60	0.11	0.296
pH 24h	5.55	5.62	0.09	0.452
L*	53.0	54.2	1.44	0.423
a*	5.43	5.24	0.52	0.725
b*	12.9	13.9	0.34	**0.013**
1h L*	52.7	54.3	1.57	0.338
1h a*	6.63	5.99	0.56	0.279
1h b*	13.9	14.5	0.38	0.137
DL (%)	2.36	2.31	0.41	0.905
Protein (%)	23.8	23.7	0.30	0.615
Ash (%)	1.31	1.34	0.07	0.704
Moisture (%)	74.9	74.9	0.17	0.868
IMF (%)	1.05	1.41	0.15	**0.042**
WBSF day 1 (N)	59.1	39.7	4.14	**0.001**
WBSF day 7 (N)	48.8	38.8	4.72	0.057
CL day 1 (%)	32.9	31.2	0.97	0.053
CL day 7 (%)	31.9	31.0	0.98	0.399

[1]Least square means for each trait.

Table 2 Fatty acid composition in *Longissimus thoracis et lumborum* muscle and percentage of fatty acid in intramuscular fat (IMF) of pigs divergent in RFI.

	Fatty Acid	mg fatty acid / 100g meat				% fatty acid in IMF			
		Low RFI[1]	High RFI[1]	SE	P-value	Low RFI[1]	High RFI[1]	SE	P-value
SFA	Myristic C14:0	17.4	25.3	0.003	**0.041**	1.17	1.23	0.001	0.486
	Palmitic C16:0	314	475	0.057	**0.016**	22.9	24.1	0.003	**0.002**
	Stearic C18:0	157	247	0.032	**0.017**	11.9	12.7	0.005	0.144
	Total SFA	491	748	0.092	**0.017**	35.9	38.0	0.008	**0.020**
MUFA	Palmitoleic C16:1	40.5	59.0	0.007	**0.031**	3.06	2.99	0.002	0.740
	Eicosenoic C20:1	9.89	13.9	0.002	0.056	0.79	0.71	0.001	0.380
	Oleic C18:1 n9	555	799	0.094	**0.025**	40.7	40.9	0.006	0.721
	Total MUFA	605	872	0.102	**0.024**	44.7	44.7	0.007	0.992
PUFA	Linoleic C18:2 n6	111	127	0.014	0.258	7.59	6.36	0.003	**<0.001**
	Alpha-linolenic C18:3 n3	10.3	11.1	0.001	0.539	0.79	0.57	0.001	**0.023**
	Total PUFA	121	139	0.015	0.265	8.36	6.94	0.003	**0.001**

[1]Least square means for each fatty acid; SFA: saturated fatty acids, MUFA: monounsaturated fatty acids, PUFA: polyunsaturated fatty acids.

Table 3 Canonical signalling pathways significantly differentially expressed in relation to RFI.

Canonical Pathways	-log (B-H p-value)	Genes
TR/RXR activation	4.90	***PIK3C2B***, ***UCP2***, *PIK3C2A*, *MDM2*, ***BCL3***, *NCOA3*, *EP300*, *PIK3R3*, ***RXRG***, ***HP***, *NCOA2*, ***PIK3CG***, *NCOA1*, ***ACACA***, *TBL1XR1*, *THRB*
PEDF signalling	2.35	***PPARG***, *PIK3R3*, ***TP53***, ***PIK3C2B***, ***GDNF***, *PIK3C2A*, ***PIK3CG***, ***RHOA***, ***SRF***, *FAS*, *BCL2*
HIF1α signalling	1.54	***SLC2A5***, *PIK3R3*, ***TP53***, ***PIK3C2B***, *EGLN1*, *PIK3C2A*, ***PIK3CG***, *NCOA1*, *MDM2*, ***MMP2***, *EP300*
Myc mediated apoptosis signalling	1.54	*PIK3R3*, ***TP53***, ***PIK3C2B***, ***CASP9***, *PIK3C2A*, ***PIK3CG***, *FAS*, *BCL2*
Aryl hydrocarbon receptor signalling	1.50	***TP53***, ***TRIP11***, ***TFF1***, *MDM2*, *NCOA3*, *FAS*, *EP300*, ***RXRG***, *HSP90B1*, *NCOA2*, ***TGFB1***, ***GSTA1***, *ALDH6A1*
Adipogenesis pathway	1.50	***PPARG***, ***TP53***, *HDAC9*, *CCNH*, ***SMAD9***, ***TGFB1***, ***SAP30L***, *CLOCK*, ***SMO***, *TBL1XR1*, *MNAT1*, *FZD7*
Integrin signalling	1.42	***ITGAM***, *PIK3R3*, *PIK3C2A*, ***PIK3C2B***, ***PARVA***, ***WIPF1***, *TLN2*, ***CAPN10***, *WASL*, ***PIK3CG***, ***RHOA***, ***RHOG***, ***FYN***, ***CAPN6***, *CRK*, *ITGA8*
Docosahexaenoic acid (DHA) signalling	1.40	*PIK3R3*, *PIK3C2A*, *BCL2*, ***CASP9***, ***PIK3C2B***, ***PIK3CG***
Lymphotoxin β receptor signalling	1.34	*PIK3R3*, *PIK3C2A*, ***LTA***, *EP300*, ***CASP9***, ***PIK3C2B***, ***PIK3CG***
IL-12 signalling and production in macrophages	1.34	***APOA4***, *PIK3R3*, *NCOA1*, ***MYD88***, ***TGFB1***, *PIK3C2A*, ***APOD***, *STAT6*, *EP300*, ***PIK3C2B***, ***PPARG***, ***PIK3CG***

Up-regulated genes in low RFI pigs are highlighted in bold and down-regulated genes in normal typeface.

Table 4 Comparison of the microarray and qPCR data of the differentially expressed genes selected for downstream validation.

Gene	Microarray fold change	qPCR fold change	Spearman's rho
ACACA	**1.80***	**1.40**	0.80***
ACSL1	1.24*	1.25*	0.56*
BCL2	1.98*	1.40	0.84***
MMP2	**1.16***	**1.10**	0.74***
SDHB	1.29**	1.23*	0.66**
TFAM	1.43***	1.56*	0.75***

*P < 0.05, **P < 0.01, ***P < 0.001; up-regulated genes in low RFI pigs are highlighted in bold and down-regulated genes in normal typeface. *ACACA* - acetyl-CoA aarboxylase alpha; *ACSL1* - acyl-CoA synthetase long-chain family member 1; *BCL2* - BCL2 apoptosis regulator; *MMP2* - matrix metallopeptidase 2; *SDHB* - succinate dehydrogenase complex iron sulfur subunit B; *TFAM* - transcription factor A, mitochondrial.

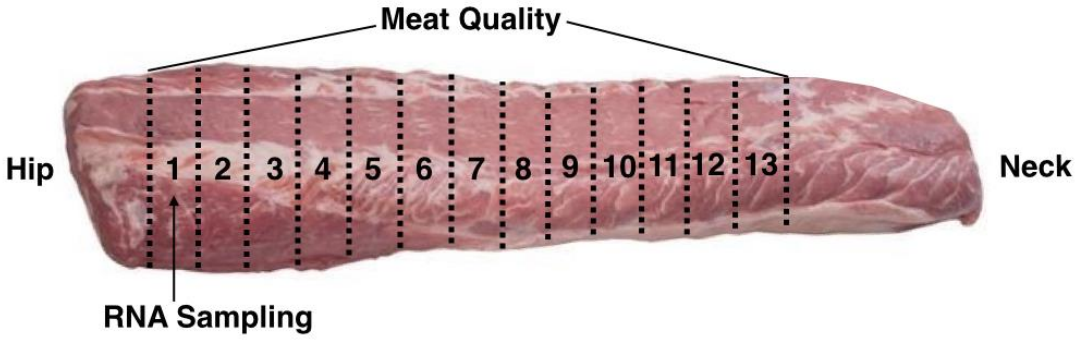

Fig. 1 Assignment of *Longissimus thoracis et lumborum* muscle for transcriptome and meat quality analysis. 1: RNA sampling & colour; 1-3: Warner Bratzler shear force day 1; 4-6: *Warner Bratzler shear force* day 7; 7-10: sensory analysis; 11: drip loss, 12: protein, moisture & intramuscular fat content; 13: fatty acid profile.

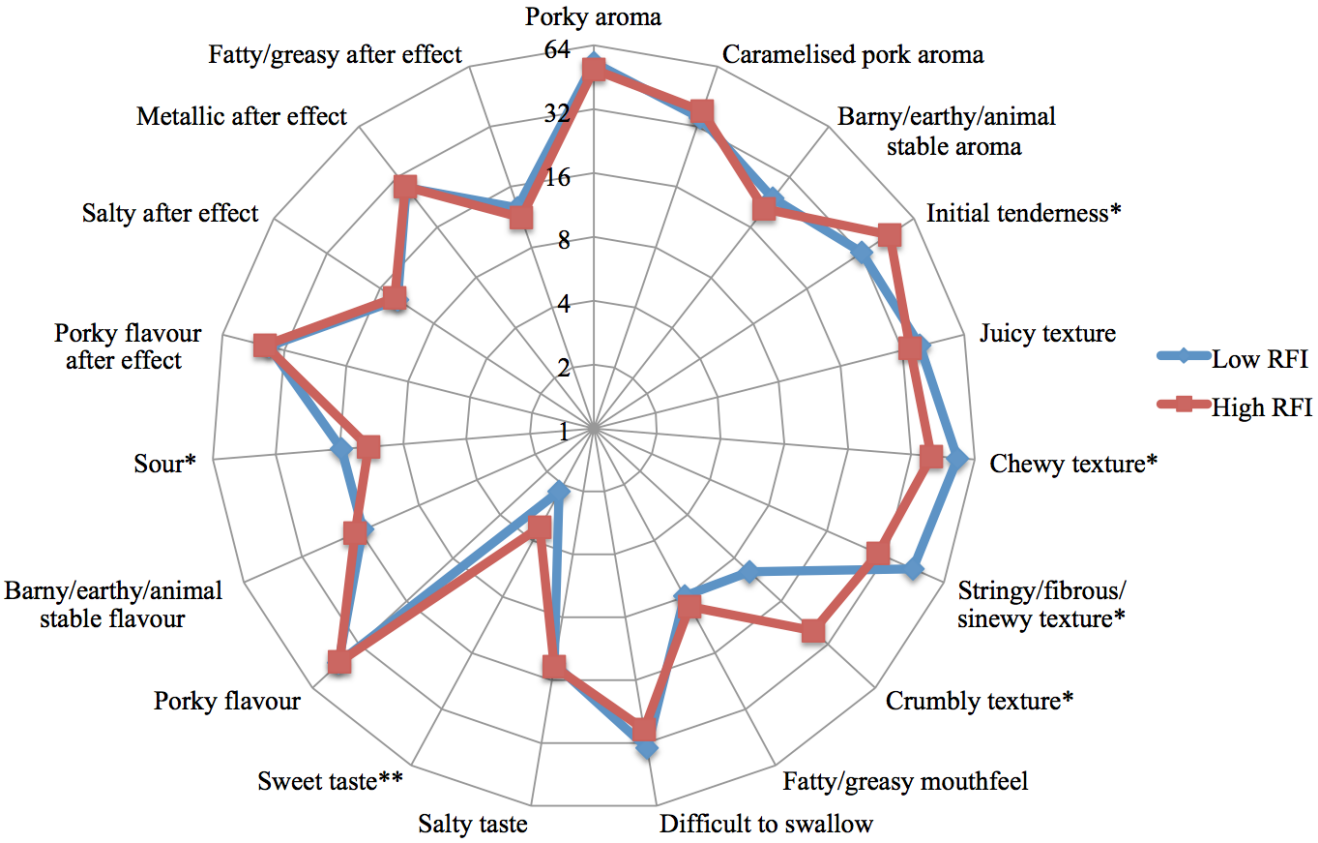

Fig. 2 Meat sensory attributes of *Longissimus thoracis et lumborum* muscle from low and high RFI pigs (least square means) scored from 0 (not detectable) to 100 (extremely detectable); $^{**}P < 0.01$, $^{*}P < 0.05$.

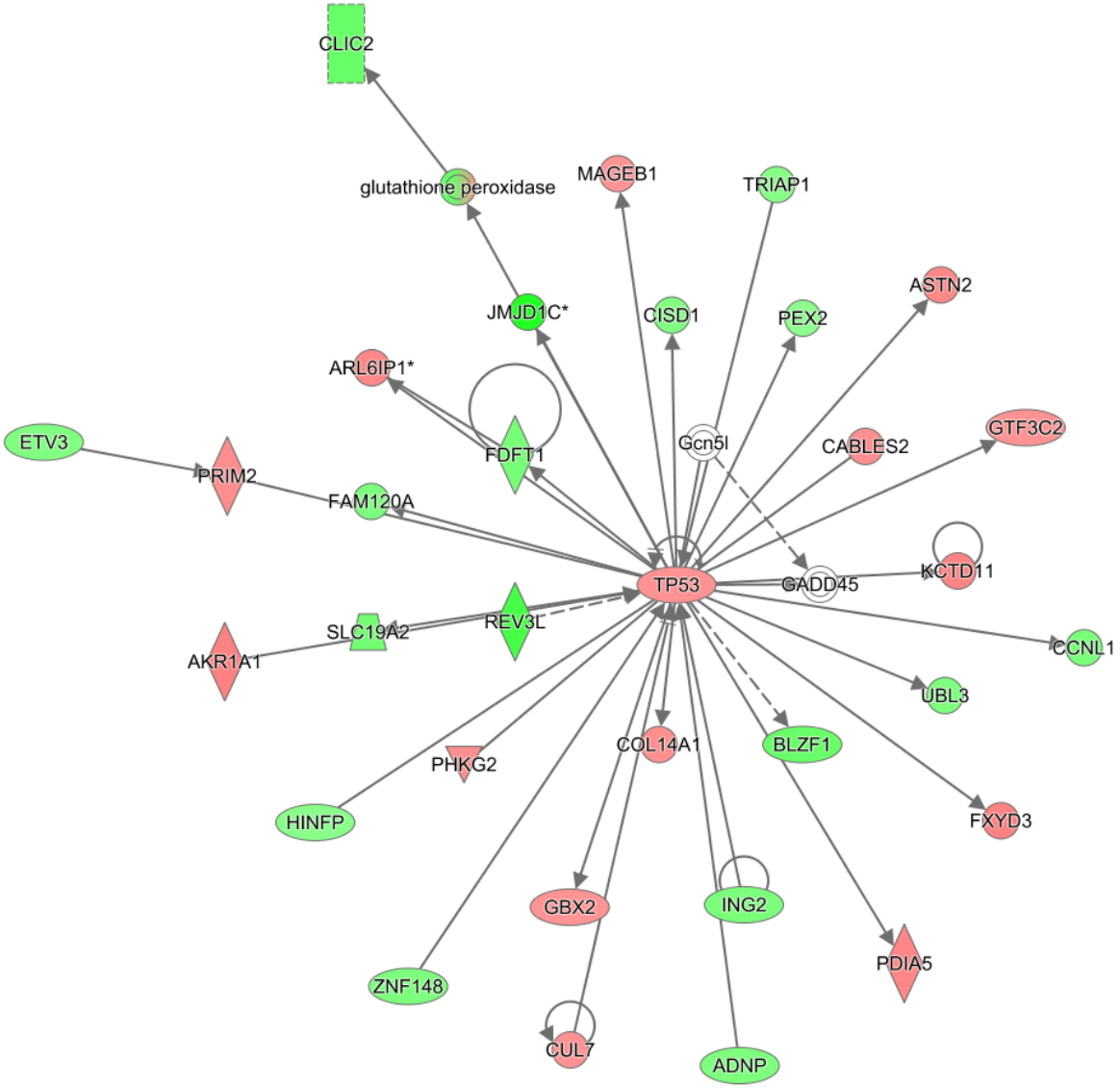

Fig. 3 Network #1 (mRNA genes): molecular transport, nucleic acid metabolism and small molecule biochemistry. Genes are denoted as nodes and the biological relationship between two nodes is denoted as an edge/line. Node colour represents up- (red) and down- (green) regulated genes in low RFI pigs.

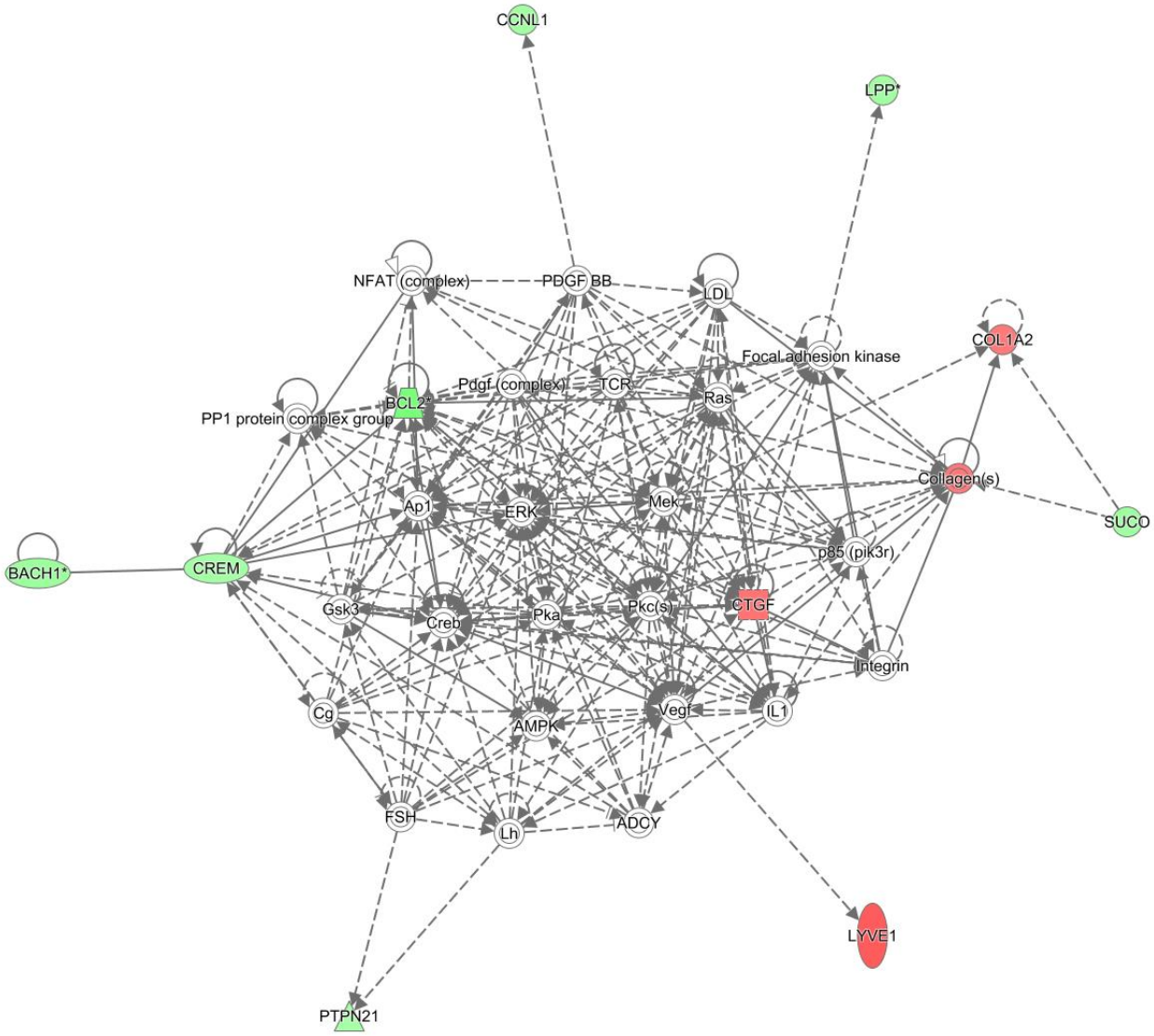

Fig. 4 Network #9 (target genes of the miRNAs involved in the network): Embryonic development, connective tissue development and function, organ morphology. Genes are denoted as nodes and the biological relationship between two nodes is denoted as an edge/line. Node colour represents up- (red) and down- (green) regulated genes in low RFI pigs.

Supplementary data

Table S1 Growth performance parameters of the pigs (10 low and 10 high RFI) selected for meat quality and transcriptomic analysis.

Table S2 Forward and reverse primers for microarray validation through qPCR.

Table S3 Differentially expressed probe sets (n=1,035) between LRFI and HRFI groups.

Table S4 Molecular and cellular functions significantly over-represented among differentially expressed genes including list of molecules contained within each function.
Table S5 Differentially expressed miRNAs in relation to RFI and the number of targeted differentially expressed transcripts.

Figure S1 Network #1(miRNA target genes): cellular development, growth and proliferation, respiratory system development and function.

RNA-seq of muscle from pigs divergent in feed efficiency and product quality identifies differences in immune response, growth, and macronutrient and connective tissue metabolism

Justyna Horodyska[1,2], Klaus Wimmers[2,3], Henry Reyer[2], Nares Trakooljul[2], Anne Maria Mullen[1], Peadar G. Lawlor[4], Ruth M. Hamill[1*]

[1]Teagasc, Food Research Centre, Ashtown, Dublin 15, Ireland
[2]Leibniz Institute for Farm Animal Biology (FBN), Institute for Genome Biology, Dummerstorf, Germany
[3]Faculty of Agricultural and Environmental Sciences, University Rostock, Germany
[4]Teagasc, Pig Development Department, AGRIC, Moorepark, Fermoy, Co. Cork, Ireland
*Corresponding author

In review at BMC Genomics

Abstract

Background: Feed efficiency (FE) is an indicator of efficiency in converting energy and nutrients from feed into a tissue that is of major environmental and economic significance. The molecular mechanisms contributing to differences in FE are not fully elucidated, therefore the objective of this study was to profile the porcine *Longissimus thoracis et lumborum* (LTL) muscle transcriptome, examine the product quality from pigs divergent in FE and investigate the functional networks underpinning the potential relationship between product quality and FE.

Results: RNA-Seq (n = 16) and product quality (n = 40) analysis were carried out in the LTL of pigs differing in FE status. A total of 272 annotated genes were differentially expressed with a $P < 0.01$. Functional annotation revealed a number of biological events related to immune response, growth, carbohydrate & lipid metabolism and connective tissue indicating that these might be the key mechanisms governing differences in FE. Five most significant bio-functions altered in FE groups were 'haematological system development & function', 'lymphoid tissue structure & development', 'tissue morphology', 'cellular movement' and

‘immune cell trafficking’. Top significant canonical pathways represented among the differentially expressed genes included ‘IL-8 signalling’, ‘leukocyte extravasation signalling, ‘sphingosine-1-phosphate signalling’, ‘PKCθ signalling in T lymphocytes’ and ‘fMLP signalling in neutrophils’. A minor impairment in the quality of meat, in relation to texture and water holding capacity, produced by high-FE pigs was observed. High-FE pigs were also associated with reduced intramuscular fat content and improved nutritional profile in terms of fatty acid composition.

Conclusions: Ontology analysis revealed enhanced activity of adaptive immunity and phagocytes in high-FE pigs suggesting more efficient conserving of resources, which can be utilised for other important biological processes. Shifts in carbohydrate conversion into glucose in FE-divergent muscle may underpin the divergent evolution of pH profile in meat from the FE-groups. Moreover, altered amino acid metabolism and increased mobilisation & flux of calcium may influence growth in FE-divergent muscle. Furthermore, decreased degradation of fibroblasts in FE-divergent muscle could impact on collagen turnover and alter tenderness of meat, whilst enhanced lipid degradation in high-FE pigs may potentially underlie a more efficient fat metabolism in these animals.

Key Words – FE, RFI, Residual feed intake, Gene expression, Transcriptomics, RNA

Background

Pork consumption accounts for over 36 percent of the world’s meat intake [1]. Porcine muscle is a significant source of high biological value proteins, vitamins and minerals, as well as dietary fats such as saturated fatty acids (SFA), monounsaturated fatty acids (MUFA), polyunsaturated fatty acids (PUFA), cholesterol and triacylglycerol [2]. SFA and cholesterol content, have been linked to obesity, cardiovascular disease and type 2 diabetes mellitus [3, 4], therefore consumers perceive leaner pork, which is lower in these components as a more healthy option [5, 6].

Feed efficiency (FE) is an indicator of efficiency in converting energy and nutrients from feed into a tissue that is of major nutritional and economic significance [7]. FE is a complex trait involving many organs and can be influenced by environmental and health related factors [8,

9]. Skeletal muscle, being the largest organ in the body and an important location of carbohydrate and lipid metabolism [10-12], plays a particularly important role in the utilisation and storage of a large proportion of the energy acquired from feed. Therefore enhancing our understanding of the biological processes occurring in muscle from FE-divergent pigs could optimise the strategies to improving FE and ease the production cost and ecological footprint from pork production. Furthermore, FE has been shown to be associated with product quality and nutritive profile in several studies, with evidence that the muscle of high-FE pigs exhibits reduced adiposity [13, 14], lower SFA and MUFA, and an enhanced proportion of PUFA [14], which is known for its protective properties against cardiovascular disease [15], and altered overall product quality [13, 14, 16, 17]. Thus divergence in FE is not only of importance to animal production, but it also impacts consumers' preference with regards to quality, nutritive value and wholesomeness of meat.

The molecular mechanisms contributing to differences in FE are not fully elucidated. To date, few studies have conducted transcriptome profiling of skeletal muscle in FE-divergent pigs e.g. [18-20]. Furthermore, these studies did not examine the consequences of divergence in FE on product quality. Here we investigate the impact of divergence in residual feed intake (RFI; the difference between actual feed intake and predicted feed requirements) on product quality of the porcine *Longissimus thoracis et lumborum* (LTL) muscle. Furthermore, we identify in that muscle important biological functions and pathways enriched with differentially expressed (DE) genes in relation to FE, and the functional networks underpinning the relationship between product quality and FE.

Results

Differential gene expression profile

An average of 104.4 million high quality paired-end reads per sample were mapped to the reference with a mean of 80.9% mapping efficiency. A total of 14,497 genes were expressed in the muscle (Fig 1) and of these 306 (272 annotated) genes were differentially expressed between high- and low-FE samples with a $P < 0.01$ corresponding to false discovery rate (q) ≤ 0.47. Of these annotated genes, 176 were up- and 96 were down-regulated, whilst 140 were found to be at least 1.5-fold differentially expressed in high- versus low-FE pigs

(Additional File: Table S1). The most altered genes were *TREH* (fold change = 4.49; high-FE > low-FE) and *SDC4* (fold change = -2.35; high-FE < low-FE). Transcripts with a $P < 0.01$ corresponding to a $q \leq 0.47$ were considered significantly differentially expressed, which is not a highly stringent cut-off because the differences in mRNA abundances between the FE groups were relatively small. However to offset this lower statistical stringency for differential expression profiling, B-H corrected p-values were used to refine the data that was further utilised to extract bio-functions, pathways and networks.

Gene ontology analysis

Enrichment analysis of the DE genes was utilised to investigate biological processes and pathways altered in response to differences in FE. Thirty nine biological functions and thirty eight canonical pathways were significantly ($P < 0.01$) enriched with DE genes. Most affected biological functions were 'haematological system development & function', 'lymphoid tissue structure & development', 'tissue morphology', 'cellular movement' and 'immune cell trafficking' (Table 1). A list of sub-categories enclosed within each function is presented in Additional file 2: Table S2. A number of functions ranged from significantly repressed to significantly activated state, including 'haematological system development and function' (z-score range: -2.13 – 3.52), 'tissue morphology' (z-score range: -2.13 – 2.87) and 'cell death and survival' (z-score range: -2.27 – 2.20). Functions containing a positive z-score range included 'immune cell trafficking' (z-score range: 0.58 – 3.52), cell-to-cell signalling and interaction' (z-score range: 0.12 – 3.19), cell-mediated immune response' (z-score range: 0.58 – 2.94), 'tissue development' (z-score range: 0.78 – 2.30) and 'vitamin and mineral metabolism' (z-score range: 2.36 – 2.89). Furthermore, most affected pathways were 'IL-8 signalling', 'leukocyte extravasation signalling', 'sphingosine-1-phosphate signalling', 'PKCθ signalling in T lymphocytes' and 'fMLP signalling in neutrophils' (Table 2 and Additional File 3: Table S3). Analysis of molecule connectivity revealed nineteen networks enriched with DE genes, of which network #2 (Fig 2) contained 21 DE molecules related to macronutrients metabolism, specifically 'protein synthesis', 'lipid metabolism' and 'molecular transport'.

Validation of RNA-seq results

Expression patterns of four randomly selected genes (*FAM134B*, *FOXO1*, *SPP1* and *TRIM63*) were confirmed through qPCR using *RPL32* as a reference gene to normalise expressions of these target transcripts. Significant differences in the mRNA abundances of *FAM134B*, *FOXO1* and *TRIM63* transcripts between the FE groups were verified and expression of *SPP1* was altered in the same direction when compared to the RNA-seq. Spearman correlations between RNA-seq and qPCR data, ranging from 0.89 to 0.94, were significant at $P < 0.001$ for all four assessed mRNAs (Table 3).

Product quality

Carcass and product quality traits of FE-divergent pigs are depicted in Table 4, whereby sensory attributes of LTL muscle in FE-divergent pigs are illustrated in Fig 3. Intramuscular fat (IMF) content significantly differed between the FE groups ($P < 0.05$), with the high-FE carcasses having leaner muscle (1.49% IMF) comparing to low-FE carcasses (1.89% IMF). Muscle depth and percent lean meat did not differ significantly between the FE groups however pH at 45min *post-mortem* (*pm)* showed a tendency toward decreased values in the high-FE pigs ($P < 0.1$) while pH measured at 2h, 3h, 4h, 5h and 24h *pm* was significantly lower in the high-FE group ($P < 0.05$), and changes in pH evolution over time are depicted in Fig 4. Drip loss did not vary between the FE groups. Muscle from high-FE pigs had increased cook loss at day 1 *pm* ($P < 0.01$) but there was no difference detected at day 7 *pm*. Although meat produced by high-FE pigs was significantly associated with increased Warner Bratzler shear force values (WBSF, less tender) at day 1 *pm* ($P < 0.05$) and had a tendency towards increased WBSF values at day 7 *pm* ($P < 0.1$), this difference in tenderness between the FE groups was not detected by sensory panellists. However, pork sensory assessment revealed that meat produced from high-FE pigs had higher scores for salty taste ($P < 0.05$) and a tendency towards increased barny/earthy/animal stable flavour ($P < 0.1$). Nutritive profile in relation to fatty acid (FA) proportions in LTL muscle (mg FA/100g meat), and percentage of FA in IMF of FE-divergent pigs are shown in Fig 5. SFA did not differ significantly in LTL muscle of FE-divergent pigs, however, a tendency towards decreased proportions for each of palmitic and stearic acids in high-FE muscle was observed ($P < 0.1$). Muscle from high-FE group contained significantly lower amounts of the MUFA, palmitoleic acid ($P < 0.05$) and had a tendency towards decreased proportions of eicosenoic and oleic acids ($P < 0.1$). While

PUFA content of muscle did not differ, when comparing the IMF *per se*, high-FE muscle had significantly greater concentrations of linoleic and alpha-linolenic acids ($P < 0.05$). Furthermore, a number of significant correlations at a $P < 0.05$ were identified between product quality traits and genes differentially expressed in FE-divergent pigs (Table 5). The strongest positive linear relationships were observed between percentage lean and *HK3* (r = 0.679), cook loss at day 7 *pm* and *PON3* (r = 0.621), and MUFA and *FOXO1* (r = 0.618). The strongest negative linear relationships were observed between cook loss at day 1 *pm* and *NFATC2* (r = -0.809), MUFA and *HK3* (r = -0.741), and cook loss at day 1 *pm* and *MYC* (r = -0.724).

Discussion

Functional annotation of divergent genes revealed a number of biological events related to immune response, growth, carbohydrate & lipid metabolism and connective tissue indicating that these might be important mechanisms governing differences in FE. Alongside attaining insights of the biological processes contributing to differences in muscle of FE-divergent pigs, we also investigated the consequences of the divergence in FE on product quality and the functional networks within muscle that underpin the relationship between FE and product quality. Divergence in FE affected various aspects of product quality and nutritive value, such as pH, tenderness, cook loss, as well as IMF content and fatty acid proportions, and this study provided clues with regards to biological mechanisms driving the relationship between FE and the observed alteration in product quality traits of economic significance.

Immune response

Ontology analysis revealed a number of pathways and biological functions related to immune response as being relevant to FE in porcine muscle. Greater amounts of leucocytes [21] and higher cellular immune response [22], were previously observed in pigs selected for lean growth. In the present study ‘protein kinase C-theta (PKCθ) signalling in T lymphocytes’ and ‘cluster of differentiation 28 (CD28) signalling in T helper cells’, which activate and promote differentiation of T cells, were significantly enriched cell-mediated immune responses. These features were also observed in pigs selected for lean growth that were subjected to an immunological challenge i.e. tetanus toxoid [22]. Furthermore, ‘tec-kinase signalling’,

involved in development and function of cellular immune response T-cells [23] was significantly activated (z-score = 2.12) in high-FE pigs exhibiting leaner growth. This pathway, alongside many other significantly over-represented pathways, was enriched with Phosphatidylinositol-4-Phosphate 3-Kinase Catalytic Subunit Type 2 Beta (*PIK3C2B*) belonging to a family of enzymes modulating immune cell development, differentiation and function [24]. *PIK3C2B* was specifically shown to play a key role in T-cell activation [25]. Functional annotation also exposed 'Interleukin 8 (IL-8) signalling', controlling trafficking of neutrophils and macrophages to the site of inflammation [26], to be significantly activated in high-FE pigs (z-score = 2.50). 'Accumulation of phagocytes' and 'phagocytosis', contained within the broader 'immune cell trafficking and tissue development' and 'cellular function and maintenance' categories, respectively, were also predicted to be significantly activated in high-FE pigs (z-score = 2.15 and 2.12, respectively). Additionally pathways playing a role in stimulating phagocytes activity [27] and muscle repair capabilities [28], 'N-formyl-Met-Leu-Phe (fMLP) signalling in neutrophils' and 'production of nitric oxide in macrophages', tended towards activation in high-FE pigs. Fuelling immune response is an energetically expensive process, which would be suspected to lower animal's feed efficiency due to prioritizing nutrients towards the immune-related processes [8]. Previous literature has reported decreased immune response in muscle from high-FE pigs [18]. On the contrary, a study conducted in cattle identified a number of immune-related processes, representing both innate and adaptive response, significantly activated in muscle of high-FE individuals i.e., 'immune response of antigen presenting cells and leukocytes', 'response of mononuclear leukocytes and myeloid cells', and 'immune response of phagocytes' [29]. Here, our findings suggest that muscle from high-FE pigs exhibit activated immune response. Furthermore, more reliance on adaptive rather than innate immunity, which could reduce feed requirements, may stimulate faster growth of muscle [30] from high-FE pigs.

Carbohydrate metabolism and glycolytic potential

pH evolution in the *pre-rigor* period was highly divergent in relation to FE status. At the earliest time-point measured (45m *pm*), pH did not significantly differ. However, pH at all later stages in the early *pm* period- up to 5 hours- as well as ultimate pH monitored the next day significantly differed between the two groups, with the high-FE pigs showing decreased pH values in the muscle. This is consistent with previous studies demonstrating greater

glycolytic potential in high-FE pigs, wherein pH 30m *pm* did not differ but ultimate pH was significantly reduced in high-FE pigs [13, 16]. Low pH in meat can increase the perception of sour taste due to a higher concentration of free hydrogen ions [31, 32]. Nevertheless, the significant difference in ultimate pH was not detected as increased acidity by sensory panellists in this study, who perceived no difference in sour taste of meat from high- versus low-FE. However, the reduced ultimate pH may have contributed to significantly higher scores for 'salty taste' that were observed in high-FE meat. This is in agreement with Lipinski et al. [33] who previously found that meat with lower pH can be perceived by sensory panellists as more salty.

Genes involved in glycolysis and energy metabolism were previously reported to be up-regulated in chickens exhibiting lower ultimate pH [34]. Here, pH evolution was significantly different in the FE-divergent muscle, and trehalase (*TREH*) that codes for an enzyme catalysing the conversion of trehalose to glucose [35] was the most up-regulated gene (fold change = 4.49) in high-FE pigs. This might indicate that this group of pigs could potentially exhibit more efficient energy conversion in growth, but with potential consequences for *post-mortem* energy metabolism and product quality. Indeed, ontology analysis highlighted the molecular function 'catabolism of oligosaccharides', which was enclosed within a broader 'carbohydrate metabolism' category, as being highly relevant to the gene expression changes in divergent FE muscle. Moreover genes enriched in this sub-category, *GM2* ganglioside activator (*GM2A*, fold change = 1.60; high-FE > low-FE) and neuraminidase 3 (*NEU3*, fold change = 1.29; high-FE > low-FE), were negatively correlated with ultimate pH and positively correlated with drip loss, respectively. These findings suggest that differences in carbohydrate conversion into glucose underpin the differential evolution of pH profile in FE-divergent muscle.

Carbohydrate metabolism has an important influence on water-holding capacity of meat [36]. Water-holding capacity traits, alongside tenderness, are closely linked with pH and here unfavourable associations between FE, lower ultimate pH and increased cook loss at day 1 with a reduced tenderness (6N increase in WBSF) were observed. However, sensory tenderness remained unchanged and, other than saltiness, no other sensory attributes were altered. It has been previously postulated that lower water holding capacity of meat with

decreased ultimate pH can result in tougher beef (increased WBSF) [37], which is consistent with our (WBSF) observations in the present study.

Growth

Syndecan-4 (*SDC4)* was the most down-regulated gene (fold change = -2.35) in high-FE muscle. *SDC4* is a gene encoding plasma membrane proteoglycans and has been previously shown to have an impact on muscle cell proliferation and differentiation [38]. Knock down of *SDC4* has been associated with increased myogenic regulatory transcription factor [39] and myogenin expressions, as well as increased muscle differentiation [40], which signify its importance to muscle growth. Integrating functional annotations of DE genes revealed a number of biological processes related to growth. 'Tissue development' and 'cardiovascular system development & function' were significantly enriched categories amongst the DE genes, with forkhead box O1 (*FOXO1*) being included (fold change = -1.49) in both categories. FOXO1 belongs to the FOXO forkhead type family of transcription factors and it plays a role in modulation of skeletal muscle angiogenesis and function [41]. Mice over-expressing *FOXO1* were found to weigh less and had a decreased skeletal muscle mass [42].

'Mobilisation and flux of Ca^{2+}', contained within a 'vitamin and mineral metabolism' category, were significantly activated in high-FE pigs (z-score = 2.9 and 2.4, respectively). Calcium plays a key role in function and plasticity of skeletal muscle. It regulates skeletal muscle formation [43, 44], homeostasis and regeneration as well as being a crucial component triggering muscle contraction that enables movement [44] and furthermore plays an important role *post-mortem* in tenderness development [45]. Moreover 'synthesis of alpha-amino acids' and 'catabolism of L-tryptophan', enclosed within an 'amino acid metabolism' category, as well as 'production of protein', contained within 'protein metabolism' category, were significantly enriched amongst DE genes. L-tryptophan is an alpha-amino acid that positively influences production of protein in skeletal muscle and growth performance [46]. L-tryptophan is also a precursor of a broad range of compounds regulating appetite therefore playing a role in FE [46]. Although muscle and adipose depth did not significantly differ between the FE groups, down-regulation of *SDC4* & *FOXO1,* altered amino acid metabolism and increased mobilisation & flux of Ca2+ may impact, at least to some extent, growth in FE-divergent pigs.

FE, connective tissue and tenderness

Collagen type XI alpha 1 chain *(COL11A1)* and collagen type VI alpha 5 chain (*COL6A5)* were up-regulated (fold change = 1.52 and 1.77, respectively) in high-FE pigs. Over-expression of *COL11A1* has been associated with decreased tenderness in heifers [47]. Also, a single-nucleotide polymorphism in this gene was identified to have a consistent association with meat tenderness across three cattle breeds [48]. This study highlights that its relevance to tenderness development is also conserved in porcine muscle. Ontology analysis highlighted several functions also related to connective tissue, for example 'apoptosis of fibroblast cell lines', enclosed within 'cell death and survival' category, was significantly inhibited in high-FE pigs (z-score = -2.27). All of the DE genes represented in this category were also enriched in 'cell death of connective tissue' (z-score = -1.18), which also falls under the broader 'cell death and survival' function. Apoptosis and the stress response have been implicated as important factors in tenderisation. Specifically, apoptosis and cell death is considered the first step in promotion of tenderisation and factors which down-regulate apoptosis, such as heat shock protein expression can inhibit tenderisation [49-51]. In the present study, the more efficient pigs produced muscle that tenderised more slowly, with significantly tougher pork on day 1 *pm* compared with less efficient counterparts. Even by day 7 *pm*, while the differences in shear force were small, a tendency towards increased toughness remained. In this scenario the modulation of apoptosis as observed through our gene expression studies may have contributed to this differential ageing associated with FE and should be a matter of consideration in further driving improvements in FE. Fibroblasts are the key players in the synthesis of extracellular matrix components such as collagen [52, 53]. Amongst down-regulated transcripts in muscle of high-FE pigs were nuclear factor of activated T-cells 1 (*NFATC1*), nuclear factor of activated T-cells 2 (*NFATC2*) and transcription factor P64 (*MYC*) (fold change = -1.30, -1.25 and -1.57, respectively) that have previously been shown to induce apoptosis in fibroblasts [54-56]. Correlation analysis between DE genes and product quality traits showed a negative correlation between *NFATC2* and cook loss at day 1 *pm*, whilst *NTAFC1* had a tendency towards being negatively correlated with cook loss at day 1 *pm* (Table 5). Surprisingly, *NFATC1* was also positively correlated with WBSF (higher values indicate decreased tenderness). Moreover, a negative correlation between *MYC* and cook loss at day 1 *pm* was noted and this is in support with a previous study which identified a SNP in *MYC* to be associated with pH and cook loss in

pork [57]. Besides connective tissue, tenderness of meat is vastly influenced by greater calpastatin activity through decreased pm protein degradation [17]. In the present study, calpastatin (*CAST*) had a tendency towards being down-regulated ($P < 0.1$, fold change = -1.17) in high-FE pigs suggesting an enhancing effect on tenderness, which is in contrast to our observation that tenderness was impaired in high-FE pigs, furthermore tenderness development was slower in this group. Nevertheless, the altered tenderness of FE-divergent meat could be partially impacted by shifts in collagen turnover resulting from decreased degradation of fibroblasts.

Lipid metabolism changes associated with FE

Muscle depth and leanness did not differ between the FE groups, which contrast previous reports [13, 14, 16, 17]. However, here and in prior studies, selection for high-FE was associated with reduced IMF [14, 16, 17]. Over the past decades, consumers have become more conscious with regards to wholesome eating and seeking healthier options [6]. Meat from high-FE pigs exhibited tendencies towards decreased levels of SFA and MUFA, which are known to be the major constituents of triacylglycerol [58, 59] and are associated with increased risk of cardiovascular disease [60, 61]. Higher proportions of PUFA, whilst lower levels of SFA and MUFA, has been previously associated with reduced IMF content [59, 62, 63]. Indeed, the IMF of meat from high-FE pigs was 12 percent richer in PUFA compared to IMF from low-FE group. PUFA has been shown to reduce low-density lipoprotein cholesterol levels and exhibit protective properties against cardiovascular disease [15], therefore suggesting that meat from high-FE pigs may have a healthier fatty acid profile. Underpinning these changes, functions and pathways important in metabolism of lipids were also affected by FE, as evident from the ontology analysis, specifically ‘concentration of lipids, cholesterol & triacylglycerol’ and ‘fatty acid metabolism’, enclosed within a broader ‘lipid metabolism’ category. Correlation analysis between DE genes, enriched in ‘lipid metabolism’ category, and product quality traits revealed a number of significant correlations. *FOXO1* (fold change = -1.49), which was previously shown to play a role in adipogenesis in cattle [64], was positively correlated with fat depth, SFA and MUFA, and also negatively correlated with lean percentage. Cytochrome B-245 beta chain (*CYBB;* fold change = 1.56) was positively correlated with percent lean and negatively correlated with IMF, SFA and MUFA. A previous study conducting expression profiling of porcine adipose

tissue suggested CYBB to play a role in fat metabolism and adipogenic differentiation [65]. Correlation analysis has also revealed Perilipin 1 (*PLIN 1*; fold change = -1.42) to be positively correlated with IMF, SFA, MUFA and PUFA and this is in keeping with a previous study reporting its higher abundance being associated with increased IMF in porcine muscle [66]. Moreover, C-X-C motif chemokine ligand 10 (*CXCL10*, fold change = 2.24), which was previously associated to marbling in cattle [67], was negatively correlated with IMF, SFA and MUFA.

Furthermore, the second most significant network (network #2), identified through the functional annotation analysis, contained several features related to 'lipid metabolism', 'molecular transport' and 'protein synthesis'. Paraoxonase 3 (*PON3*) and triacylglycerol lipase (*LIPC*) were the most up-regulated genes in this network (fold change = 4.40 and 3.51, respectively). PON3, an enzyme belonging to the PON family, associates with high density lipoproteins (HDL) [68], which are lipid particles that function to export excess cholesterol from muscle and adipose tissue to the liver [69]. PON3 knockout mice have previously been shown to exhibit increased body weight [70], which points towards a PON3 role in promoting a leaner muscle growth. The enzyme LIP catalyses hydrolysis of phospholipids and triacylglycerols [71]. Over-expression of *LIPC* in high-FE muscle suggests enhanced lipid degradation in this group of pigs and potentially underlies a more efficient fat metabolism in these animals.

Conclusions

Gene expression profiling of muscle from FE-divergent pigs provided mechanistic insights on the biological events prevailing differences in FE, which impact product quality. Small but significant changes in the quality of meat, in relation to texture and water holding capacity, from high-FE pigs, were observed. High-FE muscle was characterised by reduced intramuscular fat content and improved nutritional profile in terms of fatty acid composition. Ontology analysis revealed enhanced activity of adaptive immunity and phagocytes in high-FE pigs, which may indicate that these animals are more efficient in conserving resources that can be utilised for other important biological processes. Shifts in carbohydrate conversion into glucose in FE-divergent muscle may underpin the altered evolution of pH profile in meat from the divergent groups. Although muscle depth did not significantly differ

between the FE groups, our transcriptomic findings indicate that altered amino acid metabolism and increased mobilisation & flux of calcium may influence, at least to some extent, growth in FE-divergent muscle. Moreover, decreased degradation of fibroblasts, the key players in the synthesis of the extracellular matrix, could impact on collagen turnover and alter tenderness of meat. Biological functions important in metabolism of lipids were also affected by FE. Specifically, enhanced lipid degradation in more efficient pigs may potentially underlie a more efficient fat metabolism in these animals.

Materials and Methods

Animals and experimental design

Animal housing, diets and tests were previously described in details in Metzler-Zebeli and colleagues [72]. 138 pigs from the intact litters of 12 sows (Landrace x Large White; Hermitage Genetics, Kilkenny, Ireland) inseminated with semen from 6 boars (Maxgro; Hermitage Genetics; 2 litters per boar, each having a high estimated breeding value for FE), were utilised in this study. Pigs, weaned at 28 days of age and group-housed (entire sibling groups), were provided with *ad libitum* access to feed and water. Diets were provided in the same sequence with the same ingredient and chemical composition (starter, link, weaner and finisher) and were delivered to pigs via Feed Intake Recording Equipment (FIRE) feeders (Schauer Agrotonic, Wels, Austria). Pigs were tested from day 42 until 91 post-weaning. Feed intake was recorded daily, whereas pig weight, back-fat depth and muscle depth were recorded weekly between day 70 and day 120 of age. Average daily feed intake (ADFI) and average daily gain (ADG) were calculated for each pig weekly. Residual feed intake (RFI, a measure of FE defined as the difference between actual feed intake and predicted feed requirements) was calculated after day 120 of age as the residual from a least squares regression model of ADFI on ADG, metabolic live weight, gender and also all relevant two-way interactions, and the effects of back-fat and muscle depth using the PROC REG procedure in SAS (version 9.4; SAS Inst. Inc., Cary, NC, USA). Based on RFI values, pigs were categorised within litter and gender as low (L) RFI and high (H) RFI and of these a total of 40 (20 extremes from LRFI (high-FE) - 10 males and 10 females, and 20 extremes from HRFI (low-FE) - 10 males and 10 females) were selected for gene expression profiling and meat quality analysis. The mean RFI (g/day) of the LRFI and HRFI pigs was -100.2 (SD: 97.9) and 150.7 (SD: 163.3) respectively, whereas

the mean of feed conversion ratio (FCR, ratio of feed intake and weigh gain) of the LRFI (high-FE) and HRFI (low-FE) pigs was 1.98 (SD: 0.16) and 2.27 (SD: 0.25) respectively. The slaughter of animals, fasted for 18 hours with an average final body weight of 99 kg (SD: 11.4kg), occurred on 2 slaughter days, a week apart, and was by electronic stunning followed by exsanguination. Samples of the LTL muscle were collected and snap frozen in liquid nitrogen within 10 minutes *pm* followed by storage at -80°C until RNA isolation. The LTL muscle was excised 24 hours *pm* from each carcass and utilised for meat quality analysis.

RNA library preparation, differential expression analysis and functional annotation

Sixteen muscle samples selected from the most FE-divergent siblings of the same gender (8 from LRFI (high-FE) - 4 males and 4 females, and 8 from HRFI (low-FE) - 4 males and 4 females), were snap frozen following which they were ground into fine powder in liquid nitrogen. Total RNA was isolated using Tri-Reagent (Sigma-Alrich, Taufkirchen, Germany), followed by DNase treatment and a column-based purification using the Nucleospin RNA II kit (Macherey-Nagel, Düren, Germany). RNA library preparation was carried out using the TruSeq Stranded mRNA protocol. Following RNA sequencing with Illumina HiSeq2500, paired-end reads were mapped to the reference Sscrofa10.2 (Ensembl release 84) [73] using TopHat (2.1.0). Read counts were assigned to the gene features using the HTSeq 0.6.1 program [74]. Differential gene expression analysis in relation to FE was performed using DESeq2 package (3.4.0, www.R-project.org), including RFI groups and sow as fixed effects. Gene symbols for significantly altered genes ($P < 0.01$) and related fold changes were submitted to Ingenuity Pathway Analysis (IPA; Ingenuity® Systems, www.ingenuity.com), whereby Benjamini-Hochberg (B-H) corrected *P*-values were used to detect significantly enriched bio-functions and canonical pathways ($P < 0.01$). Functional annotations with a z-score greater than 2 and lower than -2 were considered significantly activated and inhibited in high-FE pigs, respectively. Information enclosed in the Ingenuity® Knowledge Base was utilised to generate potential important interaction networks amongst the DE genes.

Validation of RNA sequencing results

For cDNA synthesis, 1 µg of total RNA was utilized in the presence of random primers (Promega, Mannheim, Germany), oligo (dT) primer and Superscript® III reverse transcriptase (Invitrogen Corp., San Diego, CA, USA). Four DE genes were selected for validation through

quantitative real-time PCR (qPCR). Primers for target genes (Additional file 4: Table S4) were designed using Primer-BLAST software in the NCBI (https://www.ncbi.nlm.nih.gov/tools/primer-blast) based on *Sus scrofa* nucleotide sequences and their specificity was determined with the BLAST search tool database (http://www.ncbi.nlm.nih.gov/BLAST). qPCR was carried out with LightCycler 96 system (Roche Mannheim, Germany). 2 µl of cDNA was amplified in a 10 µl reaction volume using 6 µl SYBR Green I Master (Roche) and 0.6 µl (10 µM) of each forward and reverse primer. Cycling conditions for reference and DE genes consisted of initial denaturation at 95 °C for 5 min and 45 cycles of amplification (95 °C for 10 sec, 60 °C for 15 sec and 72 °C for 25 sec). A melting curve analysis was included at the end of the amplification to confirm the specificity of all amplification reactions. Normalised qPCR data were analysed using ANOVA test in R, including RFI groups as a fixed effect and sow as a random effect. Correlation analysis between the RNA-seq and qPCR data were carried out with R package considering the results as significant at $P < 0.05$.

Product quality

Carcass grading along with technological and sensory meat quality traits as well as nutritional profiling of meat were measured using methods as described in detail by Horodyska and colleagues [14]. The carcass grading included fat depth, muscle depth, lean percent and IMF content, whilst the technological meat quality included pH (45m, 2h, 3h, 4h, 5h and 24h *pm*), drip loss, cook loss and tenderness (WBSF). Fatty acids were profiled to assess the nutritive value of meat. PROC MIXED procedure in the SAS system was used to evaluate associations between FE and meat quality traits in the Maxgro x (Landrace x Large White) pigs (n = 40). The model included RFI groups, gender & slaughter day as fixed effects, sow as a random effect, live weight as a covariate and the absolute values of RFI as a weight statement. Moreover, Spearman's correlations (r) between product quality traits and normalised expression values of selected DE genes, out of a total number of identified DE genes in RFI-divergent pigs (n =16), were determined using the PROC CORR procedure in the SAS system (version 9.4).

Abbreviations

FE: feed efficiency; **RFI:** residual feed intake; **LTL:** *Longissimus thoracis et lumborum;* **IMF:** Intramuscular fat content; ***pm:*** *post-mortem;* **LRFI:** low RFI; **HRFI:** high RFI; **WBSF:** Warner Bratzler shear force; **SFA**: saturated fatty acids; **MUFA**: monounsaturated fatty acids; **PUFA**: polyunsaturated fatty acids.

Acknowledgements

The authors wish to thank Carol Griffin for training sensory panellists and conducting sensory assessment of the samples, as well as staff and students at Teagasc who assisted in animal sampling.

Funding

The ECO-FCE project was funded by the European Union Seventh Framework Programme (FP7 2007/2013) under grant agreement No. 311794.

Availability of data

Raw RNA-seq data were deposited in the ArrayExpress database at EMBL-EBI (www.ebi.ac.uk/arrayexpress) (accession number: E-MTAB-6174).

Author's contributions

JH collected samples, extracted RNA, prepared libraries, validated RNA-seq via qPCR, measured meat quality traits, carried out data analysis and wrote the manuscript; KW designed the experiment and edited the manuscript; HR participated in statistical analysis and edited the manuscript; NT assisted in library preparation, performed RNA-seq and data analysis, and edited the manuscript; AMM participated in animal sampling and edited the manuscript; PGL provided the animals, participated in data collection and analysis, and edited the manuscript; RMH conceived and designed the experiment, collected samples and edited the manuscript.

Competing interests

The authors declare that they have no competing interests.

Ethics approval

In this study, all procedures were conducted in accordance with national regulations concerning animal research and commercial slaughtering under experimental licence from the Irish Department of Health in accordance with the Cruelty to Animals Act 1876 and the European Communities (Amendments of the cruelty of Animals Act 1976) Regulations, 1994, and were authorized by Teagasc Animal Ethics Committee.

References

1. The Food and Agriculture Organization of the United Nations: **Sources of meat**. 2014. [http://www.fao.org/ag/againfo/themes/en/meat/backgr_sources.html]. Accessed on 30 Sept 2017.
2. Hathwar SC, Rai AK, Modi VK, Narayan B: **Characteristics and consumer acceptance of healthier meat and meat product formulations—a review**. *J Food Sci Technol* 2012, **49**(6):653-664.
3. Micha R, Michas G, Mozaffarian D: **Unprocessed Red and Processed Meats and Risk of Coronary Artery Disease and Type 2 Diabetes – An Updated Review of the Evidence**. *Curr Atheroscler Rep* 2012, **14**(6):515-524.
4. Wang Y, Beydoun MA: **Meat consumption is associated with obesity and central obesity among US adults**. *Int J Obes (2005)* 2009, **33**(6):621-628.
5. Cordts A, Nitzko S, Spiller A: **Consumer response to negative information on meat consumption in germany**. *IFAMA* 2014, **17** (A).
6. McNeill SH: **Inclusion of red meat in healthful dietary patterns**. *Meat Sci* 2014, **98**(3):452-460.
7. Wilkinson JM: **Re-defining efficiency of feed use by livestock**. *Animal* 2011, **5**(7):1014-1022.
8. Patience JF, Rossoni-Serão MC, Gutiérrez NA: **A review of feed efficiency in swine: biology and application**. *J Anim Sci Biotechnol* 2015, **6**(1):33.
9. Tizioto PC, Coutinho LL, Oliveira PSN, Cesar ASM, Diniz WJS, Lima AO, Rocha MI, Decker JE, Schnabel RD, Mourao GB *et al*: **Gene expression differences in Longissimus muscle of Nelore steers genetically divergent for residual feed intake**. *Sci Rep* 2016, **6**.
10. Morales PE, Bucarey JL, Espinosa A: **Muscle lipid letabolism: role of lipid droplets and perilipins**. *J Diabetes Res* 2017, **2017**:10.
11. Pedersen BK: **Muscle as a secretory organ**. *Compr Physiol* 2013, **3**(3):1337-1362.
12. Turner N, Cooney GJ, Kraegen EW, Bruce CR: **Fatty acid metabolism, energy expenditure and insulin resistance in muscle**. *J Endocrinol* 2014, **220**(2):T61-79.
13. Faure J, Lefaucheur L, Bonhomme N, Ecolan P, Meteau K, Coustard SM, Kouba M, Gilbert H, Lebret B: **Consequences of divergent selection for residual feed intake**

in pigs on muscle energy metabolism and meat quality. *Meat Sci* 2013, **93**(1):37-45.
14. Horodyska J, Oster M, Reyer H, Mullen AM, Lawlor PG, Wimmers K, Hamill RM: **Analysis of meat quality traits and gene expression profiling of pigs divergent in residual feed intake**. *Meat Sci* 2018, **137**:265–274.
15. Czernichow S, Thomas D, Bruckert E: **n-6 Fatty acids and cardiovascular health: a review of the evidence for dietary intake recommendations**. *Br J Nutr* 2010, **104**(6):788-796.
16. Lefaucheur L, Lebret B, Ecolan P, Louveau I, Damon M, Prunier A, Billon Y, Sellier P, Gilbert H: **Muscle characteristics and meat quality traits are affected by divergent selection on residual feed intake in pigs**. *J Anim Sci* 2011, **89**(4):996-1010.
17. Smith RM, Gabler NK, Young JM, Cai W, Boddicker NJ, Anderson MJ, Huff-Lonergan E, Dekkers JC, Lonergan SM: **Effects of selection for decreased residual feed intake on composition and quality of fresh pork**. *J Anim Sci* 2011, **89**(1):192-200.
18. Gondret F, Vincent A, Houee-Bigot M, Siegel A, Lagarrigue S, Causeur D, Gilbert H, Louveau I: **A transcriptome multi-tissue analysis identifies biological pathways and genes associated with variations in feed efficiency of growing pigs**. *BMC Genomics* 2017, **18**(1):244.
19. Jing L, Hou Y, Wu H, Miao YX, Li XY, Cao JH, Brameld JM, Parr T, Zhao SH: **Transcriptome analysis of mRNA and miRNA in skeletal muscle indicates an important network for differential Residual Feed Intake in pigs**. *Sci Rep* 2015, **5**.
20. Vincent A, Louveau I, Gondret F, Trefeu C, Gilbert H, Lefaucheur L: **Divergent selection for residual feed intake affects the transcriptomic and proteomic profiles of pig skeletal muscle**. *J Anim Sci* 2015, **93**(6):2745-2758.
21. Clapperton M, Bishop SC, Glass EJ: **Selection for lean growth and food intake leads to correlated changes in innate immune traits in Large White pigs**. *Anim Sci* 2006, **82**:867-876.
22. Adler M, Murani E, Ponsuksili S, Wimmers K: **PBMC transcription profiles of pigs with divergent humoral immune responses and lean growth performance**. *Int J Biol Sci* 2013, **9**(9):907-916.
23. Schaeffer EM, Yap GS, Lewis CM, Czar MJ, McVicar DW, Cheever AW, Sher A, Schwartzberg PL: **Mutation of Tec family kinases alters T helper cell differentiation**. *Nat Immunol* 2001, **2**(12):1183-1188.
24. Okkenhaug K: **Signalling by the phosphoinositide 3-kinase family in immune cells**. *Annu Rev Immunol* 2013, **31**:675-704.
25. Srivastava S, Di L, Zhdanova O, Li Z, Vardhana S, Wan Q, Yan Y, Varma R, Backer J, Wulff H *et al*: **The class II Phosphatidylinositol 3 kinase C2β is required for the activation of the K(+) channel KCa3.1 and CD4 T-Cells**. *Mol Biol Cell* 2009, **20**(17):3783-3791.
26. Jundi K, Greene CM: **Transcription of Interleukin-8: How Altered Regulation Can Affect Cystic Fibrosis Lung Disease**. *Biomolecules* 2015, **5**(3):1386-1398.
27. Sato T, Hongu T, Sakamoto M, Funakoshi Y, Kanaho Y: **Molecular mechanisms of N-Formyl-methionyl-leucyl-phenylalanine-induced superoxide generation and degranulation in mouse neutrophils: phospholipase D is dispensable**. *Mol Cell Biol* 2013, **33**(1):136-145.
28. MacMicking J, Xie QW, Nathan C: **Nitric oxide and macrophage function**. *Annu Rev Immunol* 1997, **15**:323-350.

29. Weber KL, Welly BT, Van Eenennaam AL, Young AE, Porto-Neto LR, Reverter A, Rincon G: **Identification of Gene Networks for Residual Feed Intake in Angus Cattle Using Genomic Prediction and RNA-seq**. *PLoS One* 2016, **11**(3):e0152274.
30. Leshchinsky TV, Klasing KC: **Divergence of the inflammatory response in two types of chickens**. *Dev Comp Immunol* 2001, **25**(7):629-638.
31. Da Conceicao Neta ER, Johanningsmeier SD, Drake MA, McFeeters RF: **A chemical basis for sour taste perception of acid solutions and fresh-pack dill pickles**. *J Food Sci* 2007, **72**(6):S352-359.
32. Ramos Da Conceicao Neta ER, Johanningsmeier SD, McFeeters RF: **The chemistry and physiology of sour taste--a review**. *J Food Sci* 2007, **72**(2):R33-38.
33. Lipinski K, Stasiewicz M, Purwin C, Zuk-Golaszewska K: **Effects of magnesium on pork quality**. *J Elementol* 2011, **16**(2):325-337.
34. Beauclercq S, Hennequet-Antier C, Praud C, Godet E, Collin A, Tesseraud S, Metayer-Coustard S, Bourin M, Moroldo M, Martins F *et al*: **Muscle transcriptome analysis reveals molecular pathways and biomarkers involved in extreme ultimate pH and meat defect occurrence in chicken**. *Scie Rep* 2017, **7**(1):6447.
35. Sode K, Akaike E, Sugiura H, Tsugawa W: **Enzymatic synthesis of a novel trehalose derivative, 3,3′-diketotrehalose, and its potential application as the trehalase enzyme inhibitor**. *FEBS Lett* 2001, **489**(1):42-45.
36. Pösö AR, Puolanne E: **Carbohydrate metabolism in meat animals**. *Meat Sci* 2005, **70**(3):423-434.
37. Silva JA, Patarata L, Martins C: **Influence of ultimate pH on bovine meat tenderness during ageing**. *Meat Sci* 1999, **52**(4):453-459.
38. Velleman SG, Coy CS, McFarland DC: **Effect of syndecan-1, syndecan-4, and glypican-1 on turkey muscle satellite cell proliferation, differentiation, and responsiveness to fibroblast growth factor 2**. *Poult Sci* 2007, **86**(7):1406-1413.
39. Shin J, McFarland DC, Velleman SG: **Heparan sulfate proteoglycans, syndecan-4 and glypican-1, differentially regulate myogenic regulatory transcription factors and paired box 7 expression during turkey satellite cell myogenesis: implications for muscle growth**. *Poult Sci* 2012, **91**(1):201-207.
40. Ronning SB, Carlson CR, Stang E, Kolset SO, Hollung K, Pedersen ME: **Syndecan-4 regulates muscle differentiation and is internalized from the plasma membrane during myogenesis**. *PLoS One* 2015, **10**(6).
41. Nwadozi E, Roudier E, Rullman E, Gustafsson T, Haas T: **Endothelial FoxO proteins regulate obesity associated skeletal muscle capillary rarefaction**. *Faseb J* 2015, **29**.
42. Kamei Y, Miura S, Suzuki M, Kai Y, Mizukami J, Taniguchi T, Mochida K, Hata T, Matsuda J, Aburatani H *et al*: **Skeletal muscle FOXO1 (FKHR) transgenic mice have less skeletal muscle mass, down-regulated type I (slow twitch/red muscle) fiber genes, and impaired glycemic control**. *J Biol Chem* 2004, **279**(39):41114-41123.
43. Przybylski RJ, Szigeti V, Davidheiser S, Kirby AC: **Calcium regulation of skeletal myogenesis. II. Extracellular and cell surface effects**. *Cell Calcium* 1994, **15**(2):132-142.
44. Tu MK, Levin JB, Hamilton AM, Borodinsky LN: **Calcium signaling in skeletal muscle development, maintenance and regeneration**. *Cell Calcium* 2016, **59**(2-3):91-97.
45. Tizioto PC, Gromboni CF, Nogueira AR, de Souza MM, Mudadu Mde A, Tholon P, Rosa Ado N, Tullio RR, Medeiros SR, Nassu RT *et al*: **Calcium and potassium**

content in beef: influences on tenderness and associations with molecular markers in Nellore cattle. *Meat Sci* 2014, **96**(1):436-440.
46. Wang H, Ji Y, Wu G, Sun K, Sun Y, Li W, Wang B, He B, Zhang Q, Dai Z *et al*: **l-Tryptophan activates mammalian target of rapamycin and enhances expression of tight junction proteins in intestinalporcine epithelial cells**. *J Nutr* 2015, **145**(6):1156-1162.
47. Afonso J, Tizioto PC, Oliveira PSN, Diniz WJS, Lima AOD, Souza MMD, Rocha MIP, Silva JVD, Buss CE, Gromboni CF *et al*: **0903 Differentially expressed genes in genetically divergent Nellore steers for calcium content in the Longissimus dorsi muscle**. *J Anim Sci* 2016, **94**:435-435.
48. Ramayo-Caldas Y, Renand G, Ballester M, Saintilan R, Rocha D: **Multi-breed and multi-trait co-association analysis of meat tenderness and other meat quality traits in three French beef cattle breeds**. *Genet Sel Evol* 2016, **48**(1):37.
49. Hamill RM, McBryan J, McGee C, Mullen AM, Sweeney T, Talbot A, Cairns MT, Davey GC: **Functional analysis of muscle gene expression profiles associated with tenderness and intramuscular fat content in pork**. *Meat Sci* 2012, **92**(4):440-450.
50. Ouali A, Gagaoua M, Boudida Y, Becila S, Boudjellal A, Herrera-Mendez CH, Sentandreu MA: **Biomarkers of meat tenderness: Present knowledge and perspectives in regards to our current understanding of the mechanisms involved**. *Meat Sci* 2013, **95**(4):854-870.
51. Ouali A, Herrera-Mendez CH, Coulis G, Becila S, Boudjellal A, Aubry L, Sentandreu MA: **Revisiting the conversion of muscle into meat and the underlying mechanisms**. *Meat Sci* 2006, **74**(1):44-58.
52. Scherzer MT, Waigel S, Donninger H, Arumugam V, Zacharias W, Clark G, Siskind LJ, Soucy P, Beverly L: **Fibroblast-derived extracellular matrices: an alternative cell culture system that increases metastatic cellular properties**. *PLoS One* 2015, **10**(9).
53. Russell SB, Russell JD, Trupin KM: **Collagen synthesis in human fibroblasts: effects of ascorbic acid and regulation by hydrocortisone**. *J Cell Physiol* 1981, **109**(1):121-131.
54. Neal JW, Clipstone NA: **A constitutively active NFATc1 mutant induces a transformed phenotype in 3T3-L1 fibroblasts**. *J Biol Chem* 2003, **278**(19):17246-17254.
55. Robbs BK, Cruz AL, Werneck MB, Mognol GP, Viola JP: **Dual roles for NFAT transcription factor genes as oncogenes and tumor suppressors**. *Mol Cell Biol* 2008, **28**(23):7168-7181.
56. Evan GI, Wyllie AH, Gilbert CS, Littlewood TD, Land H, Brooks M, Waters CM, Penn LZ, Hancock DC: **Induction of apoptosis in fibroblasts by c-myc protein**. *Cell* 1992, **69**(1):119-128.
57. Oh JD, Kim ES, Lee HK, Song KD: **Effect of a c-MYC gene polymorphism (g.3350G>C) on meat quality traits in berkshire**. *Asian-Australas J Anim Sci* 2015, **28**(11):1545-1550.
58. Kasprzyk A, Tyra M, Babicz M: **Fatty acid profile of pork from a local and a commercial breed**. *Arch Anim Breed* 2015, **58**(2):379-385.
59. Wood JD, Enser M, Fisher AV, Nute GR, Sheard PR, Richardson RI, Hughes SI, Whittington FM: **Fat deposition, fatty acid composition and meat quality: A review**. *Meat Sci* 2008, **78**(4):343-358.
60. Austin MA: **Triacylglycerol and coronary heart disease**. *Proc Nutr Soc* 1997, **56**(2):667-670.

61. Athyros VG, Kakafika AI, Papageorgiou AA, Tziomalos K, Skaperdas A, Pagourelias E, Pirpasopoulou A, Karagiannis A, Mikhailidis DP: **Atorvastatin decreases triacylglycerol-associated risk of vascular events in coronary heart disease patients**. *Lipids* 2007, **42**(11):999-1009.
62. Dominguez R, Lorenzo JM: **Effect of genotype on fatty acid composition of intramuscular and subcutaneous fat of Celta pig breed**. *Grasas Y Aceites* 2014, **65**(3).
63. Dugan MER, Vahmani P, Turner TD, Mapiye C, Juárez M, Prieto N, Beaulieu AD, Zijlstra RT, Patience JF, Aalhus JL: **Pork as a source of omega-3 (n-3) fatty acids**. *J Clin Med* 2015, **4**(12):1999-2011.
64. Moisá SJ, Shike DW, Faulkner DB, Meteer WT, Keisler D, Loor JJ: **Central role of the PPARγ gene network in coordinating beef cattle intramuscular adipogenesis in response to weaning age and nutrition**. *Gene Regul Syst Bio* 2014, **8**:17-32.
65. Huang W, Zhang X, Li A, Xie L, Miao X: **Differential regulation of mRNAs and lncRNAs related to lipid metabolism in two pig breeds**. *Oncotarget* 2017, **8**(50):87539-87553.
66. Li B, Weng Q, Dong C, Zhang Z, Li R, Liu J, Jiang A, Li Q, Jia C, Wu W *et al*: **A key gene, PLIN1, can affect porcine intramuscular fat content based on transcriptome analysis**. *Genes* 2018, **9**(4).
67. Lim D, Lee SH, Kim NK, Cho YM, Chai HH, Seong HH, Kim H: **Gene co-expression analysis to characterize genes related to marbling trait in hanwoo (Korean) cattle**. *Asian-Australas J Anim Sci* 2013, **26**(1):19-29.
68. Getz GS, Reardon CA: **Paraoxonase, a cardioprotective enzyme: continuing issues**. *Curr Opin Lipidol* 2004, **15**(3):261-267.
69. Feingold KR, Grunfeld C, : **Introduction to lipids and lipoproteins. In: De Groot L.J., Chrousos G., Dungan K., et al., editors.** . South Dartmouth (MA): MDText.com, Inc.; 2000. Available from: https://www.ncbi.nlm.nih.gov/books/NBK305896/.
70. Shih DM, Yu JM, Vergnes L, Dali-Youcef N, Champion MD, Devarajan A, Zhang P, Castellani LW, Brindley DN, Jamey C *et al*: **PON3 knockout mice are susceptible to obesity, gallstone formation, and atherosclerosis**. *FASEB J* 2015, **29**(4):1185-1197.
71. Chatterjee C, Sparks DL: **Hepatic lipase, high density lipoproteins, and hypertriglyceridemia**. *The American Journal of Pathology* 2011, **178**(4):1429-1433.
72. Metzler-Zebeli BU, Lawlor PG, Magowan E, McCormack UM, Curiao T, Hollmann M, Ertl R, Aschenbach JR, Zebeli Q: **Finishing pigs that are divergent in feed efficiency show small differences in intestinal functionality and structure**. *PLoS One* 2017, **12**(4):e0174917.
73. Kim D, Pertea G, Trapnell C, Pimentel H, Kelley R, Salzberg SL: **TopHat2: accurate alignment of transcriptomes in the presence of insertions, deletions and gene fusions**. *Genome Biol* 2013, **14**(4).
74. Anders S, Pyl PT, Huber W: **HTSeq-a Python framework to work with high-throughput sequencing data**. *Bioinformatics* 2015, **31**(2):166-169.

Table 1 Molecular, cellular and physiological categories significantly over-represented among the differentially expressed genes.

Category	B-H p-value range*	Z-score range[$]
Haematological System Development & Function	1.72E-11-5.74E-03	-2.13 – 3.52[£]
Lymphoid Tissue Structure & Development	1.72E-11-5.00E-03	-0.65 – 2.94[£]
Tissue Morphology	1.72E-11-5.16E-03	-2.13 – 2.87[£]
Cellular Movement	1.72E-11-5.74E-03	-0.36 – 3.52[£]
Immune Cell Trafficking	6.54E-11-5.74E-03	0.58 – 3.52[£]
Cellular Function & Maintenance	6.54E-11-4.56E-03	-0.06 – 2.83[£]
Cellular Development	1.29E-10-5.00E-03	-0.65 – 1.64
Cellular Growth & Proliferation	1.29E-10-5.00E-03	-0.65 – 1.73
Cell-To-Cell Signalling & Interaction	2.21E-09-5.74E-03	0.12 – 3.19[£]
Protein Synthesis	6.50E-09-2.32E-03	0.24 – 1.18
Humoral Immune Response	9.96E-09-3.58E-03	-0.57 – 1.89
Cellular Compromise	1.14E-08-2.80E-03	-1.51 – 2.20[£]
Cell-mediated Immune Response	1.79E-07-5.74E-03	0.58 – 2.94[£]
Free Radical Scavenging	2.33E-07-8.89E-07	1.13
Cell Death & Survival	2.42E-06-4.57E-03	-2.27 – 2.20[£]
Tissue Development	3.60E-06-4.56E-03	0.78 – 2.30[£]
Embryonic Development	5.77E-06-3.53E-03	0.54 – 1.50
Haematopoiesis	5.77E-06-1.11E-03	0.78 – 1.77
Organ Development	5.77E-06-3.94E-03	-0.66 – 1.50
Organismal Development	5.77E-06-4.95E-03	0.72 – 1.64
Cell Morphology	1.39E-05-4.95E-03	-0.08 – 2.09[£]
Lipid Metabolism	1.48E-05-1.19E-03	-1.23 – 0.60
Small Molecule Biochemistry	1.48E-05-5.74E-03	-1.23 – 0.60
Organ Morphology	1.70E-05-4.95E-03	1.06 – 1.77
Molecular Transport	1.97E-05-1.81E-03	-0.01 – 2.89[£]
Cardiovascular System Development & Function	2.63E-05-4.95E-03	-0.95 – 2.12[£]
Digestive System Development & Function	6.90E-05-5.38E-03	-0.66
Organismal Survival	8.09E-05-8.09E-05	-0.04
Cell Signalling	1.05E-04-1.81E-03	0.12 – 3.19[£]
Vitamin & Mineral Metabolism	1.05E-04-1.81E-03	2.36 – 2.89[£]
Cell Cycle	5.91E-04-3.94E-03	-0.49 – -1.98
Gene Expression	5.91E-04-3.53E-03	-1.98 – -0.49
Cellular Assembly & Organization	7.30E-04-5.74E-03	0.33 – 1.89
Renal & Urological System Development & Function	1.74E-03-3.94E-03	-0.15 – 0.76
Carbohydrate Metabolism	2.09E-03-2.09E-03	NA
Amino Acid Metabolism	2.74E-03-5.74E-03	NA
Hepatic System Development & Function	3.20E-03-3.20E-03	-0.66
Skeletal & Muscular System Development & Function	3.54E-03-3.54E-03	NA
Nervous System Development & Function	4.63E-03-4.63E-03	NA

*Range of B-H multiple testing correction p-values of enriched functions within the category; [$]range of z-scores for sub-categories contained within a particular category; [£]annotations with a z-score > 2 and z-score < -2 were considered significantly activated and inhibited in high-FE pigs, respectively; NA: no activity pattern available.

Table 2 Most significant canonical pathways observed among differentially expressed genes in relation to feed efficiency (FE).

Canonical Pathway	-log (B-H p-value)	Z-score	Genes
IL-8 signalling	4.13	2.50[£]	***RND2***, ***PIK3C2B***, ***PLCB2***, ***VCAM1***, ***PTK2B***, ***PIK3C2G***, ***GNB5***, *MAPK8*, ***RAC3***, *ROCK2*, ***ITGB2***, ***FGFR4***, ***NCF2***, ***CYBB***
Leukocyte extravasation signalling	3.38	1.73	***PIK3C2B***, ***VCAM1***, ***PTK2B***, ***CXCR4***, ***PIK3C2G***, *MAPK8*, *RAPGEF3*, *ROCK2*, ***ITGB2***, ***FGFR4***, ***NCF2***, ***CYBB***, ***VAV1***
Sphingosine-1-phosphate signalling	3.38	1.67	***RND2***, ***PIK3C2B***, ***NAAA***, ***PLCB2***, ***PTK2B***, ***FGFR4***, *ADCY4*, ***PIK3C2G***, *SPHK1*, ***CASP1***
PKCθ signalling in T lymphocytes	3.22	0.63	***PIK3C2B***, *MAP3K14*, ***FGFR4***, ***PIK3C2G***, *MAPK8*, ***CD86***, *NFATC2*, ***VAV1***, ***RAC3***, *NFATC1*
fMLP signalling in neutrophils	2.86	1.41	***PIK3C2B***, ***PLCB2***, ***FGFR4***, ***NCF2***, ***PIK3C2G***, ***CYBB***, ***GNB5***, *NFATC2*, *NFATC1*
B cell receptor signalling	2.86	0.91	***PIK3C2B***, *MAP3K14*, *FOXO1*, ***PTK2B***, ***FGFR4***, ***PIK3C2G***, *MAPK8*, *NFATC2*, ***VAV1***, ***PIK3AP1***, *NFATC1*
Myc mediated apoptosis signalling	2.86	NA	*MYC*, ***PIK3C2B***, ***FGFR4***, ***PIK3C2G***, *MAPK8*, *CYCS*, ***SFN***
Chemokine signalling	2.86	1.13	*ROCK2*, ***PLCB2***, ***PTK2B***, ***CXCR4***, ***PIK3C2G***, *MAPK8*, ***CCL5***
Gαq signalling	2.86	1.00	***RND2***, *ROCK2*, ***PIK3C2B***, ***PLCB2***, ***PTK2B***, ***FGFR4***, ***PIK3C2G***, ***GNB5***, *NFATC2*, *NFATC1*
CD28 signalling in T helper cells	2.86	0.33	***PIK3C2B***, ***FGFR4***, ***PIK3C2G***, *MAPK8*, ***CD86***, *NFATC2*, ***VAV1***, ***CTLA4***, *NFATC1*

[£]Significantly activated (z-score > 2) pathways in high-FE pigs; NA: no activity pattern available; up-regulated genes in high-FE pigs are highlighted in bold and down-regulated genes in normal typeface.

Table 3 Comparison of RNA-seq and qPCR data of selected genes affected by feed efficiency (FE).

Gene	qPCR fold change	RNA-seq fold change	Spearman's rho
FAM134B	2.2***	2.1**	0.938***
FOXO1	1.6**	1.5**	0.888***
SPP1	**3.6**	**2.5***	0.944***
TRIM63	2.2**	2.0**	0.921***

*$P < 0.05$, **$P < 0.01$, ***$P < 0.001$; up-regulated genes in high-FE pigs are highlighted in bold and down-regulated genes in normal typeface.

Table 4 Product quality traits of *Longissimus thoracis et lumborum* muscle divergent in feed efficiency (FE).

Trait	High-FE[1]	Low-FE[1]	SE	P-value
Fat depth (mm)	14.6	15.5	0.95	0.364
Muscle depth (mm)	54.6	56.8	2.36	0.367
Lean (%)	56.2	55.5	0.87	0.477
IMF (%)	1.49	1.89	0.19	**0.046**
Drip loss (%)	4.71	4.16	0.68	0.428
Tenderness day 1 (N)	37.0	31.8	2.33	**0.036**
Tenderness day 7 (N)	28.9	26.4	1.46	0.089[$]
Cook loss day 1 (%)	36.4	34.0	0.67	**0.001**
Cook loss day 7 (%)	37.8	37.2	0.58	0.250

[1]Least square means for each trait; [$]$P < 0.1$.

Table 5 Correlations between product quality traits and selected differentially expressed genes, out of the 272, in pigs divergent for feed efficiency.

Gene	pH 45m	pH 24h	DL	Tend. D1	Tend. D7	CL D1	CL D7	Fat depth	Muscle depth	Lean	IMF	SFA	MUFA	PUFA
CCR2	0.00	-0.51	0.44	0.01	0.16	0.20	0.06	0.01	-0.08	0.01	-0.38	-0.26	-0.22	-0.37
	0.99	**0.04**	0.09	0.98	0.56	0.45	0.83	0.96	0.77	0.97	0.15	0.34	0.41	0.16
COL11A1	0.44	-0.45	-0.13	0.04	-0.46	0.25	0.24	-0.32	-0.42	0.14	-0.03	0.00	-0.02	0.14
	0.09	0.08	0.64	0.88	0.07	0.36	0.38	0.23	0.11	0.60	0.92	1.00	0.93	0.59
COL6A5	0.34	-0.46	0.27	0.24	0.31	0.42	0.21	-0.11	0.12	0.29	-0.22	-0.41	-0.43	-0.18
	0.20	0.07	0.31	0.37	0.24	0.11	0.44	0.69	0.67	0.28	0.42	0.12	0.10	0.51
CXCL10	0.31	-0.25	0.22	-0.07	-0.13	0.37	-0.29	-0.34	0.04	0.36	-0.63	-0.61	-0.65	-0.46
	0.24	0.35	0.41	0.80	0.64	0.16	0.27	0.19	0.88	0.16	**0.01**	**0.01**	**0.01**	0.07
CYBB	0.28	-0.40	0.30	-0.04	0.21	0.11	-0.04	-0.44	0.06	0.50	-0.59	-0.53	-0.54	-0.36
	0.29	0.13	0.26	0.89	0.44	0.70	0.89	0.09	0.82	**0.04**	**0.02**	**0.04**	**0.03**	0.16
FOXO1	-0.43	0.52	-0.20	0.02	0.08	-0.63	-0.35	0.54	0.16	-0.53	0.26	0.50	0.62	0.09
	0.10	**0.04**	0.46	0.93	0.77	**0.01**	0.19	**0.03**	0.55	**0.04**	0.32	**0.04**	**0.01**	0.74
GM2A	0.39	-0.57	0.28	-0.14	-0.09	0.40	0.33	-0.41	-0.28	0.39	-0.33	-0.37	-0.43	-0.10
	0.14	**0.02**	0.29	0.61	0.73	0.12	0.22	0.12	0.29	0.14	0.22	0.16	0.10	0.71
HK3	0.09	-0.35	0.08	-0.23	-0.05	0.35	-0.31	-0.70	0.07	0.68	-0.54	-0.63	-0.74	-0.37
	0.75	0.19	0.76	0.40	0.85	0.19	0.24	**<0.01**	0.81	**<0.01**	**0.03**	**0.01**	**<0.01**	0.16
ITGB2	0.36	-0.52	0.35	-0.09	0.10	0.41	0.06	-0.49	-0.14	0.53	-0.50	-0.54	-0.60	-0.37
	0.17	**0.04**	0.18	0.75	0.71	0.12	0.84	**0.04**	0.60	**0.04**	**0.04**	**0.03**	**0.01**	0.15
LIPC	-0.04	-0.08	0.24	0.00	0.27	0.15	-0.05	-0.06	0.41	0.17	-0.24	-0.36	-0.44	-0.28
	0.87	0.78	0.38	0.99	0.32	0.59	0.85	0.82	0.12	0.52	0.37	0.16	0.09	0.29
MYC	0.01	0.46	-0.21	-0.23	0.09	-0.72	-0.14	0.10	0.25	-0.03	0.24	0.28	0.26	0.20
	0.97	0.07	0.44	0.39	0.73	**<0.01**	0.60	0.70	0.36	0.92	0.38	0.29	0.32	0.47
NEU3	-0.24	-0.24	0.54	0.23	0.62	0.12	0.06	0.14	-0.11	-0.14	-0.06	-0.07	-0.06	-0.06
	0.38	0.38	**0.03**	0.39	**0.01**	0.65	0.84	0.62	0.69	0.61	0.84	0.80	0.81	0.82
NFATC1	-0.23	0.12	0.21	0.28	0.70	-0.49	-0.32	0.34	0.36	-0.24	0.14	0.21	0.25	-0.13
	0.39	0.65	0.42	0.29	**<0.01**	0.06	0.23	0.19	0.17	0.36	0.61	0.43	0.36	0.63
NFATC2	-0.29	0.38	0.07	-0.12	0.35	-0.81	-0.27	0.57	0.35	-0.44	0.28	0.38	0.46	-0.08
	0.28	0.15	0.80	0.66	0.18	**<0.01**	0.31	**0.02**	0.18	0.09	0.30	0.15	0.07	0.76
PDK4	-0.41	0.46	-0.59	0.14	-0.10	-0.27	-0.25	0.18	0.08	-0.25	0.33	0.48	0.51	0.26
	0.11	0.08	**0.02**	0.62	0.72	0.32	0.35	0.50	0.77	0.35	0.21	0.06	0.05	0.32
PIK3C2B	-0.02	-0.22	0.51	-0.09	0.16	0.13	0.27	0.22	-0.50	-0.40	0.06	0.19	0.21	0.18
	0.95	0.42	**0.04**	0.73	0.55	0.63	0.31	0.41	0.05	0.13	0.84	0.47	0.44	0.50
PLIN1	0.18	0.30	-0.49	-0.26	-0.32	-0.22	0.34	-0.02	-0.17	-0.11	0.51	0.61	0.61	0.59
	0.51	0.27	0.05	0.33	0.23	0.41	0.20	0.95	0.52	0.69	**0.04**	**0.01**	**0.01**	**0.02**
PON3	0.32	-0.30	-0.04	0.25	-0.14	0.56	0.62	-0.13	-0.31	0.07	-0.01	-0.06	-0.05	0.28
	0.23	0.26	0.88	0.34	0.62	**0.02**	**0.01**	0.63	0.24	0.80	0.98	0.82	0.86	0.30
SDC4	-0.32	0.54	-0.19	-0.04	0.21	-0.50	-0.58	0.14	0.41	0.00	-0.05	0.02	0.07	-0.22
	0.23	**0.03**	0.49	0.87	0.44	0.05	**0.02**	0.59	0.11	1.00	0.85	0.93	0.80	0.41
SLC1A2	0.09	-0.53	0.29	0.35	0.20	0.51	-0.24	-0.52	-0.23	0.44	-0.61	-0.47	-0.53	-0.29
	0.76	**0.04**	0.29	0.21	0.48	0.05	0.38	0.05	0.41	0.10	**0.02**	0.08	**0.04**	0.29
TREH	0.23	-0.27	0.45	-0.28	0.15	0.05	0.33	-0.06	-0.23	0.01	-0.16	-0.18	-0.19	0.02
	0.41	0.33	**0.09**	0.31	0.59	0.85	0.23	0.83	0.42	0.97	0.58	0.52	0.49	0.95

Correlation coefficient is presented in the upper row and a *P*-value is shown in the bottom row. Significant correlations are highlighted in bold. DL: drip loss (%); Tend. D1: tenderness day 1 (N), Tend. D7: tenderness day 7 (N), CL D1: cook loss day 1 (%), CL D7: cook loss day 7 (%), Fat depth (mm), Muscle depth (mm), Lean (%), IMF: intramuscular fat content (%), SFA: saturated fatty acid (mg), MUFA: monounsaturated fatty acid (mg), PUFA: polyunsaturated fatty acid (mg).

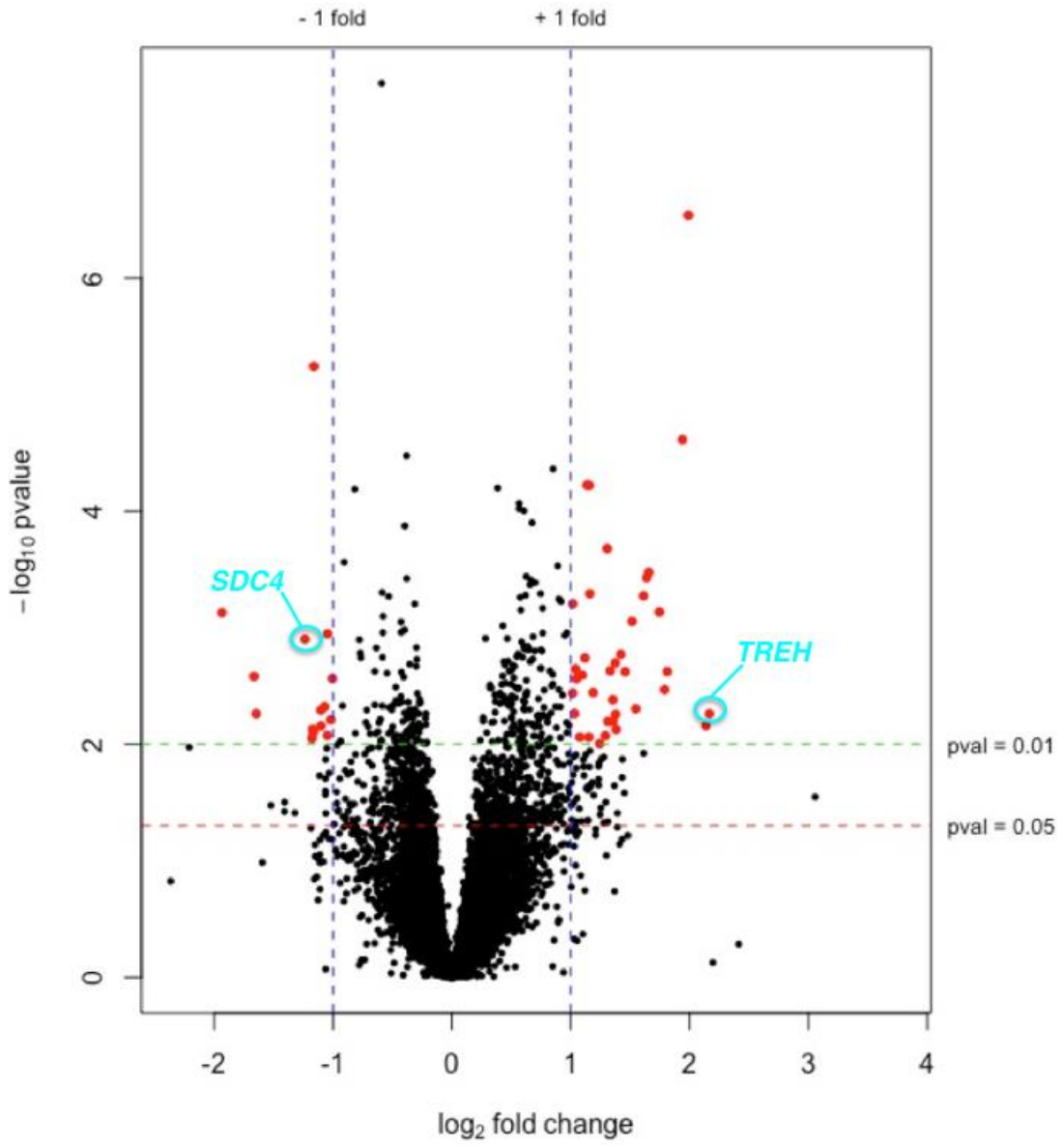

Fig 1 Volcano plot depicting a total of 14,497 genes expressed in muscle from pigs divergent in feed efficiency. The horizontal green and red lines indicate the suggestive significance thresholds of differentially expressed (DE) genes at $P < 0.01$ and 0.05, respectively. The vertical blue lines represent the threshold of log2 fold change ≥ |1| (fold change ≥ |2|) and the red dots depict significantly DE genes at $P < 0.01$ and log2 fold change ≥ |1| (fold change ≥ |2|). Positive and negative fold changes refer to up- and down-regulated genes in high-FE pigs, respectively. The most up- and down-regulated annotated genes are highlighted in a circle.

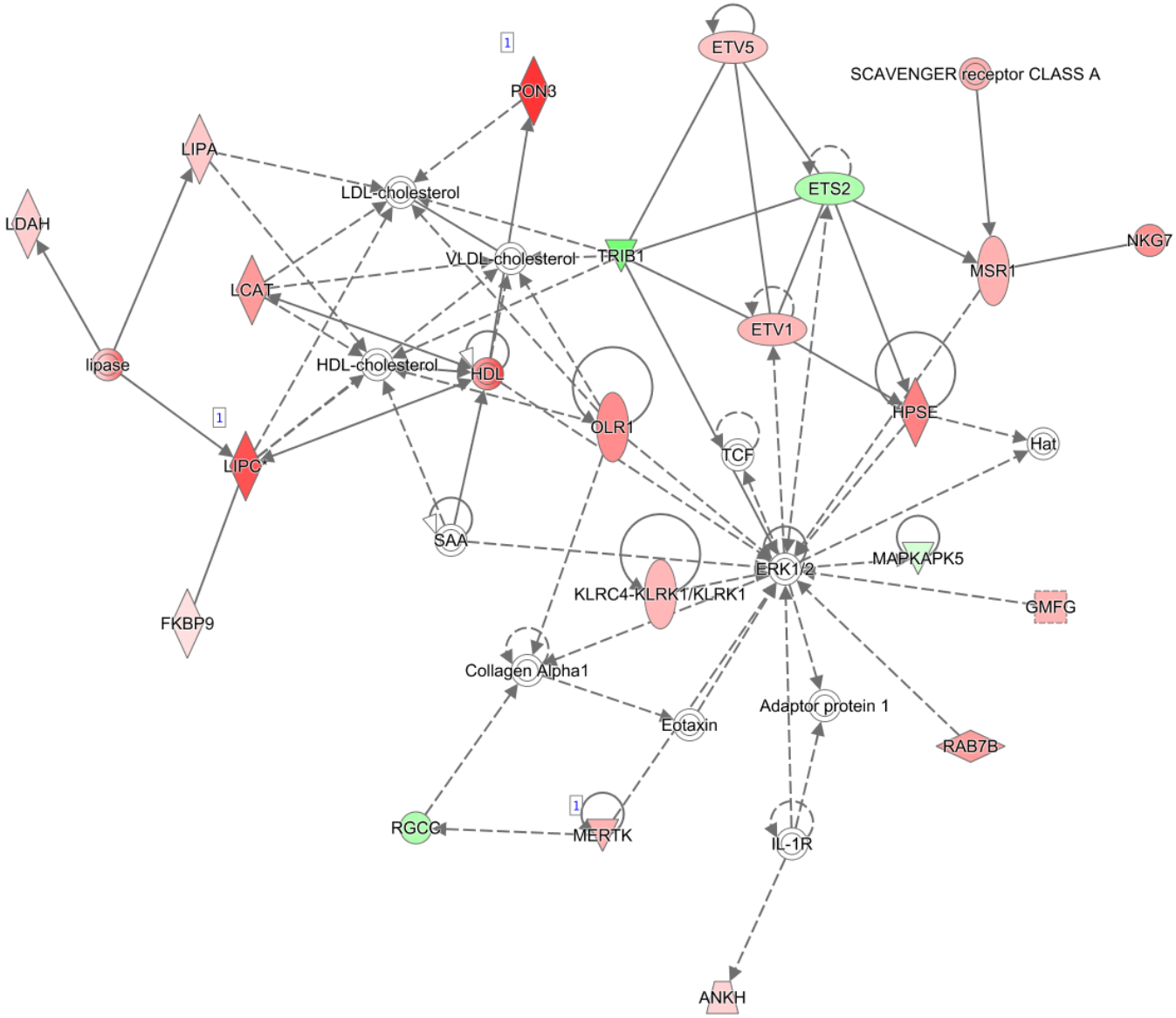

Fig 2 Network #2 containing functions related to 'protein synthesis', 'lipid metabolism', and 'molecular transport'. Genes are denoted as nodes and the biological relationship between two nodes is denoted as an edge/line. Node colour represents up- (red) and down- (green) regulated genes in high-FE pigs.

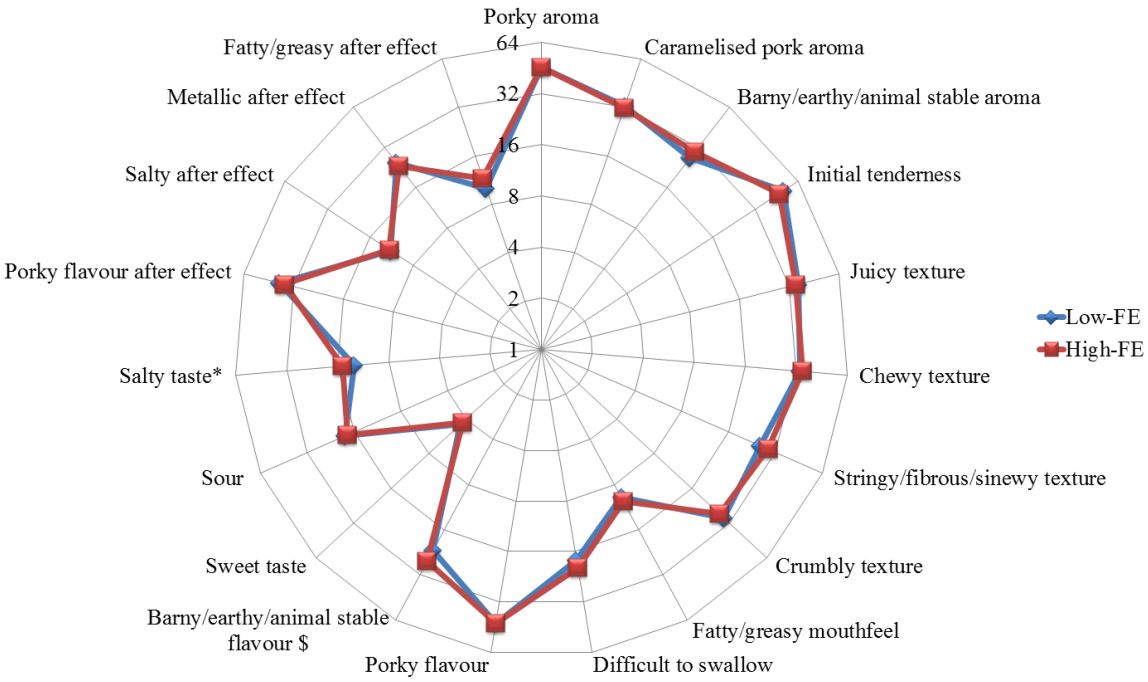

Fig 3 Radar chart illustrating meat sensory attributes of *Longissimus thoracis et lumborum* muscle from FE-divergent pigs. Panellists scored meat from 0 (not detectable) to 100 (extremely detectable). $^{\$}P < 0.1$, $^{*}P < 0.05$.

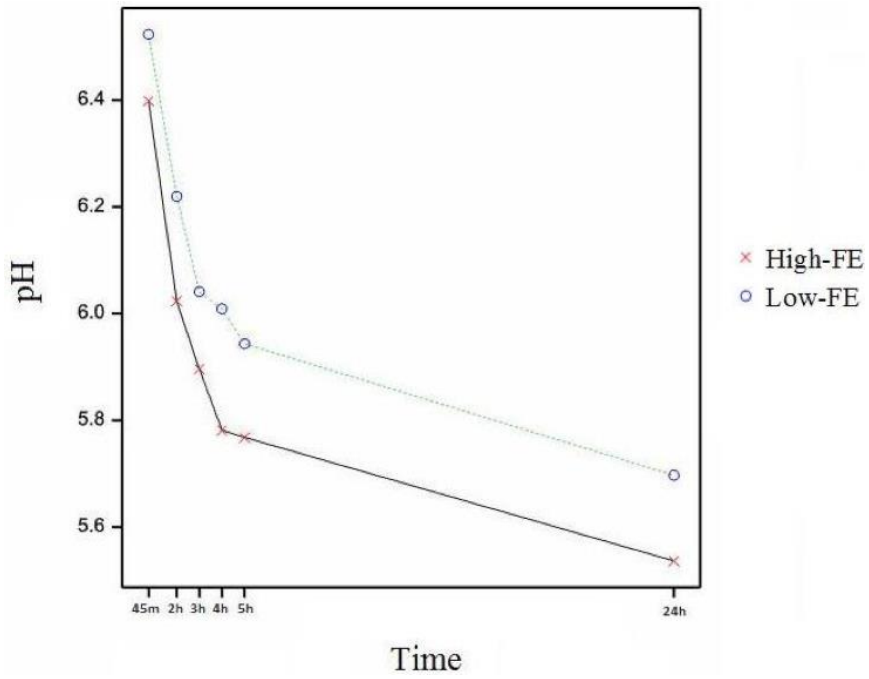

Fig 4 Timeplot depicting *post-mortem* pH evolution of *Longissimus thoracis et lumborum* muscle divergent in feed efficiency. pH 45m: $P < 0.1$; pH 2h, 3h, 4h, 5h, 24h: $P < 0.05$.

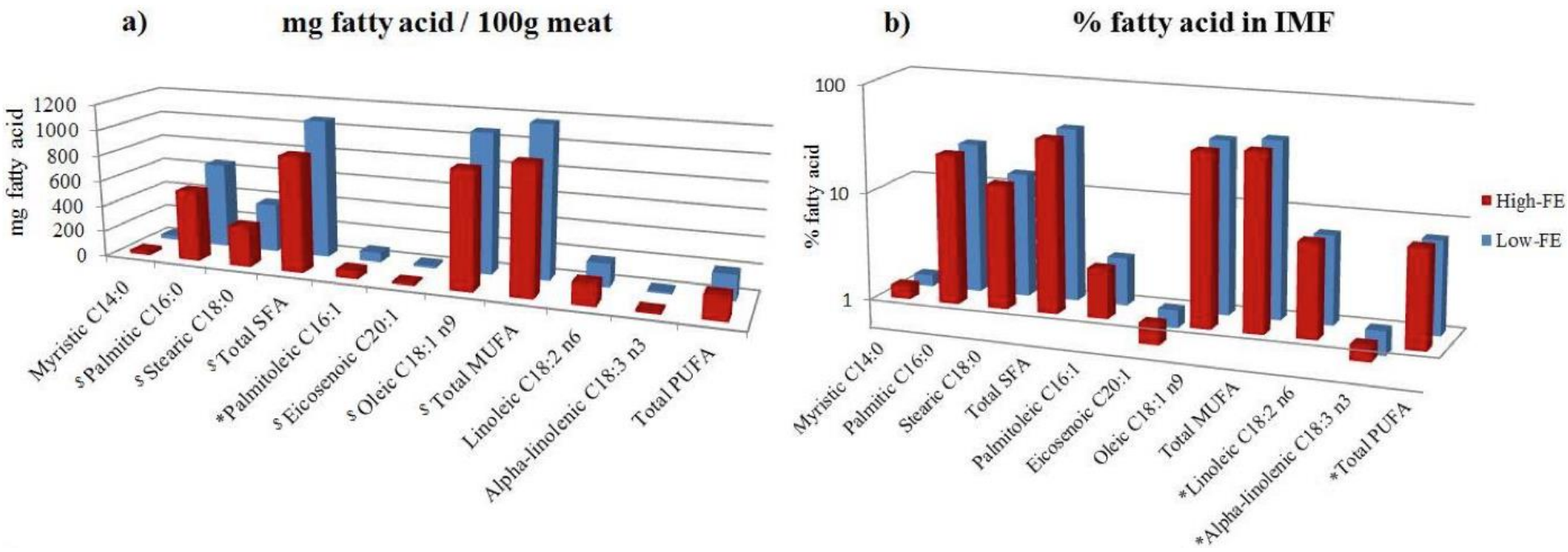

Fig 5 Bar chart illustration of fatty acids composition of pigs divergent in feed efficiency (FE). Bar chart a) displays fatty acid composition in *Longissimus thoracis et lumborum* muscle and b) shows percentage of fatty acid in intramuscular fat (IMF). SFA: saturated fatty acids, MUFA: monounsaturated fatty acids, PUFA: polyunsaturated fatty acids. $^{\$}P < 0.1$, $^{*}P < 0.05$.

Additional files

Additional file 1: Table S1 Differentially expressed transcripts (n = 272) at a $P < 0.01$ between high-FE and low-FE groups (XLSX 30 KB).

Additional file 2: Table S2 Biological functions significantly enriched with differentially expressed genes, including a list of sub-categories contained within each function (XLSX 19 KB).

Additional file 3: Table S3 All canonical pathways significantly enriched with differentially expressed genes (XLSX 12 KB).

Additional file 4: Table S4 Forward and reverse primers for RNA-seq validation through qPCR (DOCX 16 KB).

Transcriptome analysis of adipose tissue from pigs divergent in feed efficiency reveals alteration in gene networks related to adipose growth, lipid metabolism, extracellular matrix and immune response

Justyna Horodyska[1,2], Henry Reyer[2], Klaus Wimmers[2,3], Nares Trakooljul[2], Peadar G. Lawlor[4], Ruth M. Hamill[1*]

[1]Teagasc, Food Research Centre, Ashtown, Dublin 15, Ireland

[2]Leibniz Institute for Farm Animal Biology (FBN), Institute for Genome Biology, Dummerstorf, Germany

[3]Faculty of Agricultural and Environmental Sciences, University Rostock, Germany

[4]Teagasc, Pig Development Department, AGRIC, Moorepark, Fermoy, Co. Cork, Ireland

*Corresponding author

In review at Molecular Genetics and Genomics

Abstract

Adipose tissue is hypothesized to play a vital role in regulation of feed efficiency (FE; efficiency in converting energy and nutrients into tissue), of which improvement will simultaneously reduce environmental impact and feed cost per pig. The objective of the present study was to sequence the subcutaneous adipose tissue transcriptome in FE-divergent pigs (n = 16) and identify relevant biological processes underpinning observed differences in FE. We previously demonstrated that high-FE pigs were associated with lower fatness when compared to their counterparts. Here, ontology analysis of a total of 209 annotated genes that were differentially expressed at a $P < 0.01$ revealed establishment of a dense extracellular matrix and inhibition of capillary formation as one underlying mechanism to achieve suppressed adipogenesis. Moreover, mechanisms ensuring an efficient utilization of lipids in high-FE pigs might be orchestrated by upstream regulators including CEBPA and EGF. Consequently, high-FE adipose tissue could exhibit more efficient cholesterol disposal, whilst inhibition of inflammatory and immune response in high-FE pigs may be an indicator of an optimally functioning adipose tissue. Taken together, adipose tissue growth, extracellular

matrix formation, lipid metabolism and inflammatory & immune response are key biological events underpinning the differences in FE. Further investigations focusing on elucidating these processes would assist the animal production industry in optimizing strategies related to nutrient utilization and product quality.

Key Words – FE, RFI, residual feed intake, gene expression, transcriptomics

Introduction

Adipose tissue is a specialized connective tissue that functions as the largest energy reservoir in the body (Konige et al. 2014). Besides being a master regulator of systemic lipid storage in the form of triacylglycerol (Konige et al. 2014), adipose tissue is also an active endocrine organ (Mohamed-Ali et al. 1998). It secretes a number of inflammatory cytokines, known as adipocytokines, including leptin and adiponectin to communicate with skeletal muscle, liver and brain and influence various processes such as appetite, lipid and glucose metabolism, energy homeostasis, vasculature formation and also inflammatory response (Guerre-Millo 2002; Komolka et al. 2014; Trayhurn and Bing 2006). For these reasons, adipose tissue is suspected to play a vital part in feed efficiency (FE), which is a measure of efficiency in converting energy and nutrients from feed into body mass. Feed efficiency has been widely researched in livestock as its improvement will simultaneously reduce environmental impact and feed cost per pig (Wilkinson 2011). In terms of animal production, subcutaneous as well as intramuscular adipose tissues are economically important traits. Although both tissues have a unique metabolism (Hausman et al. 2009), there is a moderate positive genetic correlation between subcutaneous and intramuscular adipose (Newcom et al. 2005). Therefore the molecular mechanisms in subcutaneous adipose tissue may resemble those in the intramuscular fat.

High-FE pigs were shown to deposit less subcutaneous and intramuscular adipose tissue (Faure et al. 2013; Horodyska et al. 2018a; Horodyska et al. 2018b; Lefaucheur et al. 2011) indicating that these animals do not allocate the same resources to the energetically expensive process of adipose tissue accretion (Gaines et al. 2012) compared to their low-FE counterparts. Nevertheless the understanding of underlying molecular mechanisms in the adipose tissue of FE-divergent pigs is limited. Few studies carried out on the adipose tissue,

using residual feed intake (RFI; difference between actual feed intake and its expected nutritional requirements) as the metric for FE, identified changes in a diverse suite of responses including phosphate, glucose & lipid metabolism, oxidative and antioxidant processes, cellular homeostasis, immune response and regulation of developmental processes (Gondret et al. 2017; Lkhagvadorj et al. 2010; Louveau et al. 2016). These studies were carried out using a microarray platform and to the best of our knowledge, and to date, no RNA sequencing approach was performed on adipose tissue from FE-divergent pigs. With the aim to gain deeper insights of biological processes governing differences in FE, other metabolically important organs e.g. skeletal muscle, liver and intestine have been investigated by researchers. In these studies, skeletal muscle was shown to exhibit shifts in mitochondrial energy and lipid metabolism, protein synthesis and degradation, skeletal muscle growth and connective tissue adhesion (Horodyska et al. 2018a; Jing et al. 2015; Vincent et al. 2015). Furthermore, liver displayed alterations in cell proliferation, vitamin A metabolism, protein synthesis and catabolism, lipid and carbohydrate metabolism, reverse cholesterol transport, integrin signaling, as well as oxidative stress and immune responses (Gondret et al. 2017; Ramayo-Caldas et al. 2018; Reyer et al. 2017a; Zhao et al. 2016). Finally, studies carried out on the intestine reported energy, lipid and protein metabolism, ion transport, immune and oxidative stress responses, as well as gastrointestinal peristalsis to be differentially regulated in association with FE (Ramayo-Caldas et al. 2018; Tan et al. 2017).

The pig also serves as an *in vivo* model for biomedical research, especially metabolic studies because of the resemblance of its digestive system anatomy and physiology, e.g. lipoprotein and cholesterol metabolism, to human (Bassols et al. 2014; Kobayashi et al. 2012; Nafikov and Beitz 2007; Swindle et al. 2012). Considering that within the past three decades worldwide obesity has increased two-fold, with 39 percent of adults now being overweight and 13 percent being obese (www.who.int/), a deeper understanding of metabolic changes associated with lipid metabolism would be of great benefit.

In this study the transcriptome of subcutaneous adipose tissue of pigs divergent for FE was sequenced aiming to identify differentially expressed (DE) genes contributing to differences in FE, and to deduce affected molecular pathways via ontology analysis. This approach contributes to illuminate the biological processes underpinning the differences in FE, as well

as to explore the functional networks driving the relationship between animal adiposity and FE.

Materials and methods

Animals, experimental design and phenotypes

Animal housing, diets and FE tests of a total of 138 Maxgro (Hermitage Genetics) x (Landrace x Large White) pigs used in this study were as previously described (Horodyska et al. 2018a). Briefly, pigs were categorized within litter and gender as high (H) and low (L) RFI according to their RFI values, measured individually using transponders within pens. The minimum and maximum RFI values for the 138 pigs were -329 g/day and 494 g/day, respectively. At an average body weight of 99 kg, 40 pigs (20 extremes from LRFI (high-FE) - 10 males and 10 females, and 20 extremes from HRFI (low-FE) - 10 males and 10 females) were selected based on RFI-divergent siblings from each litter. Subcutaneous adipose tissues samples, representing outer, middle and inner layers, were taken in an area above the *Longissimus thoracis et lumborum* muscle and snap frozen within ten minutes of stunning. Samples were then stored at -80°C until RNA isolation. Phenotypic measurements including subcutaneous adipose tissue depth and *Longissimus thoracis et lumborum* muscle adiposity were measured using probe-based methods described in detail in Horodyska et al. (2018a).

Gene expression profiling and functional enrichment

Adipose tissue of four sets of full siblings was selected from the 40 RFI-divergent pigs. Each set consisted of 2 males - 1 LRFI (high-FE) and 1 HRFI (low-FE) and 2 females 1 LRFI (high-FE) and 1 HRFI (low-FE) so that 8 LRFI (high-FE) pigs - 4 males and 4 females and 8 HRFI pigs (low-FE) - 4 males and 4 females were utilized for RNA analysis. Samples were ground into fine powder in liquid nitrogen followed by total RNA extraction (Tri-Reagent, Sigma-Alrich, Taufkirchen, Germany), which was carried out in two batches and according to the manufacturer's instructions with slight modifications i.e., 1.5 times the volume of TRI-Reagent was used and an additional centrifugation step was performed to remove the fatty phase. RNA was treated with DNase and purified using the column-based Nucleospin RNA II kit (Macherey-Nagel, Düren, Germany). RNA samples were quantified using Nanodrop ND-1000 spectrophotometer (PEQLAB, Erlangen, Germany) and quality assesses with Agilent

2100 Bioanalyzer (Agilent Technologies Inc., California, USA). The RIN number ranged from 6.4 - 7.7. RNA samples were also checked for DNA contamination by PCR of the porcine *GAPDH* gene (forward primer: AAGCAGGGATGATGTTCTGG, reverse primer: ATGCCTCCTGTACCACCAAC) and *PACTB* (forward primer: GAGAAGCTCTGCTACGTCGC, reverse primer: CCTGATGTCCACGTCGCACT). Ribosomal RNA (rRNA) was removed from total RNA using Ribo-Zero Gold kit (Illumina, San Diego, CA, USA). RNA libraries were prepared with 1 µg RNA template according to the TruSeq Stranded mRNA protocol (Illumina, San Diego, CA, USA). The libraries were quality validated using an Agilent DNA-1000 chip kit on an Agilent 2100 Bioanalyzer (Agilent Technologies Inc., California, USA) and normalized to 2 nM concentration each prior to multiplexing balanced for experimental groups and sequencing on 3 lanes of a high-throughput flowcell of an Illumina HiSeq2500 at the Leibniz-Institute for Farm Animal Biology (FBN), Dummerstorf, Germany (more details are available through the ArrayExpress repository at EMBL-EBI (www.ebi.ac.uk/arrayexpress) under accession number: E-MTAB-6255). Paired-end reads were mapped to the reference (Ensembl release 84) using TopHat (2.1.0) (Kim et al. 2013). The number of aligned sequencing reads mapped to corresponding gene features was analyzed using the HTSeq 0.6.1 program (Anders et al. 2015). Entries which had more than or equal to 5 read counts in more than or equal to 6 of the samples were considered for further analysis. DESeq2 package (3.4.0, www.R-project.org) was utilized for differential gene expression analysis, whereby RFI groups and dams were included as fixed effects. Ingenuity Pathway Analysis (IPA; Ingenuity® Systems, www.ingenuity.com) was carried out upon submitting all gene symbols of significantly differentially expressed genes at a $P < 0.01$ along with their fold changes. Fisher's exact test *P*-values were used to identify significantly over-represented biological functions and canonical pathways at a $P < 0.01$. Ingenuity® Knowledge Base was used to produce potential important interaction networks containing the DE genes. Additionally, functional annotations of the differentially expressed as well as all genes expressed in the adipose tissue were extracted using PANTHER Functional Classification Tool 13.1 (Mi et al. 2017). Themes represented amongst DE genes were compared to those represented amongst all expressed genes in order to identify functional shifts related to divergence in FE. Furthermore IPA Upstream Regulator analysis, based on a dataset gathered from the literature and contained in the Ingenuity® Knowledge Base, was utilized to identify potential transcriptional regulators, growth factors etc. and their expected effects on target genes in order to elucidate the differences in gene expression. *P*-

values were calculated to evaluate the overlap between the DE genes and known genes controlled by a particular upstream regulator (overlap *P*-value) and were considered significant at $P < 0.01$. Activation states (z-score), examining whether the expression directions of target DE genes in the dataset are consistent with the activation state of a particular biological function/upstream regulator (Kramer et al. 2014), were also inferred. Functions and regulators were considered significantly activated and inhibited in LRFI (high-FE) pigs with a z-score greater than 2 and lower than -2, respectively.

Quantitative Real-Time PCR (qPCR)

Real-time PCR analyses were performed for *COL8A1*, *MMP16*, and *PLCE1* using gene-specific primers (Table 1). The primers specificity was verified with the primer-BLAST tool (www.ncbi.nlm.nih.gov/BLAST). cDNA was synthesized with 1 µg of a previously extracted total RNA accompanied by random primers (Promega, Mannheim, Germany), oligo (dT) primer and Superscript® III reverse transcriptase (Invitrogen Corp., San Diego, CA, USA). qPCR was performed using LightCycler 96 system (Roche Mannheim, Germany), wherein reactions consisting of 2 µl of cDNA, 6 µl SYBR Green I Master (Roche) and 0.6 µl (10 µM) of each forward and reverse primer were carried out in duplicates in 10 µl final volume. Upon initial denaturation at 95 °C for 5 min and 45 cycles of amplification (95 °C for 10 sec, 60 °C for 15 sec and 72 °C for 25 sec), specificity of the amplification reactions was examined by a melting curve analysis. Normalized gene expression was compared between RFI (FE) groups including dams as a random effect in a linear mixed-effects model using the lme4 R package. Correlation analysis between the RNA-seq and qPCR data were examined in R.

Results

Phenotypes

The mean RFI, weight and feed conversion ratio (FCR, ratio of feed intake and weight gain), along with the highest and lowest values, of the high-FE (LRFI) and low-FE (HRFI) pigs are shown in Table 2. Thickness of subcutaneous adipose tissue did not differ significantly between the RFI groups (high-FE: 14.6 mm and low-FE: 15.5 mm). As described in details in Horodyska et al. (2018b), muscle adiposity was significantly altered between the FE groups

($P < 0.05$). High-FE muscle contained 1.49% intramuscular fat content as opposed to their counterparts having 1.89% intramuscular fat content.

Adipose transcripts differentially expressed between FE groups

Upon sequencing and data processing of a total of 16 RNA libraries from subcutaneous adipose tissue of FE-divergent pigs, high quality reads were mapped with 87.5% efficiency to the reference yielding an average of 105.5 million paired-end reads per sample. Assigning of read counts to gene features revealed expressed transcripts assigned to in total 15,477 genes. Based on a significance threshold of $P < 0.01$ (corresponding to a false discovery rate of $q \leq 0.64$), 209 (111 up- and 98 down-regulated) annotated genes were found to be associated to high/low feed efficiency (Fig S1). List of most altered genes is presented in Table 3. A detailed list of all differentially expressed genes is shown in Table S1. Validation of RNA-seq results was carried out through qPCR of three genes, selected based on their abundance and functionality related to feed efficiency, *COL8A1* (collagen type VIII alpha 1), *MMP16* (matrix metallopeptidase 16) and *PLCE1* (phospholipase C epsilon 1). Expressions of these transcripts were normalized against a reference gene (*RPL32*), which was observed to be stable amongst the samples from FE-divergent groups. Spearman correlation coefficients of the comparison of RNA-seq and qPCR fold changes were found to be significant for *COL8A1*, *MMP16* and *PLCE1* (rho = 0.989, 0.832, 0.911 respectively; $P < 0.001$). RNA-seq validation through qPCR confirmed three selected genes to be significantly up-regulated in high-FE pigs (Fig 1).

Functional enrichment analysis

The lower statistical stringency in differential expression profiling introduces a risk of Type I error. Therefore to further refine the data, the list of DE genes was integrated via gene ontology analysis to extract biological functions and pathways. Nineteen molecular and cellular functions (Fig 2A and Table S2), were significantly ($P < 0.001$) enriched with genes associated to FE. Most altered themes were 'cellular movement' (78 DE genes, 10% distribution of all DE genes entries), 'cell death and survival' (89 DE genes, 11% distribution of all DE genes entries), 'cellular development' (85 DE genes, 11% distribution of all DE genes entries), 'cellular growth and proliferation' (72 DE genes, 9% distribution of all DE genes entries), 'cell morphology' (73 DE genes, 9% distribution of all DE genes entries) and

'lipid metabolism' (28 DE genes, 4% distribution of all DE genes entries). Ontology analysis also revealed twenty-one physiological system development and function categories (Fig 2B and Table S3) significantly ($P < 0.001$) over-represented with genes associated to FE. Most significant biological themes affected by divergence in FE were 'cardiovascular system development & function' (54 DE genes, 6% distribution of all DE genes entries), 'organismal development' (91 DE genes, 11% distribution of all DE genes entries), 'tissue morphology' (78 DE genes, 9% distribution of all DE genes entries) and 'haematological system development & function' (61 DE genes, 7% distribution of all DE genes entries), 'immune cell trafficking'(37 DE genes, 4% distribution of all DE genes entries), and 'lymphoid tissue structure and development'(44 DE genes, 5% distribution of all DE genes entries). Furthermore, nine canonical signaling pathways (Fig 2C) were significantly ($P < 0.01$) enriched with DE genes in relation to FE, of which most altered were 'axonal guidance signaling' (14 DE genes, 29% distribution of all DE genes entries), 'complement system' (4 DE genes, 8% distribution of all DE genes entries), 'granulocyte adhesion and diapedesia' (7 DE genes, 15% distribution of all DE genes entries), 'antiproliferative role of TOB in T cell signaling' (3 DE genes, 6% distribution of all DE genes entries), 'factors promoting cardiogenesis in vertebrates' (5 DE genes, 10% distribution of all DE genes entries) and 'p38 MAPK signaling' (5 DE genes, 10% distribution of all DE genes entries). Additionally, comparison of molecular and physiological themes represented amongst DE genes against those represented with all expressed genes in the adipose tissue (Fig 3A and 3B) revealed 'receptor and signal transducer activities' and 'growth and developmental processes' to be over-represented in relation to FE. Specifically, 'signal transducer activity' and 'growth and developmental processes' were enriched with up-regulated genes whilst 'receptor activity' was enriched with down-regulated genes. Sixteen networks were inferred by integration of genes affected by FE (Table S4), whereby the most significant network (network#1) comprised twenty-four DE genes involved in cell death and survival, embryonic development and cancer. Another important network (network#2), was represented by eighteen DE genes including the most altered gene, *COL11A2*, and related to connective tissue development, function and disorders, as well as organismal injury and abnormalities (Fig 4).

Analysis of potential upstream regulators predicted CCAAT/enhancer binding protein alpha (CEBPA; z-score = -2.41 and overlap *P*-value = 7.73E-05) and epidermal growth factor (EGF; z-score = -2.51 and overlap *P*-value = 4.03E-03) to be inhibited in adipose tissue of

high-FE pigs. CEBPA and EGF were predicted to control expression of 11 and 10 DE genes, respectively, in the direction consistent with the activation state of the particular regulator. Specifically, *MMP8*, *LTF*, *CSF3R*, *SULT2A1*, *NFIL3*, *PLIN2*, *BTG*, *ITGAM*, *TGFB2*, *PLOD2* and *EPH2* were inferred to be inhibited by CEBPA, whilst *LTF*, *ANPEP*, *VEGFA*, *BTG2*, *ETS2*, *GPER1*, *ITGAM*, *TGFB1*, *KRT19*, and *CYP1A1* were inferred to be inhibited by EGF. Predicted inhibition of these transcripts, except TGFB2, PLOD2, EPH2, KRT19 and CYP1A1, was consistent with their observed down-regulation in adipose tissue of high-FE pigs. In addition a number of EGF target genes down-regulated in our dataset, such as *BTG2*, *ITGAM*, *LTF*, *ETS2* and *TGFB1*, were significantly enriched in 'cell survival' function, which was predicted to be suppressed (z-score = -2.18) in high-FE pigs.

Discussion

The aim of this study was to examine the transcriptome of subcutaneous adipose tissue and identify biological processes contributing to differences in FE and explore the functional networks driving the relationship between animal adiposity and FE. In our prior study (Horodyska et al. 2018b) we demonstrated that high-FE pigs exhibit reduced muscle adiposity, however muscle and subcutaneous fat tissue depth remained unaffected by FE despite previously reported links between FE (RFI indexes) and back-fat (Lefaucher et al. 2008; Tizioto et al. 2015). Gene ontology analysis identified a number of candidate biological functions and pathways affiliated with adipose tissue growth, extracellular matrix formation, lipid metabolism and immune response suggesting that these may be some of the key mechanisms underpinning the tissue changes associated with FE.

Growth

Sulfiredoxin 1(*SRXN1),* which codes for an endogenous antioxidant protein (Zhou et al. 2015), was the most down-regulated gene (fold change = -3.85) in high-FE pigs. Previous studies have reported over-expression of *SRXN1* during oxidative stress in astrocytes (Zhou et al. 2015) and in lung tissue (Tahmasbpour Marzony et al. 2016). Increased oxidative stress has been observed in adipose tissue of obese mice (Furukawa et al. 2004). In this study high-FE (LRFI) pigs exhibited suppression of *SRXN1* in the subcutaneous adipose tissue, although no significant differences in depth of this tissue were detected between the FE groups.

Nevertheless muscle adiposity (intramuscular fat content), exhibiting a positive genetic correlation with subcutaneous adipose tissue (Newcom et al. 2005), was relatively lower (1.49% in high-FE pigs as opposed to 1.89% in low-FE pigs) in high-FE pigs and this is in keeping with the suppression of *SRXN1*. Gene ontology analysis revealed several significant biological functions related to adipose tissue growth, specifically 'connective tissue development and function' wherein 'quantity of connective tissue' was significantly inhibited (z-score = -2.44) and 'stimulation of connective tissue cells' tended towards suppression (z-score = -1.41) in high-FE pigs. In these functions, expression of lactotransferrin *(LTF)* and oncostatin M *(OSM)* was down-regulated (fold change = -2.85 and -1.88, respectively). A study conducted on human pre-adipocytes demonstrated that induced expression of *LTF* led to increased differentiation of adipocytes (Moreno-Navarrete et al. 2014; Moreno-Navarrete et al. 2013), whilst elevated expression of *OSM* was observed in obese mice and humans (Elks et al. 2016). Furthermore, sub-categories enclosed within a broader 'cardiovascular system development and function' category, including 'movement of endothelial cells' and 'quantity of blood vessels' were repressed (z-score = -2.05 and -1.94, respectively) in high-FE pigs. Growth of adipose tissue is angiogenesis dependent and inhibition of vascular growth has been previously shown to prevent adipose tissue expansion (Rupnick et al. 2002). Here, an important regulator of angiogenesis in adipose tissue (Ledoux et al. 2008), vascular endothelial growth factor A *(VEGFA)*, was down-regulated (fold change = -1.35) in high-FE pigs. Furthermore the most significantly enriched pathway with DE genes, 'axonal guidance signaling', has been implicated in angiogenesis (Larrivee et al. 2009). Interestingly, *VEGFA* was also represented in this pathway confirming its role in promoting axon guidance (Mackenzie and Ruhrberg 2012). Additionally, when comparing functional annotations of the DE genes against all genes expressed in the adipose tissue, *VEGFA* was also enriched in 'growth and developmental processes'. These findings are in keeping with a previous study reporting 'regulation of developmental processes' being enriched with down-regulated genes in the adipose tissue of high-FE pigs (Lkhagvadorj et al. 2010).

Prediction of potential upstream regulators predicted inhibition of CEBPA and EGF to control expression of a total of 16 genes that were observed to be down-regulated in the adipose tissue of high-FE. CEBPA, together with peroxisome proliferators activated receptor gamma (PPARG), is a master regulator of adipogenesis (Prokesch et al. 2009). EGF has previously been linked to proliferation and differentiation of adipose-derived stem cells

(Hebert et al. 2009) and obesity (Kurachi et al. 1993). In the present study this growth factor, along with CEBPA, was predicted to be inhibited in adipose tissue of high-FE pigs. mRNAs coding for these transcription regulators were not significantly differentially expressed between the FE-divergent groups *per se*, albeit abundance of transcripts encoding these factors is not expected to affect their activity (Filtz et al. 2014).

Extracellular matrix

Analysis of molecule connectivity revealed network#2 enriched with functions related to 'connective tissue development & function' and 'connective tissue disorders'. The most up-regulated gene (fold change = 25.7) in high-FE pigs, collagen type XI alpha 2 chain (*COL11A2*) coding for extracellular minor fibrillar collagen (Fang et al. 2010) was represented in this network. Matrix metallopeptidase 8 (*MMP8*) which degrades collagen type I and III (Van Doren 2015), was down-regulated (fold change = -3.23) in this network. While collagen type I and III *per se* were not differentially expressed between the FE-divergent groups, a number of other collagen types, such as collagen type XI alpha 1 chain (*COL11A1*), collagen type XIV alpha 1 chain (*COL14A1*) and collagen type XXVIII alpha 1 chain (*COL28A1*) were up-regulated (fold change = 4.80, 1.35 and 5.27, respectively) in the subcutaneous fat of high-FE pigs. When comparing themes represented amongst DE genes to those represented amongst all expressed genes, 'growth and developmental processes' were identified to be enriched with up-regulated genes in relation to FE such as *COL11A1*, *COL11A2* and transforming growth factor beta-2 (*TGFB2*). *TGFB2* modulates the synthesis of extracellular matrix components (Fuchshofer et al. 2005), whilst collagen is a predominant structural element of interstitial extracellular matrix (Frantz et al. 2010) providing mechanical support to the cellular constituents (Neve et al. 2014). These suggest that adipose tissue of high-FE animals may be characterized by a dense extracellular matrix. Indeed, a connection between extracellular matrix formation and body fat has been reported in a pig population selected for leanness (Reyer et al. 2017b). Furthermore, there is evidence that extracellular matrix regulates angiogenesis (Neve et al. 2014). Formation of a dense extracellular matrix may suppress adipogenesis through inhibiting capillary formation (Bouloumié et al. 2002).

Lipid metabolism

Previous reports revealed that 'fatty acid metabolism' (Lkhagvadorj et al. 2010) was a functional category enriched with down-regulated genes in adipose tissue of high-FE pigs, whilst up-regulated genes were predominantly involved in 'lipid catabolism', 'fatty acid beta-oxidation' (Gondret et al. 2017) and 'mitochondrial oxidative metabolism' (Louveau et al. 2016). These findings are consistent with our gene ontology analysis wherein 'synthesis of fatty acids and lipids', enclosed within 'lipid metabolism' category, were significantly enriched with DE genes and tended towards inhibition (z-score = -1.77 and -1.25, respectively) in high-FE pigs. In these themes, ATP binding cassette subfamily A member 8 (*ABCA8*), clusterin (*CLU*), paraoxonase 3 (*PON3*) and cytochrome p450 family 1 subfamily A member 1 (*CYP1A1*) were over-expressed (fold change = 1.27, 1.46, 2.10 and 3.87, respectively) in the high-FE group. ABCA8 is a membrane protein (Locher 2009) that has previously been shown to be involved in modulating cholesterol efflux and high density lipoprotein cholesterol level (Trigueros-Motos et al. 2017). Studies carried out in liver elucidated a role of CLU protein in transporting cholesterol from tissues to the liver (de Silva et al. 1990). PON3 is known for associating with high density lipoproteins (Getz and Reardon 2004). In addition, PON3 knockout mice experienced increased body weight (Shih et al. 2015). CYP1A1 belongs to a family of enzymes playing a crucial part in cholesterol biosynthesis (Sridhar et al. 2017). Accordingly, a number of polymorphisms in *CYP1A1* have been associated with high and low density lipoprotein cholesterol as well as triglyceride levels (Almeida et al. 2005; Bailon-Soto et al. 2014). These alterations in cholesterol metabolism in the adipose tissue of high-FE animals suggest increased mobilization of fat depots towards hepatic metabolism and utilization of fat resources (Reyer et al. 2017a). Over-expression of these lipid-associated transcripts was accompanied with suppression of adipogenesis-related mRNAs, i.e. *LTF* and *VEGFA*.

Immune response

'High mobility group box 1 (HMGB1) signaling' and 'p38 mitogen-activated protein kinase (p38MAPK) signaling' were pathways significantly affected by FE. p38MAPK and HMGB1 are involved in the mounting of an immune response through synthesis of pro-inflammatory cytokines (Cuenda and Rousseau 2007; Lee et al. 2014; Yang et al. 2005). A previous study postulated that production of HMGB1 in adipose tissue is triggered by inflammatory signals

associated with obesity (Gunasekaran et al. 2013). Accordingly ‘complement system’, which is a major constituent of the innate immunity (Rus et al. 2005), was inferred from ontology analysis. Selectin L (*SELL*), involved in leukocyte adhesion to blood vessels during inflammatory and immunological response (Nelson et al. 1992), was found to be down-regulated in high-FE pigs and significantly enriched in ‘granulocyte adhesion and diapedesis’ pathway. Interestingly, a single nucleotide polymorphism in *SELL* gene was identified as a positional and functional candidate gene for FE through a genome-wide association study (Horodyska et al. 2017). Furthermore ‘proliferation of immune cells’ contained within ‘haematological system development and function’, ‘chemotaxis of phagocytes’ contained within ‘immune cell trafficking’ and ‘phagocytosis’ contained within ‘cellular function and maintenance’ were significantly inhibited (z-score = -2.36, -2.32 and -2.01, respectively) in high-FE adipose tissue, and ‘prostaglandin synthesis’ had a tendency towards suppression (z-score = -1.33) in high-FE pigs. Cytokines and prostaglandins are inflammatory molecules that are synthesized and secreted by macrophages upon tissue exposure to inflammatory stimuli (Arango Duque and Descoteaux 2014). Studies carried out on obese mice and humans reported a strong positive correlation between adipocyte size and accumulation of pro-inflammatory macrophages in adipose tissue (Cinti et al. 2005; Ortega Martinez de Victoria et al. 2009). In addition, cytokines communicate with skeletal muscle, liver and brain and regulate appetite and lipid and glucose metabolism (Guerre-Millo 2002). Supporting prior evidence reported by Gondret et al. (2017), our findings clearly indicate that high-FE adipose tissue display inhibition of immune and inflammatory responses, which otherwise would lead to expansion of this organ and dysregulation of systemic energy homeostasis.

To conclude, a number of differentially expressed genes were significantly enriched in growth, extracellular matrix formation, lipid metabolism and inflammatory & immune response pathways, suggesting that these may be the main mechanisms governing the differences in adipose tissue from FE-divergent pigs. Specifically, establishment of a dense extracellular matrix and inhibition of capillary formation may be one underlying mechanism to achieve suppressed adipogenesis and increased utilization of fatty acids. Accordingly, lipid metabolism was also affected by FE whereby over-expression of cholesterol-related genes suggests more efficient cholesterol disposal from high-FE adipose tissue. The mechanisms ensuring an efficient utilization of lipids in high-FE pigs might be orchestrated by upstream regulators including CEBPA and EGF. Moreover, inhibition of inflammatory and immune

responses in high-FE pigs may be an indicator of an optimally functioning adipose tissue, which is a central organ involved in systemic lipid metabolism and energy homeostasis. Further studies dedicated to deciphering these processes will assist in optimizing strategies related to nutrient utilization and animal adiposity.

List of abbreviations

FE: feed efficiency; RFI: residual feed intake; LRFI: low RFI; HRFI: high RFI; high-FE = LRFI; low-FE = HRFI.

Author's contributions

JH collected samples, extracted RNA, prepared libraries, validated RNA-seq via qPCR, carried out data analysis and wrote the manuscript; HR participated in statistical analysis and edited the manuscript; KW contributed to experimental design, established lab protocols and edited the manuscript; NT assisted in library preparation, performed RNA-seq and data analysis, and edited the manuscript; PGL provided and screened the animals on RFI, participated in data collection and analysis, and edited the manuscript; RMH conceived the experiment and contributed to experimental design, collected samples and edited the manuscript.

Funding: The ECO-FCE project was funded by the European Union Seventh Framework Programme (FP7 2007/2013) under grant agreement No. 311794.

Compliance with ethical standards

Conflict of interest: The authors declare that they have no competing interests.

Ethical approval: Animal care, slaughter and tissue collection of the animals used in this study were performed in compliance with national regulations related to animal research and commercial slaughtering and were approved by the Teagasc Animal Ethics Committee.

References

Almeida, S., Zandona, M. R., Franken, N., Callegari-Jacques, S. M., Osorio-Wender, M. C., Hutz, M. H. (2005). Estrogen-metabolizing gene polymorphisms and lipid levels in women with different hormonal status. *Pharmacogenomics J, 5*(6), 346-351.

Anders, S., Pyl, P. T., Huber, W. (2015). HTSeq--a Python framework to work with high-throughput sequencing data. *Bioinformatics, 31*(2), 166-169.

Arango-Duque, G., Descoteaux, A. (2014). Macrophage cytokines: involvement in immunity and infectious diseases. *Front Immunol, 5*, 491.

Bailon-Soto, C. E., Galaviz-Hernandez, C., Lazalde-Ramos, B. P., Hernandez-Velazquez, D., Salas-Pacheco, J., Lares-Assef, I., Sosa-Macias, M. (2014). Influence of CYP1A1*2C on high triglyceride levels in female Mexican indigenous Tarahumaras. *Arch Med Res, 45*(5), 409-416.

Bassols, A., Costa, C., Eckersall, P. D., Osada, J., Sabria, J., Tibau, J. (2014). The pig as an animal model for human pathologies: A proteomics perspective. *Proteomics Clin Appl, 8*(9-10), 715-731.

Bouloumié, A., Lolmède, K., Sengenès, C., Galitzky, J., M., L. (2002). Angiogenesis in adipose tissue. *Ann Endocrinol, 63*(2).

Cinti, S., Mitchell, G., Barbatelli, G., Murano, I., Ceresi, E., Faloia, E., Wang, S., Fortier, M., Greenberg, A. S., Obin, M. S. (2005). Adipocyte death defines macrophage localization and function in adipose tissue of obese mice and humans. *J Lipid Res, 46*(11), 2347-2355.

Cuenda, A., Rousseau, S. (2007). p38 MAP-Kinases pathway regulation, function and role in human diseases. *Biochim Biophys Acta, 1773*(8), 1358-1375.

de Silva, H. V., Stuart, W. D., Duvic, C. R., Wetterau, J. R., Ray, M. J., Ferguson, D. G., Albers, H. W., Smith, W. R., Harmony, J. A. (1990). A 70-kDa apolipoprotein designated ApoJ is a marker for subclasses of human plasma high density lipoproteins. *J Biol Chem, 265*(22), 13240-13247.

Elks, C. M., Zhao, P., Grant, R. W., Hang, H., Bailey, J. L., Burk, D. H., McNulty, M. A., Mynatt, R. L., Stephens, J. M. (2016). Loss of oncostatin M signaling in adipocytes induces insulin resistance and adipose tissue inflammation in vivo. *J Biol Chem, 291*(33), 17066-17076.

Fang, M., Adams, J. S., McMahan, B. L., Brown, R. J., Oxford, J. T. (2010). The expression patterns of minor fibrillar collagens during development in zebrafish. *Gene Expr Patterns, 10*(7-8), 315-322.

Faure, J., Lefaucheur, L., Bonhomme, N., Ecolan, P., Meteau, K., Coustard, S. M., Kouba, M., Gilbert, H., Lebret, B. (2013). Consequences of divergent selection for residual feed intake in pigs on muscle energy metabolism and meat quality. *Meat Sci, 93*(1), 37-45.

Filtz, T. M., Vogel, W. K., Leid, M. (2014). Regulation of transcription factor activity by interconnected, post-translational modifications. *Trends Pharmacol Sci, 35*(2), 76-85.

Frantz, C., Stewart, K. M., Weaver, V. M. (2010). The extracellular matrix at a glance. *J Cell Sci., 123*(24), 4195-4200.

Fuchshofer, R., Birke, M., Welge-Lussen, U., Kook, D., Lutjen-Drecoll, E. (2005). Transforming growth factor-beta 2 modulated extracellular matrix component expression in cultured human optic nerve head astrocytes. *Invest Ophthalmol Vis Sci, 46*(2), 568-578.

Furukawa, S., Fujita, T., Shimabukuro, M., Iwaki, M., Yamada, Y., Nakajima, Y., Nakayama, O., Makishima, M., Matsuda, M., Shimomura, I. (2004). Increased

oxidative stress in obesity and its impact on metabolic syndrome. *J Clin Invest, 114*(12), 1752-1761.

Gaines, A. M., Peterson, B. A., Mendoza, O. F. (2012). Herd management factors that influence whole herd feed efficiency. In J. F. Patience (Ed.), *Feed efficiency in swine*, (pp. 15-39). Wageningen: Wageningen Academic Publishers.

Getz, G. S., Reardon, C. A. (2004). Paraoxonase, a cardioprotective enzyme: continuing issues. *Curr Opin Lipidol, 15*(3), 261-267.

Gondret, F., Vincent, A., Houée-Bigot, M., Siegel, A., Lagarrigue, S., Causeur, D., Gilbert, H., Louveau, I. (2017). A transcriptome multi-tissue analysis identifies biological pathways and genes associated with variations in feed efficiency of growing pigs. *BMC Genomics, 18*, 244.

Guerre-Millo, M. (2002). Adipose tissue hormones. *J Endocrinol Invest, 25*(10), 855-861.

Gunasekaran, M. K., Viranaicken, W., Girard, A. C., Festy, F., Cesari, M., Roche, R., Hoareau, L. (2013). Inflammation triggers high mobility group box 1 (HMGB1) secretion in adipose tissue, a potential link to obesity. *Cytokine, 64*(1), 103-111.

Hausman, G. J., Dodson, M. V., Ajuwon, K., Azain, M., Barnes, K. M., Guan, L. L., Jiang, Z., Poulos, S. P., Sainz, R. D., Smith, S., Spurlock, M., Novakofski, J., Fernyhough, M. E., Bergen, W. G. (2009). Board-invited review: the biology and regulation of preadipocytes and adipocytes in meat animals. *J Anim Sci, 87*(4), 1218-1246.

Hebert, T. L., Wu, X., Yu, G., Goh, B. C., Halvorsen, Y. D., Wang, Z., Moro, C., Gimble, J. M. (2009). Culture effects of epidermal growth factor (EGF) and basic fibroblast growth factor (bFGF) on cryopreserved human adipose-derived stromal/stem cell proliferation and adipogenesis. *J Tissue Eng Regen Med, 3*(7), 553-561.

Horodyska, J., Hamill, R. M., Varley, P. F., Reyer, H., Wimmers, K. (2017). Genome-wide association analysis and functional annotation of positional candidate genes for feed conversion efficiency and growth rate in pigs. *PLoS One, 12*(6), e0173482.

Horodyska, J., Oster, M., Reyer, H., Mullen, A. M., Lawlor, P. G., Wimmers, K., Hamill, R. M. (2018a). Analysis of meat quality traits and gene expression profiling of pigs divergent in residual feed intake. *Meat Sci, 137*, 265–274.

Horodyska, J., Wimmers, K., Reyer, H., Trakooljul, N., Mullen, A. M., Lawlor, P. G., Hamill, R. M. (2018b). RNA-seq of muscle from pigs divergent in feed efficiency and product quality identifies differences in immune response, growth, and macronutrient and connective tissue metabolism

Jing, L., Hou, Y., Wu, H., Miao, Y., Li, X., Cao, J., Brameld, J. M., Parr, T., Zhao, S. (2015). Transcriptome analysis of mRNA and miRNA in skeletal muscle indicates an important network for differential Residual Feed Intake in pigs. *Sci Rep, 5*, 11953.

Kim, D., Pertea, G., Trapnell, C., Pimentel, H., Kelley, R., Salzberg, S. L. (2013). TopHat2: accurate alignment of transcriptomes in the presence of insertions, deletions and gene fusions. *Genome Biol, 14*(4), R36.

Kobayashi, E., Hishikawa, S., Teratani, T., Lefor, A. T. (2012). The pig as a model for translational research: overview of porcine animal models at Jichi Medical University. *Transplant Res, 1*(1), 8.

Komolka, K., Albrecht, E., Wimmers, K., Michal, J. J., Maak, S. (2014). Molecular heterogeneities of adipose depots - potential effects on adipose-muscle cross-talk in humans, mice and farm animals. *J Genomics, 2*, 31-44.

Konige, M., Wang, H., Sztalryd, C. (2014). Role of adipose specific lipid droplet proteins in maintaining whole body energy homeostasis. *Biochim Biophys Acta, 1842*(3), 393-401.

Kramer, A., Green, J., Pollard, J., Jr., Tugendreich, S. (2014). Causal analysis approaches in Ingenuity Pathway Analysis. *Bioinformatics, 30*(4), 523-530.

Kurachi, H., Adachi, H., Ohtsuka, S., Morishige, K., Amemiya, K., Keno, Y., Shimomura, I., Tokunaga, K., Miyake, A., Matsuzawa, Y., et al. (1993). Involvement of epidermal growth factor in inducing obesity in ovariectomized mice. *Am J Physiol, 265*(2 Pt 1), E323-331.

Larrivee, B., Freitas, C., Suchting, S., Brunet, I., Eichmann, A. (2009). Guidance of vascular development: lessons from the nervous system. *Circ Res, 104*(4), 428-441.

Ledoux, S., Queguiner, I., Msika, S., Calderari, S., Rufat, P., Gasc, J. M., Corvol, P., Larger, E. (2008). Angiogenesis associated with visceral and subcutaneous adipose tissue in severe human obesity. *Diabetes, 57*(12), 3247-3257.

Lee, S.-A., Kwak, M. S., Kim, S., Shin, J.-S. (2014). The role of high mobility group box 1 in innate immunity. *Yonsei Med J, 55*(5), 1165-1176.

Lefaucher, L., Lebret, B., Ecolan, P., Galian, M., Damon, M., Louveau, I., Prunier, A., Sellier, P., Gilbert, H. (2008). Divergent selection on "residual feed intake" in pigs: Impact on growth performance, muscle compositional traits and meat quality. *AAB*(40), 83–84.

Lefaucheur, L., Lebret, B., Ecolan, P., Louveau, I., Damon, M., Prunier, A., Billon, Y., Sellier, P., Gilbert, H. (2011). Muscle characteristics and meat quality traits are affected by divergent selection on residual feed intake in pigs. *J Anim Sci, 89*(4), 996-1010.

Lkhagvadorj, S., Qu, L., Cai, W., Couture, O. P., Barb, C. R., Hausman, G. J., Nettleton, D., Anderson, L. L., Dekkers, J. C., Tuggle, C. K. (2010). Gene expression profiling of the short-term adaptive response to acute caloric restriction in liver and adipose tissues of pigs differing in feed efficiency. *Am J Physiol Regul Integr Comp Physiol, 298*(2), R494-507.

Locher, K. P. (2009). Structure and mechanism of ATP-binding cassette transporters. *Philos Trans R Soc Lond B Biol Sci, 364*(1514), 239-245.

Louveau, I., Vincent, A., Tacher, S., Gilbert, H., Gondret, F. (2016). Increased expressions of genes and proteins involved in mitochondrial oxidation and antioxidant pathway in adipose tissue of pigs selected for a low residual feed intake. *J Anim Sci, 94*(12), 5042-5054.

Mackenzie, F., Ruhrberg, C. (2012). Diverse roles for VEGF-A in the nervous system. *Development, 139*(8), 1371-1380.

Mi, H., Huang, X., Muruganujan, A., Tang, H., Mills, C., Kang, D., Thomas, P. D. (2017). PANTHER version 11: expanded annotation data from Gene Ontology and Reactome pathways, and data analysis tool enhancements. *Nucleic Acids Res, 45*(Database issue), D183-D189.

Mohamed-Ali, V., Pinkney, J. H., Coppack, S. W. (1998). Adipose tissue as an endocrine and paracrine organ. *Int J Obes Relat Metab Disord, 22*(12), 1145-1158.

Moreno-Navarrete, J. M., Ortega, F., Moreno, M., Serrano, M., Ricart, W., Fernández-Real, J. M. (2014). Lactoferrin gene knockdown leads to similar effects to iron chelation in human adipocytes. *J Cell Mol Med, 18*(3), 391-395.

Moreno-Navarrete, J. M., Serrano, M., Sabater, M., Ortega, F., Serino, M., Pueyo, N., Luche, E., Waget, A., Rodriguez-Hermosa, J. I., Ricart, W., Burcelin, R., Fernandez-Real, J. M. (2013). Study of lactoferrin gene expression in human and mouse adipose tissue, human preadipocytes and mouse 3T3-L1 fibroblasts. Association with adipogenic and inflammatory markers. *J Nutr Biochem, 24*(7), 1266-1275.

Nafikov, R. A., Beitz, D. C. (2007). Carbohydrate and lipid metabolism in farm animals. *J Nutr, 137*(3), 702-705.

Nelson, R. M., Aruffo, A., Dolich, S., Cecconi, O., Mannori, G., Bevilacqua, M. P. (1992). Quantitative determination of selectin-carbohydrate interactions. *Cold Spring Harb Symp Quant Biol, 57*, 271-279.

Neve, A., Cantatore, F. P., Maruotti, N., Corrado, A., Ribatti, D. (2014). Extracellular matrix modulates angiogenesis in physiological and pathological conditions. *BioMed Res Int., 2014*, 10.

Newcom, D. W., Baas, T. J., Schwab, C. R., Stalder, K. J. (2005). Genetic and phenotypic relationships between individual subcutaneous backfat layers and percentage of longissimus intramuscular fat in Duroc swine. *J Anim Sci, 83*(2), 316-323.

The World Health Organization. Obesity and overweight. (2016). [http://www.who.int/mediacentre/factsheets/fs311/en/]. Accessed on 6 Oct 2017.

Ortega Martinez de Victoria, E., Xu, X., Koska, J., Francisco, A. M., Scalise, M., Ferrante, A. W., Jr., Krakoff, J. (2009). Macrophage content in subcutaneous adipose tissue: associations with adiposity, age, inflammatory markers, and whole-body insulin action in healthy Pima Indians. *Diabetes, 58*(2), 385-393.

Prokesch, A., Hackl, H., Hakim-Weber, R., Bornstein, S. R., Trajanoski, Z. (2009). Novel insights into adipogenesis from omics data. *Curr Med Chem, 16*(23), 2952-2964.

Ramayo-Caldas, Y., Ballester, M., Sanchez, J. P., Gonzalez-Rodriguez, O., Revilla, M., Reyer, H., Wimmers, K., Torrallardona, D., Quintanilla, R. (2018). Integrative approach using liver and duodenum RNA-Seq data identifies candidate genes and pathways associated with feed efficiency in pigs. *Sci Rep, 8*(1), 558.

Reyer, H., Oster, M., Magowan, E., Dannenberger, D., Ponsuksili, S., Wimmers, K. (2017a). Strategies towards Improved Feed Efficiency in Pigs Comprise Molecular Shifts in Hepatic Lipid and Carbohydrate Metabolism. *Int J Mol Sci, 18*(8), 1674.

Reyer, H., Varley, P. F., Murani, E., Ponsuksili, S., Wimmers, K. (2017b). Genetics of body fat mass and related traits in a pig population selected for leanness. *Int J Mol Sci, 18*(8), 1674.

Rupnick, M. A., Panigrahy, D., Zhang, C.-Y., Dallabrida, S. M., Lowell, B. B., Langer, R., Folkman, M. J. (2002). Adipose tissue mass can be regulated through the vasculature. *Proc Natl Acad Sci U S A, 99*(16), 10730-10735.

Rus, H., Cudrici, C., Niculescu, F. (2005). The role of the complement system in innate immunity. *Immunol Res, 33*(2), 103-112.

Shih, D. M., Yu, J. M., Vergnes, L., Dali-Youcef, N., Champion, M. D., Devarajan, A., Zhang, P., Castellani, L. W., Brindley, D. N., Jamey, C., Auwerx, J., Reddy, S. T., Ford, D. A., Reue, K., Lusis, A. J. (2015). PON3 knockout mice are susceptible to obesity, gallstone formation, and atherosclerosis. *Faseb j, 29*(4), 1185-1197.

Sridhar, J., Goyal, N., Liu, J., Foroozesh, M. (2017). Review of ligand specificity factors for CYP1A subfamily enzymes from molecular modeling studies reported to-date. *Molecules, 22*(7).

Swindle, M. M., Makin, A., Herron, A. J., Clubb, F. J., Frazier, K. S. (2012). Swine as models in biomedical research and toxicology testing. *Vet Pathol, 49*(2), 344-356.

Tahmasbpour-Marzony, E., Ghanei, M., Panahi, Y. (2016). Oxidative stress and altered expression of peroxiredoxin genes family (PRDXS) and sulfiredoxin-1 (SRXN1) in human lung tissue following exposure to sulfur mustard. *Exp Lung Res, 42*(4), 217-226.

Tan, Z., Wang, Y., Yang, T., Xing, K., Ao, H., Chen, S., Zhang, F., Zhao, X., Liu, J., Wang, C. (2017). Differentially expressed genes in the caecal and colonic mucosa of

Landrace finishing pigs with high and low food conversion ratios. *Sci Rep, 7*(1), 14886.

Tizioto, P. C., Coutinho, L. L., Decker, J. E., Schnabel, R. D., Rosa, K. O., Oliveira, P. S., Souza, M. M., Mourão, G. B., Tullio, R. R., Chaves, A. S., Lanna, D. P., Zerlotini-Neto, A., Mudadu, M. A., Taylor, J. F., Regitano, L. C. (2015). Global liver gene expression differences in Nelore steers with divergent residual feed intake phenotypes. *BMC Genomics, 16*(1), 242.

Trayhurn, P., Bing, C. (2006). Appetite and energy balance signals from adipocytes. *Philos Trans R Soc Lond B Biol Sci, 361*(1471), 1237-1249.

Trigueros-Motos, L., van Capelleveen, J. C., Torta, F., Castano, D., Zhang, L. H., Chai, C., Kang, M., Dimova, L. G., Schimmel, A. W. M., Tietjen, I., Radomski, C., Tan, L. J., Hwee, T. C., Narayanaswamy, P., Wu, D., Dorninger, F., Yakala, G. K., Barhdadi, A., Angeli, V., Dube, M. P., Berger, J., Dallinga-Thie, G. M., Tietge, U. J. F., Wenk, M. R., Hayden, M. R., Hovingh, G. K., Singaraja, R. R. (2017). ABCA8 regulates cholesterol efflux and high-density lipoprotein cholesterol levels. *Arterioscler Thromb Vasc Biol*.

Van Doren, S. R. (2015). Matrix metalloproteinase interactions with collagen and elastin. *Matrix Biol, 44*, 224-231.

Vincent, A., Louveau, I., Gondret, F., Trefeu, C., Gilbert, H., Lefaucheur, L. (2015). Divergent selection for residual feed intake affects the transcriptomic and proteomic profiles of pig skeletal muscle. *J Anim Sci, 93*(6), 2745-2758.

Wilkinson, J. M. (2011). Re-defining efficiency of feed use by livestock. *Animal, 5*(7), 1014-1022.

Yang, H., Wang, H., Czura, C. J., Tracey, K. J. (2005). The cytokine activity of HMGB1. *J Leukoc Biol, 78*(1), 1-8.

Zhao, Y., Hou, Y., Liu, F., Liu, A., Jing, L., Zhao, C., Luan, Y., Miao, Y., Zhao, S., Li, X. (2016). Transcriptome Analysis Reveals that Vitamin A Metabolism in the Liver Affects Feed Efficiency in Pigs. *G3, 6*(11), 3615-3624.

Zhou, Y., Duan, S., Zhou, Y., Yu, S., Wu, J., Wu, X., Zhao, J., Zhao, Y. (2015). Sulfiredoxin-1 attenuates oxidative stress via Nrf2/ARE pathway and 2-Cys Prdxs after oxygen-glucose deprivation in astrocytes. *J Mol Neurosci, 55*(4), 941-950.

Table 1 Primer sequences for RNA-seq validation via qPCR.

Gene	NCBI accession no.	Forward	Reverse	Product size	Efficiency
COL8A1	XM_001926443.5	CCACACCTACCCCAGTATATGAAG	CCTTGCTCCCCTCGTAAACTAG	116 bp	100 %
MMP16	XM_001926617.5	GCTATTCTTCGCCGTGAGATG	GGCAAGCCTCTCCAGAAGTAAG	116 bp	101 %
PLCE1	XM_013990458.1	AGGGATATGTTGGCAGGATTG	GGACAAAGAAACTCTCCTCCTCTG	117 bp	97 %
RPL32	NM_001001636.1	AGCCCAAGATCGTCAAAAAG	TGTTGCTCCCATAACCAATG	165 bp	93 %

Table 2 Phenotypic data of pigs divergent in feed efficiency (FE).

FE group	Body weight (kg)*	Residual feed intake (g/day)*	Feed conversion ratio *
n = 40 FE-divergent pigs utilised for phenotypic measurements			
High-FE (LRFI; n = 20)	97.53 ±12.8 (123.6; 74.6)	-100.2 ±97.7 (-329.3; 53.81)	1.98 ±0.16 (2.23; 1.70)
Low-FE (HRFI; n = 20)	100.4 ±9.93 (116.2; 83.8)	150.7 ±163 (494.1; -186.6)	2.27 ±0.25 (2.93; 1.86)
n = 16 FE-divergent pigs (selected out of the 40) utilised for RNA-seq			
High-FE (LRFI; n = 8)	101.5 ±13.7 (123.6; 76.2)	-73.06 ±39.5 (-17.92; -130.6)	1.99 ±0.15 (2.20; 1.80)
Low-FE (HRFI; n = 8)	101.8 ±8.9 (116.2; 87.2)	193.8 ±89.8 (324.2; 100.2)	2.32 ±0.16 (2.54; 2.12)

* Values represent means and standard deviations of phenotypic traits. Maximum and minimum values are shown in parenthesis.

Table 3 Most differentially expressed transcripts in relation to feed efficiency (FE).

Gene*	FC	P-value	q-value	Top molecular and physiological function	Top pathway	Network[$]
COL11A2	+25.7	0.009	0.64	Organismal dev, cellular development	Intrinsic prothrombin activation	2
PLEKHB1	+7.49	0.004	0.55	-	-	3
DIRAS3	+7.37	0.009	0.61	Cellular movement, organismal development	HMGB1 signalling	8
KCNMA1	+6.16	0.001	0.40	Cellular movement, cardiovascular system d & f	-	4
COL28A1	+5.27	0.002	0.45	-	-	7
GARNL3	+4.95	0.002	0.47	-	-	11
COL11A1	+4.80	0.008	0.61	Cellular movement, organismal development	-	7
NFASC	+4.25	0.001	0.45	Cellular movement, tissue morphology	-	5
BMPR1B	+4.16	<0.001	0.21	Cellular movement, organismal development	TGF-β signalling	3
CYP1A1	+3.86	0.005	0.55	Cellular movement, organismal development	Oestrogen biosynthesis	8
MRAP2	+3.63	0.004	0.55	Cell morphology, connective tissue d & f	-	5
KRT18	+3.60	0.003	0.50	Cell death and survival, organismal development	ILK signalling	1
COLGALT2	+3.32	0.003	0.53	-	-	12
ADIRF	+3.21	0.006	0.56	Cellular development, connective tissue d & f	-	12
SHISA2	+2.99	0.005	0.55	Organismal development & survival	-	8
SRXN1	-3.85	<0.001	0.09	Cell death, organismal survival	-	6
AKR1C4	-3.59	0.002	0.45	Lipid metabolism	Oestrogen biosynthesis	4, 9
MMP8	-3.23	<0.001	0.13	Cellular movement, cardiovascular system d & f	Axonal guidance signalling	2
FAT2	-2.93	0.009	0.63	-	-	10
LTF	-2.85	0.002	0.45	Cellular movement, cardiovascular system d & f	-	1
TEX33	-2.72	0.001	0.40	-	-	5
TREH	-2.28	0.007	0.61	-	Trehalose degradation II (Trehalase)	9
TXK	-2.25	0.008	0.61	Cellular movement, organismal development	Leukocyte Extravasation signalling	2
NLRP12	-2.24	<0.001	0.22	Cellular movement, organismal development	TREM1 signalling	13
OSM	-1.88	0.005	0.55	Cellular movement, cardiovascular system d & f	HMGB1 signalling	3
CSF3R	-1.87	0.001	0.42	Cellular movement, organismal development	Granulocyte adhesion & diapedesis	1
ADORA3	-1.73	<0.001	0.09	Cellular movement, cardiovascular system d & f	Gαi signalling	7
CBFA2T3	-1.71	0.002	0.50	Cellular and organismal development	-	1
RPH3A	-1.70	0.001	0.38	-	-	12
AHSA2	-1.68	0.005	0.55	-	-	5

FC: fold change with positive and negative fold changes correspond to high-FE > low-FE and high-FE < low-FE, respectively; * A total of 87 annotated genes were found to be at least 1.5-fold differentially expressed in FE-divergent pigs; $ Network IDs: d & f: development and function; **1.** Cell death and survival, embryonic development, cancer; **2.** Connective tissue development and function, connective tissue disorders, organismal injury and abnormalities; **3.** Organ development, respiratory system development and function, cardiovascular system development and function; **4**. Glomerular injury, organismal injury and abnormalities, renal fibrosis; **5**. Cardiovascular disease, organismal injury and abnormalities, cancer; **6.** Humoral immune response, protein synthesis, antimicrobial response; **7.** Cell signalling, cellular function and maintenance, vitamin and mineral metabolism; **8.** Cellular development, cellular growth and proliferation, dermatological diseases and conditions; **9.** Cell morphology, cellular function and maintenance, drug metabolism; **10.** Cell-to-cell signalling and interaction, inflammatory response, cell cycle; **11.** Amino acid metabolism, molecular transport, small molecule biochemistry; **12.** Cell death and survival, developmental disorder, embryonic development; **13.** Dermatological diseases and conditions, hereditary disorder, inflammatory disease; **14.** Cardiovascular disease, cardiovascular system development and function, cell morphology; **15.** DNA replication, recombination, and repair, dermatological diseases and conditions, developmental disorder; **16.** Developmental disorder, hereditary disorder, metabolic disease.

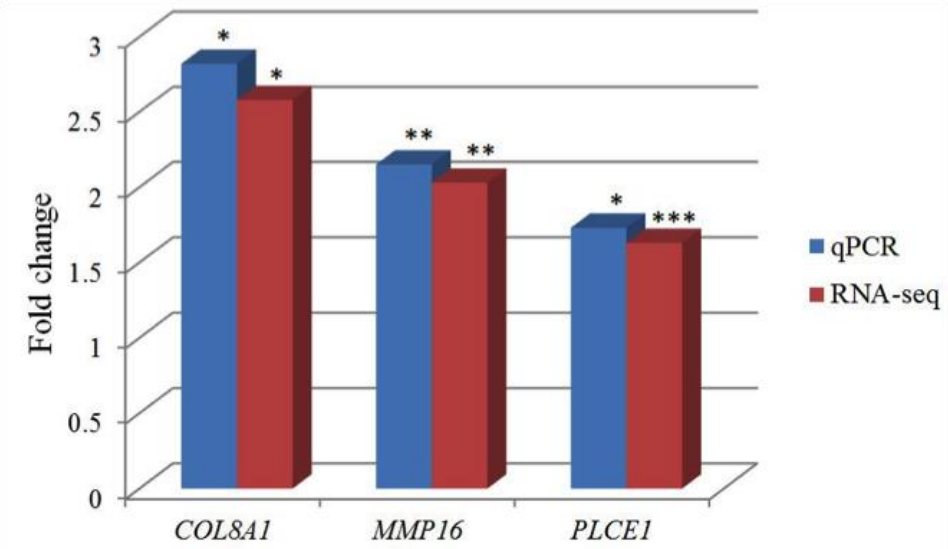

Fig 1 Bar chart illustrating the RNA-seq and qPCR fold changes of three selected up-regulated genes in high-FE pigs. Significance levels of differences affected by selection for feed efficiency: *$P < 0.05$, **$P < 0.01$, ***$P < 0.001$.

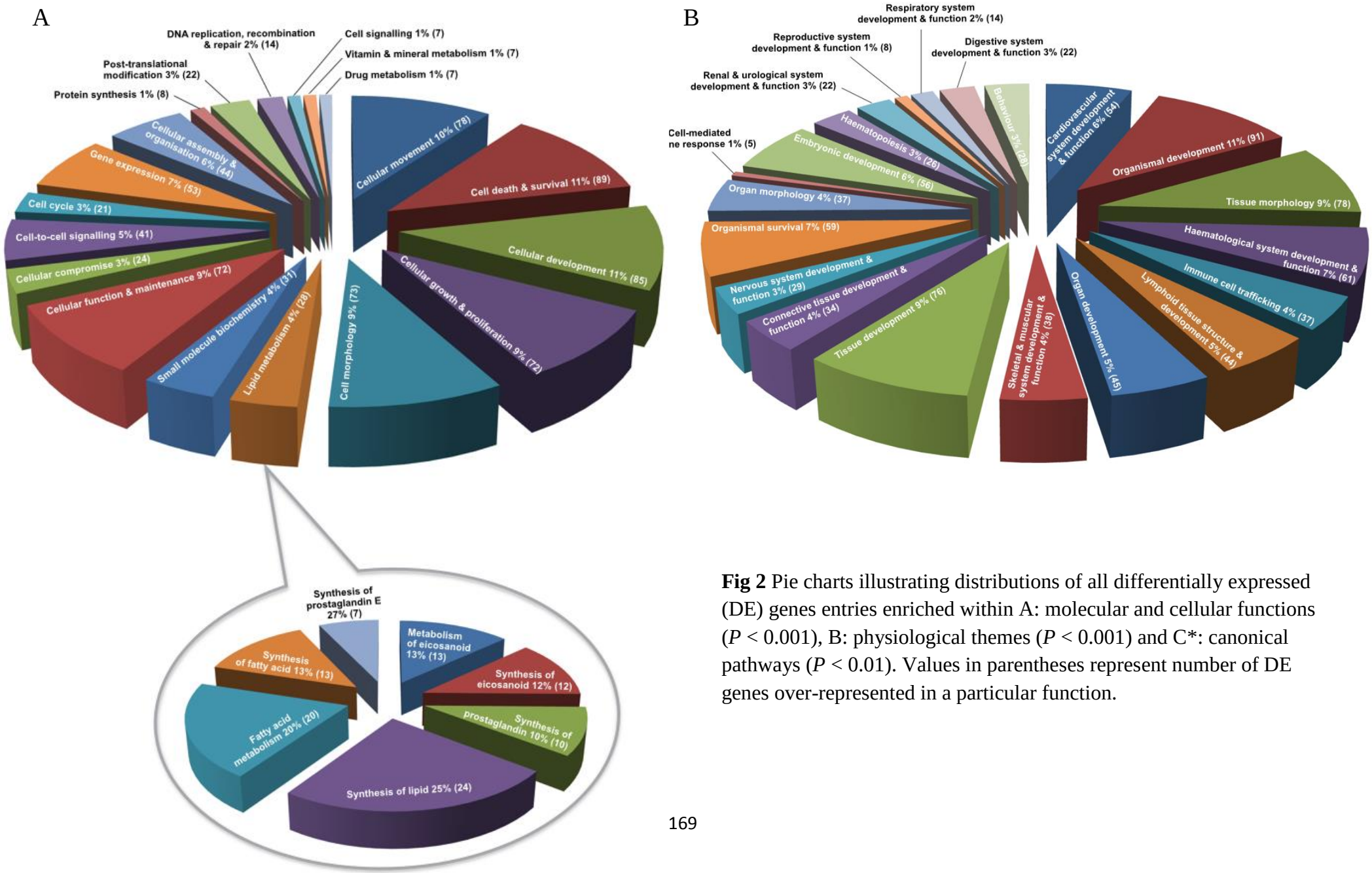

Fig 2 Pie charts illustrating distributions of all differentially expressed (DE) genes entries enriched within A: molecular and cellular functions ($P < 0.001$), B: physiological themes ($P < 0.001$) and C*: canonical pathways ($P < 0.01$). Values in parentheses represent number of DE genes over-represented in a particular function.

C

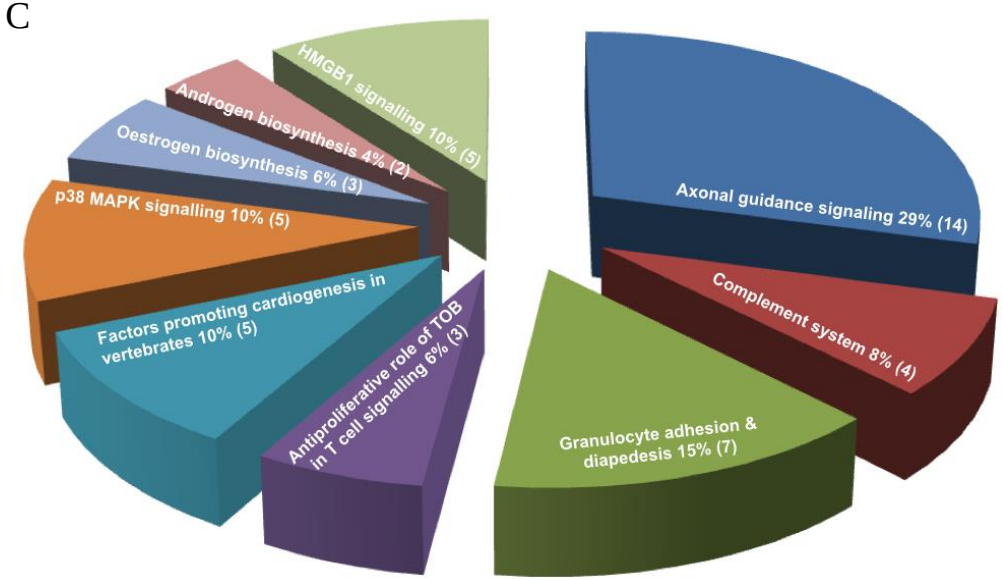

Fig 2 cont. *Axonal guidance signaling: [-log(p-value) = 3.88]; *EPHA7*, *UNC5A*, *ARHGEF15*, *MET*, *VEGFA*, *PLCE1*, *FZD4*, *ADAMTS6*, *GLIS2*, *SEMA3D*, *MMP8*, *ROBO2*, *SEMA3B*, *SEMA3C*. Complement system: [-log(p-value) = 3.36]; *C5AR1*, *ITGAM*, *CFI*, *CFB*. Granulocyte adhesion and diapedesis: [-log(p-value) = 2.76]; *CSF3R*, *SELL*, *C5AR1*, *ITGAM*, *MMP16*, *MMP8*, *TNFRSF1B*. Antiproliferative role of TOB in T cell signaling: [-log(p-value) = 2.70]; *CCNE2*, *TGFB1*, *TGFB2*. Factors promoting cardiogenesis in vertebrates: [-log(p-value) = 2.69]; *CCNE2*, *FZD4*, *TGFB1*, *TGFB2*, *BMPR1B*. p38 MAPK signaling: [-log(p-value) = 2.24]; *PLA2G4A*, *TGFB1*, *TGFB2*, *TNFRSF1B*, *IRAK1*. Oestrogen biosynthesis: [-log(p-value) = 2.20]; *CYP1A1*, *AKR1C4*, *HSD17B14*. Androgen biosynthesis: [-log(p-value) = 2.10]; *AKR1C4*, *HSD17B14*. HMGB1 signaling: [-log(p-value) = 2.02]; *TGFB1*, *DIRAS3*, *TGFB2*, *OSM*, *TNFRSF1B*.

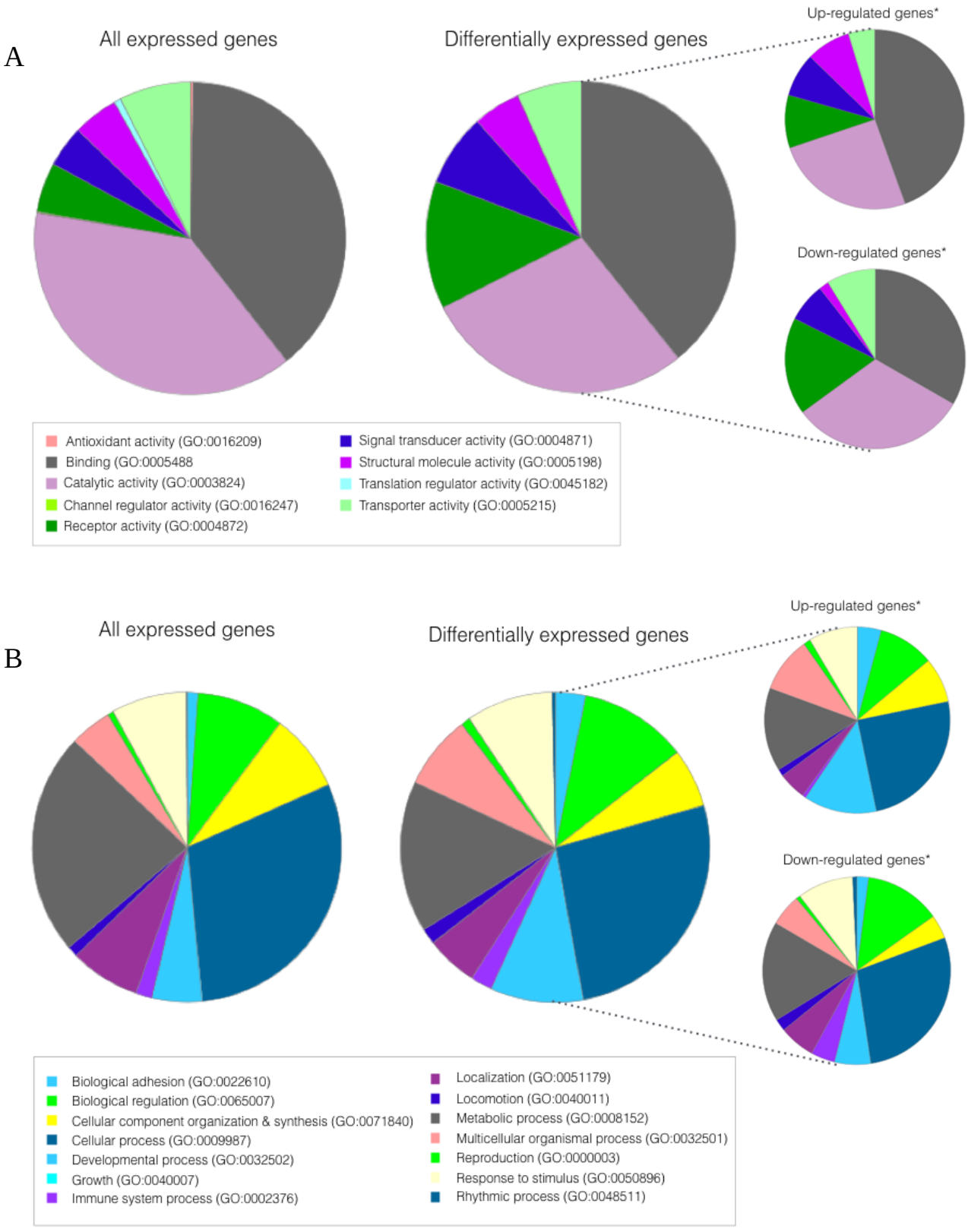

Fig 3 Pie charts depicting A: molecular and B: physiological functions enriched with differentially expressed genes in adipose tissue of pigs divergent in feed efficiency (FE) when compared against all genes expressed in the adipose tissue. *Up- and down-regulated genes in high-FE.

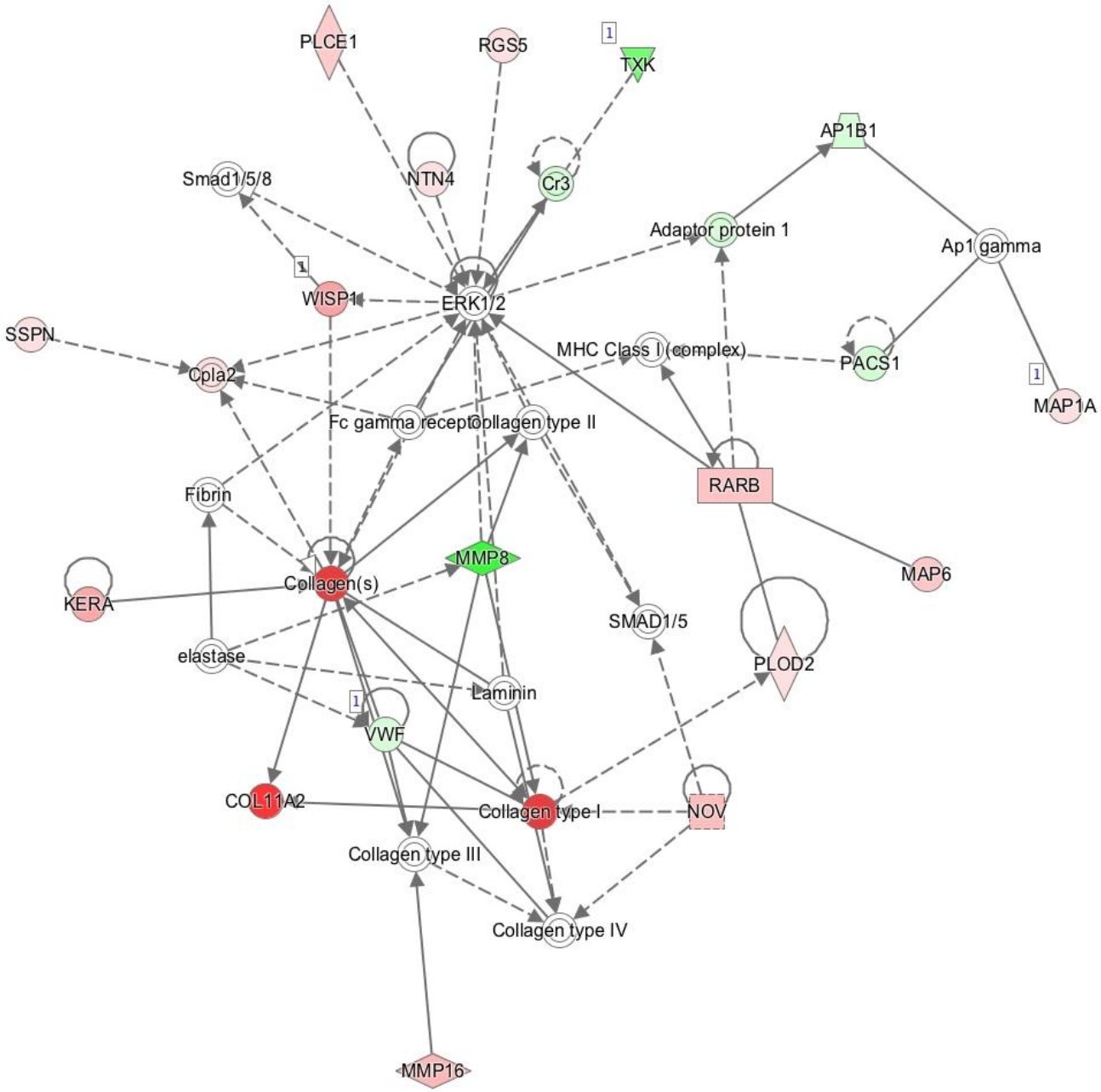

Fig 4 Gene network (#2) containing functions related to 'connective tissue development & function', 'connective tissue disorders' and 'organismal injury & abnormalities'. Genes are denoted as nodes and the biological relationship between two nodes is denoted as an edge/line. Node color represents up- (red) and down- (green) regulated genes in high-FE pigs.

Supplementary files

Table S1 (PDF 259 KB) Differentially expressed transcripts (n = 209) at a $P < 0.01$ in FE-divergent pigs.

Table S2 (PDF 29 KB) Molecular and cellular functions significantly enriched with differentially expressed genes including a list of sub-functions contained within each category.

Table S3 (PDF 105 KB) Physiological system development and function categories significantly enriched with differentially expressed genes including a list of sub-categories contained within each function.

Fig S1 (PDF 131 KB) Volcano plot representing $\log_2$ fold changes and $-\log_{10}$(p-values) of genes expressed in adipose tissue from high-FE pigs.

RNA-Seq of liver from pigs Divergent in feed efficiency highlights shifts in macronutrient metabolism, hepatic growth and immune response

Justyna Horodyska[1,2], Ruth M. Hamill[1]*, Henry Reyer[2], Nares Trakooljul[2], Peadar G. Lawlor[3], Ursula M. McCormack[3], Klaus Wimmers[2,4]

[1]Teagasc, Food Research Centre, Ashtown, Dublin 15, Ireland
[2]Leibniz Institute for Farm Animal Biology (FBN), Institute for Genome Biology, Dummerstorf, Germany
[3]Teagasc, Pig Production Department, AGRIC, Moorepark, Fermoy, Co. Cork, Ireland
[4]Faculty of Agricultural and Environmental Sciences, University Rostock, Germany
*Corresponding author

In review at Frontiers in Genetics

Abstract

Liver is a metabolically complex organ that influences nutrient partitioning and potentially modulates the efficiency of converting energy acquired from macronutrients ingestion into a muscle and/or adipose tissue (referred to as feed efficiency, FE). The objective of this study was to sequence the hepatic tissue transcriptome of closely related but differently feed efficient pigs (n = 16) and identify relevant biological processes that underpin the differences in liver phenotype between FE groups. Liver weight did not significantly differ between the FE groups, however blood parameters showed that total protein, glucose, cholesterol and percentage of lymphocytes were significantly greater in high-FE pigs. Ontology analysis revealed carbohydrate, lipid and protein metabolism to be significantly enriched with differentially expressed genes. In particular, high-FE pigs exhibited gene expression patterns suggesting improved absorption of carbohydrates and cholesterol as well as enhanced reverse cholesterol transport. Furthermore, the inferred decrease in bile acid synthesis in high-FE pigs may contribute to the observed greater levels of serum glucose, which can be then delivered to cells and utilized for growth and maintenance. Gene ontology analysis also suggested that livers of more efficient pigs may be characterized by higher protein turnover and increased epithelial cell differentiation, whereby an enhanced quantity of invariant natural killer T-cells

and viability of natural killer cells could induce a quicker and more effective hepatic response to inflammatory stimuli. Our findings suggest that this prompt hepatic response to inflammation in high-FE group may contribute to the more efficient utilization of nutrients for growth in these animals.

Key Words – FE, RFI, residual feed intake, gene expression, transcriptomics

Introduction

Liver is a central organ for systemic metabolism (Rui 2014; Shimizu et al., 2015) and plays an important role in modulating the efficiency of converting energy acquired from macronutrients into muscle and/or adipose tissue affecting feed efficiency (FE). Energy from ingested macronutrients can be stored by the liver in the form of glycogen, which during food deprivation is broken down into glucose and delivered to the bloodstream (Sherwin 1980; Zhang et al., 2014). Liver can also convert energy from a dietary source to triacylglycerol and export it by very low density lipoproteins (VLDL) either to muscle for use there or to adipose tissue for storage (Gruffat et al., 1996). Moreover liver is a key organ for synthesis of cholesterol, a vital constituent of cell membrane, and lipoproteins that function as cholesterol transporting particles (Charlton-Menys et al., 2008). Low density lipoproteins (LDL) deliver cholesterol to peripheral organs, whilst high density lipoproteins (HDL) transport excess cholesterol from these tissues back to the liver (Feingold et al., 2000), which is then utilized e.g. for synthesis of bile acids that enable intestinal absorption of dietary fats (Boyer 2013).

Being continually subjected to antigens entering from the gut via blood supply, liver also exhibits immunological properties (Gao 2016; Peng et al., 2016). The lymphocyte population of the liver is primarily represented by macrophages, natural killer and natural killer T cells that are involved in innate immune defense and regulation of liver regeneration (Gao 2016; Racanelli et al., 2006). Fueling immune response is an energetically expensive process resulting in less nutrients available for growth (Patience et al., 2015). This alteration in prioritizing nutrients towards stimulating immune response would be suspected to negatively impact animal's feed efficiency. Nevertheless, it has been postulated that high-FE animals have a more efficient immune response to fight off inflammation and therefore more energy available for growth and muscle deposition (Paradis et al., 2015).

Transcriptomic approach is a relevant tool in developing a deeper understanding of the physiological processes in liver which may be related to feed efficiency. To date only a few studies have analyzed the transcriptome of liver from FE-divergent pigs wherein shifts in biological processes that were observed to be differentially regulated in association with FE included cell proliferation, vitamin A metabolism, protein synthesis and catabolism, lipid and carbohydrate metabolism, reverse cholesterol transport, integrin signaling, as well as oxidative stress, inflammation and immune responses (Gondret et al., 2017; Ramayo-Caldas et al., 2018; Reyer et al., 2017; Zhao et al., 2016). Although these studies have offered insights on the regulation of feed efficiency via liver physiology, the biological processes governing the differences in FE are not fully elucidated and further research is needed. Hence the purpose of the present study was to characterize phenotypes relevant to liver physiology and to perform RNA sequencing of liver tissue in pigs divergent for FE to gain deeper insights into differences in hepatic transcriptome architecture and its relationship to liver function in more efficient pigs.

Materials and methods

Ethics statements

The care, slaughter and sample collection of the animals fulfilled the national regulations of animal research and commercial slaughtering and were approved by the Teagasc Animal Ethics Committee for the care and use of animals.

Animals and experimental design

A total of 138 Maxgro (Hermitage Genetics) x (Landrace x Large White) pigs were used in this study. Housing, diets, and selection on FE were as previously described (Horodyska et al., in review). According to RFI (a measure of FE defined as the difference between actual feed intake and predicted feed requirements) values, pigs were assigned within litter and gender as high (H) and low (L) RFI. A total of 40 pigs (20 extremes from LRFI (high-FE) group - 10 males and 10 females, and 20 extremes from HRFI (low-FE) group - 10 males and 10 females) were sampled considering the relatedness of pigs.

Phenotypic measurements

For each animal (n = 40), liver weights were recorded and blood samples were collected in vacuette tubes (ROI: Labstock, Dublin, Ireland; AT: Sarstedt, Nürnbrecht, Germany) during slaughter. For biochemical analysis, upon allowing the blood to clot at room temperature, the samples were centrifuged at 1,500 × g for 10 min and the serum was collected and stored at -80 °C until analyzed. Creatinine, creatine kinase, total protein, blood urea nitrogen, triglycerides, glucose and cholesterol were analyzed with a calibrated ABS Pentra 400 clinical chemistry analyzer (Horiba, ABX, North Hampton, UK). In order to determine analyzer accuracy, every fifth sample was run in duplicate. For hematological analysis, blood was treated with EDTA to prevent clotting. It was then subjected to analysis, within 4 hours of sample collection, whereby white blood cells, lymphocytes, monocytes, granulocytes, red blood cells, red blood cell distribution width, hemoglobin, hematocrit, mean corpuscular volume, mean corpuscular hemoglobin, platelets and mean platelet volume were measured with a Beckman Coulter Ac T Diff analyzer (Beckman Coulter Ltd., High Wycombe, UK). The PROC MIXED procedure in the SAS was used to evaluate associations between FE and liver weight as well as biochemical and hematological parameters in the Maxgro x (Landrace x Large White) pigs (n = 40). The model included RFI group as a fixed effect, slaughter day as a random effect, and the absolute values of RFI as a weight statement. Additionally for liver weight, final live body weight was incorporated in the model as a covariate. Moreover, correlations between RFI and hematological and biochemical parameters were determined using the PROC CORR procedure in the SAS system (version 9.4; SAS Inst. Inc., Cary, NC, USA).

RNA sequencing of liver samples, data processing and ontology analysis

Samples of the right liver lobe (*Lobus Spigelii*) tissue were collected and snap frozen in liquid nitrogen within 10 minutes *post-mortem* followed by storage at -80°C until RNA isolation. Of these 40 liver tissues from RFI-divergent pigs, 16 samples from four sets of full siblings were selected and each set consisted of 2 males - 1 LRFI (high-FE) and 1 HRFI (low-FE) and 2 females 1 LRFI (high-FE) and 1 HRFI (low-FE) so that 8 LRFI (high-FE) pigs - 4 males and 4 females and 8 HRFI pigs (low-FE) - 4 males and 4 females were analyzed. Total RNA of these liver samples was isolated with Tri-Reagent (Sigma-Alrich, Taufkirchen, Germany), and subjected to DNase treatment and a column-based purification (Nucleospin RNA II kit,

Macherey-Nagel, Düren, Germany). Total RNA was used as input for the library preparation according to the TruSeq Stranded mRNA protocol (Illumina, San Diego, CA, USA). Subsequently, sequencing was performed on an Illumina HiSeq2500 generating paired-end reads. Reads were mapped to the reference (Ensembl release 84) using TopHat (2.1.0) (Kim et al., 2013) and read counts were assigned to the gene features employing HTSeq 0.6.1 (Anders et al., 2015). The assessment of the differentially expressed genes included RFI groups and slaughter dates as fixed effects and was performed using the Wald test implemented in DESeq2 (3.4.0, www.R-project.org). To integrate gene expression data, the list of DE genes ($P < 0.01$) and corresponding fold changes were passed to Ingenuity Pathway Analysis (IPA; Ingenuity® Systems, www.ingenuity.com) and significantly enriched bio-functions and canonical pathways ($P < 0.01$) were extracted. They were considered significantly activated and inhibited at an absolute z-score greater than 2. In addition, potential important interaction networks enriched with DE genes were generated using the Ingenuity® Knowledge Base.

Verification of RNA-seq through quantitative real-time PCR (qPCR)

Following cDNA synthesis from 1 µg of total RNA and in presence of random primers (Promega, Mannheim, Germany), oligo (dT) primer and Superscript® III reverse transcriptase (Invitrogen Corp., San Diego, CA, USA), qPCR were carried out on a LightCycler 96 system (Roche Mannheim, Germany). Gene-specific primers (Table 1) were designed using the Primer-BLAST software (https://www.ncbi.nlm.nih.gov/tools/primer-blast) and the BLAST search tool database (http://www.ncbi.nlm.nih.gov/BLAST). PCR reactions were carried out in a final volume of 12 µl consisting of 2 µl cDNA, 6 µl SYBR Green I Master (Roche), 0.6 µl (10 µM) of each forward and reverse primer, and 2.8 µl qPCR grade water (Roche). After an initial denaturation at 95 °C for 5 min, 45 cycles of amplification followed (95 °C for 10 sec, 60 °C for 15 sec and 72 °C for 25 sec). Melting curve analysis was performed at the end of the amplification to verify the specificity of all amplification reactions. *RPL32* expression values were used to normalize qPCR results. Subsequently, qPCR data was analyzed in a mixed model including RFI group as a fixed effect and slaughter date as a random effect (lme4; R). The correlation between RNA-seq and qPCR data were assessed in R considering a significance threshold of $P < 0.05$.

Results

Phenotypic measurements

Liver weight did not significantly differ between the FE groups (high-FE = 1.62 kg ±0.04 kg and low-FE = 1.67 kg ±0.04 kg). The effect of divergence in FE on biochemical and hematological parameters are shown in Table 2. Biochemical analysis of serum revealed that total protein, glucose and cholesterol were significantly ($P < 0.05$) higher in high-FE pigs compared to low-FE pigs. Creatinine, creatine kinase, blood urea nitrogen and triglycerides did not differ significantly between the groups. Hematological analysis exposed significantly ($P < 0.05$) reduced number of white blood cells but increased percentage of lymphocytes in high-FE pigs. The number of platelets and mean platelet volume was significantly ($P < 0.001$ and $P < 0.05$, respectively) lower in high-FE pigs. Remaining hematological parameters were not significantly altered by FE group. Spearman correlations between phenotypic parameters of pigs divergent in FE are depicted in Table 3. A number of significant correlations at a $P < 0.001$ were observed between phenotypes. The strongest linear relationships were noted between total protein and cholesterol (r = 0.781), glucose and cholesterol (r = 0.737), red blood cells and hemoglobin (r = 0.726), creatinine and cholesterol (r = 0.723), creatinine and total protein (r = 0.704), total protein and triglycerides (r = 0.629), total protein and glucose (r = 0.608), as well as creatinine and glucose (r = 0.601). This was followed by moderate linear relationships between triglycerides and creatinine (r = 0.566), cholesterol (r = 0.563) and blood urea nitrogen (r = 0.560).

Differentially expressed genes and ontological interpretation

89.2% of the revealed sequences were successfully mapped to the reference resulting in an average of 105.6 million high quality paired-end reads per sample assigned to 14,910 genes expressed in liver. A total of 922 genes were differentially expressed with a $P < 0.01$ (Figure 1) corresponding to false discovery rate (q) ≤ 0.16, and of these 818 were annotated (Figure 2 and Table S1). Twenty-one molecular & cellular functions and twenty-one physiological system development & function categories were significantly enriched ($P < 0.01$) amongst the DE genes in relation to FE, as inferred from functional enrichment analysis (Figure 3 and Table S3). The highest distribution of all DE genes entries were observed in ‘cell death and survival’ (12%), ‘cellular development’ (11%), ‘organismal development’ (11%) and

'organismal survival' (10%). Twenty canonical pathways were significantly associated with DE genes in relation to FE at $P < 0.01$ (Table 4 and Table S4), wherein the highest distribution of DE genes were observed in 'protein ubiquitination pathway' (8%) and 'role of NFAT in regulation of the immune response' (8%), followed by 'EIF2 signaling' (7%), 'ILK signaling'(7%), 'B cell receptor signaling'(7%), 'aldosterone signaling in epithelial cells' (7%) and 'gap junction signaling' (7%). Twenty-five networks were obtained upon integration of all DE genes. The most significant network (network 1) contained functions related to gastrointestinal and hepatic system disease and liver cirrhosis. Carbohydrate and lipid metabolism, and small molecule biochemistry were represented by 25 DE molecules in network 12 (Figure 4).

Verification of RNA-seq results

Three transcripts, *KIT* (KIT proto-oncogene receptor tyrosine kinase), *PON3* (paraoxonase 3) and *SAA3* (serum amyloid A3), selected based on their abundance and functionality related to feed efficiency were amplified through qPCR. Significant differences in the expression levels of all three measured transcripts between the FE groups were confirmed. Spearman correlations attained by comparing gene expression levels measured using RNA-seq and qPCR, were found to be significant for *KIT* ($r = 0.604$, $P < 0.05$), *PON3* ($r = 0.968$, $P < 0.001$), and *SAA3* ($r = 0.946$, $P < 0.001$) (Figure 5)**.**

Discussion

In this study we investigated the hepatic transcriptome of pigs divergent in FE and identified a number of biological functions and pathways affiliated with lipid, protein and carbohydrate metabolism as well as hepatic growth and immune response. These differences help explain the physiological differences associated with divergence in FE and the recorded biochemical and hematological parameters.

Macronutrients metabolism

Paraoxonase 3 (*PON3*) was the most up-regulated (fold change = 10.1) gene in high-FE pigs. *PON3* codes for an enzyme that associates with HDL (Getz et al., 2004) and prevents oxidation of LDL (Reddy et al., 2001) which otherwise would result in endothelial

dysfunction (Leiva et al., 2015). Increased adipose deposition observed in PON3 knockout mice (Shih et al., 2015) is consistent with a potential role of PON3 in promoting lean growth and this is in keeping with decreased intramuscular fat content in the high-FE pigs found in our previous report (Horodyska et al., in review). Enrichment of DE genes in lipid metabolism networks was further portrayed by molecule connectivity analysis (Figure 4). Suppression of ATP binding cassette subfamily A member 1 (*ABCA1*) in mouse liver increased absorption of dietary cholesterol (Oram et al., 2001). In the present study, the network illustrates *ABCA1* being down-regulated (fold change = -1.37) in high-FE pigs. Other members of the *ABCA* family, (*ABCA5* and *ABCA8*) were over-expressed (fold change = 1.67 and 1.52, respectively) in high-FE pigs. In mice, abundance of *ABCA5* expression was previously associated with increased macrophage cholesterol efflux to HDL (Ye et al., 2010), whilst hepatic abundance of *ABCA8* led to significantly increased plasma HDL level and reverse cholesterol transport (Trigueros-Motos et al., 2017). Indeed, serum analysis pointed towards enhanced cholesterol level in high-FE pigs (Table 1). In addition, a positive correlation between serum cholesterol and total protein, which mainly constitutes of albumin, was observed. Interestingly, serum albumin mediates cholesterol efflux and may be a significant player in reverse cholesterol transport (Ha et al., 2003). Moreover, a previous study has also shown reverse cholesterol transport to be over-expressed in the livers of high-FE pigs (Gondret et al., 2017).

'Fibroblast growth factor (FGF) signaling', which is involved in bile acid metabolism (Ornitz et al., 2015), was predicted to be activated in high-FE livers (z-score = 3.00). In this pathway, fibroblast growth factor receptor substrate 2 (FRS2) was up-regulated (fold change = 1.31) in high-FE pigs. FRS2α deficiency led to increased bile acid synthesis in mouse liver (Wang et al., 2014) therefore it seems probable that high-FE pigs experience decreased bile acid production. In support of this, a previous study showed a lower abundance of genes involved in bile acid metabolism, nuclear receptor subfamily 1 group H member 4 (*NR1H4*) and squalene epoxidase (*SQLE*), in the liver of more feed efficient pigs (Reyer et al., 2017). Besides its well established functions, bile acids are also involved in lowering glucose levels (Staels et al., 2009) and hindering gluconeogenesis (Chai et al., 2015). Differential expression of cholesterol-related genes in the livers of pigs divergent for FE points towards increased absorption of dietary cholesterol and reverse cholesterol transport in high-FE pigs. Therefore, the inferred reduction in bile acid synthesis may be a measure to prevent drops in serum

glucose level rather than explained by HDL cholesterol shortage. This presumption is in accordance with the higher glucose and cholesterol concentrations found in the serum of high-FE pigs. Gene ontology analysis also revealed 'uptake & conversion of carbohydrates', enclosed within a broader 'carbohydrate metabolism' category, significantly enriched with DE genes and 'aldosterone signaling in epithelial cells' significantly activated (z-score = 2.12) in high-FE pigs. Alongside its role in the regulation of sodium absorption (Briet et al., 2010), Aldosterone was shown to be involved in glucose transport through molecular regulation of SGLT1 (sodium-dependent glucose co-transporter) and GLUT2 (glucose transporter) in the chicken intestine (Garriga et al., 2001).

The increased serum total protein concentration observed in high-FE pigs supports the suggested activation of 'protein degradation and trafficking' sub-categories such as 'protein catabolism and secretion' (z-score = 2.16 and 1.00, respectively) in the high-FE livers inferred from the functional enrichment analysis. Moreover, the greater serum protein concentration could have stimulated endogenous glucose synthesis (Promintzer et al., 2006), which is consistent with the positive correlation between total protein and glucose concentrations in the serum of FE-divergent pigs. Over-expression of genes involved in protein synthesis and degradation have been reported in livers of high-FE pigs (Gondret et al., 2017). Lobley (2003) postulated that protein synthesis is much more energetically expensive in comparison to protein degradation. In our previous report (Horodyska et al., 2018), we have suggested that high-FE muscle exhibits increased protein turnover and potentially reuses existing proteins, while directing the conserved energy towards more efficient growth. This phenomenon could also be occurring in the liver of high-FE pigs.

Hepatic growth

'Hepatocyte growth factor (HGF) signaling', 'epidermal growth factor (EGF) signaling' and 'FGF signaling' were significantly activated pathways (z-score = 2.33, 2.12 and 3.00, respectively) in high-FE pigs. Previous studies revealed a role for growth factors, e.g. HGF, EGF and FGF, in stimulating proliferation and differentiation of hepatic oval cells (Hu et al., 1993; Jones et al., 2009; Sánchez et al., 2010) and also in liver regeneration (Jiang et al., 1993; Steiling et al., 2003; Zimmers et al., 2017). Over-expression of growth factor receptor bound protein 2-associated protein 1 (*GAB1*) was a common feature shared between the three

pathways. A study in GAB1 knockout mice reported defects in liver regeneration (Bard-Chapeau et al., 2006) and also reduced embryonic liver size (Sachs et al., 2000). AKT serine/threonine kinase 3 (*AKT3*) was another over-expressed gene enriched in these pathways. Akt3 is a member of AKT kinase family playing a role in modulation of cell survival and proliferation (Xu et al., 2012). Accordingly, 'differentiation of epithelial cells', enclosed within a 'cellular development' function, was activated (z-score = 2.13). Moreover a 'cell cycle' sub-category, 'senescence of cells', which is characterized by cell cycle arrest leading to loss of its ability to divide (Hoare et al., 2010), was suppressed (z-score = -2.90) in high-FE pigs. In the present study liver weights did not significantly differ between the FE groups, although a previous report found significantly heavier liver weights in high-FE pigs (Reyer et al., 2017). Cyclin T2 (*CCNT2*), coding for a protein regulating cell differentiation through activation of cyclin-dependent kinase 9 (CDK9) (Garriga et al., 2003; Simone et al., 2002), was the most down-regulated (fold change = -5.40) gene in high-FE pigs. CDK9 also functions in the inflammatory response (Han et al., 2014). Here, *CDK9* was down-regulated (fold change = -1.22) in high-FE pigs at a $P < 0.05$. It is possible that suppression of *CCNT2* could influence CDK9 function in differentiation of monocytes (De Falco et al., 2005) rather than hepatic epithelial cells.

Immune response

The 'role of nuclear factor of activated T cells (NFAT) in regulation of the immune response' was significantly activated (z-score = 2.14) in high-FE pigs. NFAT proteins play a role in the first line of defense through regulating innate leukocyte response to inflammatory stimuli (Zanoni et al., 2012). Myocyte enhancer factor 2C (*MEF2C*), which orchestrates immune cell activation and differentiation (Schuler et al., 2008), was enriched in this pathway and up-regulated in high-FE animals. Additionally, MEF2C belongs to a family of transcriptional factors that acts in conjunction with NFAT (Mancini et al., 2009). 'Quantity of invariant natural killer T-cells' and 'cell viability of natural killer cells', falling under the broader 'hematological system development and function' theme, were also significantly activated (z-score = 2.10 and 2.20, respectively) in high-FE pigs. In these sub-categories, ETS proto-oncogene 1 transcription factor (*ETS1*) and KIT proto-oncogene receptor tyrosine kinase (*KIT*) were up-regulated. KIT is crucial for survival and maturation of natural killer cells (Colucci et al., 2000), whereas ETS1 plays an essential role in the development and function

of natural killer T cells, a group of cells exhibiting properties of both natural killer cells and T cells (Choi et al., 2011). Consistent with the gene ontology, hematological analysis found an increased percentage of serum lymphocytes in the high-FE group. It is widely considered that during immune response dietary nutrients are shifted away from growth, which may lower animal's feed efficiency, towards the immune-related processes (Patience et al., 2015). Nevertheless, a prompt response to hepatic pro-inflammatory stimuli may result in less energy consumed for combating systemic inflammation and hence more efficient utilization of nutrients for growth and protein accretion (Paradis et al., 2015).Several studies have reported a diverse hepatic inflammatory response in high- versus low-FE pigs (Gondret et al., 2017) and cattle (Alexandre et al., 2015; Paradis et al., 2015), thereby supporting this connection.

Conclusions

Hepatic nutrient partitioning has a direct influence on the efficiency of energy utilization and potentially plays an important role in FE. In this study, carbohydrate, lipid and protein metabolism were significantly over-represented within the DE genes, confirming the hepatic influence on divergent energy utilization in high- versus low-FE pigs. In particular, high-FE pigs exhibited gene expression patterns suggesting improved hepatic absorption of carbohydrates and cholesterol as well as enhanced reverse cholesterol transport. Furthermore, the inferred decrease in bile acid synthesis in high-FE pigs may contribute to the increased concentrations of serum glucose observed. This increased glucose can be delivered to cells and utilized for increased growth. Gene ontology analysis also suggests that the liver of more feed efficient pigs may be characterized by higher protein turnover and increased epithelial cell differentiation, whilst enhanced quantity of invariant natural killer T-cells and viability of natural killer cells could induce a faster and more effective hepatic response to inflammatory stimuli.

Declarations

List of abbreviations

FE: feed efficiency; **RFI:** residual feed intake; **LRFI:** low RFI; **HRFI:** high RFI; **HDL:** high density lipoprotein; **LDL:** low density lipoprotein.

Acknowledgements

The ECO-FCE project was funded by the European Union Seventh Framework Programme (FP7 2007/2013) under grant agreement No. 311794.

Conflict of interest statement

The authors declare that the research was conducted in the absence of any commercial or financial relationships that could be construed as a potential conflict of interest.

Author's contributions

JH collected samples, extracted RNA, prepared libraries, validated RNA-seq via qPCR, carried out data analysis and wrote the manuscript; RMH conceived the experiment and contributed to experimental design, collected samples and edited the manuscript; HR participated in statistical analysis and edited the manuscript; NT assisted in library preparation, performed the RNA-seq and data analysis, and edited the manuscript; PGL provided the animals screened on RFI, participated in data collection and analysis, and edited the manuscript; UMM determined serum and blood parameters, and edited the manuscript; KW contributed to experimental design, established lab protocols and edited the manuscript.

Availability of data

RNA-seq data generated during the current study are available on ArrayExpress at EMBL-EBI (www.ebi.ac.uk/arrayexpress) (accession number: E-MTAB-6256).

References

Alexandre, P. A., Kogelman, L. J. A., Santana, M. H. A., Passarelli, D., Pulz, L. H., Fantinato-Neto, P., Silva, P. L., Leme, P. R., Strefezzi, R. F., Coutinho, L. L., Ferraz, J. B. S., Eler, J. P., Kadarmideen, H. N., Fukumasu, H. (2015). Liver transcriptomic networks reveal main biological processes associated with feed efficiency in beef cattle. *BMC Genomics, 16*(1), 1073.

Anders, S., Pyl, P. T., Huber, W. (2015). HTSeq—a Python framework to work with high-throughput sequencing data. *Bioinformatics, 31*(2), 166-169.

Bard-Chapeau, E. A., Yuan, J., Droin, N., Long, S. N., Zhang, E. E., Nguyen, T. V., Feng, G. S. (2006). Concerted functions of Gab1 and Shp2 in liver regeneration and hepatoprotection. *Mol Cell Biol, 26*(12), 4664-4674.

Boyer, J. L. (2013). Bile Formation and Secretion. *Compr Physiol, 3*(3), 1035-1078.

Briet, M., Schiffrin, E. L. (2010). Aldosterone: effects on the kidney and cardiovascular system. *Nat Rev Nephrol, 6*(5), 261-273.

Chai, J., Zou, L., Li, X., Han, D., Wang, S., Hu, S., Guan, J. (2015). Mechanism of bile acid-regulated glucose and lipid metabolism in duodenal-jejunal bypass. *Int J Clin Exp Pathol, 8*(12), 15778-15785.

Charlton-Menys, V., Durrington, P. N. (2008). Human cholesterol metabolism and therapeutic molecules. *Exp Physiol, 93*(1), 27-42.

Choi, H. J., Geng, Y., Cho, H., Li, S., Giri, P. K., Felio, K., Wang, C. R. (2011). Differential requirements for the Ets transcription factor Elf-1 in the development of NKT cells and NK cells. *Blood, 117*(6), 1880-1887.

Colucci, F., Di Santo, J. P. (2000). The receptor tyrosine kinase c-kit provides a critical signal for survival, expansion, and maturation of mouse natural killer cells. *Blood, 95*(3), 984-991.

De Falco, G., Bellan, C., D'Amuri, A., Angeloni, G., Leucci, E., Giordano, A., Leoncini, L. (2005). Cdk9 regulates neural differentiation and its expression correlates with the differentiation grade of neuroblastoma and PNET tumors. *Cancer Biol Ther, 4*(3), 277-281.

Easton, R. M., Cho, H., Roovers, K., Shineman, D. W., Mizrahi, M., Forman, M. S., Lee, V. M. Y., Szabolcs, M., de Jong, R., Oltersdorf, T., Ludwig, T., Efstratiadis, A., Birnbaum, M. J. (2005). Role for Akt3/Protein kinase B gamma in attainment of normal brain size. *Mol Cell Biol, 25*(5), 1869-1878.

Feingold, K. R., Grunfeld, C. (2000). Introduction to Lipids and Lipoproteins. In L. J. De Groot, G. Chrousos, K. Dungan, K. R. Feingold, A. Grossman, J. M. Hershman, C. Koch, M. Korbonits, R. McLachlan, M. New, J. Purnell, R. Rebar, F. Singer & A. Vinik (Eds.), *Endotext*). South Dartmouth (MA): MDText.com, Inc.

Gao, B. (2016). Basic liver immunology. *Cell Mol Immunol, 13*(3), 265-266.

Garriga, C., Planas, J. M., Moretó, M. (2001). Aldosterone mediates the changes in hexose transport induced by low sodium intake in chicken distal intestine. *J Physiol, 535* (Pt 1), 197-205.

Garriga, J., Bhattacharya, S., Calbo, J., Marshall, R. M., Truongcao, M., Haines, D. S., Grana, X. (2003). CDK9 is constitutively expressed throughout the cell cycle, and its steady-state expression is independent of SKP2. *Mol Cell Biol, 23*(15), 5165-5173.

Getz, G. S., Reardon, C. A. (2004). Paraoxonase, a cardioprotective enzyme: continuing issues. *Curr Opin Lipidol, 15*(3), 261-267.

Gondret, F., Vincent, A., Houée-Bigot, M., Siegel, A., Lagarrigue, S., Causeur, D., Gilbert, H., Louveau, I. (2017). A transcriptome multi-tissue analysis identifies biological pathways and genes associated with variations in feed efficiency of growing pigs. *BMC Genomics, 18*, 244.

Gruffat, D., Durand, D., Graulet, B., Bauchart, D. (1996). Regulation of VLDL synthesis and secretion in the liver. *Reprod Nutr Dev, 36*(4), 375-389.

Ha, J. S., Ha, C. E., Chao, J. T., Petersen, C. E., Theriault, A., Bhagavan, N. V. (2003). Human serum albumin and its structural variants mediate cholesterol efflux from cultured endothelial cells. *Biochim. Biophys. Acta, 1640*(2), 119-128.

Han, Y., Zhan, Y., Hou, G., Li, L. I. (2014). Cyclin-dependent kinase 9 may as a novel target in downregulating the atherosclerosis inflammation (Review). *Biomed Rep, 2*(6), 775-779.

Hoare, M., Das, T., Alexander, G. (2010). Ageing, telomeres, senescence, and liver injury. *J Hepatol, 53*(5), 950-961.

Horodyska, J., Oster, M., Reyer, H., Mullen, A. M., Lawlor, P. G., Wimmers, K., Hamill, R. M. (2018). Analysis of meat quality traits and gene expression profiling of pigs divergent in residual feed intake. *Meat Sci, 137*, 265–274.

Horodyska, J., Wimmers, K., Reyer, H., Trakooljul, N., Mullen, A. M., Lawlor, P. G., Hamill, R. M. (in review). RNA-seq of muscle from pigs divergent in feed efficiency and product quality identifies differences in immune response, growth, and macronutrient and connective tissue metabolism

Hu, Z., Evarts, R. P., Fujio, K., Marsden, E. R., Thorgeirsson, S. S. (1993). Expression of hepatocyte growth factor and c-met genes during hepatic differentiation and liver development in the rat. *Am J Pathol, 142*(6), 1823-1830.

Jiang, W. G., Hallett, M. B., Puntis, M. C. A. (1993). Hepatocyte growth factor/scatter factor, liver-regeneration and cancer metastasis. *Br J Surg, 80*(11), 1368-1373.

Jones, C. N., Tuleuova, N., Lee, J. Y., Ramanculov, E., Reddi, A. H., Zern, M. A., Revzin, A. (2009). Cultivating liver cells on printed arrays of hepatocyte growth factor. *Biomaterials, 30*(22), 3733-3741.

Kim, D., Pertea, G., Trapnell, C., Pimentel, H., Kelley, R., Salzberg, S. L. (2013). TopHat2: accurate alignment of transcriptomes in the presence of insertions, deletions and gene fusions. *Genome Biol, 14*(4), R36.

Leiva, E., Wehinger, S., Guzmán, L., Orrego, R. (2015). Role of Oxidized LDL in Atherosclerosis. In S. A. Kumar (Ed.), *Hypercholesterolemia*, (pp. Ch. 03). Rijeka: InTech.

Lobley, G. E. (2003). Protein turnover—what does it mean for animal production? *Canadian J Anim Sci, 83*(3), 327-340.

Mancini, M., Toker, A. (2009). NFAT Proteins: Emerging Roles in Cancer Progression. *Nat Rev Cancer, 9*(11), 810-820.

Olsen, H. G., Skovgaard, K., Nielsen, O. L., Leifsson, P. S., Jensen, H. E., Iburg, T., Heegaard, P. M. (2013). Organization and biology of the porcine serum amyloid A (SAA) gene cluster: isoform specific responses to bacterial infection. *PLoS One, 8*(10), e76695.

Oram, J. F., Lawn, R. M. (2001). ABCA1. The gatekeeper for eliminating excess tissue cholesterol. *J Lipid Res, 42*(8), 1173-1179.

Ornitz, D. M., Itoh, N. (2015). The Fibroblast Growth Factor signaling pathway. *Wiley Interdiscip Rev Dev Biol, 4*(3), 215-266.

Paradis, F., Yue, S., Grant, J. R., Stothard, P., Basarab, J. A., Fitzsimmons, C. (2015). Transcriptomic analysis by RNA sequencing reveals that hepatic interferon-induced genes may be associated with feed efficiency in beef heifers. *J Anim Sci, 93*(7), 3331-3341.

Patience, J. F., Rossoni-Serão, M. C., Gutiérrez, N. A. (2015). A review of feed efficiency in swine: biology and application. *J Anim Sci Biotechnol, 6*(1), 33.

Peng, H., Wisse, E., Tian, Z. (2016). Liver natural killer cells: subsets and roles in liver immunity. *Cell Mol Immunol, 13*(3), 328-336.

Promintzer, M., Krebs, M. (2006). Effects of dietary protein on glucose homeostasis. *Curr Opin Clin Nutr Metab Care, 9*(4), 463-468.

Racanelli, V., Rehermann, B. (2006). The liver as an immunological organ. *Hepatology, 43*(2 Suppl 1), S54-62.

Ramayo-Caldas, Y., Ballester, M., Sánchez, J. P., González-Rodríguez, O., Revilla, M., Reyer, H., Wimmers, K., Torrallardona, D., Quintanilla, R. (2018). Integrative approach using liver and duodenum RNA-Seq data identifies candidate genes and pathways associated with feed efficiency in pigs. *Sci Rep, 8*(1), 558.

Reddy, S. T., Wadleigh, D. J., Grijalva, V., Ng, C., Hama, S., Gangopadhyay, A., Shih, D. M., Lusis, A. J., Navab, M., Fogelman, A. M. (2001). Human paraoxonase-3 is an HDL-associated enzyme with biological activity similar to paraoxonase-1 protein but is not regulated by oxidized lipids. *Arterioscler Thromb Vasc Biol, 21*(4), 542-547.

Reyer, H., Oster, M., Magowan, E., Dannenberger, D., Ponsuksili, S., Wimmers, K. (2017). Strategies towards Improved Feed Efficiency in Pigs Comprise Molecular Shifts in Hepatic Lipid and Carbohydrate Metabolism. *Int J Mol Sci, 18*(8).

Rui, L. (2014). Energy Metabolism in the Liver. *Compr Physiol, 4*(1), 177-197.

Sachs, M., Brohmann, H., Zechner, D., Müller, T., Hülsken, J., Walther, I., Schaeper, U., Birchmeier, C., Birchmeier, W. (2000). Essential Role of Gab1 for Signaling by the C-Met Receptor in Vivo. *J Cell Biol, 150*(6), 1375-1384.

Sánchez, A., Fabregat, I. (2010). Growth factor- and cytokine-driven pathways governing liver stemness and differentiation. *World J Gastroenterol, 16*(41), 5148-5161.

Schuler, A., Schwieger, M., Engelmann, A., Weber, K., Horn, S., Muller, U., Arnold, M. A., Olson, E. N., Stocking, C. (2008). The MADS transcription factor Mef2c is a pivotal modulator of myeloid cell fate. *Blood, 111*(9), 4532-4541.

Sherwin, R. S. (1980). Role of Liver in Glucose Homeostasis. *Diabetes Care, 3*(2), 261-265.

Shih, D. M., Yu, J. M., Vergnes, L., Dali-Youcef, N., Champion, M. D., Devarajan, A., Zhang, P., Castellani, L. W., Brindley, D. N., Jamey, C., Auwerx, J., Reddy, S. T., Ford, D. A., Reue, K., Lusis, A. J. (2015). PON3 knockout mice are susceptible to obesity, gallstone formation, and atherosclerosis. *FASEB J, 29*(4), 1185-1197.

Shimizu, N., Maruyama, T., Yoshikawa, N., Matsumiya, R., Ma, Y., Ito, N., Tasaka, Y., Kuribara-Souta, A., Miyata, K., Oike, Y., Berger, S., Schutz, G., Takeda, S., Tanaka, H. (2015). A muscle-liver-fat signalling axis is essential for central control of adaptive adipose remodelling. *Nat Commun, 6*, 6693.

Simone, C., Stiegler, P., Bagella, L., Pucci, B., Bellan, C., De Falco, G., De Luca, A., Guanti, G., Puri, P. L., Giordano, A. (2002). Activation of MyoD-dependent transcription by cdk9/cyclin T2. *Oncogene, 21*(26), 4137-4148.

Staels, B., Fonseca, V. A. (2009). Bile Acids and Metabolic Regulation: Mechanisms and clinical responses to bile acid sequestration. *Diabetes Care, 32*(Suppl 2), S237-S245.

Steiling, H., Wustefeld, T., Bugnon, P., Brauchle, M., Fassler, R., Teupser, D., Thiery, J., Gordon, J. I., Trautwein, C., Werner, S. (2003). Fibroblast growth factor receptor signalling is crucial for liver homeostasis and regeneration. *Oncogene, 22*(28), 4380-4388.

Trigueros-Motos, L., van Capelleveen, J. C., Torta, F., Castaño, D., Zhang, L.-H., Chai, C., Kang, M., Dimova, L. G., Schimmel, A. W. M., Tietjen, I., Radomski, C., Tan, L. J., Hwee, T. C., Narayanaswamy, P., Wu, D., Dorninger, F., Yakala, G. K., Barhdadi, A., Angeli, V., Dubé, M.-P., Berger, J., Dallinga-Thie, G. M., Tietge, U. J. F., Wenk, M. R., Hayden, M. R., Hovingh, G. K., Singaraja, R. R. (2017). ABCA8 Regulates Cholesterol Efflux and High-Density Lipoprotein Cholesterol Levels. *Arterioscler Thromb Vasc Biol, 37*(11):2147-2155.

Wang, C., Yang, C., Chang, J. Y., You, P., Li, Y., Jin, C., Luo, Y., Li, X., McKeehan, W. L., Wang, F. (2014). Hepatocyte FRS2alpha is essential for the endocrine fibroblast growth factor to limit the amplitude of bile acid production induced by prandial activity. *Curr Mol Med, 14*(6), 703-711.

Xu, N., Lao, Y., Zhang, Y., Gillespie, D. A. (2012). Akt: A Double-Edged Sword in Cell Proliferation and Genome Stability. *J Oncol, 2012*, 15.

Ye, D., Meurs, I., Ohigashi, M., Calpe-Berdiel, L., Habets, K. L., Zhao, Y., Kubo, Y., Yamaguchi, A., Van Berkel, T. J., Nishi, T., Van Eck, M. (2010). Macrophage

ABCA5 deficiency influences cellular cholesterol efflux and increases susceptibility to atherosclerosis in female LDLr knockout mice. *Biochem Biophys Res Commun, 395*(3), 387-394.

Zanoni, I., Granucci, F. (2012). Regulation and dysregulation of innate immunity by NFAT signaling downstream of pattern recognition receptors (PRRs). *Eur J Immunol, 42*(8), 1924-1931.

Zhang, Y., Xu, D., Huang, H., Chen, S., Wang, L., Zhu, L., Jiang, X., Ruan, X., Luo, X., Cao, P., Liu, W., Pan, Y., Wang, Z., Chen, Y. (2014). Regulation of Glucose Homeostasis and Lipid Metabolism by PPP1R3G-mediated Hepatic Glycogenesis. *Mol Endocrinol, 28*(1), 116-126.

Zhao, Y., Hou, Y., Liu, F., Liu, A., Jing, L., Zhao, C., Luan, Y., Miao, Y., Zhao, S., Li, X. (2016). Transcriptome Analysis Reveals that Vitamin A Metabolism in the Liver Affects Feed Efficiency in Pigs. *G3, 6*(11), 3615-3624.

Zimmers, T. A., Jin, X., Zhang, Z., Jiang, Y., Koniaris, L. G. (2017). Epidermal Growth Factor Receptor Restoration Rescues the Fatty Liver Regeneration in Mice. *Am J Physiol Endocrinol Metab, 313(4):E440-E449*.

Table 1 Forward and reverse primers and amplicon length used for qPCR analysis.

Gene	NCBI accession no.	Forward	Reverse	Product size (bp)
KIT	NM_001044525.1	TTCTCGTGTCCAATGCTGATG	TCGGTGCCTGGACAGAAATAC	166
PON3	NM_001044604.1	CAATGGGATCACAGTCTCATCAG	TGCCCAAATATCTCCCGTATC	178
*SAA3**	NM_001044552.1	CTCAAGGAAGCTGGTCAAGG	GGACATTCTCTCTGGCATCG	178
RPL32	NM_001001636.1	AGCCCAAGATCGTCAAAAAG	TGTTGCTCCCATAACCAATG	165

* Olsen et al., (2013).

Table 2 Effect of divergence in feed efficiency (FE) on biochemical and hematological parameters.

	Measurement	High-FE[1]	Low-FE[1]	SE	P-value
Biochemistry	Creatinine (µmol/L)	117.7	98.27	11.0	0.085
	Creatine kinase (µmol/L)	89.83	87.56	16.8	0.893
	Total protein (g/L)	61.03	48.21	6.26	**0.048**
	Blood urea nitrogen (mg/dL)	14.56	9.444	3.54	0.157
	Triglycerides (mmol/L)	0.620	0.549	0.07	0.351
	Glucose (mmol/L)	4.892	3.968	0.37	**0.016**
	Cholesterol (mmol/L)	2.329	1.811	0.25	**0.045**
Hematology	White blood cells (x10^3 cells/µl)	22.66	27.30	1.84	**0.016**
	Lymphocytes (%)	51.94	42.93	3.43	**0.013**
	Monocytes (%)	7.226	6.466	1.04	0.469
	Granulocytes (%)	42.06	38.77	5.60	0.561
	Lymphocyte number (x10^3 cells/µl)	11.51	11.24	1.08	0.809
	Monocyte number (x10^3 cells/µl)	1.430	1.648	0.24	0.371
	Granulocyte number (x10^3 cells/µl)	9.990	10.30	1.73	0.859
	Red blood cells (x10^6 cells/µl)	6.386	6.772	0.35	0.274
	Hemoglobin (g/dL)	11.20	11.74	0.62	0.388
	Hematocrit (%)	0.352	0.353	0.01	0.870
	Mean corpuscular volume (fL)	52.69	52.57	0.70	0.864
	Mean corpuscular hemoglobin (%)	17.37	17.31	0.26	0.809
	Mean corpuscular hemoglobin conc (pg)	32.35	32.52	0.45	0.705
	Red cell distribution width (fL)	19.24	20.27	0.84	0.229
	Platelets (10^6 cells/µl)	178.3	272.2	29.9	**0.003**
	Mean platelet volume (fL)	7.778	8.937	0.54	**0.039**

[1] Least square means for each parameter.

Table 3 Correlations between hematological and biochemical parameters.

	C	CK	TP	BUN	Tg	Glu	Chol	WBC	Lc	Mc	Gc	LcN	McN	GcN	RBC	Hg	Hc	MCV	MCH	MCHC	RCDW	P
CK	-0.070																					
	0.674																					
TP	0.704	-0.084																				
	<.001	0.613																				
BUN	0.380	0.058	0.418																			
	0.017	0.727	**0.008**																			
Tg	0.566	0.032	0.629	0.560																		
	<.001	0.846	**<.001**	**<.001**																		
Glu	0.601	-0.003	0.608	0.363	0.191																	
	<.001	0.985	**<.001**	**0.023**	0.245																	
Chol	0.723	-0.075	0.781	0.439	0.563	0.737																
	<.001	0.651	**<.001**	**0.005**	**<.001**	**<.001**																
WBC	-0.083	-0.025	-0.173	-0.365	-0.237	-0.121	-0.048															
	0.614	0.881	0.292	**0.023**	0.147	0.463	0.774															
Lc	0.188	-0.085	0.290	0.317	0.110	0.378	0.295	-0.476														
	0.253	0.606	0.074	0.050	0.506	**0.018**	0.068	**0.002**														
Mc	0.292	0.009	0.440	0.235	0.410	0.173	0.264	-0.539	0.577													
	0.071	0.959	**0.005**	0.150	**0.010**	0.292	0.105	**<.001**	**<.001**													
Gc	-0.158	0.033	-0.062	-0.009	-0.061	-0.176	-0.257	0.085	-0.434	-0.421												
	0.336	0.842	0.709	0.955	0.714	0.285	0.114	0.605	**0.006**	**0.008**												
LcN	0.131	-0.110	0.174	0.087	-0.063	0.377	0.307	0.214	0.690	0.180	-0.362											
	0.428	0.503	0.290	0.598	0.703	**0.018**	0.057	0.192	**<.001**	0.274	**0.024**											
McN	0.247	-0.021	0.429	0.101	0.306	0.186	0.295	-0.264	0.476	0.902	-0.525	0.331										
	0.129	0.897	**0.006**	0.542	0.059	0.258	0.068	0.104	**0.002**	**<.001**	**0.001**	**0.040**										
GcN	-0.154	-0.030	-0.014	-0.088	-0.059	-0.174	-0.184	0.323	-0.406	-0.392	0.930	-0.129	-0.388									
	0.350	0.856	0.932	0.596	0.722	0.290	0.261	**0.045**	**0.010**	**0.014**	**<.001**	0.432	**0.015**									
RBC	0.397	-0.054	0.461	0.079	0.213	0.287	0.466	0.134	0.105	-0.017	0.001	0.289	0.103	0.091								
	0.013	0.746	**0.003**	0.632	0.193	0.077	**0.003**	0.415	0.527	0.918	0.994	0.075	0.532	0.580								
Hg	0.254	-0.016	0.220	-0.065	0.062	0.199	0.345	0.125	0.028	-0.148	0.011	0.214	-0.101	0.074	0.726							
	0.119	0.921	0.177	0.692	0.708	0.225	**0.032**	0.447	0.863	0.367	0.946	0.191	0.540	0.656	**<.001**							
Hc	0.355	0.025	0.317	-0.010	0.161	0.274	0.445	0.240	0.015	-0.046	-0.028	0.250	0.014	0.062	0.656	0.742						
	0.026	0.882	**0.049**	0.954	0.326	0.091	**0.005**	0.141	0.927	0.780	0.866	0.125	0.933	0.707	**<.001**	**<.001**						
MCV	-0.173	0.201	-0.328	-0.259	-0.346	-0.030	-0.148	0.254	-0.316	-0.310	0.146	-0.137	-0.299	0.151	-0.304	0.140	0.320					
	0.293	0.220	**0.041**	0.111	**0.031**	0.857	0.369	0.119	0.050	0.055	0.375	0.407	0.065	0.360	0.060	0.397	**0.047**					
MCH	-0.146	0.323	-0.159	-0.229	-0.129	0.047	-0.012	0.220	-0.345	-0.290	0.178	-0.161	-0.250	0.170	-0.208	0.159	0.354	0.852				
	0.375	**0.045**	0.333	0.161	0.434	0.774	0.944	0.179	**0.032**	0.073	0.279	0.328	0.125	0.301	0.203	0.333	**0.027**	**<.001**				
MCHC	0.146	0.163	0.309	-0.100	0.149	0.303	0.336	**0.019**	-0.147	-0.104	0.060	-0.082	-0.029	0.039	0.135	0.321	0.427	0.288	0.614			
	0.376	0.320	0.056	0.546	0.364	0.061	**0.037**	0.908	0.373	0.529	0.719	0.621	0.862	0.815	0.413	**0.046**	**0.007**	0.076	**<.001**			
RCDW	-0.144	-0.066	-0.155	0.101	0.007	-0.282	-0.187	0.267	-0.020	-0.097	-0.123	0.127	-0.025	-0.083	0.164	-0.025	-0.123	-0.525	-0.488	-0.371		
	0.383	0.689	0.345	0.541	0.964	0.082	0.253	0.100	0.905	0.555	0.455	0.442	0.882	0.614	0.318	0.882	0.456	**0.001**	**0.002**	**0.020**		
P	-0.175	0.080	-0.189	0.106	0.009	-0.067	-0.077	0.193	-0.188	-0.259	-0.117	-0.041	-0.176	-0.086	-0.036	-0.047	-0.041	0.105	0.113	-0.013	0.025	
	0.287	0.628	0.249	0.521	0.957	0.687	0.641	0.240	0.253	0.112	0.479	0.803	0.283	0.601	0.827	0.776	0.803	0.524	0.492	0.937	0.878	
MPV	-0.131	-0.042	-0.186	-0.210	-0.166	-0.010	0.066	0.375	-0.409	-0.468	**0.024**	-0.174	-0.461	0.023	0.036	0.304	0.343	0.487	0.418	0.172	-0.060	0.334
	0.425	0.798	0.256	0.200	0.313	0.953	0.688	**0.019**	**0.010**	**0.003**	0.884	0.291	**0.003**	0.892	0.829	0.060	0.033	**0.002**	**0.008**	0.295	0.715	**0.038**

Abbreviations:
C: Creatinine (µmol/L), **CK**: Creatine kinase (µmol/L), **TP**: Total protein (g/L), **BUN**: Blood urea nitrogen (mg/dL), **Tg**: Triglycerides (mmol/L), **Glu**: Glucose (mmol/L), **Chol**: Cholesterol (mmol/L), **WBC**: White blood cells (x 103 cells/µl), **Lc**: Lymphocytes (%), **LcN**: Lymphocyte number (x 103 cells/µl), **Mc**: Monocytes (%), **McN**: Monocyte number (x 103 cells/µl), **Gc**: Granulocytes (%), **GcN**: Granulocyte number (x 103 cells/µl), **RBC**: Red blood cells (106 cells/µL), **RCDW**: Red cell distribution width (fL), **Hg**: Hemoglobin (g/dL), **Hc**: Hematocrit (%), **MCV**: Mean corpuscular volume (fL), **MCH**: Mean corpuscular hemoglobin (%), **MCHC**: Mean corpuscular hemoglobin concentration (pg), **P**: Platelets (106 cells /µL), **MPV**: Mean platelet volume (fL).

Correlation coefficient is presented in the upper row and a *P*-value is shown in the bottom row.

Table 4 Most significantly enriched canonical signaling pathways identified in liver samples of feed efficiency (FE)-divergent pigs.

Canonical Pathways	-log(p-value)	Z-score	Gene
Role of NFAT in Regulation of Immune Response	4.07	2.14[£]	***AKAP5***, ***AKT3***, ***BLNK***, ***FRS2***, ***GAB1***, *GNA11*, *GNAZ*, ***GNG2***, *GSK3A*, ***ITPR1***, *ITPR3*, ***MEF2A***, ***MEF2C***, ***MS4A2***, *NFKBIB*, *ORAI1*, ***PLCB1***, ***SOS1***, ***SOS2***
HGF Signaling	3.36	2.33[£]	***AKT3***, *CCND1*, ***ELF1***, ***ELF2***, *ELF3*, ***ETS1***, ***FRS2***, ***GAB1***, ***MAP3K1***, ***MAPK9***, ***MET***, ***SOS1***, ***SOS2***
Aldosterone Signaling in Epithelial Cells	3.21	2.12[£]	***DNAJB4***, *DNAJB12*, ***DNAJC6***, *DNAJC11*, ***DNAJC13***, *DNAJC16*, *DNAJC17*, *DNAJC22*, ***FRS2***, ***GAB1***, ***ITPR1***, *ITPR3*, ***PIKFYVE***, ***PLCB1***, ***SOS1***, ***SOS2***
Gap Junction Signaling	3.10	NA	***AKT3***, ***CAV1***, ***FRS2***, ***GAB1***, ***GUCY1B3***, ***ITPR1***, *ITPR3*, *NPR1*, ***PLCB1***, ***PRKG1***, ***SOS1***, ***SOS2***, *TUBA1B*, *TUBB4B*, *TUBB*, *TUBG1*
Cell Cycle Regulation by BTG Family Proteins	2.73	NA	*CCND1*, *E2F1*, *E2F4*, *PPM1J* , *PRMT1*, ***PPP2R5A***
B Cell Receptor Signaling	2.71	2.00	***AKT3***, ***BLNK***, *CARD10*, ***ETS1***, ***FRS2***, ***GAB1***, *GSK3A*, ***MAP2K6***, ***MEF2C***, ***MAP3K1***, ***MAPK9***, *NFKBIB*, ***PAG1***, ***PTEN***, ***SOS1***, ***SOS2***
tRNA Charging	2.48	NA	*AARS*, *EARS2*, *FARSA*, *HARS*, *MARS*, *YARS*
ILK Signaling	2.46	0.00	*ACTN1*, ***AKT3***, ***BMP2***, *CCND1*, ***FRS2***, ***GAB1***, *GSK3A*, *KRT18*, ***MAPK9***, ***MAP2K6***, *MYH9*, *PPP1R14B*, ***PPP2R5A***, ***PTEN***, *PPM1J*, ***RICTOR***
14-3-3-mediated Signaling	2.39	2.12[£]	***AKT3***, ***FRS2***, ***GAB1***, *GSK3A*, ***MAPK9***, ***PLCB1***, *STK11*, *TUBA1B*, *TUBB4B*, *TUBG1*, *TUBB*, *YWHAH*
EGF Signaling	2.38	2.12[£]	***AKT3***, ***FRS2***, ***GAB1***, ***ITPR1***, *ITPR3*, ***MAP3K1***, ***SOS1***, ***SOS2***

[£]Significantly activated (z-score > 2) pathways in high-FE pigs; up-regulated genes in high-FE pigs are highlighted in bold and down-regulated genes in normal typeface; NA: no activity pattern available.

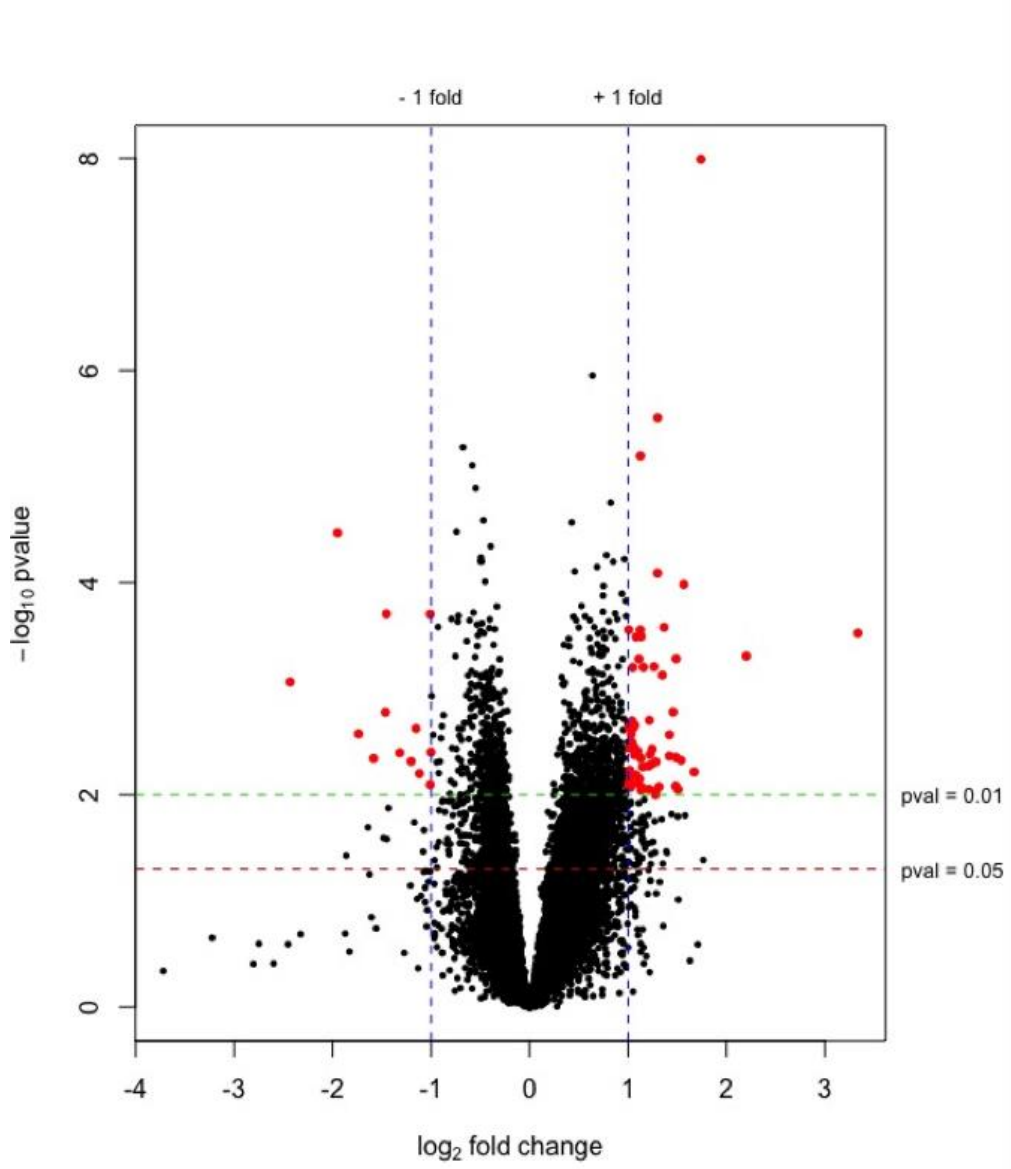

Figure 1 Plot of $-\log_{10}$(p-values) versus $\log_2$ fold changes for genes expressed in liver from high-FE pigs. The green and red lines indicate P = 0.01 and 0.05, respectively. Blue lines represent the threshold of genes with a log2 fold change ≥ |1| (fold change ≥ |2|). Significantly differentially expressed genes (P < 0.01, log2 fold change ≥ |1| [fold change ≥ |2|]) are highlighted by red dots. Up-regulated genes in high-FE pigs are indicated by positive fold changes.

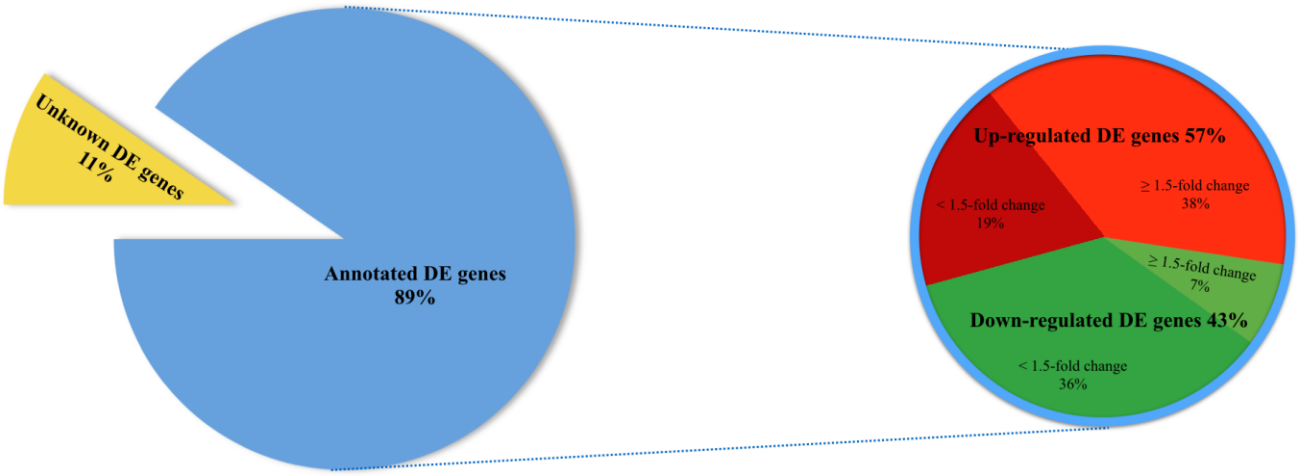

Figure 2 Pie chart depicting a total of 922 differentially expressed (DE) genes ($P < 0.01$) in liver of FE-divergent pigs and a percentage of annotated up- and down-regulated genes in high-FE pigs. The most up-regulated gene was *PON3* (fold change = 10.08) and the most down-regulated gene was *CCNT2* (fold change = -5.40) in high FE pigs.

(A)

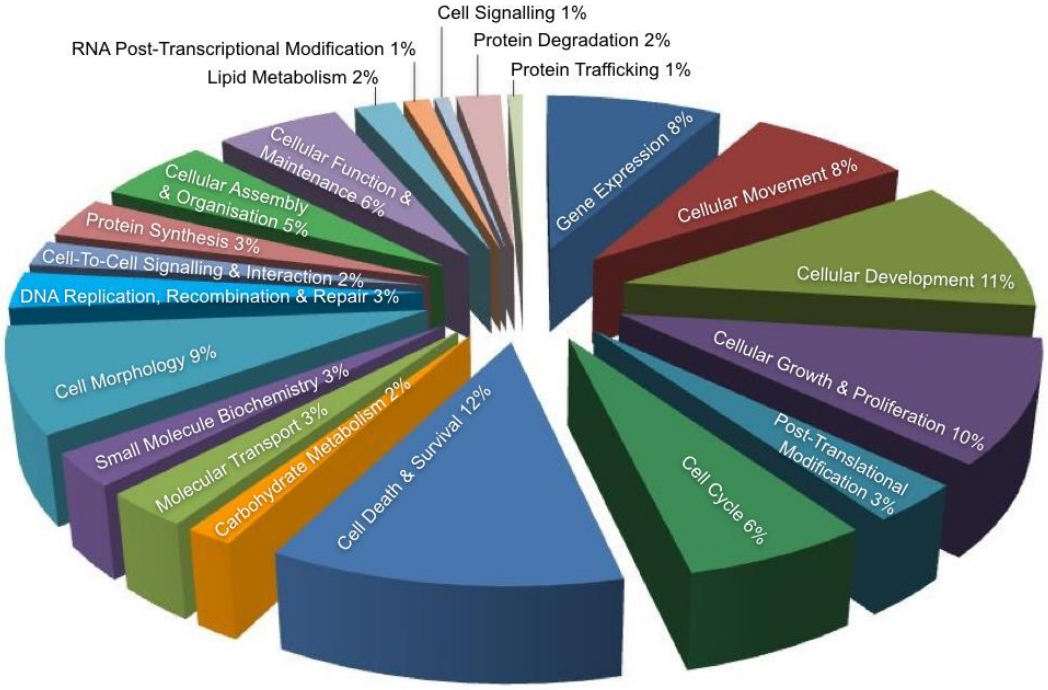

(B)

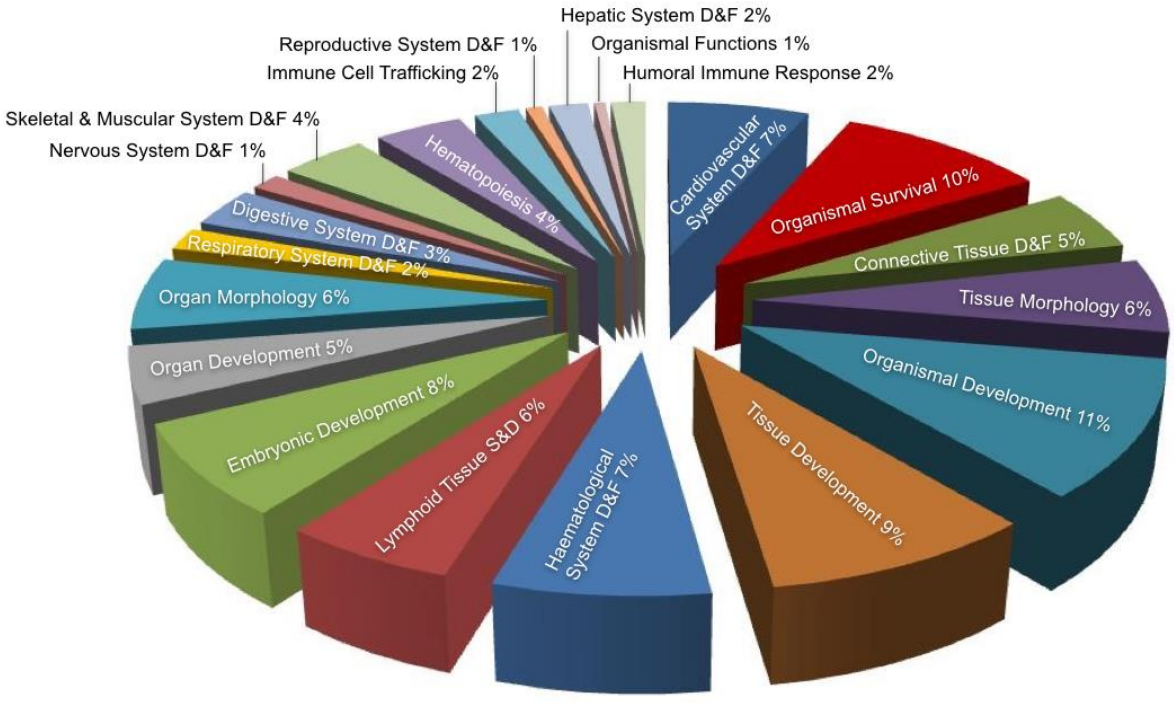

Figure 3 Pie charts illustrating entry distributions of differentially expressed genes within (A) molecular and cellular functions, and (B) physiological system development and function categories significantly ($P < 0.01$). F&D: Function & Development; S&D: Structure & Development.

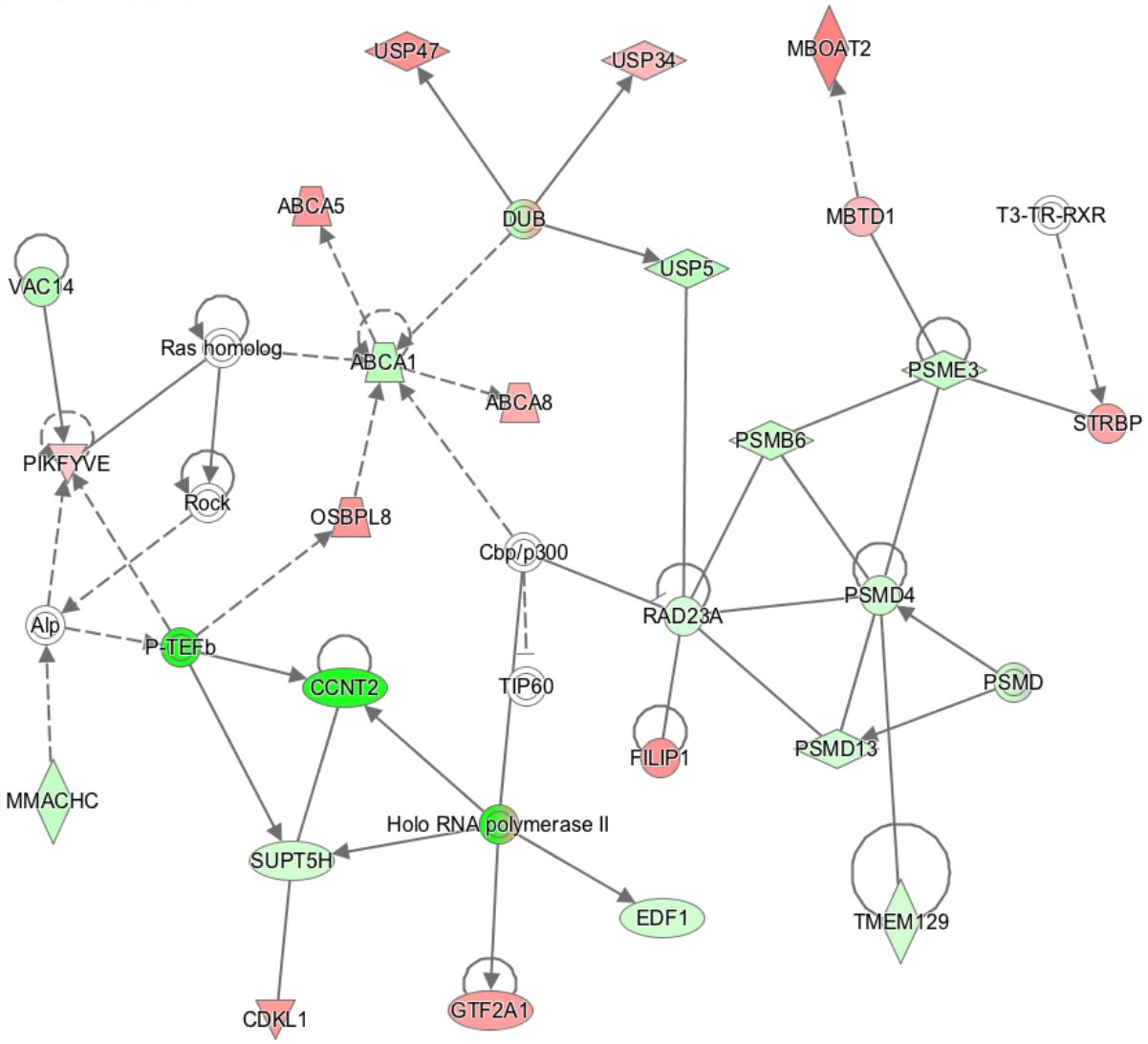

Figure 4 Connection of genes affecting functions related to 'carbohydrate metabolism', 'lipid metabolism' and 'small molecule biochemistry' represented in a gene network (network 12). Biological relationship between genes is depicted as an edge/line (solid lines and dashed lines show direct and indirect interactions, respectively). Colors represent up- (red) and down- (green) regulated genes in high-feed efficient pigs.

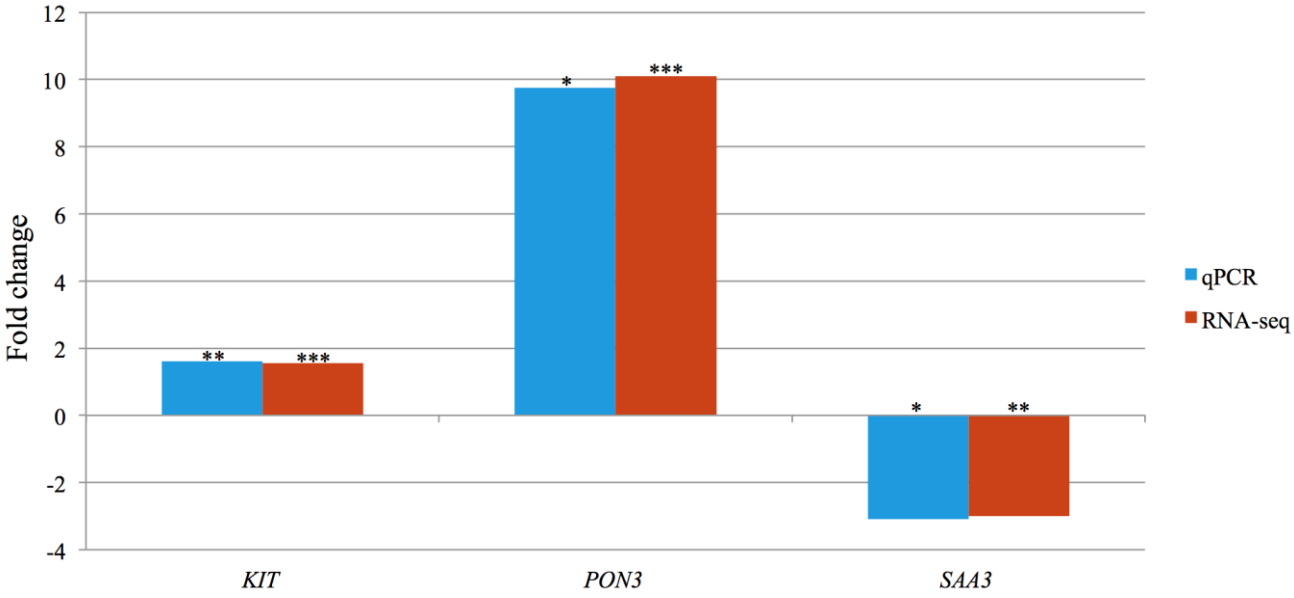

Figure 5 Bar chart portraying the RNA-seq and qPCR fold changes of three selected differentially expressed genes in high-FE pigs. Significance levels of differences affected by feed efficiency: *P < 0.05, **P < 0.01, ***P < 0.001.

Supplementary data

Table S1 Differentially expressed transcripts (n = 818) at a *P* < 0.01 between high-FE and low-FE groups.

Table S2 Molecular and cellular functions significantly over-represented among differentially expressed.

Table S3 Physiological system development and function categories significantly over-represented among differentially expressed.

Table S4 Significantly enriched canonical signaling pathways identified in liver samples of feed efficiency divergent pigs.

ANNEX B

List of Figures and Tables

List of figures

List of tables

ANNEX C

Abbreviations

List of abbreviations

AKR1C3	aldo-keto reductase family 1 member C3
CAPN1	calpain 1
CAST	calpastatin
CCNT2	cyclin T2
CDK9	cyclin dependent kinase 9
cDNA	complementary DNA
CEBPA	CCAAT/enhancer binding protein alpha
CL	cook loss
COL11A2	collagen type XI alpha 2 chain
COL1A1	collagen type I alpha 1 chain
cRNA	complementary RNA
D110	days to 110 kg
DE	differentially expressed
EBV	estimated breeding value
EGF	epidermal growth factor
FA	fatty acids
FCR	feed conversion ratio
FE	feed efficiency
FGF	fibroblast growth factor
FRS2	fibroblast growth factor receptor substrate 2
GWAS	genome-wide association study
HDL	high density lipoproteins
HGF	hepatocyte growth factor
HMGB1	high mobility group box 1
HWE	Hardy–Weinberg equilibrium
IBS	identity-by-state
IGF2	insulin-like growth factor 2
IMF	intramuscular fat
L*, a*, b*	lightness, redness, yellowness
LIPC	lipase
LTL	*Longissimus thoracis et lumborum*
MAF	minor allele frequency

MBD5	methyl-CpG binding domain protein 5
miRNA	microRNA
MMP2	matrix metallopeptidase 2
mRNA	messenger RNA
MUFA	monounsaturated fatty acids
MYC	transcription factor P64
NFAT	nuclear factor of activated T cells
NFATC1	nuclear factor of activated T-cells 1
NFATC2	nuclear factor of activated T-cells 2
NFE2L2	nuclear factor, erythroid 2 like 2
NGS	next-generation sequencing
NR2E1	nuclear receptor subfamily 2 group E member 1
OPRD1	opioid receptor delta 1
p38MAPK	p38 mitogen-activated protein kinase
PPARG	peroxisome proliferator activated receptor gamma
PRKDC	protein kinase, DNA-activated, catalytic polypeptide
PUFA	polyunsaturated fatty acids
QTL	quantitative trait locus
RFI	residual feed intake
RMA	robust multi-array average
SDC4	syndecan-4
SDHB	succinate dehydrogenase complex iron sulphur subunit B
SELL	selectin L
SFA	saturated fatty acids
SNP	single nucleotide polymorphism
SSC	pig (Sus scrofa) chromosome
TFAM	transcription factor A mitochondrial
TP53	tumor suppressor p53
TREH	trehalase
VEGFA	vascular endothelial growth factor A
WBSF	Warner Bratzler shear force
WHC	water holding capacity

ANNEX D

Acknowledgement

Acknowledgement

First and foremost, I would like to take this opportunity to express my sincere special thanks and appreciation to Dr. Ruth Hamill (Teagasc, Food Research Centre, Dublin, Ireland), who was my primary PhD project supervisor. It was her encouragement and support that started me on my path into scientific research. Whilst studying for my bachelor degree, Dr. Hamill introduced me to the field of molecular biology, an area that I have since developed a great interest in and it was her guidance that enabled me to pursue this PhD project. Throughout the four years of my PhD, Dr. Hamill has been a great mentor to me and was always very giving of her time. Dr. Hamill's professionalism is second to none and she went above and beyond in helping me to strengthen my knowledge, skill-set and research competency. Such was achieved by providing me with the opportunities to conduct my research not only in Ireland but also in Germany and the U.S.A, as well as attending and presenting my research findings at many international conferences. It was through our many discussions and constructive feedback from Dr. Hamill that helped me to craft my expertise. I will always be very grateful to Dr. Hamill for proving me with this invaluable experience.

I had the pleasure and was honoured to have Prof. Dr. Klaus Wimmers (Leibniz Institute for Farm Animal Biology, Dummerstorf, Germany) as my academic supervisor. It was thanks to his expertise and knowledge that I was afforded such vital scrutiny and critical feedback of my work throughout the four years of my PhD project. I would like to personally thank Prof. Wimmers for helping me integrate with other scientists, alongside guiding me to adapt to the customs and practices within his research facility.

I am also immensely grateful to Dr. Henry Reyer (Leibniz Institute for Farm Animal Biology, Dummerstorf, Germany) for his critical assistance and in-depth advice. Dr. Reyer was never short of fruitful ideas and provided knowledgeable and technical assistance, as well as ongoing support. He too was very giving of his time, making himself readily available to assist with the many queries I had throughout my PhD. I would also like to thank him personally for his mentoring and strengthening my research competency.

Thank you also to Dr. Michael Oster and Dr. Nares Trakooljul (Leibniz Institute for Farm Animal Biology, Dummerstorf, Germany) for their assistance and support. They were always very welcoming with any queries I had and were very prompt when furnishing me with

detailed explanations to same. I would also like to thank Dr. Peadar Lawlor (Teagasc, Pig Development Department, Fermoy, Cork, Ireland) for providing the experimental animals, Dr. Anne Maria Mullen (Teagasc, Food Research Centre, Dublin, Ireland) for assisting in animal sampling and Ms. Carol Griffin (Teagasc, Food Research Centre, Dublin, Ireland) for training sensory panellists and conducting sensory assessment of the samples. Finally, I would also like to thank the laboratory team at Leibniz Institute for Farm Animal Biology, Dummerstorf, Germany, especially Ms. Janine Wetzel, Ms. Angela Garve, Ms. Hannelore Tychsen and Ms. Anette Jugert, for their excellent technical assistance.

It is through the combined efforts, assistance and guidance from all the named persons listed above that have enabled me to complete my research. I now have the pleasure to submit my PhD thesis.

Justyna Horodyska